Lubos Matejicek

Assessment of Energy Sources Using GIS

Assessment of Energy Sources Using GIS

Lubos Matejicek

Assessment of Energy Sources Using GIS

Lubos Matejicek
Institute for Environmental Studies
Charles University
Prague, Czech Republic

Printed on acid-free paper

Preface

Power supply is one of the most important factors for living standards, human evolution, and socioeconomic development. But during the last few decades, the increasing need for new energy sources has led to a rapidly growing awareness in the field of environmental protection, with focuses on overexploitation and environmental pollution. In order to provide sustainable development, detailed knowledge and quantitative characterizations of our energy sources, distributions of energy and power supply are needed for prediction at local and global scales in time and space.

Assessment of energy sources and power supply optimization can improve situations. Using new methods based on Geographic Information Systems (GISs) enables more complex analyses dealing with spatial and temporal phenomena. Computer analysis and modeling will provide better deployment of existing power sources in order to reduce the operational and maintenance costs of the energy generation units.

This new and important book gathers the latest research in the field and related topics such as the outlook of energy sources and power supplies, key environmental issues, mapping of energy from fossil fuels, optimization of using renewable energy sources, and optimized deployment of existing power sources and renewable energy sources. Chapters are complemented by case-oriented studies that show practical applications.

The first chapter provides an introduction to the assessment of energy sources in the spatial and time scales of the universe, our solar system, Earth, continents and their regions, and mankind. It also introduces basic laws, principles, and physical units. The environmental issues are discussed from a view point of energy consumption by types and regions. The case studies deal with the presentation of spatial data using extensions of spreadsheets such as 3D Maps, development kits for data visualization on websites, and statistical programs.

The second chapter focuses on the introduction of spatial and temporal analyses using the Geographic Information System (GIS). It explains spatial data models in GIS, which are helpful for the assessment of energy sources. The description contains a number of examples to demonstrate GIS functionality. Desktop GISs and other related information systems give an overview of available software tools for

issues described in the next chapters. The case studies show web-based applications for spatial analysis of energy sources, GIS projects, and modeling tools for prediction of air pollution.

The third chapter focuses on energy outlook using data presented by a number of national and multinational agencies and companies, such as the US Energy Information Administration (EIA), the International Energy Agency (IEA), European Environmental Agency (EEA), British Petroleum (BP), and a number of others. Energy production, redistribution, and consumption are illustrated by Sankey diagrams complemented by a number of other charts. Also, various scenarios are discussed in order to decrease global emissions and total cumulative emissions of carbon dioxide. The case studies show spatial data management and datasets related to energy consumption.

The fourth chapter describes energy sources based on fossil fuels. It contains a number of tables and graphs that show global and regional trends of consumption. Mapping of fossil sources is provided by GIS datasets extended with data from GPS and remote sensing. The chapter includes an exploration of environmental effects related to fossil fuel use. The case studies are focused on using GPS and mobile GIS for mapping fossil fuels at a local scale and mapping surface coal mines at a regional scale with satellite images.

The fifth chapter contains information about using hydropower at the global and local scales. It explains types of hydropower sources and provides an overview of existing installations, as well as explores environmental effects of operational hydropower plants. The chapter also introduces hydrological modeling focused on nutrient flows in the basin. The case studies are focused on mapping the largest hydropower plants with data from remote sensing and mapping potential sources for small hydropower plants at the local scale.

The sixth chapter deals with wind power. It explains the basic principles and shows various types of hydropower installations. The wind power sources are explored by mapping wind speed at global and local scales. Thematic mapping contains installed capacity and production of wind power for leading countries. The GIS utilization is provided for risk assessment of wind turbines and wind farms projects. The case studies show data processing related to wind power sources in GIS and mapping potential sources for wind turbines at a local scale.

The seventh chapter shows estimates of solar energy potential and discusses environmental issues. It explains the modeling of solar irradiation with data from ground sensors and satellite systems. GIS is used for the exploration of potential solar sources with the regional and country maps, which can be used for the assessment of electricity generation from photovoltaic and thermal systems in Europe, Africa, and Southwest Asia. The studies are focused on estimates of solar energy by GIS advanced functionality including ArcGIS. Methods for area solar radiation and point solar radiation are tested at the local scale of urban environments.

The eighth chapter describes the assessment of bioenergy potential in the context of existing energy systems. The description is focused on modern solid biomass heating systems, liquid biofuels, and biogas systems. Flow diagrams show global bioenergy flows and provide an overview of different renewable energy sources, and

main technologies to convert them into direct heat, or heat and power. The attached case studies demonstrate spatial data processing related to mapping of potential bioenergy sources and optimization of transport management.

The ninth chapter deals with nuclear power, provides its historical overview, and discusses environmental issues. It also compares nuclear fission and fusion, which represents a great challenge for research and development. The chapter also includes mapping of world uranium mining production, which is documented with a number of thematic maps and charts. An overview of nuclear reactor generations with their deployment is illustrated in diagrams and tables. Environmental effects of using nuclear energy are discussed and complemented by flow diagrams for power generation by fuel and demand by sector for selected regions. The case studies provide mapping of global and regional environmental impacts of operational nuclear installations in relation to population density.

The tenth chapter is principally devoted to the energy storage systems, which are increasingly important for the integration of variable power from renewables in the electricity grid. In particular, pumped storage hydropower and compressed air energy storage systems are explored together with their environmental impacts. The case studies are focused on selected installations of energy storage systems and their environmental evaluation. GIS is used for risk assessment mapping of related ecologies and natural systems, physical environments, and human impacts.

This book is the successor to earlier research activities on environmental consequences of energy use and many years of teaching, as well as research and teaching in the field of GIS and remote sensing. The book incorporates much information from recent reports, papers, and books, which summarize new developments in the assessment of energy sources and GIS. The materials are presented in such a way that they can be understood on different levels, in order to enable students and professionals to make quantitative estimates and form sound judgments. Case studies of energy projects taken from around the world provide examples of using GIS in selected stages of decision-making processes.

Prague, Czech Republic   Lubos Matejicek

Acknowledgments

Contents

Chapter 1
Introduction

Our standard of life and our advanced technology are highly dependent on an adequate supply of energy. More and more energy is needed to supply our homes with electricity, to drive our transport, to power our communications, and to support our industry. Our living standards are dependent on energy consumption, which is strikingly illustrated by the connection to average life expectancy. People in rich well-developed countries like Japan and in continents like North America and Europe use considerably more energy per person and have longer average life expectancy. At the other end of the scale, people in poorer countries, such as in some parts of Africa and Asia, have significantly lower energy consumption and average life expectancy. Without energy, all the conveniences of modern life would be impossible on the scale needed, and our civilization would soon collapse into barbarism.

Supply of energy is increasingly dependent on consumption of fossil and nuclear fuels needed to support the operation of our services such as the production of food and water, heating, transportation, communication, housing, clothing, and other human services. The amount and concentration of energy used in industrialized countries results in environmental degradation of nature on a local and regional scale. Moreover, it causes the global warming, which can irreversibly damage our world. Global climate changes result from the accumulation of gaseous emissions to the upper layers of the atmosphere. The gaseous emissions containing carbon dioxide mostly originate from combustion of fossil fuels. An expanding consumption of fossil energy sources by seeking to improve the living standards of world population can contrarily result in damage of our health and degradation of our environment. It cannot be solved on the national level, because the energy sources and energy usage are intimately involved in nations' and world's economies, which can cause some adverse effects on the economic and social circumstances of national populations. For example, the average daily fossil fuel use per capita in some highly industrialized nations, such as the United States, may amount to more than 50 times the necessary daily food intake, which expend 20 times the energy used by some developing nations. Evidently, the energy intake is closely linked to the degree of industrialization. Also it can approximately indicate the living level of populations.

An analysis of the spatial supply and demand relationships for energy potential in the global and local scale is needed in order to optimize cost, transportation, and use of energy. Many of the previous studies have identified potential for energy generation at individual sites, according to local factors. The research presented here takes more generalized approach, to allow national and multinational scale assessment of capability to meet local and global energy demands, and potential energy supply under relevant scenarios. The approach is illustrated for selected areas of interest in the world and in the author's country, although techniques are applicable elsewhere when suitable data are available.

The geographic information system (GIS) is used as a key tool for data management, analysis, and modeling. GIS was originally designed to capture, store, analyze, and present spatial data derived from cartography. But today, the world of GIS has changed dramatically. Data management is based on database tools that represent commonplace for sharing of a large amount of information. Advanced mobile computing systems can display detailed view of spatial objects and their interactions in space and time. All information can be shared via the cloud, which offers to perform analysis, such as assessment of energy sources, in seconds, and display results on a mobile computer or even a smart phone or tablet.

1.1   Energy Sources in the Scale of the Universe

Nowadays, the Universe is presented as everything that exists in the past, the present, and the future. According to current understanding, the Universe is formed by space-time and energy that include electromagnetic radiation and matter. The Big Bang theory describes the development of the Universe as a creation of space and time from a fixed amount of energy and matter. After the initial expansion, the Universe cooled sufficiently to allow the formation of subatomic particles and later of simple atoms. Clouds of these initial elements coalesced through gravity to form primordial stars, which were transformed to the next generation of stars (Fig. 1.1). Now, our Solar System is located in a galaxy composed of billions of stars, the Milky Way, which is just one of many (Fig. 1.2). It is assumed that the distribution of galaxies is uniform in all directions, with no edges or centers, on the largest scales. Assuming that the described scenario is correct, the age of the Universe is estimated to be 13.799 ± 0.021 billion years, and its diameter is about 28 billion parsecs (91 billion light-years) at the present time. Final observations indicate the increasing rate of the expansion of the Universe. Also the latest theory indicates that the Universe is composed almost completely of dark energy and dark matter. Ordinary matter, which forms galaxies and atoms including supposed life, accounts for approximately 4.9%. Dark energy permeates all of space. It accelerates the expansion of the Universe, contributing to approximately 68.3% of the world's energy. Dark matter contributes approximately 26.8%. The existence is inferred from its gravitational effects on visible matter and radiation in the large-scale structure of the Universe. The residuum containing only 4.9% of the mass-energy of the Universe is ordinary matter that is based on atoms and the objects they form. Present research in physics is also focused on subatomic particles, including atomic constituents such as protons, neutrons, and

Fig. 1.1 Some visible galaxies captured by the Hubble Ultra Deep. Source: www.pixabay.com, 2016

electrons, and elementary particles that are not composed of other particles according to current understanding. Quantum mechanics can explain dynamics of particles, their behavior under certain experimental conditions including wave-particle duality. All particles and their interactions can be described by a quantum field theory called the Standard Model, which is currently formulated for mass-energy interactions of 61 elementary particles (such as quarks, leptons, gluons, photon, and bosons) that can be combined to form composite particles. This model represents a theory that is concerned with electromagnetic interactions and the weak and strong nuclear interaction. The Standard Model supports the experimental confirmation of the existence of particles. The model even predicted the existence of a new recently discovered Higgs boson.

Our Solar System was formed 4.568 billion years ago from the gravitational collapse of an interstellar molecular cloud that consisted mostly of hydrogen, helium, and small amounts of heavier chemical elements fused by previous generations of stars. It formed a protoplanetary disk with a hot and dense protostar at the center and hundreds of protoplanets in a protoplanetary disk due to the rotation of the initial cloud. The present planets were formed by accretion from the protoplanetary disk, in which protoplanets, dust, and gas gravitationally attracted each other (Fig. 1.3). The rocky planets such as Mercury, Venus, Earth, and Mars exist in the warm inner Solar System close to the Sun. Due to a very small fraction of metallic elements in
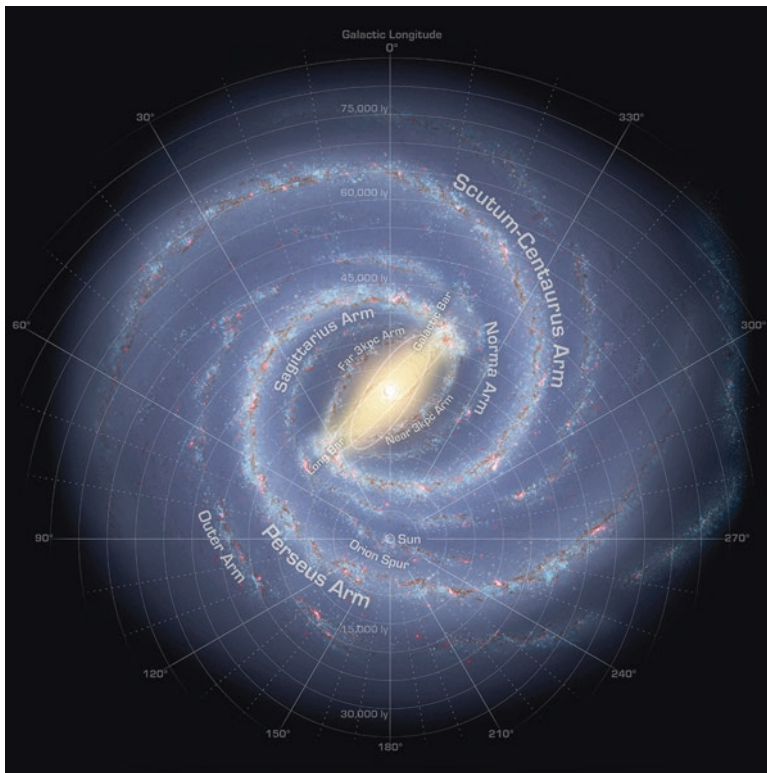
Fig. 1.2 The Milky Way, the galaxy containing our Solar System with the Sun in the center of the coordinate system under the galactic center that occupies a supermassive black hole Sagittarius A*. Source: www.pixabay.com, 2016
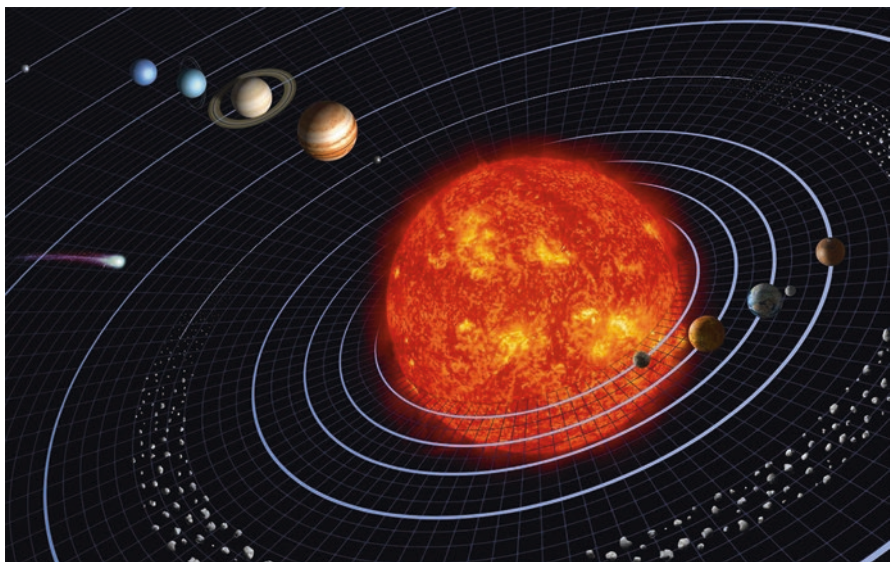
Fig. 1.3 Our Solar System with the Sun and its rocky planets Mercury, Venus, Earth, and Mars (on the right side) and its giant planets Jupiter, Saturn, Uranus, and Neptune (on the left side) behind the Kuiper Belt. Source: www.pixabay.com, 2016

the initial cloud, their size is relatively small. Beyond the frost line where other material is cool enough to remain solid, the giant planets such as Jupiter, Saturn, Uranus, and Neptune were formed by volatile ice compounds remaining solid, which allowed to capture large atmosphere of hydrogen and helium. The leftover debris, which never became planets, congregated in regions of Kuiper Belt of asteroids and Oort cloud. Once the pressure and density of hydrogen in center of the protostar became great enough, the thermonuclear fusion begin. After this period about 50 million years, the Sun became a main-sequence star, which will last about 10 billion years. The Sun's pre-remnant life is estimated to around 2 billion years. Thus, the Solar System should probably behave like today until the hydrogen in the core of the Sun has been converted to helium, which will occur after 5 billion years from now.

The Sun is the most important source of energy in our Solar System. It is an essential energy source for life on Earth, and its mass is about 330,000 times that of Earth. It accounts for 99.86% of the total mass of the Solar System. At present, its photospheric composition by mass is hydrogen (73.46%) and helium (24.85%). The smaller quantities belong to oxygen, carbon, iron, and other elements. The hydrogen fusion in its core is the primary source of energy. Above the visible surface of the Sun, the photosphere, the photosphere visible sunlight energy is free to propagate into space. The spectrum of the sunlight is similar to the electromagnetic spectrum of a black-body radiation at about 6000 K. The amount of solar energy deposited by the Sun per unit area on Earth is the solar constant, which equals to approximately 1368 W/m^2. It is composed of about 10% ultraviolet light, 40% visible light, and 50% infrared light. But less power in the mentioned parts of electromagnetic spectrum arrives at the surface of the Earth in dependence on atmospheric conditions. In case of clear conditions when the Sun is near the zenith, the amount of power can be approximated to 1000 W/m^2.

1.2   Energy Sources in the Scale of Mankind

The roots of our civilization are related to primitive technology and culture that begins in the Paleolithic Era followed by Neolithic Era and the Agricultural Revolution in the region of Western Asia, the Nile Valley, and Nile Delta between 8000 and 5000 BCE. The agriculture technology began to displace the hunter-gatherer societies. Other sources of mechanical energy related to domestic animals, wind, and water streams were developed in order to enhance agricultural production and living. As the world population increased, the demand for other sources, such as the amount of crop and pasture land, increased in proportion. Permanent replacing of natural forest and grassland ecosystems represented the major environmental impact of human activities until the beginning of the industrial revolution several centuries ago.

The industrial revolution significantly increased using fossil sources of energy such as coal, oil, and gas, which significantly changed the conditions of human societies by making available large amounts of energy for manufactory production and transport. It changed the conditions of human societies freeing up a part of the population for other beneficial activities. Manufacturing and commerce were concentrated in urban areas, which caused increasing of urban populations.

On the other hand, the growing industrialization inflicted serious damage on the environment in the local and global scale. The burning of fossil fuels caused air pollution that can even extend in high concentrations to rural areas at some distance from the pollution sources. The global atmosphere experiences a permanent increase in greenhouses gases that are thought to induce the average surface temperature to rise and climate to be modified. Unlike the local emission of pollutants, most of which are precipitated from the atmosphere within a few days, greenhouse gases are accumulated in the atmosphere for years. One of the most abundant greenhouse gases is carbon dioxide, which is produced by burning of fossil fuels.

Nowadays, the major sources of energy are fossil fuels, nuclear fuels, and, particularly, hydropower. The fossil sources remain indispensable for heating, cooking, or industrial and commerce use in developing countries and even in developed countries. In the future, it will be very difficult to reduce the global emissions of carbon dioxide, because it is not efficiently possible to utilize the full energy of fossil fuels without forming carbon dioxide. The nuclear fuels can decrease the ordinary emissions of carbon dioxide, but the nuclear power plant technology and safety systems are still technically very complex and economically quite expensive. Also the environmental problems associated with preparing the nuclear fuel and storing the spent fuel have become expensive to manage. Fossil and nuclear fuels, which store their energy in chemical or nuclear form indefinitely, are the preferred form for storing and transporting energy especially in relation to production of electrical energy that can be easily transmitted from source to final consumer, but there is no electrical storage capacity in the electrical system. It can be partially overcome by using hydropower systems to store energy for periods of hours to days in pumped-storage hydroelectricity systems. The widely used hydropower plants convert the gravitational energy of dammed up water to electrical power. Hydropower has been used since ancient times as an energy source for irrigation and the operation of various mechanical devices. Modern hydropower plants represent efficient sources of electrical energy, which are used by some countries as one of major sources for production of electrical energy. But hydropower projects can have social and environmental impacts due to the construction of a dam and power plant, along with the impounding of a reservoir.

In the future the sources of renewable energy such as solar thermal power plants, hydropower, wind turbines, photovoltaic systems, biomass-fueled power plants, and geothermal power plants could be integrated into the complex energy systems in order to produce energy in a more efficient and environment-friendly way. Most of the renewable energy systems experience low energy flux intensity, which is in addition to that dependent on actual meteorological conditions. Thus, they require larger land area that is needed for fossil fuel power stations or nuclear power plants and are often located farther away from consumers, where natural conditions and land costs are optimal. Another major sector of the energy market is represented by transportation energy where automobiles are a major consumer and emitter of air pollution. Although modern automobiles emit smaller amounts of pollutants, their growing number causes higher contribution to the urban air pollution. Considerable progress can ensure new technology of electric drive systems powered by electric storage systems and the introduction of lightweight body designs together with onboard-engine-driven systems.

1.3 Laws, Principles, and Physical Units

Energy, in physics, is the capacity for doing work. It may exist in potential, kinetic, thermal, electrical, chemical, nuclear, or other various forms (www.britannica.com/science/energy). The SI unit of energy is joule (J) or newton-meter (N·m): the energy transferred to an object by the mechanical work of moving it a distance of 1 meter against a force of 1 newton. Besides this definition, there are many other definitions, depending on the context, where definitions of energy are derived (thermal, radiant, electromagnetic, or nuclear energy). All forms of energy are convertible to other kinds of energy and obey the law of conservation of energy which says that energy can be neither created nor destroyed. For example, energy transformation includes generating electric energy from heat energy via a steam turbine in the power plant, which uses chemical energy from fossil fuels or nuclear energy from nuclear fuels. This electric energy can be easily transported and transformed by consumers into many forms using heating systems, air-conditioning systems, lights, local transport systems, and so forth (Fig. 1.4).

Also the Sun transforms nuclear energy into other forms of energy such as radiant energy, which escapes out to its surroundings. A part of this energy arrives at the surface of the Earth and is unevenly distributed over the planet, absorbed by the atmosphere and hydrosphere, and, finally, transformed into a flow of heat to space. When incoming solar energy is balanced by this flow of heat, the energy budget is in equilibrium (Fig. 1.5).

Fig. 1.4 Las Vegas at night. Source: www.pixabay.com, 2016
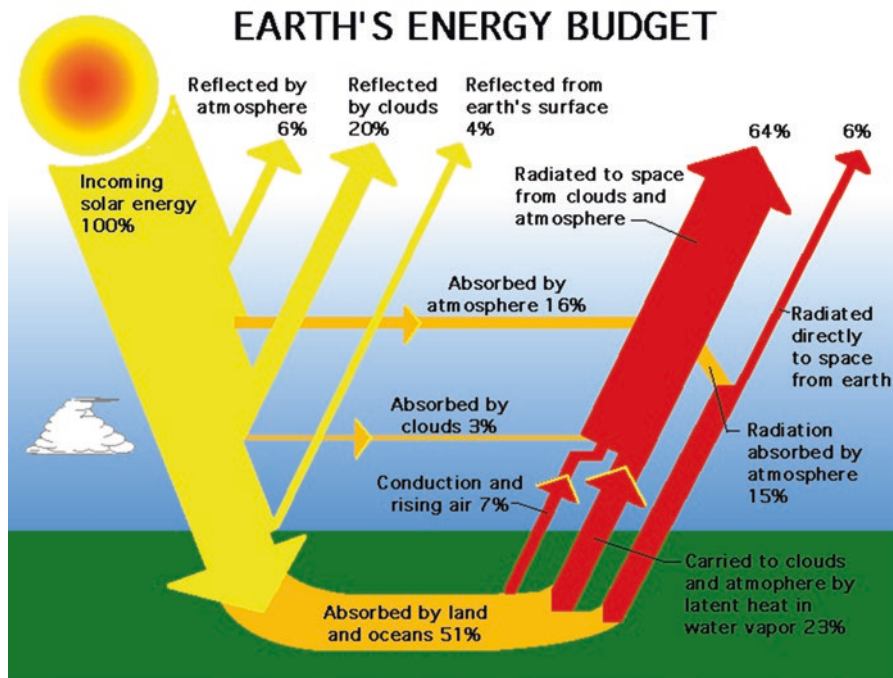
Fig. 1.5 Earth's energy budget. Source: http://www.slideshare.net/jcv57/gpm-global-energy-budget-power-point, 2016

1.4 Food Energy

Humans need intake of food energy to sustain life. Food energy is a form of chemical energy that humans and animals derive from their food and molecular oxygen in the process of cellular respiration. Foods are composed mainly of carbohydrates, fats, proteins, vitamins, minerals, and water. The physical unit for food energy is joule (J) or its multiples (kJ). Also calorie (cal) or its multiples (kcal) are still widely used as an older metric unit of energy (1 kcal = 4.184 kJ). The value of metabolizable energy for each food item can be estimated by multiplying the total amount of energy associated with a food item by approximately 85%. It results to a typical amount of energy obtained by a human after the respiration. A more precise estimate is provided in laboratories to determine a specific energy amount for each component such as fat, proteins, carbohydrates, organic acids, polyols (sugar alcohols, sweeteners), fiber, and ethanol (drinking alcohol), which better approximate the process of cellular respiration. The declared energy value of food shall be calculated using the conversion factors in Table 1.1. The selected food nutrients based on various food categories are displayed in Table 1.2. The values are compiled from the US Department of Agriculture (USDA).

Table 1.1 The declared energy value (Council Directive of September 24, 1990, on nutrition labeling for foodstuffs)

Food component	Conversion factor [kJ/g]	Conversion factor [kcal/g]
Fat	37	9
Alcohol (ethanol)	29	7
Salatrims	25	6
Protein	17	4
Carbohydrate (except polyols)	17	4
Organic acid	13	3
Polyols	10	2.4
Fiber	8	2
Erythritol	0	0

Table 1.2 Table of selected food nutrients ("T," tablespoon; "t," teaspoon)

Food category	Food	Measure	Grams	Calories (joule)	Protein	Carbohydrate	Fiber	Fat	Sat. fat
Dairy product	Cocoa	1 cup	252	235 (983)	8	26	0	11	10
Oils, fats, shortenings	Lard	½ cup	110	992 (4151)	0	0	0	110	92
Meat and poultry	Bacon, crisp	2 slices	16	95 (397)	4	1	0	8	7
Fish and seafood	Salmon, canned	3 ounce	85	120 (502)	17	0	0	5	1
Vegetables	Potato chips	10	20	110 (460)	1	10	t	7	4
Fruits	Apple juice	1 cup	250	125 (523)	t	34	0	0	0
Bread, cracked wheat	Cornflakes	1 cup	25	110 (460)	2	25	0.1	t	0
Soups	Bean soups	1 cup	250	190 (795)	8	30	0.60	5	4
Desserts and sweets	Apple betty	1 serving	100	150 (628)	1	29	0.5	4	0
Nuts and seeds	Peanuts roasted	1/3 cup	50	290 (1213)	13	9	1.2	25	16
Beverages	Beer (4% alcohol)	2 cups	480	228 (954	t	8	0	0	0

The minimum energy requirement per person per day is about 7500 kJ. The recommended energy intake is 11,300 and 8800 kJ for men and women, respectively. The recommendations are for men and women between 31 and 50 age in case of the light physical activity associated with typical day-to-day life. Food energy is mainly used for basal metabolic requirements to produce heat to maintain body temperature and to produce mechanical energy by skeletal muscle. About 20% of energy is used for brain metabolism. The efficiency of food energy conversion is highly dependent on the category of food and on the type of energy usage. For example, the efficiency of muscles to convert the energy available from respiration into mechanical energy is approximately 20%.

1.5   The Environmental Issues

World total primary energy supply is higher than the world final energy consumption because great amount of energy is lost during the process of extraction from natural resources, its refinement into usable forms, and its transport to consumers. There is a great variability in energy consumption per capita between developed and developing countries in the world. While the developed countries indicate some scope for reducing energy consumption by improvements in efficiency, many of the developing countries rapidly increase their energy consumption in the view of grooving population and using obsolescent technology for energy extraction. The trends of primary energy consumption of the world regions such as North America, South and Central America, Europe and Eurasia, Middle East, Africa, and Asia Pacific in million tonnes of oil equivalent (Mtoe) in the period 1985–2014 are illustrated in Fig. 1.6. The input datasets are based on primary fuel types such as oil, natural gas, coal, nuclear energy, hydro energy, and renewables that include solar, wind, geothermal, and biomass resources. It displays graphically the imbalance among different geographical regions. The total primary energy consumption in North America and Europe indicates constant level in the period 1985–2014. Although the final energy consumption in these regions is growing, the energy needs are slightly reduced by using more efficient technology. The significant increase of primary energy consumption is indicated by the Asia Pacific region. It is caused by a rapid growth of China's economy, in particular. Globally, fuel switching to sources with lower carbon dioxide and using advanced technology for energy extraction and transport will result in equalization of the primary energy consumption in the next decades compared with the period 1985–2014. Also the predictions should comprise the potential primary energy demand of other regions such as South and Central America and Africa. But the fossil and nuclear fuel sources over the world are being depleted at a rate that will render them scarce and more expensive in future decades, even if they are managed in a more efficient way than in the past.

A relatively new type of energy from the view of the twentieth century is represented by electric energy that today consumes more than one third of the world's
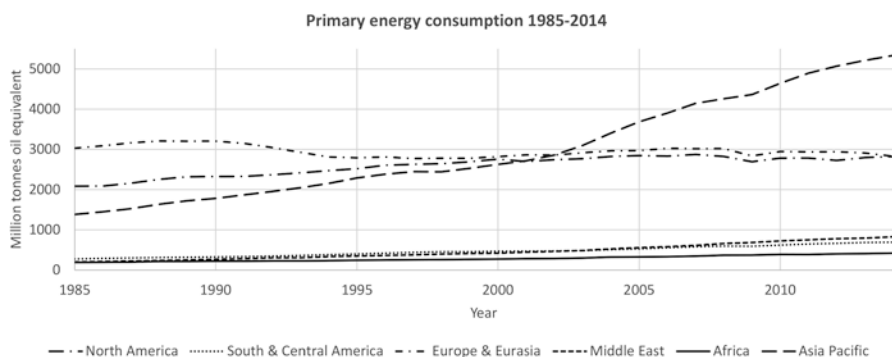
Fig. 1.6 The energy consumption in million tonnes of oil equivalent in the period 1965–2014. Source: BP Statistical Review, 2015

energy. Major part of the electric energy is produced in large utility plants, each generating in the range of 100 to 4000 MW. Fossil fuels, nuclear fuels, and hydropower are the overwhelming contributors. The remainder, which accounts for a few percent, is actually generated by renewable energy plants such as solar and wind farms. Due to higher prices, fossil fuels such as oil and gas are used as sources for reserve fossil fuel power plants. The electric energy is directly transmitted by a sophisticated network system to customers, because the possibilities to accumulate electric energy are significantly limited. The dependence of electricity generation on the energy consumption based mainly on fossil fuels is illustrated in Fig. 1.7. Again, the total electricity generation in North America and Europe indicates constant level in the period 1985–2014. The higher prices of electric energy in these regions pressurize leading manufacturers into production of energy-saving products and their economical operation. The permanent increase of electricity generation indicates the Asia Pacific region, which is mainly caused by a rapid growth of China's economy, in particular.

Total energy consumption by types and region in 2014 in absolute terms and relative terms is shown in Fig. 1.8 and Fig. 1.9, respectively. The dominant energy consumption in the world is based on fossil fuels such as oil, coal, and gas. Oil is governing fuel for transportation vehicles and also the fuel of choice for industrial use. It is more
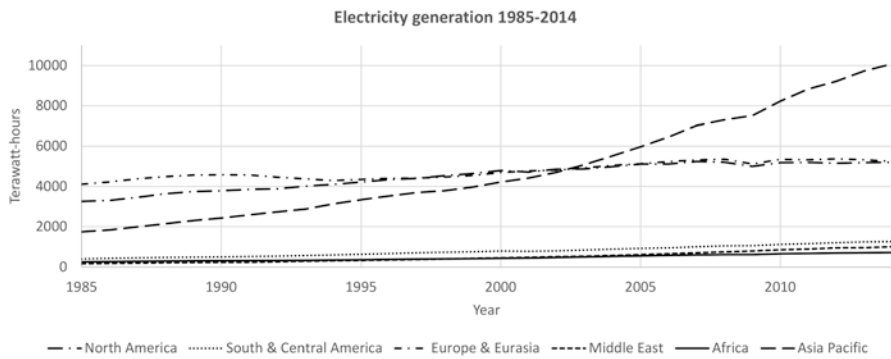
Fig. 1.7 Electricity generation in the period 1985–2014. Source: BP Statistical Review, 2015
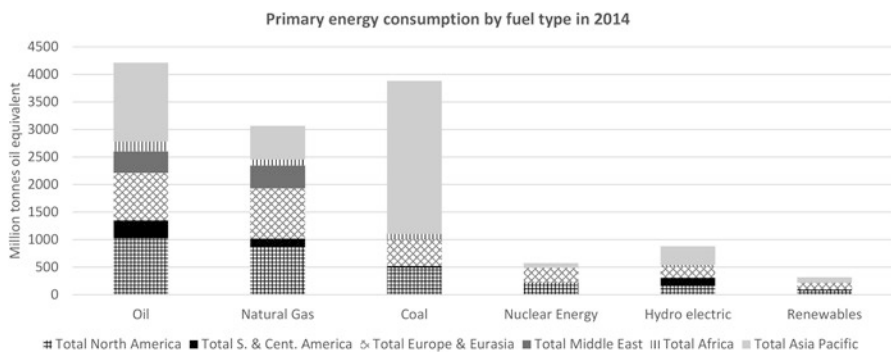
Fig. 1.8 Total energy consumption by types and region. Source: BP Statistical Review, 2015

Total energy consumption by region in 2014

5335; 41%   2823; 22%   ⊞ Total North America

                                        ■ Total S. & Cent.
                                           America

                                        ✕ Total Europe &
                                           Eurasia

                                        ■ Total Middle East

                                        ‖ Total Africa

                                        ▦ Total Asia Pacific

420; 3%   828; 7%   2830; 22%

Total energy consumption by fuel type in 2014

879; 7%   317; 2%   4211; 33%

574; 4%

                                        ■ Oil

                                        ■ Natural Gas

                                        ■ Coal

                                        ⁖ Nuclear Energy

                                        ▤ Hydro electric

                                        ▨ Renew-ables

3882; 30%   3066; 24%
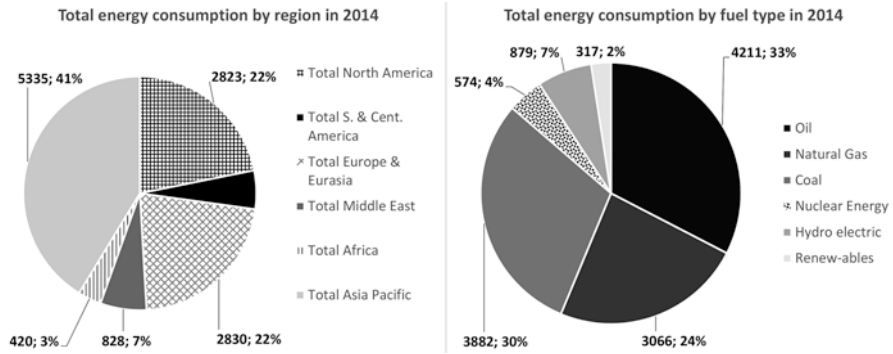
Fig. 1.9 Total energy consumption by types and region. Source: BP Statistical Review, 2015

expensive than coal due to a more complex extraction but is more easily transported by pipeline and supertankers. Coal is the cheapest fossil fuel to extract from surface mines, store, and transport. It is mainly used as an electric utility fuel and as an energy source for central and local heating in some countries. But its use is less efficient and clean than in case of oil and gas. Natural gas is widely used in industry, commerce, and residences because of its ease, efficiency, and cleanliness of combustion in comparison with coal and oil. But it is more expensive and not easily stored or shipped across oceans. A significant fraction to the world's electricity supply represents nuclear-fueled power plants that contribute about 20% of the electricity in the United States, about 80% in France, and about 30% in Japan. The capital investment for nuclear-fueled power plants is much greater in comparison with fossil-fueled plants of equal electric power. The price for electricity generation may change, if fossil-fueled plants will be mandated to install carbon capture and sequestration equipment. However, if nuclear industry will be viewed as a risk for human health after the accidents at the Three Mile Island power plant in Pennsylvania (1979), at Chernobyl in Ukraine (1986), and at Fukushima in Japan (2011), the extra capital investment for the highest levels of security can increase the cost of electricity generation from nuclear-fueled power plants.

The reserves of fossil and nuclear fuels are limited, and it is expected that their extraction at an actual rate will render them extremely scarce in future centuries. In order to replace widely used fossil sources of energy, new advanced technologies have to be created using nondepletable sources, the so-called renewable energies or renewables such as wind power, solar power, and geothermal energy. Some renewables were developed on a small scale in preindustrial societies, providing for irrigation, ocean transport, cooking, and milling of grain. New advanced technology for smart distribution and consumption of electric energy can make it possible to develop these sources on a much larger scale, but renewables have only a tiny share to current world energy consumption. Electric energy originated from renewables is more costly than fossil energy but may become more economical when pollution abatement costs of nonrenewables are factored in. In contrast with fossil fuels, renewable energy is dependent on local conditions and is not transportable by itself. After conversion to electric power, it can be transported and partially stored in pump-storage hydroelectricity, which is used by electric power systems for load

balancing, or converted into chemical energy in rechargeable batteries, which is mostly utilized in mobile electronic devices.

Besides renewables, synthetic fuels such as hydrogen, bioethanol, biodiesel, and biogas can be manufactured from biomass by transforming the molecular structure of a natural source to a synthetic one. After transformation into the secondary fuel, it can be transported and stored in a more suitable way than its parent fuel. Although the secondary fuel can provide superior combustion characteristics, the costs are not actually competitive and environmentally achievable in a large scale of fuel combustion. Historically the synthetic fuels were mostly transitioning from fossil fuels, which is transformation from one inherently depletable limited resource to another. A positive characteristic of synthetic fuel production is the ability to use multiple feedstocks such as coal, oil, gas, or, preferably, natural biomass. Because prospecting of new fossil deposits and synthetic fuels will be increasingly difficult toward the future, the only energy sources that could supply energy indefinitely beyond a time scale of centuries are nuclear fusion with combination of some renewables. Nuclear fusion can provide higher-order energy for a given weight of fuel than any fuel-consuming energy source currently in use, even more than nuclear fission. But both the energy sources, nuclear fusion and renewables, are capital-intensive technology. Nuclear fusion is still in early stages of development and substantial sums running into billions of dollars will have to be spent on fusion research in the future.

An evaluation of the standard of living in a country, not economic growth alone, can be based on the Human Development Index (HDI). HDI is a summary measure of average achievement in key dimensions of human development: a long and healthy life, being knowledgeable, and having a decent standard of living. The health dimension is assessed by life expectancy at birth; the education dimension is measured by mean years of schooling for adults aged 25 years and more and expected years of schooling for children of school entering age. The standard of living dimension is measured by gross national income (GNI) per capita. The HDI uses the logarithm of income, to reflect the diminishing importance of income with increasing GNI. The scores for the three HDI dimension indices are then aggregated into a composite index using geometric mean. HDI like other indexes can express synoptically only a part of what human development entails. The dependence of the United Nations' HDI on the primary energy consumption in tonnes of oil equivalent per capita for selected countries is depicted in Fig. 1.10. The relation between increments of both variables in the period 1990–2014 is shown in Fig. 1.11. It shows a global energy trend for each country and its influence on HDI. The primary energy consumption is expected to slightly decrease in the developed countries due to implementation of new efficient technology, while the primary consumption in developing countries will grow rapidly in dependence on growing economy and population.

Energy consumption mainly based on fossil fuels has escalated the pollution of our environment by the anthropogenic emissions of so-called greenhouse gases since the industrial revolution. During the twentieth century, industrialization proceeded even faster than population growth, which caused increased pollution of atmosphere, deposition of land, and contamination of surface water and groundwater. These effects caused permanent loss of natural species of plants and animals. Also global climate started to change, which can be observed by increasing the average atmospheric surface temperature by a greenhouse effect. The carbon dioxide emitted by

Human Development Index (HDI) in 2014
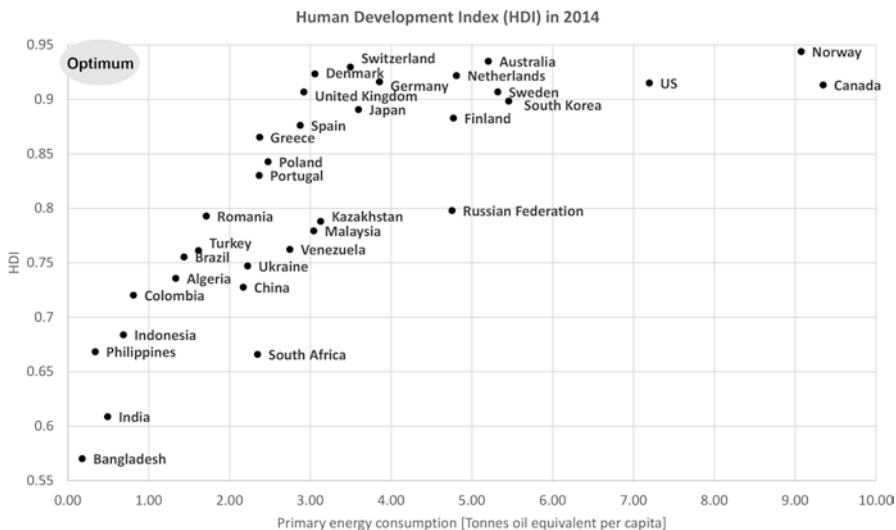
Fig. 1.10 The dependence of the United Nations' HDI and on the primary energy consumption in tonnes of oil equivalent per capita for selected countries. Source: BP Statistical Review, 2015; UN World Population Prospects, 2015

Increment of Human Development Index (HDI) in the period 1990-2014
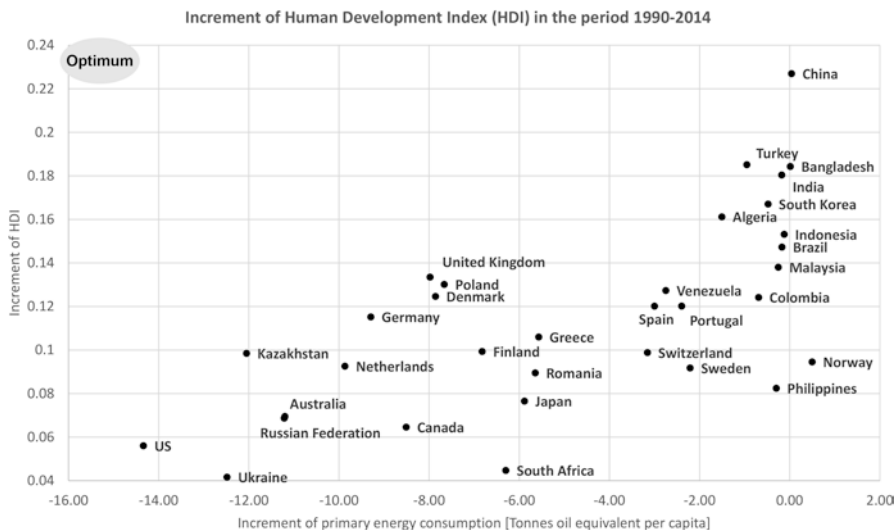
Fig. 1.11 The dependence of the increment of the United Nations' HDI on the increment of the primary energy consumption in tonnes of oil equivalent per capita for selected countries in the period 1990–2014. Source: BP Statistical Review, 2015; UN World Population Prospects, 2015

consumption of fossil fuels is one of the main greenhouse gases, which absorb infrared radiation. By this effect the atmosphere absorbs the Earth's radiation and heats up. A part of heat energy is radiated back to the Earth's surface, which gets hotter. Escalation of carbon dioxide emissions in a short period 1985–2014 is illustrated in Fig. 1.12.

Carbon Dioxide Emissions

Total North America ■ Total S. & Cent. America ⊹ Total Europe & Eurasia ■ Total Middle East ⫴ Total Africa ▩ Total Asia Pacific
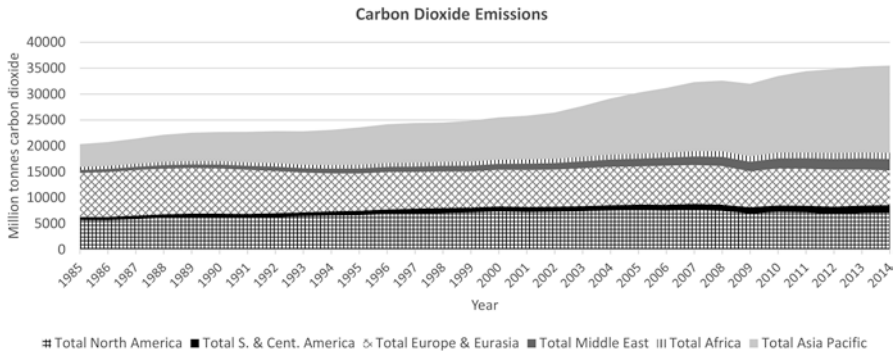
Fig. 1.12 Escalation of carbon dioxide emissions in a short period 1985–2014. Source: BP Statistical Review, 2015

In order to assess information concerning climate change, the Intergovernmental Panel on Climate Change (IPCC) was established as a scientific intergovernmental body under the auspices of the United Nations by two United Nations organizations, the World Meteorological Organization (WMO) and the United Nations Environment Programme (UNEP) in 1988. The IPCC is an internationally accepted authority and provides reports that support United Nations Framework Convention on Climate Change (UNFCCC). The reports are based on thousands of contributions from scientists and other experts in order to cover information relevant to understanding the risk of human-induced climate change. The 2007 Nobel Peace Prize was awarded for outstanding contributions in this field of activity to IPCC and Al Gore, an American politician and environmentalist who served as the Vice President of the United States under President Bill Clinton. A number of conferences have been held to negotiate a global agreement on reduction of climate change in the last decades. A key conference, the 2015 United Nations Climate Conference, was held in Paris at the end of 2015. The agreement calls for zero net anthropogenic greenhouse gas emissions to be reached during the second half of the twenty-first century in order to limit global warming. These suggested commitments were estimated to limit global warming to 2.7 degrees Celsius by 2100, but no detailed timetable or country-specific goals for emissions were incorporated into the Paris Agreement in comparison with the previous Kyoto Protocol. A final global agreement represented a consensus of the representatives of the 196 parties attending it. The agreement will become legally binding if joined by at least 55 countries which together produce at least 55% of global greenhouse emissions. The ratification took place in New York on April 22, 2016 (Earth Day), in a period of one year. The country-specific carbon dioxide (CO_2) emission totals of fossil fuel use and industrial processes (excluding short-cycle biomass burning such as agricultural waste burning, and large-scale biomass burning such as forest fires) are managed by the European Union in the Emission Database for Global Atmospheric Research (EDGAR). A comparison between emission totals in 1970 and 2013 for the top 25 CO_2-emitting countries (with population more than 1 million) extended by the top 100 CO_2-emitting countries with limited displayed range 0–1 million kton CO_2 per year is illustrated in Fig. 1.13. A comparison between emission totals, which includes estimates of population for each country in 1970 and 2013, is
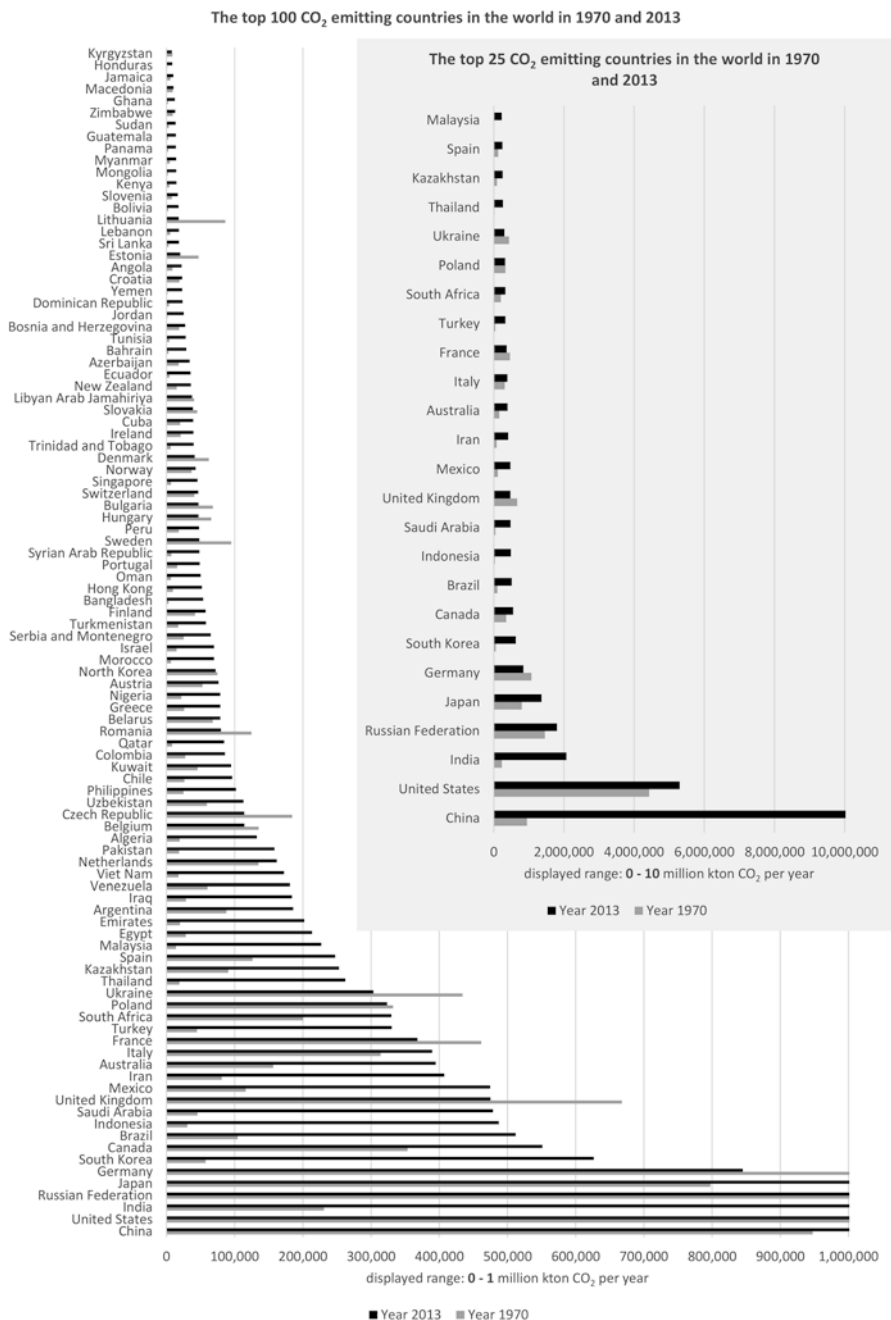
Fig. 1.13 The top 25 CO_2-emitting countries (with population more than 1 million) in the world in 1970 and 2013 extended by the top 100 CO_2-emitting countries with limited displayed range 0–1 million kton CO_2 per year. Source: EU Edgar database, 2015, UN World Population Prospects, 2015

The top 100 CO$_2$ emitting countries in the world in 1970 and 2013 per capita
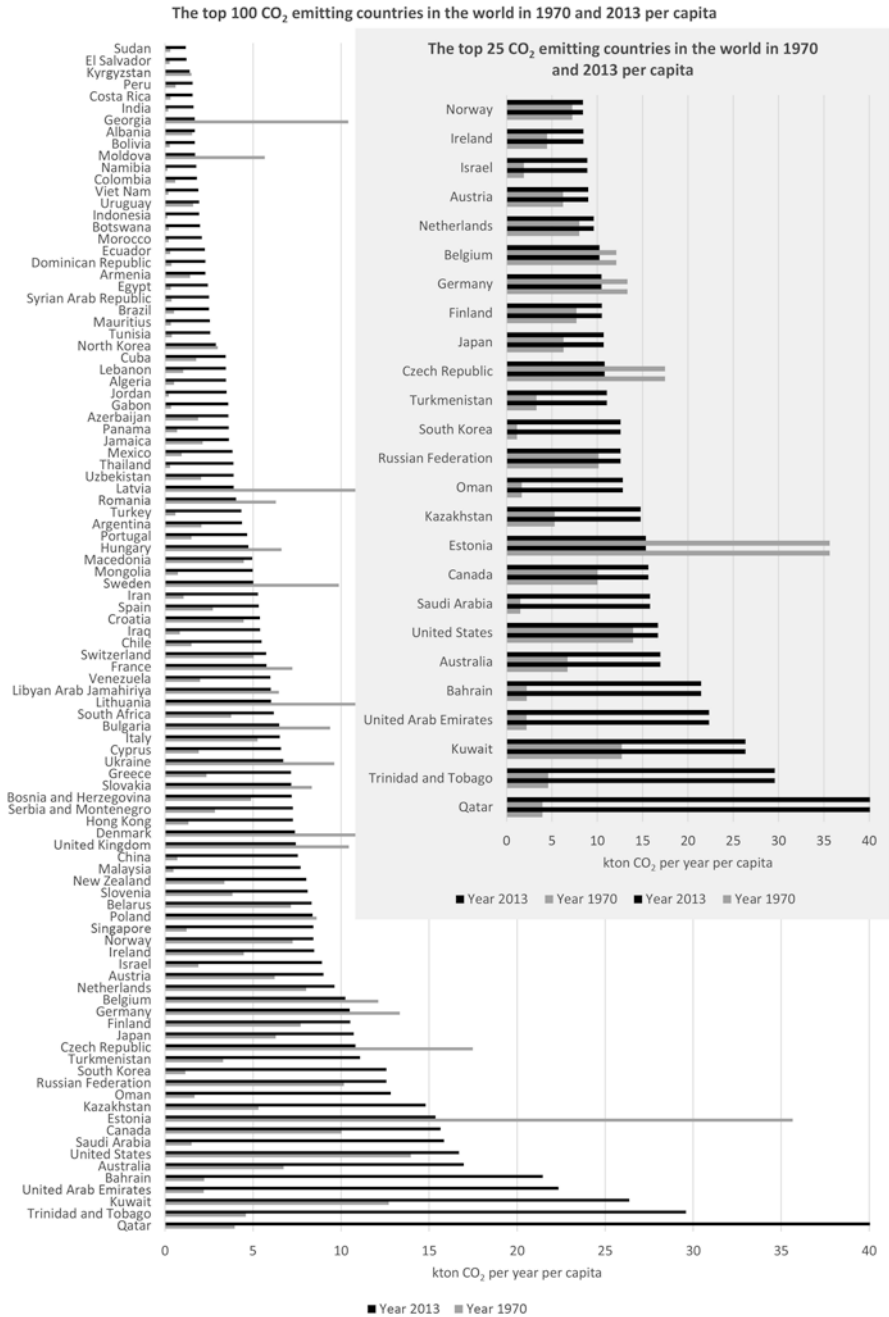
Fig. 1.14 The per capita top 25 CO$_2$-emitting countries in the world in 1970 and 2013 with population more than 1 million extended by the per capita top 100 CO$_2$-emitting countries with limited displayed range 0–1 million kton CO$_2$ per year. Source: EU Edgar database, 2015, UN World Population Prospects, 2015

illustrated in Fig. 1.14. The list and order of selected countries is changed due to recalculation of a database. Some populous countries are out of focus. Some sparsely inhabited countries with a high consumption of fossil fuels come into focus. But the total CO_2 emissions in each country are dependent on many factors such as geographic location, meteorological conditions, accessibility of fossil fuels, and industrialization.

1.6   Basic Tools for Processing and Display of Spatial and Temporal Data Dealing with Energy Assessment

The field of spatial and temporal data processing in the framework of assessment of energy sources is concerned with the exploration and prediction of patterns and processes at spatial and time scale. The spatial objects including energy sources, transport routes, consumers, and other phenomena can be described as a spatial data infrastructure. A number of various computer tools with a wide range of services can be used for this reason. They include basic computer office suites (word processors, spreadsheets, presentations tools, tools for a database management, and personal information managers), development kits for data visualization on Website, statistical programs for advance calculation and testing hypothesis, computer modeling tools using geographic information system (GIS) for complex data management and presentation, and case-oriented tools that can gain immediate insight into assessment of energy sources from a special point of view.

1.6.1   Processing Spatial and Temporal Data in Spreadsheets

Simple methods for display of spatial and temporal data arranged in tables are implemented in spreadsheets. They use a grid of cells structured in rows and columns to provide data processing such as arithmetic operations, basic statistical functions, and a wide range of optional functions. Most of them contain programming tools for development of macros. In addition to processing tools, the spreadsheets support many types of charts to display data in ways that are meaningful to the audience. The basic selection contains column, bar, line, area, surface, or radar charts. It can be extended by a variety of optional formats such as stacked column charts or pie 3D charts. Other extensions of charts are represented by combination charts such as a histogram, a box plot, and a column chart extended by a line chart. A new addition of actual versions of spreadsheets can manage basic map outputs by 3D map charts. It can plot geographical and temporal data on the Earth's surface or custom map and capture screenshots to build pictures or video. Spreadsheets can be also used as a universal tool for data input and data preprocessing. There are several ways to exchange data between spreadsheets and database systems or case-oriented tools for advanced statistical and modeling procedures. Data can be typically

exchanged by import-export functions into a wide variety of formats, shared by other programs, or simply transferred by a copy-paste functionality.

As an example from the Excel support Web pages (explore sample datasets in 3D Maps), the capacity of power stations according to an energy source in the United States is selected to demonstrate spreadsheet's capability to process data and to create tables, graphs, and 3D charts. The input dataset contains 17,635 records about the capacity of power stations in the United States. Each record gives information

Table 1.3 Capacity of power stations according to an energy source in the United States

Energy description	Energy source code	Sum of capacity (megawatts)	Number of installations	Average capacity per installation (megawatts)
Natural gas	NG	454331.5	5459	83.23
Anthracite coal, bituminous coal	BIT	186156.5	925	201.25
Subbituminous coal	SUB	132769.8	465	285.53
Nuclear (uranium, plutonium, thorium)	NUC	106147.3	104	1020.65
Water (conventional, pumped storage)	WAT	98068.3	4124	23.78
Residual fuel oil	RFO	31272.9	146	214.20
Distillate fuel oil	DFO	28481.4	3431	8.30
Wind	WND	24979.5	494	50.57
Lignite coal	LIG	14786.2	29	509.87
Black liquor	BLQ	4472.7	170	26.31
Geothermal	GEO	3280.5	228	14.39
Wood/wood waste solids	WDS	3178.5	179	17.76
Municipal solid waste	MSW	2671.0	96	27.82
Waste/other coal	WC	2162.1	25	86.48
Petroleum coke	PC	1719.1	26	66.12
Landfill gas	LFG	1532.0	1204	1.27
Other gas	OG	1267.6	69	18.37
Blast furnace gas	BFG	994.3	33	30.13
Solar (photovoltaic, thermal)	SUN	539.0	89	6.06
Jet fuel	JF	512.3	73	7.02
Purchased steam	PUR	475.7	23	20.68
Agriculture crop	AB	374.6	20	18.73
Oil – other	WO	86.7	39	2.22
Wood waste liquids	WDL	79.0	4	19.75
Other biomass solid	OBS	78.6	3	26.20
Tires	TDF	53.3	2	26.65
Other biomass liquid	OBL	17.8	5	3.56
Sludge waste	SLW	6.5	1	6.50

Source: Excel 3D Maps sample dataset

Sum of Capacity (Megawatts)
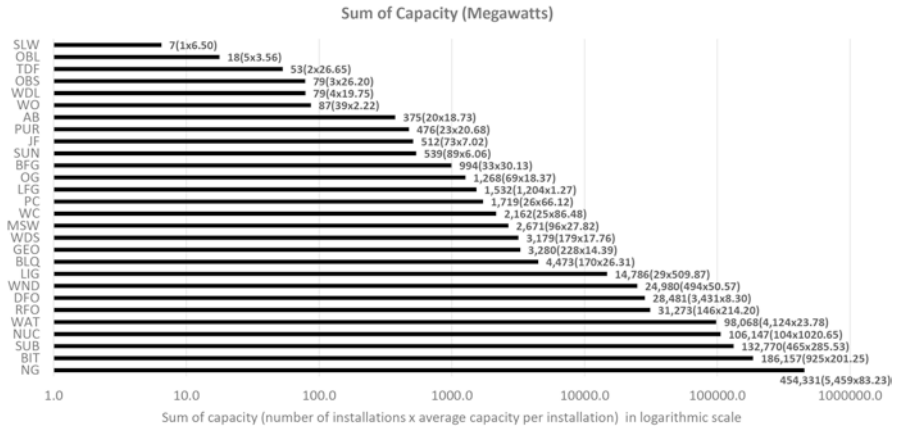
Fig. 1.15 Summarized records of power station capacities by type of energy source complemented by a number of installations and an average capacity per installation in the parenthesis. Source: Excel 3D Maps sample dataset

about company, plant name, capacity in megawatts, energy source code, initial date of operation, and energy description. Table 1.3 quotes figures concerning a sum of capacity, a number of installations, and an average capacity per an installation for each type of an energy source. The SUMIF, COUNTIF, and AVERAGEIF functions are used to sum, count, and average the values in a range of specified criteria. In this example, the criteria are applied to a range of the energy source code, and the conditional functions SUMIF and AVERAGEIF are applied to a range of a capacity in megawatts. Figure 1.15 shows simple bar charts with summarized records of power station capacities by type of energy source complemented by information about a number of installations and an average capacity per installation. It indicates the domination of energy sources supplied by fossil fuels such as natural gas and coal. These fossil energy sources are followed by nuclear energy sources and hydropower. Based on the records and displayed outputs, renewable energy sources still play a complementary role in the energy supply. There are a high number of natural gas power stations, waterpower stations, and distillate fuel oil installations in the United States. In accordance with presumption, the highest average capacity per installation indicates the nuclear power plants. Figure 1.16 demonstrates a new spreadsheet capability dealing with 3D map charts. Excel 2016 3D Maps, a fully integrated 3D geospatial visualization tool, is used for display of capacity of power stations according to the energy source in the United States. The 3D bars show the capacity of power stations in dependence on energy sources and sites on the map. The relationship between geographical locations and their associated data shows heterogenic distribution of the capacity, which is dependent on local energy resources. Solid fossil fuels can be transported at long distances by railroad, which allows to move power stations near to the energy consumers and to operate high-capacity power stations. On the other hand, renewable energy sources are highly dependent on the local conditions, which determine their location. Natural gas and oil power

Fig. 1.16 Mapping of power stations according to an energy source in the United States. Source: Excel 3D Maps sample dataset

stations have a high number of installations with a low capacity per installation and are relatively evenly distributed across the whole area near the local consumers.

1.6.2   Development Kits for Data Visualization on Website

An easy accessible way on how to visualize data is represented using Google Charts with a simple JavaScript that is embedded in the Web page. Charts are exposed as JavaScript classes that can be customized to fit the best look. During visualization, the charts are rendered using HTML5/SVG technology to provide cross browser compatibility and cross platform portability to various operating systems including mobile platforms such as phones and tablets. Google Charts provides a wide range of charts from simple line charts to complex map charts. Most charts are accessible in the chart gallery as ready-to-use chart types. As an example from the Google Developers' Web pages, the geocharts are used to display maps of primary energy consumption in 1985 and 2014 with the region mode that colors whole regions of the selected countries. In comparison with a published example in the gallery, the code in JavaScript is slightly customized in order to insert data in the helper function *arrayToDataTable* that creates and populates *DataTable* using single cells (Table 1.4). The names of data columns are specified in the header (*['Country', 'MTOE']*) and the data columns are entered in the following lines containing five selected countries with the highest primary energy consumptions in 1985 (*['United States', 1756], ['Russia', 819], ['China', 530], ['Japan', 372], ['India', 133]*).

Table 1.4 The code for display of primary energy consumptions with geocharts
Source: BP Statistical Review 2015

```
<html>
  <head>
    <script type="text/javascript" src="https://www.gstatic.com/charts/loader.js"></script>
    <script type="text/javascript" src="https://www.google.com/jsapi"></script>
    <script type="text/javascript">
      google.charts.load('current', {'packages':['geochart']});
      google.charts.setOnLoadCallback(drawRegionsMap);
      function drawRegionsMap() {
        var data = google.visualization.arrayToDataTable([
          ['Country', 'MTOE'],
          ['United States', 1756],
          ['Russia', 819],
          ['China', 530],
          ['Japan', 372],
          ['India', 133]
        ]);
        var options = {
          colorAxis: {colors: ['yellow', 'red']}
        };
        var chart = new google.visualization.GeoChart(document.getElementById('regions_div'));
        chart.draw(data, options);
      }
    </script>
  </head>
  <body>
    <div id="regions_div" style="width: 900px; height: 500px;"></div>
  </body>
</html>
```

The display of geocharts in a Web browser environment is illustrated in Fig. 1.17. Maps of the primary energy consumption in million tonnes of oil equivalent in 1985 and 2014 are displayed for 67 countries. The script options can show the primary production consumption as a range of colors and the remaining countries as grey shades.

1.6.3 Statistical Programs

Statistical programming tools are specialized computer programs for statistical analysis that include a variety of extensions such as data mining procedures, predictive modeling, clustering, classification, exploratory techniques, neural networks, and advanced data visualization options. Statistical methods can help to collect, organize, analyze, and interpret data. In standard statistical research, datasets are organized in tables that are used to explore the relationship in dependence on defined hypothesis. But many case-oriented statistical tools have been created over the last decade to improve existing methods and create new more complex data processing tools. For example, exploratory data analysis (EDA) offers an interactive view on data by using advanced visualization functions of high-resolution computer graphics. Complex automated analysis includes data mining, multivariate statistics, and neural nets. Each statistical software has been extended by development tools in order to create case-oriented data processing extensions to existing environment that can be optimized on a specific field of study. Statistical programs have been
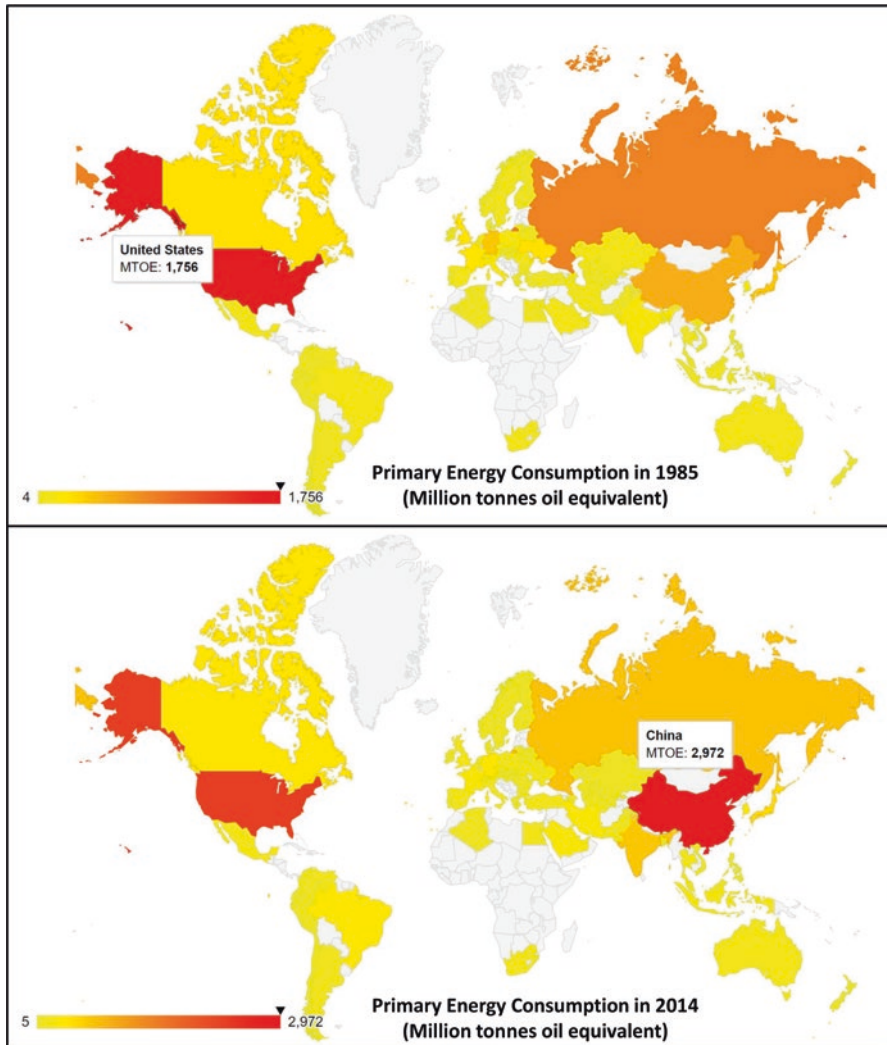
Fig. 1.17 Display of the primary energy consumption in 1985 and 2014 with geocharts. The script options (colorAxis) show the primary production consumption as a range of colors from yellow to red. Source: BP Statistical Review, 2015

complemented by a wide range of graphs that can better interpret output of statistical methods.

As an example, data about primary energy consumption (TOE – tonnes of oil equivalent) per capita, recalculated carbon dioxide emissions (tonnes of CO_2) per capita, and HDI (Human Development Index) in 2013 for 63 countries, which are dominant in primary energy consumption, are displayed in Table 1.5. The countries are sorted in descendent order of primary energy consumption per capita in order

Table 1.5 Primary energy consumption per capita (TOE – tonnes of oil equivalent), carbon dioxide emissions per capita (tonnes), and Human Development Index (HDI) for 63 countries sorted in descendent order of primary energy consumption per capita

n	Country (1–21)	TOE	CO_2	HDI	n	Country (21–42)	TOE	CO_2	HDI	n	Country (43–63)	TOE	CO_2	HDI
1	Qatar	22,01	40,27	0,85	22	Japan	3,70	10,71	0,89	43	Argentina	2,04	4,37	0,83
2	Singapore	13,76	8,43	0,91	23	Switzerland	3,69	5,75	0,93	44	Chile	1,96	5,49	0,83
3	Kuwait	10,84	26,37	0,82	24	Kazakhstan	3,20	14,80	0,79	45	Lithuania	1,91	6,02	0,84
4	United Arab Emirates	10,83	22,35	0,83	25	Denmark	3,18	7,38	0,92	46	Thailand	1,75	3,89	0,72
5	Canada	9,49	15,65	0,91	26	Iran	3,16	5,28	0,76	47	Uzbekistan	1,73	3,89	0,67
6	Norway	8,87	8,43	0,94	27	United Kingdom	3,14	7,43	0,90	48	Romania	1,65	4,04	0,79
7	Saudi Arabia	7,37	15,85	0,84	28	Slovakia	3,11	7,17	0,84	49	Turkey	1,60	4,33	0,76
8	United States	7,16	16,70	0,91	29	Israel	3,08	8,92	0,89	50	Mexico	1,55	3,84	0,75
9	Belgium	5,47	10,25	0,89	30	Malaysia	3,08	7,70	0,78	51	Brazil	1,41	2,51	0,75
10	South Korea	5,43	12,57	0,90	31	Belarus	2,98	8,33	0,80	52	Azerbaijan	1,33	3,60	0,75
11	Australia	5,42	16,97	0,93	32	Spain	2,88	5,32	0,87	53	Algeria	1,26	3,47	0,73
12	Sweden	5,33	5,01	0,91	33	Venezuela	2,83	5,98	0,76	54	Egypt	0,98	2,44	0,69
13	Netherlands	5,14	9,63	0,92	34	Italy	2,64	6,52	0,87	55	Ecuador	0,94	2,26	0,73
14	Turkmenistan	5,12	11,08	0,68	35	Ukraine	2,58	6,72	0,75	56	Colombia	0,79	1,81	0,72
15	Finland	4,97	10,52	0,88	36	Poland	2,55	8,38	0,84	57	Peru	0,73	1,56	0,73
16	Russia	4,81	12,58	0,80	37	Greece	2,53	7,15	0,86	58	Indonesia	0,68	1,94	0,68
17	New Zealand	4,45	8,02	0,91	38	Portugal	2,38	4,67	0,83	59	Vietnam	0,60	1,89	0,66
18	Germany	4,04	10,49	0,92	39	South Africa	2,31	6,17	0,66	60	India	0,47	1,62	0,60
19	Austria	4,01	9,00	0,88	40	Bulgaria	2,30	6,48	0,78	61	Pakistan	0,40	0,87	0,54
20	Czech Republic	3,94	10,82	0,87	41	China	2,13	7,55	0,72	62	Philippines	0,33	1,04	0,66
21	France	3,87	5,77	0,89	42	Hungary	2,08	4,73	0,83	63	Bangladesh	0,17	0,34	0,57

Source: BP Statistical Review 2015; EU Edgar database, 2015; UN World Population Prospects, 2015

Table 1.6 Descriptive statistics: primary energy consumption per capita (TOE – tonnes of oil equivalent), carbon dioxide emissions per capita (tonnes), Human Development Index (HDI), population density, and country area for 63 countries

Variable (number of countries: $n = 63$)	Mean	Minimum	Maximum	Standard deviation
TOE (tonnes of oil equivalent) per capita	3.75	0.17	22.01	3.61
CO_2 (tonnes) per capita	7.95	0.34	40.27	6.55
HDI	0.80	0.54	0.94	0.10
Population density (per km²)	257	3	7755	975
Area (km²)	1,566,460	697	17,098,242	3,153,217

Source: BP Statistical Review, 2015; EU Edgar database, 2015; UN World Population Prospects, 2015
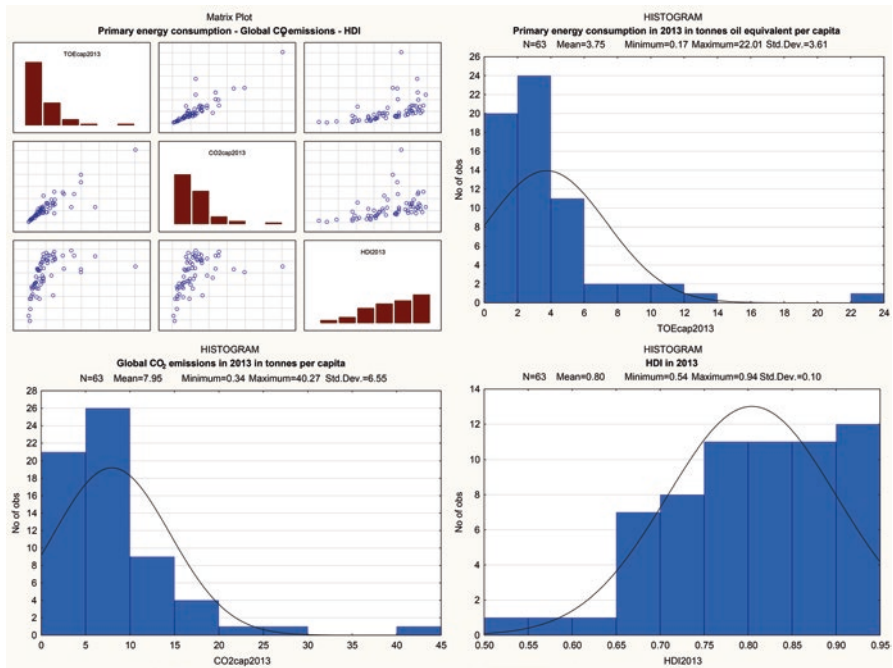
Fig. 1.18 A matrix graph and three histograms that illustrate relationship between primary energy consumption per capita (TOE – tonnes of oil equivalent), carbon dioxide emissions per capita (tonnes), and Human Development Index (HDI). Source: BP Statistical Review, 2015; EU Edgar database, 2015; UN World Population Prospects, 2015

to illustrate the highest consumers in the world. Conversion of original values of consumption and emissions to values per capita enables comparison between populous countries and densely populated countries. The basic descriptive statistics for these variables complemented by population density and country area is

shown in Table 1.6 that shows a high range of values for the population density and the country area. The relationship between these variables is illustrated in Fig. 1.18 with matrix plots that summarize the relationships between selected variables. There is a significant relationship between the primary energy consumption per capita and the carbon dioxide emissions per capita. The relationship between HDI and other variables is less evident. The histograms of frequency distribution of the respective variables are plotted on the diagonal and attached plots. The matrix plots in the form of the scatter matrix can be also considered the graphic equivalent of the correlation matrix, which gives the quantification of relationships by correlation coefficients.

Bibliography

Andrews, J., & Jelley, N. (2013). *Energy science: Principles, technologies, and impacts* (2nd ed.). New York: Oxford University Press.

Aubrecht, G. J. (2005). *Energy: Physical, environmental, and social impact* (3rd ed.). San Francisco: Prentice Hall.

Da Rosa, A. V. (2012). *Fundamentals of renewable energy processes* (3rd ed.). Amsterdam: Elsevier Science.

Dincer, I., & Zamfirescu, C. (2012). *Sustainable energy systems and applications* (2012th ed.). Oshawa, ON: Springer.

Editors of Scientific American. (2013). *The future of energy: Earth, wind, and fire*. New York: Scientific American.

Eisen, J., Hammond, E., Rossi, J., Spence, D., Weaver, J., & Wiseman, H. (2015). *Energy, economics and the environment (University Casebook Series)* (4th ed.). Goleta, CA: Foundation Press.

Fay, J. A., & Golomb, D. S. (2011). *Energy and the environment* (2nd ed.). New York: Oxford University Press.

Hazen, R. M. (2013). *The story of earth: The first 4.5 billion years, from stardust to living planet* (1st ed.). London: Penguin Books.

Hicks, T. (2011). *Handbook of energy engineering calculations* (1st ed.). New York: McGraw-Hill Education.

International Institute for Applied Systems Analysis: GEA Team (2012). *Global energy assessment* (1st ed.). Cambridge: Cambridge University Press.

May, B., Moore, P., & Lintott, C. (2013). *Bang!: The complete history of the universe* (4th ed.). London: Carlton Books.

Randolph, J., & Masters, G. M. (2008). *Energy for sustainability: Technology, planning, policy* (1st ed.). Washington, DC: Island Press.

Seagrave, W. (2012). *History of the universe* (1st ed.). London: Penny Press.

Smil, V. (2007). *Energy in nature and society: General energetics of complex systems* (1st ed.). Cambridge: MIT.

Smil, V. (2012). *Harvesting the biosphere: What we have taken from nature* (1st ed.). Cambridge: MIT.

Tester, J. W., Drake, E. M., Driscoll, M. J., Golay, M. W., & Peters, W. A. (2005). *Sustainable energy: Choosing among options* (1st ed.). Cambridge: MIT.

Vanek, F., & Albright, L. (2012). *Energy systems engineering: Evaluation and implementation* (2nd ed.). New York: McGraw-Hill Education.

Dictionaries and Encyclopedia

Cleveland, C. J., & Christopher, G. M. (2009). *Dictionary of energy: Expanded edition* (1st ed.). Amsterdam: Elsevier.

Encyclopaedia Britannica. Retrieved from www.britannica.com

Wikipedia. Retrieved from www.wikipedia.org/

Data Sources (Revised in September, 2016)

BP (British Petroleum). (2015). *Statistical review of world energy*. Retrieved from www.bp.com/en/global/corporate/energy-economics/statistical-review-of-world-energy.html

Data Distribution Centre (DDC) of the Intergovernmental Panel on Climate Change (IPCC). Retrieved from www.ipcc-data.org

Emissions Database for Global Atmospheric Research (EDGAR). Retrieved from edgar.jrc.ec.europa.eu

EPA's Environmental Dataset Gateway (EDG). Retrieved from edg.epa.gov/metadata/catalog/main/home.page

European Commission. *Energy statistical pocketbook*. Retrieved from ec.europa.eu/energy/en/statistics/energy-statistical-pocketbook

European Commission. *Energy strategy*. Retrieved from ec.europa.eu/energy/en/topics/energy-strategy

European Environment Agency. *Data and maps*. Retrieved from www.eea.europa.eu/data-and-maps

European Environment Agency. (2015). *The European environment—State and outlook*. Retrieved from www.eea.europa.eu/soer-2015/synthesis

International Energy Agency. *Statistics*. Retrieved from www.iea.org/statistics/

United Nations, Department of Economic and Social Affairs, Population Division. *World population prospects, the 2015 revision*. Retrieved from esa.un.org/unpd/wpp

United Nations, Human Development Reports. (2015). *Human development statistical tables*. Retrieved from hdr.undp.org/en/data

U.S. Department of Agriculture, Agricultural Research Service. *Nutritive value of foods, home and garden bulletin No. 72* (HG-72). Retrieved from www.ars.usda.gov/Main/docs.htm?docid=6282

U.S. Department of Energy (DOE). *Open energy data*. Retrieved from energy.gov/data/open-energy-data

U.S. Energy Information Administration (EIA). *Maps*. Retrieved from http://www.eia.gov/maps/

U.S. Energy Information Administration (EIA). *Open data*. Retrieved from www.eia.gov/open-data/index.cfm

Chapter 2
Spatial and Temporal Analysis
for Energy Systems

In this book, the concepts and procedures for assessment of energy systems are discussed in order to apply a number of spatial and temporal analyses with geographic information system (GIS). In addition to digital mapping, GIS can change the way of viewing our Earth's resources in a more complex way by integrating data from remote sensing, GPS, and a wide range of databases. Many GIS packages are freely available as open software or as commercial software broadly used in industry, government, and academia. This chapter introduces some fundamental concepts that are dealt with in next chapters. After identifying certain open issues in spatial and temporal analysis, a case-oriented approach is proposed for assessment of energy sources including nonrenewable sources and renewable sources with their temporal dynamics and spatial patterns. Also presentation of new GIS technologies will discuss the strengths and weaknesses, along with the opportunities and limitations of using GIS methods for wide-ranging applications in assessment of energy sources.

2.1 Energy Sources and Energy Consumption in the Scale of the Earth

The field of digital mapping systems is concerned with the exploration, description, explanation, and prediction of patterns and processes at geographic scales on the Earth's surface, which is illustrated by Earth's surface imageries in Figs. 2.1 and 2.2 that combine many satellite images to produce cloud-free views of the landscape.

The Earth's surface is mostly covered by water with much of the continental shelf below sea level. It represents about 361 million km^2, which is about 70.8% of the whole Earth's surface. The remaining 149 million km^2 (29.2%) consists of mountains, deserts, plains, and other landforms. About 97.5% of the water is saline. The remaining water (2.5%) is fresh with about 68.7% in ice caps and glaciers. Natural resources are available in the whole world, but the accessibility is dependent on many natural, economic, political, and social factors. Based on the Earth's
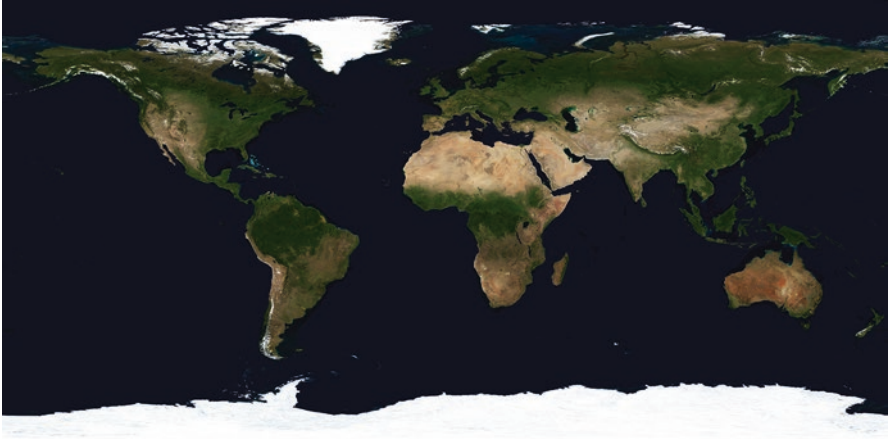
Fig. 2.1 The Earth's surface. Source: www.pixabay.com, 2016
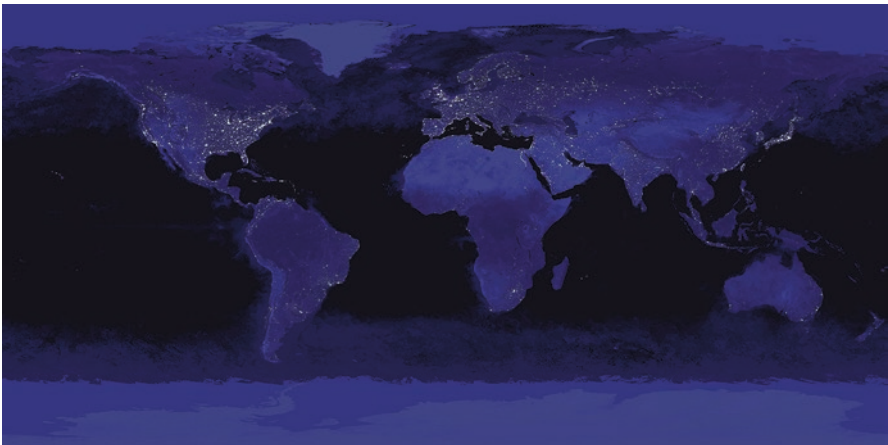
Fig. 2.2 The Earth's surface at night. Source: www.pixabay.com, 2016

surface, we can classify biotic natural resources such as forests and potentially the animals, which are obtained from the biosphere. But they represent just a part of actual, potential, or reserve resources that also include widely used fossil fuels formed from decayed organic matter.

The Earth's surface at night is very helpful for observation of spatial distribution of human activities that are mostly in the sites with easy living, plentiful resources, kindly climate, and rich harvest. The brightest areas are generally the most urbanized but not necessarily the most populated sites. Most major cities are near transportation networks, which are along coastlines and near rivers. Areas with more lights are usually more economically developed, because electricity is widely used to keep production, business in thriving cities or countries. Poor areas may have
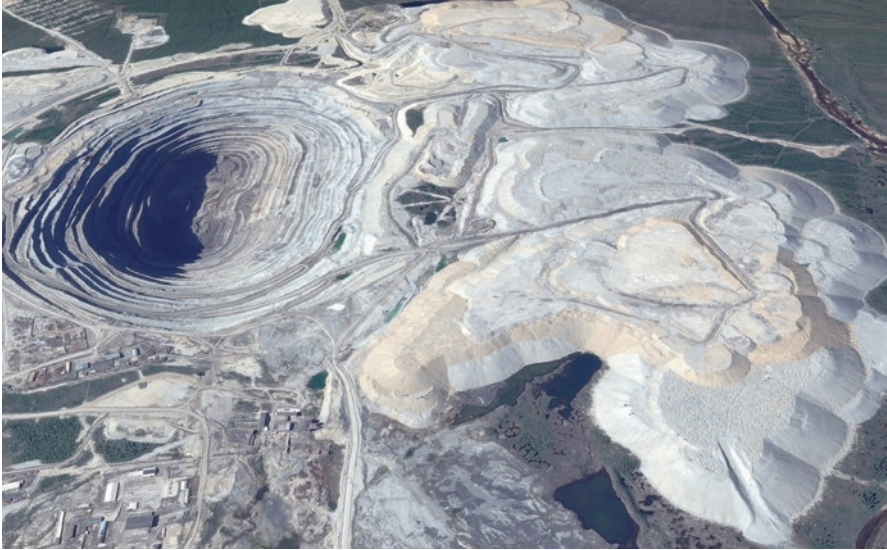
Fig. 2.3 An open-pit diamond mine in Siberia, Udachnaya pipe. Source: Google Earth, 2016

probably lower usage of electric lights to conserve money. Initial studies show that these satellite images complemented by topographic data and thematic maps can approximately estimate the economic state of certain regions.

In a local scale, more detailed view of human activities is identified with satellite images and aerial photographs. Extractive industries represent a large growing activity that cause depletion of natural resources resulting in losses of ecosystem services of many countries. They are, along with agriculture, the basis of the primary sector of economy. Apparent depletion of natural resources is directly caused by mining, petroleum extraction, forestry, as well as changes in demography, economy, and politics. As an example of a nonrenewable natural resource, an open-pit diamond mine in Siberia, Udachnaya pipe, is illustrated in Fig. 2.3.

2.2 Spatial Data Models in GIS

Our interaction with objects on the Earth's surface is diverse and can be described in many ways. Consider the first example, energy sources that include coal mines, oil wells, or renewable sources of energy such as wind power plants, solar power plants, and biogas stations. They are used for our energy supply, delimit land cover or administrative areas, and are an important feature in the shape of a surface. There are many ways how to describe energy sources in spatial modeling. Larger objects such as surface mines can be delineated by polygons that are formed by a set of lines that enclose an area. Smaller objects such as oil wells or individual installations of renewable sources can be marked with point symbols. Consider the second example,

Fig. 2.4 Manhattan Island, bounded by the East, Hudson, and Harlem Rivers in the state of New York in the United States. Source: Google Earth, 2016

transport routes that include oil pipelines, roads, railroads, water transport, or electrical power lines. They make connection between energy sources and manufacturing industry or consumers. Each route can be formed by a line that has attributes such as flow direction and flow volume. A set of routes is connected into a network that can be optimized in relation to transportation costs and transportation volume. Consider the last example, a set of consumers such as industry, transportation, and end consumers. Larger objects such as factories and residential areas are delineated by administrative boundaries that are formed with polygons. Transport lines are formed by lines. Smaller objects such as small business installations, residential buildings, and other public utilities can be marked as point symbols. An example of a complex area of interest for transformation into spatial data objects is illustrated in Fig. 2.4 that shows Manhattan, a part of New York City in the United States. The attached lines symbolized water transport, subway network, and road network.

Based on previous examples, it is evident that real objects on the Earth's surface can be represented in a variety of ways in dependence on a spatial scale and on a scope of work. The target data model has to represent an abstraction of the real world that utilizes a set of data objects in order to support map display, spatial analysis, and visualization. GIS organizes information into a series of layers that are integrated using spatial location. At a fundamental level, GIS datasets are organized as a series of thematic layers to represent and answer questions about a particular problem set, such as geology, hydrology, transportation, or environment. A simplified data model based on a few thematic map layers is illustrated in Fig. 2.5. The base map is represented by an aerial image of the area of interest. The next map layers contain a road network and central energy consumers classified in dependence on energy consumption into two thematic layers.
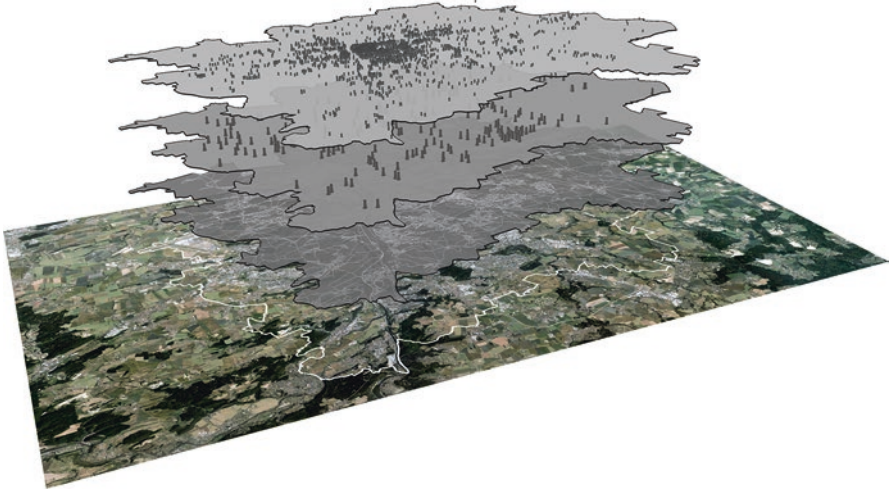
Fig. 2.5 A few thematic layers that represent a simplified data model of energy consumers in Prague (an aerial image, a road network layer, and energy consumers classified in dependence on energy consumption into two layers)
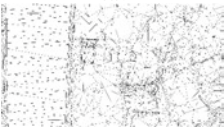
2.2.1   Representing of Spatial Data with Vectors

Vector data can represent the shapes of features precisely and compactly with associated attributes in dependence on the precision of an ordered set of coordinates. The vector representation supports geometric operations dealing with calculating length and area and set operations and finding other features that are spatially related. In a simplified way, vector data classified by dimension are represented by points, lines, polygons, and, optionally, annotations. An annotation is associated with each feature and represented by a label for display of attributes or their compositions. In real applications, labels can contain name of site, sustained yield of energy source, or transport capacity. The vector datasets are stored in dependence on their dimension and relationships in a feature container, which manage vector spatial objects and nonspatial objects and their relationships based on defined rules. In GIS, the vector layers are used to be stored in shapefiles or geodatabases (Table 2.1).

Points are zero-dimensional shapes representing spatial features too small in a selected scale to be depicted as lines or areas. Points are stored in the GIS datasets as single *x-y* coordinates with attributes. Point layers can model locations of oil wells, locations of underground mines, and installations of power plants in energy systems.

Lines are one-dimensional shapes that represent spatial features too narrow to depict as areas. Lines are stored in the GIS datasets as a series of ordered *x-y* coordinates with attributes. The segments of a line can be straight or shaped by defined functions. Line layers are used for modeling of transport networks, electrical power energy distribution, and distribution piping in energy systems.

Table 2.1 Spatial data representations in the GIS

	Vector data	Raster data	TIN
Purpose of use	-vector data are used for mapping of discrete features with precise shapes and boundaries.	-raster data are used for mapping of continuous phenomena, and satellite or aerial images.	-triangulated datasets are used for mapping of a surface that mostly represents elevation.
Source of data	-digitized from map manuscripts, raster data, satellite images or aerial photographs, -collected from GPS receivers, -contours from DEM, -imported from other software tools.	-satellite images or aerial photographs, scanned blueprints and photographs, -converted from DEM, -rasterized from vector data, -outputs of raster algebra and other complemented software tools.	-outputs of 3D tools for building of DEM, -converted from other software tools dealing with construction and editing of DEMs.
Spatial storage	-points stored as x, y, (z) coordinates, -lines stored as paths of connected x, y, (z) coordinates, -polygons stored as closed paths.	-each cell is located by its row and column position from a coordinate in the lower-left corner of the raster and cell height and width, -rasters that are combined to form a multiband image are numbered.	-each node in a triangle face has an x, y, (z) coordinate value.
Feature representation	-points represent small features in a given spatial scale, -lines represent features with a length but small width in a given spatial scale, -polygons represent features that span an area.	-points features are represented by a cell, -line features are represented by a string of adjacent cells with common value, -polygon features are represented by a region of cells with common value.	-node z values determine the shape of a surface, -breaklines determine changes in the surface such as ridges or streams, -areas of exclusion define polygons with the same elevation such as lakes or broad rivers.
Topological association	-line topology keeps track of which lines are connected to a node, -polygon topology keeps track of which polygons are to the right and left side of a common line.	-neighboring cells can be simply located by incrementing and decrementing row and column values.	-each triangle is associated with its neighboring triangles.
Spatial analysis	-topological map overlay, -buffer generation and proximity, -spatial and logical queries, -address geocoding, -network analysis.	-spatial coincidence, -proximity, -surface analysis, -dispersion, -least-cost path, -spatial interpolation.	-elevation, slope, aspect calculations, -volume estimation, -vertical profiles on alignments, -viewshed analysis.
Map output	-best for drawing the precise position and shape of point, line and polygon features, -not well suited for continuous phenomena or features with indistinct boundaries.	-best for presenting images and continuous phenomena with gradually varying attributes, -not well suited for precise drawing point and line features.	-well suited for rich presentation of surfaces, -color display can show elevation, slope, or aspect in 2D or 3D perspective.

Polygons are two-dimensional shapes that represent plane features. Polygons are stored in the GIS datasets as a series of segments that form a set of closed areas. Polygon layers model large-sized objects such as land cover structures, administrative units, and borders of towns. In mapping of energy systems, polygons can be used for delineation of surface mines, sites of biomass production, and larger power plant installations.

2.2.2 Representing of Spatial Data with Raster Datasets

Much of data are captured from aerial and satellite images that record data as pixel values in a two-dimensional grid. The two-dimensional grids can be arranged into three-dimensional grid comprised of spatial dimension in the x and y coordinates and spectral data or thematic data in the z coordinate (Table 2.1). In general, a pixel value stores reflectance of a part of the electromagnetic spectrum captured from aerial or satellite images. It can also store a thematic attribute such as land cover type, elevation, or other surface values. The grid layers are used to be stored in a wide range of various raster formats such as TIFF (Tag Image File Format), BMP (bitmap image file) or JPEG (Joint Photographic Experts Group). In case of GIS datasets, grid layers need to be embedded with georeferencing data that include spatial localization and additional information about map projection. Thus, more specific raster formats must be used such as GeoTIFF, IMG-ERDAS IMAGINE, and Multi-resolution Seamless Image Database (MrSID) developed by LizardTech. Three-dimensional grid data can be also stored in the mentioned extended raster formats. Besides these raster formats, the band-sequential (BSQ), band-interleaved-by-line (BIL), and band-interleaved-by-pixel (BIP) are used for data exchange between GIS and other advanced computer modeling tools.

2.2.3 Representing of Spatial Data with Triangulated Irregular Network

A triangulated irregular network (TIN) is designed for surface models in GIS. It is represented by a set of nodes with elevations and triangles with edge. TIN is widely used for surface analysis such as delineation and estimates of slope, aspect, and visibility. It can also depict the relief of terrain (Table 2.1).

2.2.4 Other Data Structures in Spatial Models

Many common spatial tasks deal with finding a location or an address. Thus, spatial models have to manage these locators and allow to create features for locations. Other distinctions between prevalent information systems and GIS are represented

by sharing a common coordinate system and topological associations, which enables to create spatial relationships between spatial objects, geometric networks for modeling of linear systems such as transport networks, and planar topologies model systems of line and area features as a continuous coverage of an area such as counties sharing an outer boundary with a state.

2.3   Spatial Data Types

Spatial analysis in GIS is a process for looking at spatial patterns in datasets and at relationships among them. Method and functions for spatial analysis differ in many ways. The basic difference originates from types of analyzed features: discrete or continuous. For discrete features (point locations, lines, and areas bounded by polygons), the location is pinpointed by its position and optionally by its elevation. At any given spot, the feature is either present or not. For continuous phenomena such as precipitation, temperature, or pollutant concentration, the occurrence can be measured anywhere, at any given location. Continuous data are used to be represented by raster datasets, which are represented as matrixes of cells in continuous space. Each raster is represented by a layer with one attribute. Each cell in its boundary is characterized by a value of the attribute such as precipitation, temperature, or pollutant concentration. The cell size affects the precision of mapping phenomena. Using too large a cell size will cause some information to be lost. Using too small a cell size will require a lot of storage space in order to cover the whole area of interest and will take longer processing, without adding additional precision to the map. Generally, any feature type can be represented using either model, discrete, or continuous (Fig. 2.6). While locations of discrete features are dependent on precision of coordinates, their precision after conversion into the raster datasets depends on a cell size.

Each spatial feature has attributes that contain associated information such as categories, ranks, counts, and ratios (Fig. 2.7). The categories of attributes predetermine the types of possible spatial analysis. Their data formats include integer or real numbers, strings of characters, logical values, and even multimedia files or link to them.

Categories represent features with similar properties such as categories of energy sources or transport routes. They are mostly formed as text abbreviations or numeric codes. The simple abbreviations and codes are recommended in order to reduce errors. The category attribute can support database selections and ways in which features are processed and displayed.

Ranks can express state of features or processes such as the level of source reserve or meteorological conditions. Ranks put features in order, from low to high, or in the reverse order. They are used when direct measures bring inaccurate information. For example, quantify air pollution in the surroundings of emission can be indicated by a few levels (low, middle, high, very high) instead of the local direct measures.
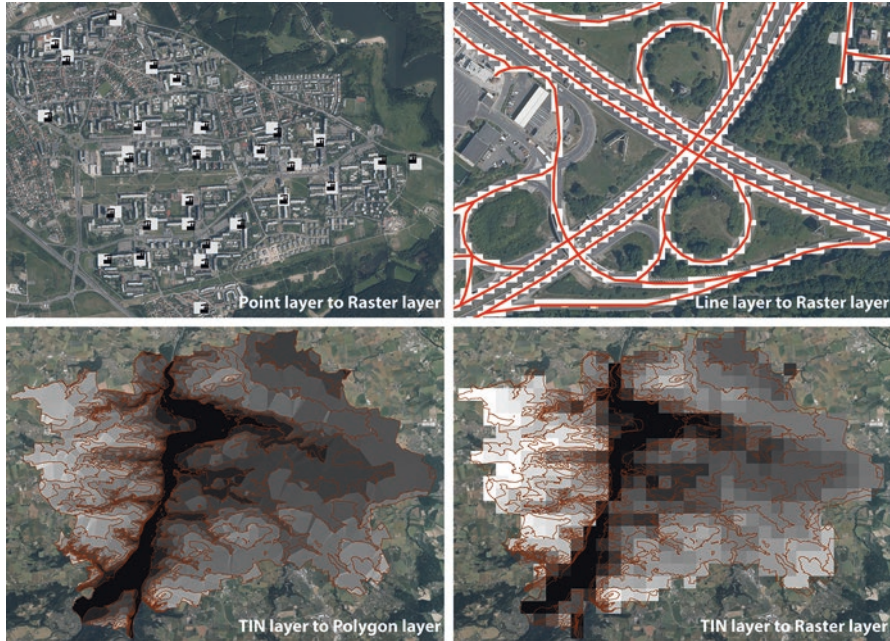
Fig. 2.6 A comparison between discrete features (location of energy systems in an urban area, roads near a crossroad, and contours complemented by DEM) and raster datasets converted from discrete features

Counts express total numbers. A number can be any measurable quantity associated with a feature such as power of a power station or consumption of a consumer. Using counts enables to see the actual value of each feature. Counts are used to be displayed in the maps by symbols with various sizes or shades. Sometimes they are transformed into the ranks in order to simplify information about amounts.

Ratios can express the relationship between two quantities such as densities that show the distribution of features per unit area. For example, dividing the number of people per area of each country gives its population density, which can better even out differences between large and small countries. Similar effects like densities can be expressed by proportions, which show what part of a total value is. For example, dividing a number of people in the selected age classes by the total population in each part of a country gives the proportions of people in this age class over the whole country.

The tables of attribute values are used to be analyzed by selection, calculating and summarizing. Selection of features is provided by using queries. The query is usually in the form of a logical expression. The subsets of features can serve for calculating and summary statistics. Calculating enables to assign new values in attribute tables such as ratios and densities or other derived characteristics of features. Summarizing of specific attributes is used to get statistics such as arithmetic average, median, modus, and standard deviation.
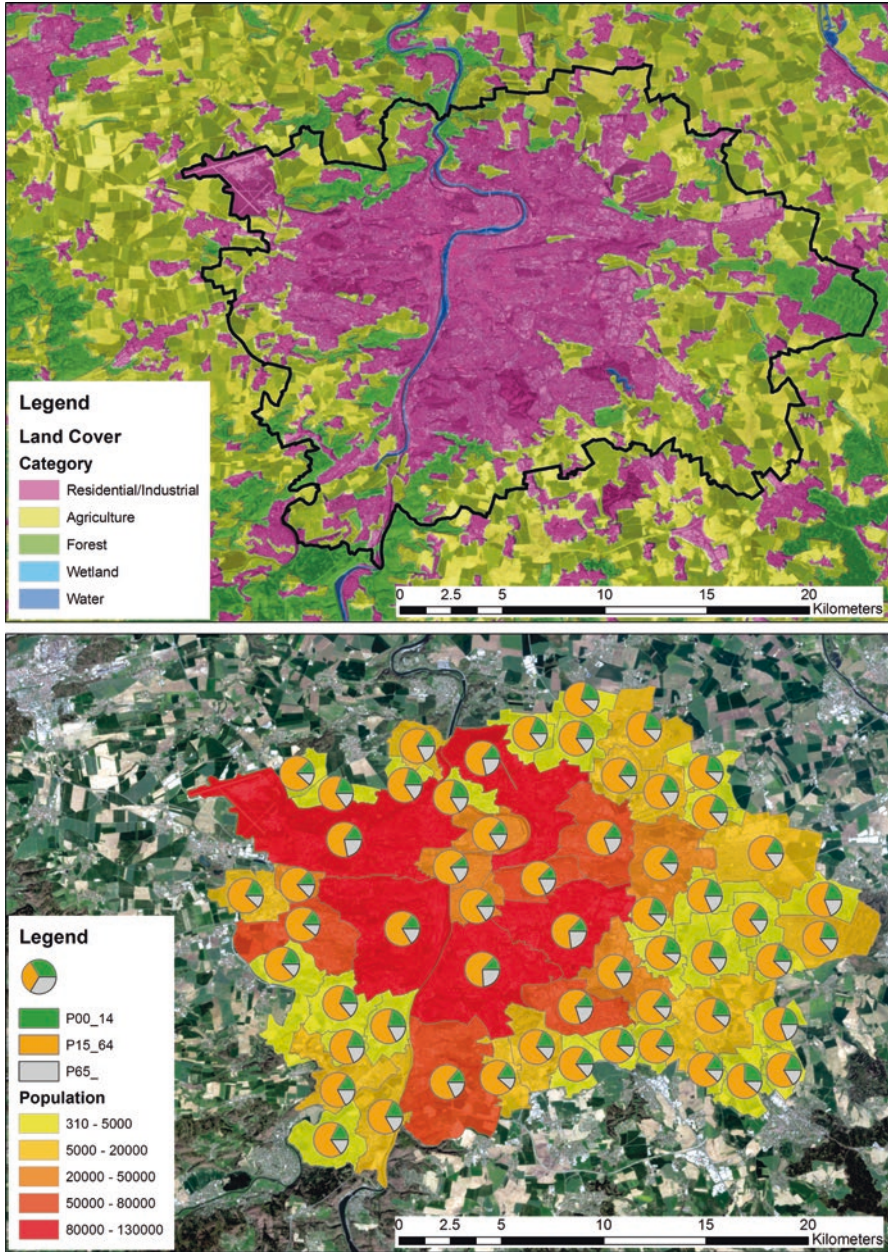
Fig. 2.7 Presentation of associated information in attributes of spatial features with categories of land cover classes, ranks of population, and counts of population classes (0–14, 15–64, 65 and higher)

2.4   Coordinate Systems

The coordinate system for spatial data provides a frame of reference in order to identify the location of features on the surface of the Earth, align data, and create maps. Dozens of map projections for displaying features from the curved surface of the Earth to a flat sheet of paper or display have been created by geodesists for a few centuries to preserve one or more specific properties of the spatial data: shape, distance, area, and direction. The shape of the Earth can be regarded approximately as a sphere, but a more accurate spatial approximation is an ellipsoid. However, the Earth's surface has irregularities above and below the approximating ellipsoid. The elevation is described with respect to a given reference datum. Once the ellipsoid and the datum are given, the location of a point is uniquely defined on the Earth's surface. Coordinates on the Earth's surface are therefore specified in terms of latitude and longitude over a reference surface and elevation above and below a datum. Elevations are used to be measured above a reference mean sea level, which gives coordinates in the framework of a geographic coordinate system (GCS). A common GCS is represented by the World Geodetic System defined in 1984 (WGS84), which has adoptions to represent region-specific data with higher accuracy in different countries.

In order to calculate lengths and areas in the local scale, the ellipsoid is approximated by a plane or another surface that can be flattened on a plane. Then the coordinates on the plane may be defined by metric distances from a reference point along two orthogonal directions. The mathematical conversion of coordinates from the ellipsoid into the corresponding coordinates on an approximating plane is called a projection. Some of the simplest projections are made onto geometric shapes that can be flattened without stretching their surface. Some examples of map projections which are widely used in GISs are shown in Table 2.2.

Thus, GISs contain geographic and projected coordinate systems that represent the world in very different ways. In geographic coordinate systems, points are referenced by their longitude and latitude values. Longitude values are measured east-west, while latitude values are measured north-south. The linear distance between two points separated by the same angular distance may differ, depending on their locations, because the reference surface is curved and lines of longitude converge at the poles. In projected coordinate systems, the Earth is simplified by mapping location on a flat surface with map projection. It has two-dimensional coordinate system with orthogonal axis. The link between geographic and projected coordinate systems involves mathematical formulas, map projection. A projected coordinate system is always dependent on definition of a geographic coordinate system, because this information is needed to properly convert locations to a projected coordinate system.

Using map datasets that were originally curved on a two-dimensional surface causes distortions in one or more of the spatial properties such as distance, area, shape, and direction. Concurrently, no map projection can preserve all these properties. Each map projection is judged by its suitability for representing a particular area of the Earth's surface from the view of preserving distance, area, shape, and direction. According to these imperfections, some map projections minimize distor-

Table 2.2 Examples of map projections which are used widely in GISs

Projection	Schema	Simplified description
Equirectangular projection (equidistant cylindrical projection)		It maps meridians to vertical straight lines of constant spacing and circles of latitude to horizontal straight lines of constant spacing. This projection is mainly used for thematic mapping, due to its distortion. It has become a standard for global raster datasets, such as Celestia and NASA World Wind.
Mercator (presented by the Flemish cartographer Gerardus Mercator in 1569)		It was the standard map projection for nautical purposes because of its ability to represent lines of constant course, as straight segments that conserve the angles with the meridians. The linear scale is equal in all directions around any point, thus preserving the angles and the shapes of small objects. It distorts the size of objects as the latitude increases from the Equator to the poles, where the scale becomes infinite. It is still used commonly for navigation.
Universal Transverse Mercator (UTM)		It divides the Earth between 80°S and 84°N latitude into 60 zones, each 6° of longitude in width. Zone numbering increases eastward to zone 60, which covers longitude 174° to 180° E. Each of the 60 zones uses a transverse Mercator projection. It is also used for the military grid reference system, which is the geocoordinate standard used by NATO militaries.
Web Mercator (Spherical Mercator or WGS 84/Pseudo-Mercator)		It is a variant of the Mercator projection that is used primarily in Web-based mapping programs. It uses the same formulas as the standard Mercator as used for small-scale maps. The Web Mercator uses the spherical formulas at all scales whereas large-scale Mercator maps normally use the ellipsoidal form of the projection.
Winkel tripel projection (Winkel III)		It is a modified azimuthal map projection of the world, one of three projections proposed by Winkel. The name "Tripel" refers to a goal of minimizing three kinds of distortion: area, direction, and distance. It is the standard projection for world maps made by the National Geographic Society and many educational institutes.
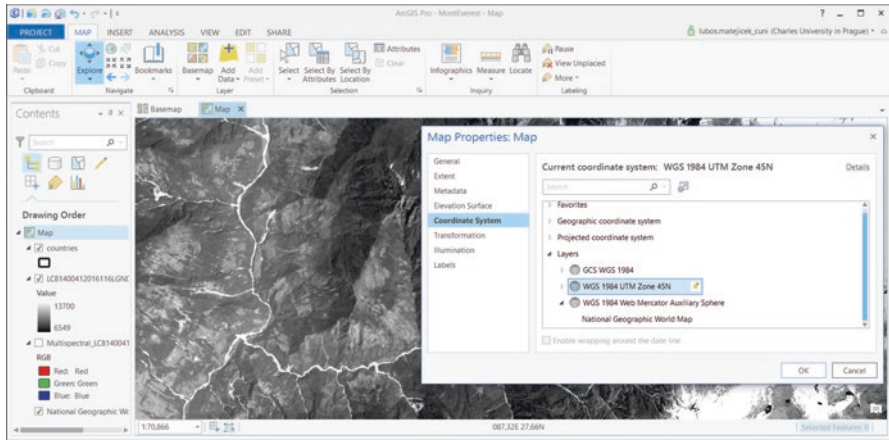
Fig. 2.8 A list of coordinate systems linked to map layers that represent: countries in the world (WGS 1984), a Landsat 8 image (UTM Zone 45 N), and a National Geographic World Map (Web Mercator Auxiliary Sphere). The map layers are preprocessed by on-the-fly projection in dependence on a projection of the first map layer on the top of a list in the table of contents (ArcGIS Pro)

tion in one property at the expense of another, while others attempt to balance the overall distortion. In comparison with projected coordinate systems, geographic coordinate systems make it easy to identify locations on a globe and contain less distortion. Projected coordinate systems offer easier to calculate spatial locations and relationships, but quantities such as distances and angles have distortions in dependence on the selected map projection.

The features in map layers with different coordinate systems cannot be displayed together, because they are transformed into different coordinates. They must be reprojected into a common coordinate system or preprocessed by on-the-fly projection, which can affect drawing performance. The datasets with a small number of simple features may display relatively quickly. The large datasets can take longer to draw. Thus, the reprojection with GIS tools is highly recommended in many cases. As an example, the GIS project in Fig. 2.8 illustrates display of a few map layers in different coordinate systems. It combines map layers in different projections preprocessed by on-the-fly projection. The map layers include countries in the world (WGS 1984), a Landsat 8 image (UTM Zone 45 N), and a National Geographic World Map (Web Mercator Auxiliary Sphere).

2.5   Spatial and Temporal Modeling in GIS

Using GIS for spatial analysis helps to find out location of spatial objects and their relationships. But GIS gets more accurate and up-to-date information, which can be extended by many methods and functions such as 3D modeling, raster map algebra,
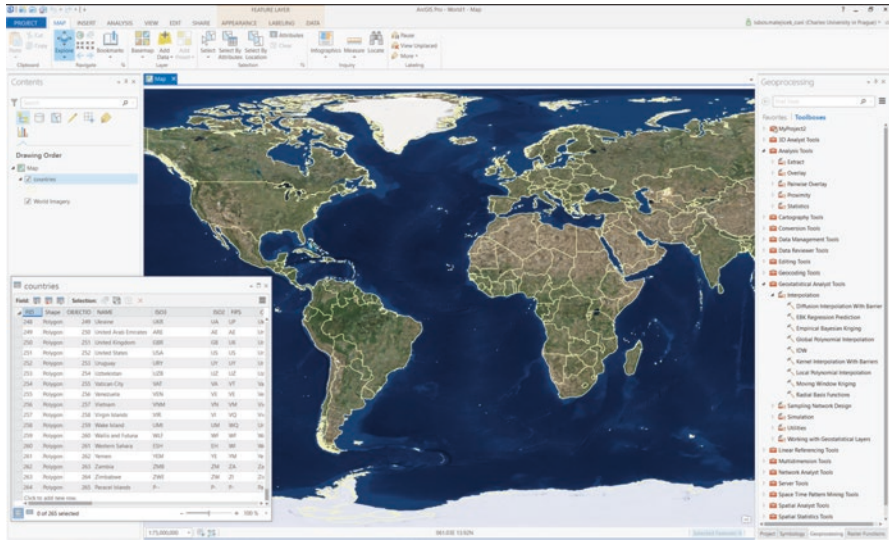
Fig. 2.9 A world map, an attribute table for the layer of countries, and an example of a list of selected groups of geoprocessing methods are displayed in the environment of ArcGIS Pro

spatial exploratory data analysis, spatial statistics, and network optimizations. As an example, a desktop image of ArcGIS Pro from ESRI is shown in Fig. 2.9. It demonstrates the rich GIS environment for spatial processing and advanced analyses. A new version of ArcGIS Pro also provides tools for visualization and analyzes and shares data in both 2D and 3D environments.

Advanced spatial processing is represented by spatial modeling, which is used to be supported by map algebra. It manages a set of raster layers that contain numerical attributes and have all exactly the same pixel size and numbers of rows and columns and are located in the same coordinates. Map algebra applies algebraic expressions for each single pixel in the same coordinates using values of individual raster layers. The results are stored in a new raster layer. For example, if the raster layer containing digital elevation model (DEM) and the raster layer of the height of buildings and infrastructure above ground are counted up, the resulting raster layer represents the digital surface model (DSM) of the area of interest (Fig. 2.10).

Besides spatial analysis described by many guidebooks, GIS can provide spatial modeling extended with temporal dynamics. Over the years, GIS has devised a limited number of ways of handling time within its data structures derived from the representation of the essentially static contents of maps. But the actual GIS can manage a number of cases that are dealing with space-time phenomena. Some tools are included in statistical methods for analyzing data distributions and patterns in the context of both space and time. For example, a new version of ArcGIS form can take time-stamped point features that are structured into Network Common Data Form (netCDF) data cube. Points are aggregating into space-time

Fig. 2.10 Raster algebra applied on building of the digital surface model (DSM) in ArcGIS Pro (ortofoto of a residential area on the left side, DEM in the middle part, and DSM on the right side; the DEM and the DSM are displayed in different elevation intervals represented by color classes in order to recognize surface objects properly)
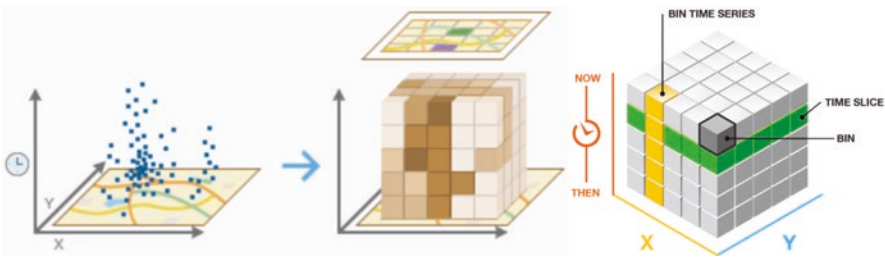
Fig. 2.11 Time-stamped point features structured into Network Common Data Form (netCDF) data cube and aggregated into space-time bins. ESRI, 2016

bins where they are counted in order to calculate summary field statistics for bin values across time at each location. It enables to examine time series trends across an area of interest (Fig. 2.11).

A typical recent approach to integration of dynamic phenomena into spatial modeling is that data are managed with GIS but processed through dedicated software tools in order to provide dynamic modeling. For example, hydrological software tools for modeling of matter flows in a river basin such as Soil and Water Assessment Tools (SWAT) are based on this architecture. The ArcGIS extension ArcSWAT represents a graphical user interface for data management in the GIS environment. After setting of input data (watershed parameters, land classes, soil properties, and meteorological data), the dedicated SWAT model starts to predict

surface water quality variables such as sediment, nitrogen, and phosphorus loadings into a system of multiple hydrologically connected watersheds. The outputs include predictions of the impacts of land management practices on surface water, sediment, and agricultural chemical yields in complex watersheds with varying hydrology, land use, soils, and management practices. Integration of dynamic models and spatial methods implemented in GIS can offer a wider range of functionality for many other decision-making tools and software applications (Fig. 2.12).

A wide range of spatial analyses implemented in GIS is described by many books, guides, and help tools inside GIS programs. A list of selected methods and functions implemented in many desktop GISs is generally presented in Table 2.3. Many methods and functions can be available through the development programming tools based on scripts that can be run in the GIS environment.

Fig. 2.12 The ArcGIS extension ArcSWAT for modeling of matter flows in a river basin such as with SWAT model (an example of a small basin with a land cover classification layer and a DEM layer on the background)

Table 2.3 A list of selected methods and functions implemented in desktop GISs

GIS functionality	List of selected methods and functions
Data management	Data creation and conversion (geodatabase, shapefile, coverage)
	Vector, raster, and TIN editing
	Projection and transformation
	Selection by location and attribute
	Archiving, data migration, and data export
Map display	Navigation
	Classification and symbolizing
	Display properties, page layout, and printing

Table 2.3 (continued)

GIS functionality	List of selected methods and functions
Spatial analysis	Set operations (clip, split, merge, union, intersect)
	Proximity methods (buffer, Thiessen polygons, point distance, polygon neighbors)
	Generalization (dissolve, eliminate)
	Summary statistics
	Vector transformation (feature to point, line, or polygon)
	Raster management (composite bands, mosaic dataset, resample, statistics)
	Relationship classes
	Sampling (random points, generate points along lines, generate tessellation with triangles, squares, or hexagons)
	Geocoding tools (create address locator, geocode and standardize addresses)
	Linear referencing tools (create routes, locate features along routes, transform route events)
	Multidimensional tools—making Network Common Data Form (netCDF) feature/raster layer
Advanced spatial analysis	Raster algebra
	Distance mapping (cost distance, Euclidian distance, path distance)
	Analyzing patterns, mapping clusters, measuring geographic distribution
	Modeling spatial relationships (exploratory regression, geographically weighted regression)
	Groundwater (Darcy flow, particle track, porous puff)
	Hydrology (flow accumulation, flow direction, stream link, stream order)
	Multivariate analysis (band collection statistics, supervised and unsupervised classifications, principal components)
	Fuzzy membership
	Solar radiation (area solar radiation, points solar radiations)
	Surface (aspect, contour generation, curvature, hillshade, observer points, slope)
	Zonal statistics
Geostatistics	Exploratory spatial data analysis
	Spatial interpolation with deterministic functions and statistical methods
Network analysis	Creating a network dataset
	Finding the best route
	Finding the closest services
	Calculating service area and origin-destination cost matrix
3D tools	DEM creation and conversion (TIN, raster)
	Editing and shape interpolations, surface volume
	Visibility (sight lines, observer points, skyline barrier, viewshed)
Spatial and temporal modeling	Creating space-time cube
	Analysis spatiotemporal data
	Visualization space-time cube in 2D and 3D
Case-oriented extensions from other developers	ArcSWAT: http://swat.tamu.edu/software/arcswat/
	Geospatial Modelling Environment: http://www.spatialecology.com/gme/

2.6   Computer Systems for Spatial Data Management in GIS

Apart from a wide range of various data models, which are bind into specific data formats, implementation of database models linked to GIS is highly used way for management of spatial and temporal data. In a simplified way, a database contains a set of related data organized into collection of tables, forms, queries, reports, and other objects. The content of data is adapted to model aspects of reality in order to support processes requiring information, such as querying the capacity of energy sources in a way that supports finding the optimal energy sources near the area of interest. Access to all data in a database is provided by database management system (DBMS) that consists software tools for entry, storage, and retrieval of information. Modern database systems are supported by the relation model that is managed with the structured query language (SQL). Each user can control data in a database in dependence on access rules that are linked to database administration, data definition and update, data retrieval, and data view.

Physically, database systems are running on dedicated computers, which are supported by servers designated for network administration, World Wide Web, and other complemented services. Administration of database systems in data centers is extended by expert groups on data collection and data analysis besides other services. A simplified schema of a data center that is dealing with database management and public data services is illustrated in Fig. 2.13.

Spatial data models require a database that can store and query data representing objects in a geometric space such as points, lines, and polygons. In addition to previous database systems, extended functionality is required for databases to process spatial data types efficiently. An Open Geospatial Consortium (OGC) and International Organization for Standardization (ISO) created Simple Feature Access that specifies a common storage and access model of mostly managed two-dimensional spatial data such as point, line, polygon, and other features. Instead of using basic index practices, spatial databases use a spatial index to speed up database methods such as spatial selection, measurement, and topology.
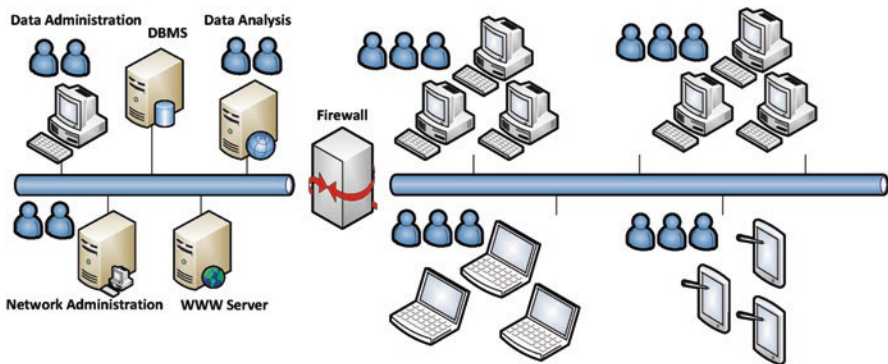
Fig. 2.13 A simplified schema of a computer center for database management and public data services
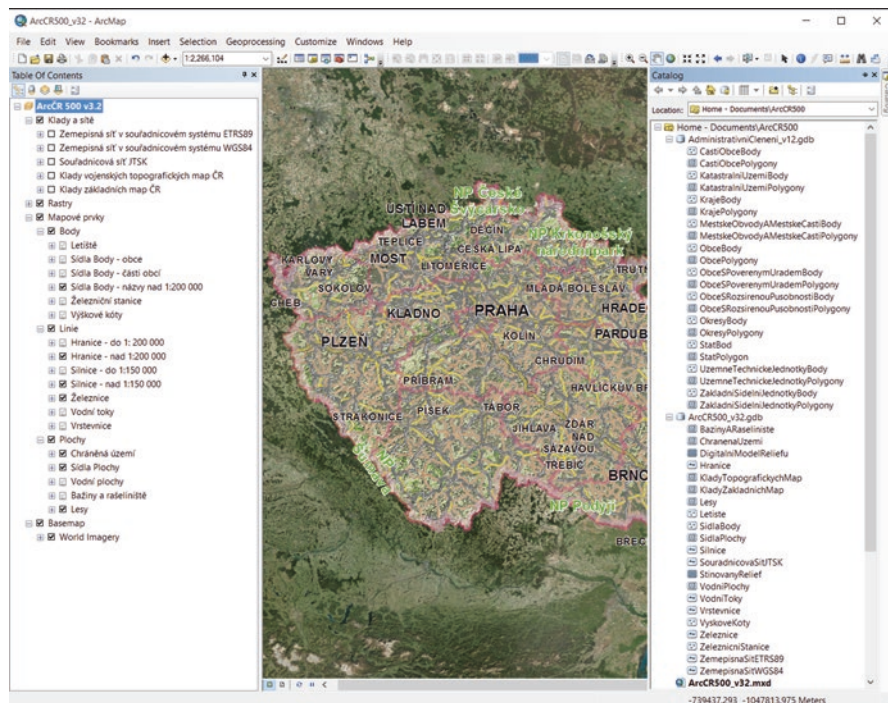
Fig. 2.14 Processing of digital vector geographic database of the Czech Republic ArcČR® 500 in the ArcGIS environment (the list of map layers is on the left side and the structure of geodatabase is on the right side)

A new complex object-oriented data model, geodatabase, was also introduced by Environmental Systems Research Institute (ESRI). A geodatabase, likewise other GIS data models, can manage four representations of geographic data: vector data for symbolizing features, raster data for representing images and gridded thematic data, triangulated irregular network (TIN) for designing surfaces, and addresses and locators for finding a geographic position (Fig. 2.14). The geodatabase is a collection of spatial datasets of various types held in a common file system folder, a Microsoft Access database, or a multiuser relational DBMS of many platforms such as Oracle, Microsoft SQL Server, PostgreSQL, Informix, or IBM DB2. It enables to manage spatial data in many sizes and have varying numbers of users in the scale from a single user to large workgroups. Main benefits of the geodatabase data model are:

– Uniform repository of spatial data: spatial data can be stored and managed in a database, which allows common data entry, more accurate data editing, and advanced validation.
– User works with more intuitive data objects: a geodatabase can contain data objects that better correspond to the reality such as producers of energy, power lines, transformers, and consumers instead of generic points, lines, and areas.

– Objects can be extended by relationships: definition of feature quantities is extended with topological associations and general relationships, which enables to specify what happens to features when related features are modified.
– Advanced map design can be implemented: drawing methods can be extended by writing scripts and features on a map display and can respond to changes in neighboring features.
– Larger datasets can be managed simultaneously: sets of features are continuous without tiles or other spatial partitions and can be edited by many users in a local area with reconciliation of any conflicts that emerge.
– Common setting of coordinate systems and map projections in feature datasets and raster datasets: all the data layers have to be in the same map projection and coordinate system in order to draw them on top of each other or combine them by analytical tools to see relationships.

The spatial datasets managed by database systems or saved as stand-alone files are used by desktop GISs, which are listed in Table 2.4. A list of selected GISs represents just a few software applications from a broad range of tools, which involve desktop GIS, Web map servers, software development frameworks and libraries (for Web and non-Web applications), extensions of computer-aided design (CAD), and mobile GIS implemented on mobile computing tools such as smartphones and tablets. The Web map server is implemented with ArcGIS for server dealing with accessing maps and geographic information on desktop applications and mobile computing tools. Its extensions can provide complete range of ArcGIS functionality such as manage Web services for mapping, spatial analysis, dataset editing, and geodata management. Also ArcGIS for server can manage the geodatabase, apply rules, define data models, maintain data integrity, and enable multiuser data processing. Similarly, MapServer on an open-source platform can be used for interactive mapping applications to the Web. The applications can be complemented by extensions developed with a scripting programming language.

2.7 GIS Tools for Processing and Presentation of Data Focused on Energy Sources

GIS can change the way of viewing our Earth's resources. GIS-based spatial modeling enables analysis of aerial and satellite images together with terrain properties such as digital terrain models, river network, road and railroad transport, industrial sites, and residential areas. The optional using of renewable resources can be improved by more precise prediction of local wind, solar, biomass, and surface water conditions. The next examples are focused on new applications of methods implemented in GIS and related computer systems. The selected methods dealing with mapping and spatial analysis will be presented using tools that can address a wider audience of energy researchers, academics, and practitioners.

Table 2.4 A list of selected desktop GISs and other related software tools

| GIS	Description and the key features	Website and development
ArcGIS family Environmental Systems Research Institute (ESRI) [commercial]	Advanced analysis and data management capabilities, including geostatistical and topological analysis tools. It includes desktop GIS, server GIS and other tools such as ArcPad and mobile GIS for mobile computers. ESRI created a number of spatial data formats such as shapefile, geodatabase, and coverage	www.esri.com Environmental Systems Research Institute was founded in 1969 as a land-use consulting firm. The company has a network of many international distributors and hosts an annual International User's Conference complemented by European User's Conference and many meetings on the national level
GeoMedia [commercial]	Managing geospatial databases, creating maps, publishing geospatial information, and analyzing mapped information	www.hexagongeospatial.com/products/producer-suite/geomedia The application was developed by Intergraph, which was acquired by Hexagon
TerrSet (formerly IDRISI) [commercial]	The package dedicated originally for education is integrated geographic information system and remote sensing software	www.clarklabs.org GIS and image processing product developed by Clark Labs at Clark University in 1987. In January 2015 Clark Labs released the TerrSet Geospatial Monitoring and Modeling Software, version 18
GRASS (Geographic Resources Analysis Support System) [open source]	Geospatial data management and analysis, image processing, spatial and temporal modeling, and visualizing. It contains over 350 modules that can handle raster, topological vector, image processing, and graphic data	grass.osgeo.org The development of GRASS was started by the USA-CERL with the involvement of many others, including universities and other federal agencies in 1982. In October 1999, the license was changed to the GNU GPL

Table 2.4 (continued)

QGIS (previously known as Quantum GIS) [open source]	Geospatial data management of raster and vector layers. Extensive functionality is given by integration with other open-source GIS packages, including PostGIS, GRASS, and MapServer	qgis.org The development of Quantum GIS started in early 2002, version 1.0, was released in January 2009. As an application under the GNU GPL, QGIS can be freely modified to perform different or more specialized tasks
Map Windows GIS [open source]	The GIS application and set of programmable mapping components. It can be reprogrammed to perform different or more specialized tasks. There are also plug-ins available to expand compatibility and functionality	www.mapwindow.org GIS package was adopted by the USEPA as the primary GIS platform for its Better Assessment Science Integrating Point and Nonpoint Sources (BASINS) watershed analysis and modeling software
ENVI (Environment for Visualizing Images) [commercial]	Written in Interactive Data Language (IDL), ENVI enhanced the text-based IDL and enabled a suite of graphical user interfaces specialized in remote sensing imagery analysis. The package contains a number of algorithms which are mostly contained in automated, wizard-based approach	www.exelisvis.com The software package was released in 1994. After a few transformation, the former division Exelis Visual Information Solutions was purchased by the Harris Corporation in 2015, becoming Harris Geospatial
ERDAS IMAGINE [commercial]	The package is designed for remote sensing application with raster graphics editor abilities. It allows users to prepare, display, and enhance digital images for mapping use in GIS and computer-aided design (CAD)	www.hexagongeospatial.com The first version of ERDAS was launched in 1978. The application was developed by ERDAS, which was acquired by Hexagon
SAGA (System for Automated Geoscientific Analyses) [open source]	The package represents a user friendly platform for the implementation of geoscientific methods. It is achieved by the unique application programming interface. It comes with a comprehensive set of free modules	www.saga-gis.org In 2007, the center of the SAGA development moved toward Hamburg, where it is linked to the Department of Physical Geography

2.7.1   Web-Based Applications

US Energy Information Administration (US EIA) collects and analyzes energy information to promote understanding of energy and its relations to the economy and the environment. Many map views with optional extensions for customization are available through the Web pages on an interactive mapping system (Fig. 2.15).

British petroleum (BP) offers data on world energy markets for a period of a few past decades. Tables, charts, and map views are available through a couple of tools that can filter and analyze information on health, safety, and environmental performance. An example of the energy charting tool is illustrated in Fig. 2.16.
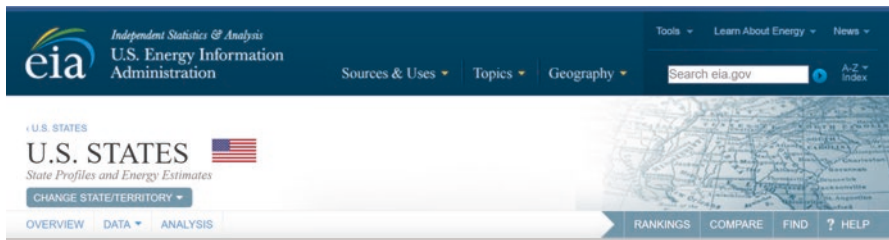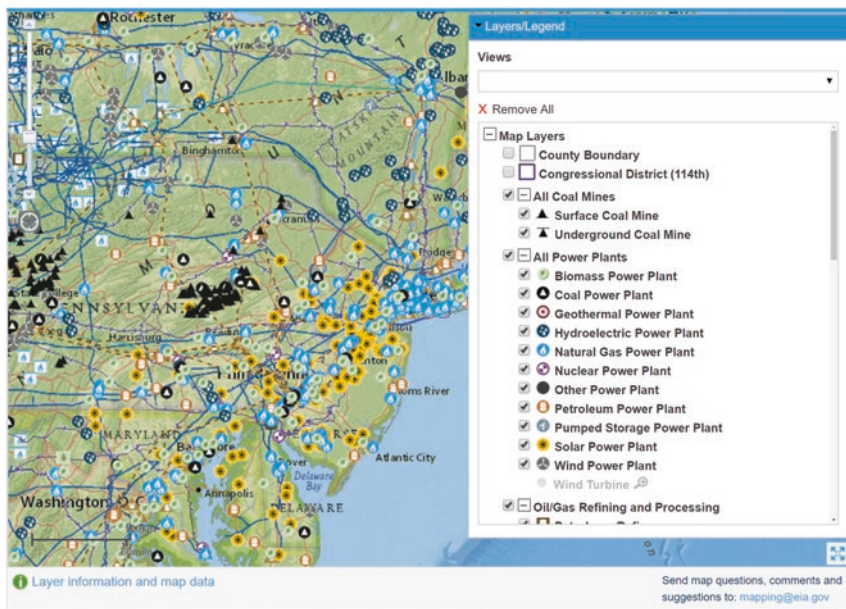

Fig. 2.15 An interactive mapping system dealing with energy sources and energy consumers managed by US EIA
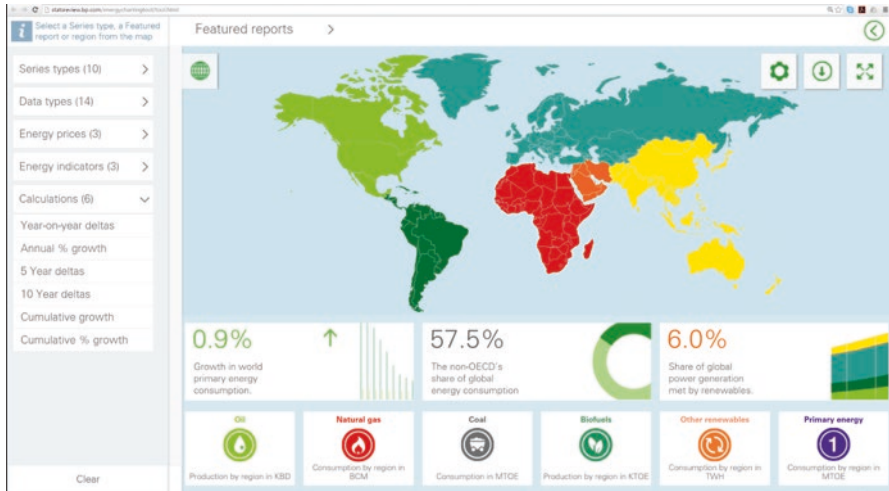
Fig. 2.16 An example of the energy charting tool managed by BP

2.7.2   GIS Projects

GIS organizes spatial datasets into projects that enable to combine a variety of data in an infinitive number of ways. As an example, a thematic map in Fig. 2.17, a layout view in Fig. 2.18, and a global scene in Fig. 2.19 show the primary energy consumption in 2013 in tonnes of oil equivalent (TOE) per capita. Ratios about primary energy per capita have been joined with attributes of the map layer: countries of the world. In order to simplify a view, the values are symbolized in the ranks (from ≤1 to ≤22 TOE per capita).

Information about the primary energy consumption in TOE per capita is used to provide comparable results for the whole world. The BP statistical review contains a majority of countries, which are significant primary energy consumers. The overview is given in a map view, which is used to display and work with geographic data in two dimensions (Fig. 2.17). It also shows the ArcGIS Pro environment for processing and analyzing data. The next step focused on finalizing of project results is represented by a layout view in Fig. 2.18. The GIS environment offers a number of items for layout design such as legends, scales, titles, north arrows, and other graphic and text symbols. The output layout views can be printed on large-format printers or exported to cloud GIS services. The results can be also visualized by a scene in a global 3D view (Fig. 2.19), which offers to work with data in three dimensions.

Other example presents mapping of energy utilities with data from US EIA. Vector datasets were imported into a GIS project and added to 2D layers. A vector dataset containing information about power plants was converted to a 3D layer thereafter, in order to provide extrusion of features to the 3D symbology. The loca-

Fig. 2.17 A map view of primary energy consumption in 2013 (TOE per capita) symbolized in the ranks (from ≤1 to ≤22 TOE per capita) in two dimensions. Source: BP Statistical Review, 2015; National Geographic World Map

Fig. 2.18 A layout view of primary energy consumption in 2013 (TOE per capita) symbolized in the ranks (from ≤1 to ≤22 TOE per capita) complemented by a legend, a scale, and a title. Source: BP Statistical Review, 2015; National Geographic World Map

tions of power plants are highlighted by vertical lines that have different lengths in dependence on the total power. A part in the southeastern region of the United States is illustrated in Fig. 2.20 with a local 3D map that is complemented by an attribute table with information about local power plants. The rows are sorted in descendent
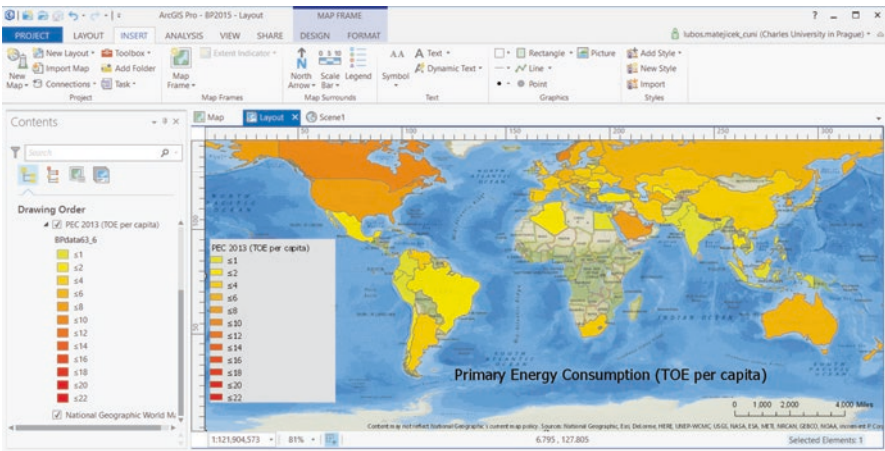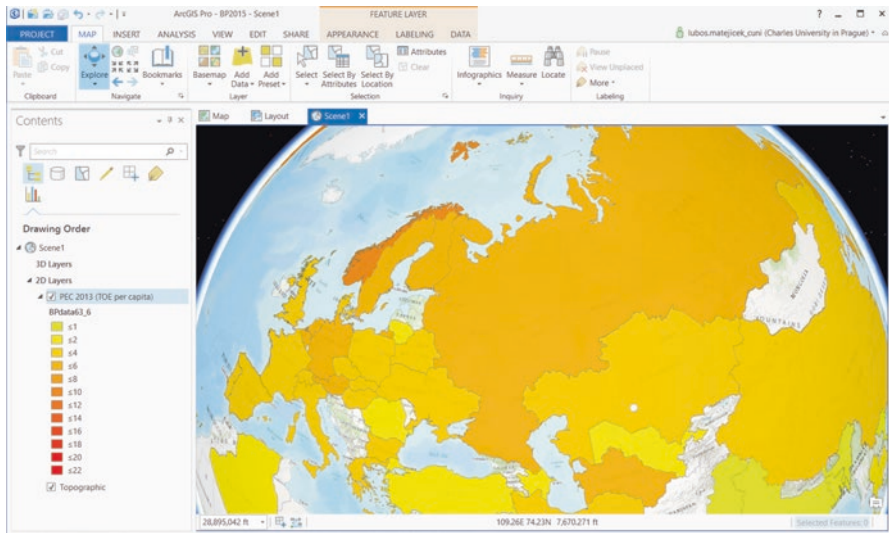
Fig. 2.19 A global 3D scene of primary energy consumption in 2013 (TOE per capita) symbolized in the ranks (from ≤1 to ≤22 TOE per capita). Source: BP Statistical Review, 2015; ESRI Topographic Map

order in dependence on the total power. Ten power plants with the highest total power are selected for indication in the 3D map. There are two natural gas power plants and one nuclear power plant in the list in the area of Florida. Also there are two coal power plants in Georgia and one nuclear power plant in Alabama. The local 3D map is complemented by a number of 2D layers that are focused on biofuel production, natural gas distribution, oil industry, and coal mines.

2.7.3　Development of Case-Oriented Software Applications

Case-oriented software applications for energy analyses mainly deal with enhancement of exiting GISs, utilization of other existing computational tools, or development of stand-alone software applications. As examples from a wide range of scientific research, environmental issues are used for presentation in a final part of this chapter. Energy extraction, transport, and consumption affect air, surface water, groundwater, and food chains. In the last 50 years, with the development of digital computers, environmental modeling has become more powerful for risk assessment of these phenomena. It is a science that uses mathematics to simulate environmental processes with computers. In case of environmental contamination, the models are based on physical and chemical phenomena such as diffusion, advection, sorption, reactions, and other thermodynamic processes. The model structure is also dependent on the spatial scale
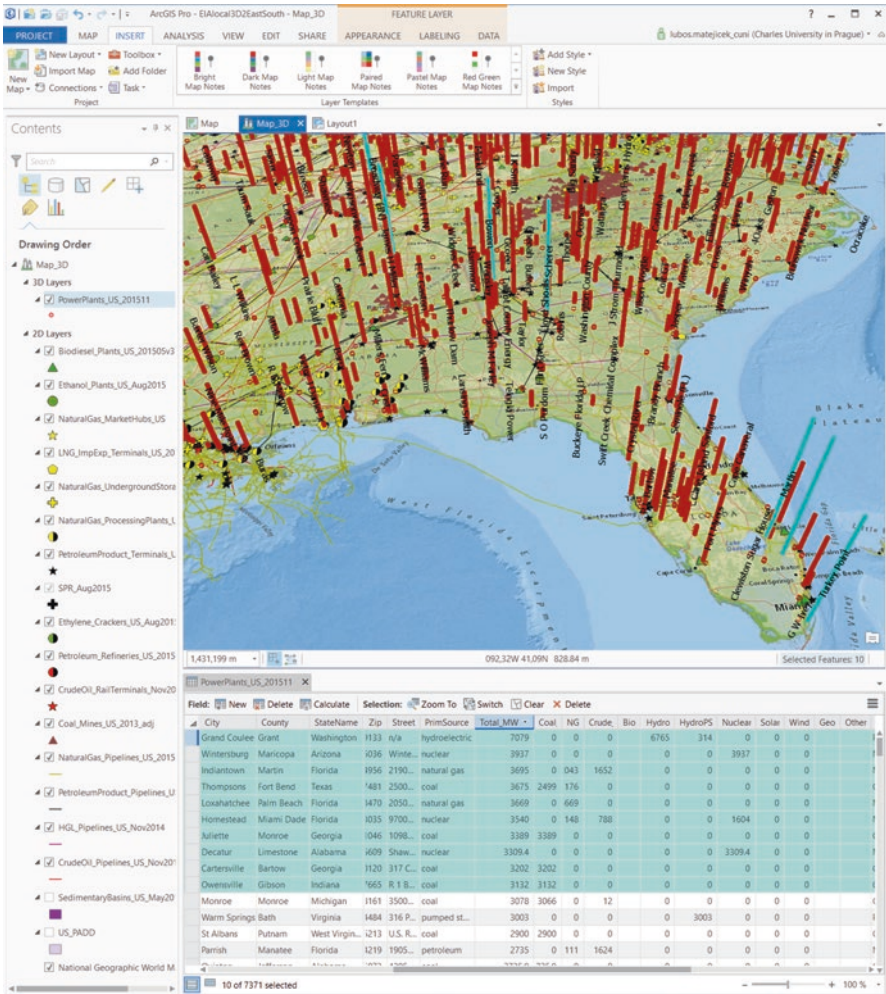
Fig. 2.20 The 3D scene of the primary energy consumption per capita in tonnes in 2013 in the ArcGIS Pro environment. Source: BP Statistical Review, 2015; ESRI Topographic Map

and the time scale of exploration. There are models of Earth's atmosphere or oceans under simulated conditions for long time periods such as hundreds of years, regional models of air pollution or contamination of surface water under simulated conditions for middle time periods such as year or months, and models of contamination caused by local accidents under simulated conditions for a few days or hours. The description of processes is translated into mathematical terms that lead to differential equations solving the change of a variable, like concentration in space and time. In mathematical models, diffusion is predicted by the Fick's second law that describes how the

concentration is changed with time and space. It is a partial differential equation, which in one dimension is

$$\frac{\partial c}{\partial t} = D \frac{\partial^2 c}{\partial x}$$

(2.1)

where c is the concentration, a function $c = c(x,t)$ depends on location x and time t, and D is the diffusion coefficient. This 1D (one-dimensional) formula can be applied to various situations in almost all environmental compartments. The derived models are used in environmental pollution in the modeling of the local concentration distribution due to air emissions from stacks or point pollution in rivers. Modeling of pollutant distribution has to be extended by other phenomena such as advection, chemical reaction, or nuclear decay in addition to diffusion. Thus, the Fick's second law is used to be extended by other terms in three dimensions. The partial differential equation that describes diffusion in three dimensions and advection in one dimension is given by

$$\frac{\partial c}{\partial t} = D_x \frac{\partial^2 c}{\partial x} + D_y \frac{\partial^2 c}{\partial y} + D_z \frac{\partial^2 c}{\partial z} + \upsilon \frac{\partial c}{\partial x} - \lambda c$$

(2.2)

where c is the concentration, a function $c = c(x,y,z,t)$ depends on location x, y, z and time t; D_x, D_y, D_z, is the diffusion coefficient in the x, y, z direction, respectively; v is the advection in x-direction; and λ is a degradation coefficient for substances that are subject to degradation or decay processes in addition. An analytical solution for the 3D instantaneous emission source in a constant unidirectional flow field is

$$c(x,,,y,,,z,,,t) = \frac{M}{\left(\sqrt{4\pi t}\right)^2 \sqrt{D_x D_y D_z}} e^{\frac{1}{4t}\left[\frac{(x-\upsilon t)^2}{D_x} \frac{y^2}{D_y} \frac{z^2}{D_z}\right] - \lambda t}$$

(2.3)

where M denotes the total mass per unit area in the fluid system.

There are many applications of this solution, mainly for air pollution modeling. Visualization of concentration distribution from a 3D Gaussian puff is illustrated in Table 2.5. It shows concentration distribution from 3D Gaussian puff for two different advections in x-direction based on an analytical solution for the 3D instantaneous emission source in a constant unidirectional flow field.

The previous simplified description of Gaussian puff has to be extended for applications in the atmosphere by terms that take the ground surface account and other meteorological conditions. Also all decay processes are neglected for which mathematical description requires a more detailed approach. It includes photochemical degradation, dry and wet deposition on the ground, washout due to precipitation, and other chemical reactions. Such more complex models are used extensively for prediction of the local development of a plume in the atmosphere. Simulation of these models often needs high-performance numerical solvers, which can be developed as stand-alone programs with high-level programming languages. More efficient way is represented by using of complex computing tools such as MATLAB,

Table 2.5 Visualization of concentration distribution from 3D Gaussian puff for two different advections in x-direction based on an analytical solution for the 3D instantaneous emission source in a constant unidirectional flow field ($D_x = D_y = D_z = 0.01$ m^2/s; $M = 1$) in MATLAB 2016a
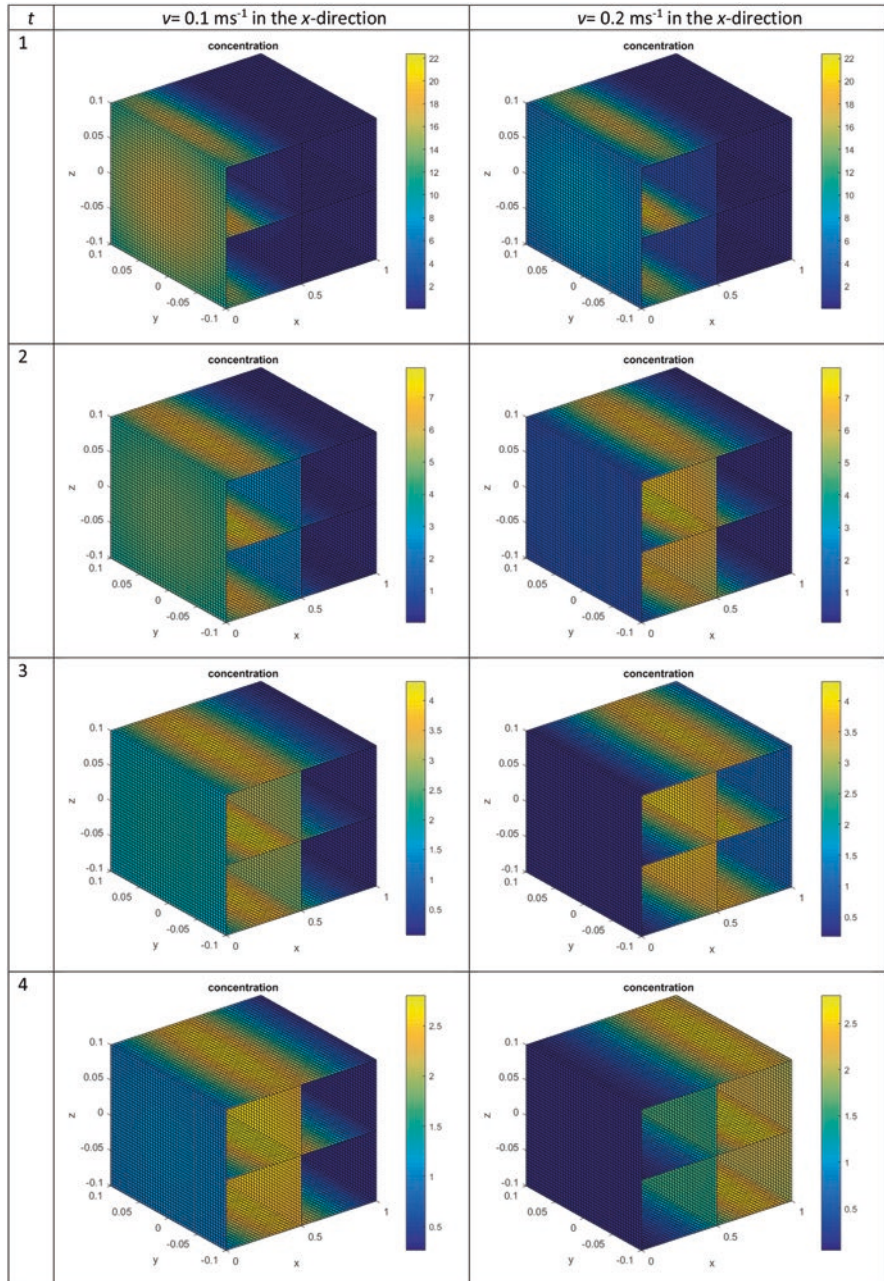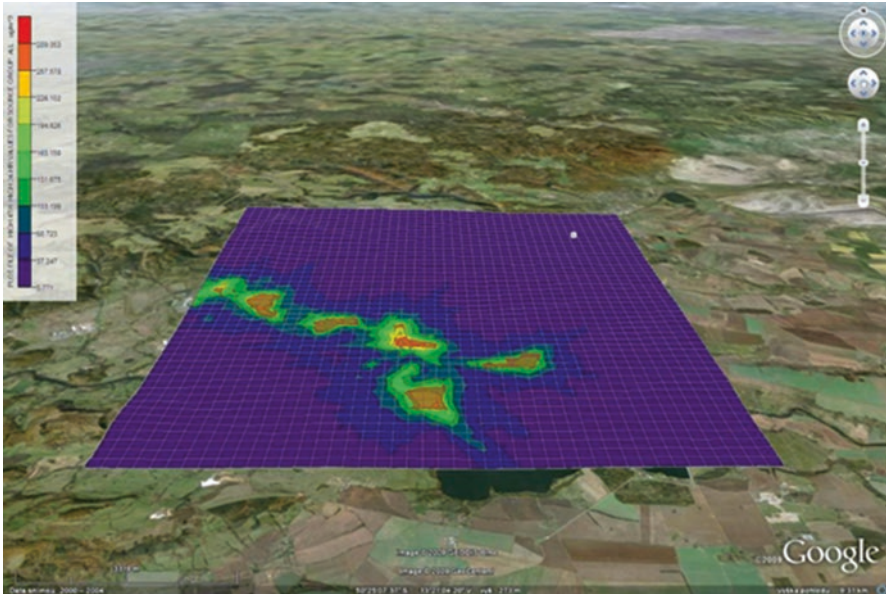
Fig. 2.21 An output of the Industrial Source Short Term (ISCST3) in the AERMOD View, a map layer of air pollution above the surface (concentration of the particulate matter with a mean aerodynamic diameter 10 μm)

Mathematica, Maple, or R. In addition to numerical solvers, they can manage input data, visualize results, and complement risk assessment with a number of optional extensions and toolboxes.

Information about national standards under a variety of environmental laws and about environmental monitoring and modeling are reported by US Environmental Protection Agency (USEPA), which was established for protecting human health and the environment. The EPA was proposed by President Richard Nixon by writing and enforcing regulations based on laws passed by Congress. An example an output of the Industrial Source Short Term (ISCST3) is illustrated in Fig. 2.21, which contains a map layer of air pollution above the surface. It displays concentration of the particulate matter with a mean aerodynamic diameter 10 μm (PM_{10}). The air dispersion model ISTST3 represents a Gaussian plume model, which is widely used to assess pollution concentrations. The model contains extensions of the simplified mathematical description of Gaussian puff in order to provide simulation of emission from more emission sources of various types such as point, line, and area emission sources. It also incorporates the ground surface account and a number of meteorological conditions such as wind speed and wind direction; atmospheric chemistry for NO_x, NO_2, and SO_2 decay; and building downwash. The model is used to be a component of air dispersion modeling packages, which implement other popular EPA models into one interface.

Bibliography

Arctur, D., & Zeiler, M. (2004). *Designing geodatabases: Case studies in GIS data modeling* (1st ed.). Redlands: ESRI Press.

Clark, M. (2009). *Transport modeling for environmental engineers and scientists* (2nd ed.). New York: Wiley.

Holzbecher, E. (2012). *Environmental modeling: Using MATLAB* (2nd ed.). Heidelberg: Springer.

Longley, A. J., Goodchild, M., Maguire, D. J., & Rhind, D. W. (2010). *Geographic information systems and science* (3rd ed.). New York: Wiley.

Law, M., & Collins, A. (2016). *Getting to know ArcGIS Pro* (1st ed.). Redlands: ESRI Press.

Maguire, D. J., Goodchild, M., & Batty, M. (Eds.). (2005). *GIS, spatial analysis, and modeling* (1st ed.). Redlands: ESRI Press.

Mitchell, A. (1999). *The ESRI guide to GIS analysis, Vol. 1: Geographic patterns & relationships* (1st ed.). Redlands: ESRI Press.

Mitchell, A. (2005). *The ESRI guide to GIS analysis, Vol. 2: Spatial measurements and statistics* (1st ed.). Redlands: ESRI Press.

Mitchell, A. (2012). *The ESRI guide to GIS analysis, Vol. 3: Modeling suitability, movement, and interaction* (1st ed.). Redlands: ESRI Press.

Pistocchi, A. (2014). *GIS based chemical fate modeling: Principles and applications* (1st ed.). Hoboken, NJ: Wiley.

Zeiler, M. (2010). *Modeling our world: The ESRI guide to geodatabase concepts* (2nd ed.). Redlands: ESRI Press.

Dictionaries and Encyclopedia

Wade, T., & Sommer, S. (Eds.). (2006). *A to Z GIS: An illustrated dictionary of geographic information systems* (2nd ed.). Redlands: ESRI Press.

Wikipedia. Retrieved from www.wikipedia.org/

Data Sources (Revised in September, 2016)

BP (British Petroleum). *Energy charting tool*. Retrieved from http://tools.bp.com/energy-charting-tool.aspx

Diva GIS. Retrieved from http://www.diva-gis.org/Data

European Environment Agency. *Data and maps*. Retrieved from www.eea.europa.eu/data-and-maps

Food and Agriculture Organization (FAO) of the United Nations GeoNetwork. Retrieved from http://www.fao.org/geonetwork/srv/en/main.home

International Steering Committee for Global Mapping (ISCGM). Retrieved from http://www.iscgm.org/

NASA Earth Observations (NEO). Retrieved from http://neo.sci.gsfc.nasa.gov/

NASA's Socioeconomic Data and Applications Center (SEDAC). Retrieved from http://sedac.ciesin.columbia.edu/

Natural Earth (free vector and raster map data at 1:10 m, 1:50 m, and 1:110 m scales). Retrieved from http://www.naturalearthdata.com/downloads/

OpenStreetMap Dataset. Retrieved from http://planet.openstreetmap.org/

OpenTopography. *High-resolution topography data and tools*. Retrieved from http://www.opento-
    pography.org/
Sentinel Satellite Data. Retrieved from https://scihub.copernicus.eu/dhus/#/home
United Nations Environment Programme (UNEP). *Environment for development*. Retrieved from
    http://geodata.grid.unep.ch/
U.S. Energy Information Administration (EIA). *Maps*. Retrieved from http://www.eia.gov/maps/
U.S. Geological Survey (USGS) Earth Explorer. Retrieved from http://earthexplorer.usgs.gov/

Chapter 3
Energy Outlook: Spatial and Temporal Mapping of Energy Sources Using GIS

Over the centuries, the energy has been extracted from nature in many ways. From ancient times to almost modern times, wood was the main fuel, which was often used more rapidly than was replaced by new growth, and therefore the forests of countries surrounding the Mediterranean were gradually destroyed, followed by the forests of central Europe and South America nowadays. The scarcity of wood stimulated utilization of other energy sources based on fossil fuels. Coal became the main energy source in many developed countries and provided the power for the industrial revolution, because it can be transported and has a higher caloric values than wood. During the twentieth century, coal is gradually displaced by oil and gas. In comparison with coal, these fossil fuels can be more easily transported over large distances by pipelines and tankers. Since the nineteenth century, the rapid development of the electrical industry has become a complex change of our civilization. The advantage of electricity being very easily transported displaced many local energy sources for heating, air-conditioning, suburban transport, and communication. It became a convenient power source for our factories and household articles. Electricity is mostly generated by turbines driven by steam produced by burning fossil fuels. It can be complemented by hydroelectric power and nuclear power. Nowadays the electrical industry makes possible to integrate a number of other sources, such as solar farms, wind and biofuel production, and small hydro energy plants.

3.1 Global Primary Energy Consumption

World energy consumption represents the total energy used by human civilization per all industrial sectors and across every country. It has significant implications for social, economic, and political sphere. Energy data are periodically published by local authorities in each country and by international institutions and companies such as the US Energy Information Administration (EIA), the International Energy Agency (IEA), European Environmental Agency (EEA), and British Petroleum (BP).

Fig. 3.1 US EIA online mapping: International energy information, including overviews, rankings, data, and analyses (an example focused on a map presentation of the total primary energy production in 2013). Source: EIA, 2016

The EIA is an agency of the US Federal Statistical System responsible for collection and analysis of energy information. The Department of Energy Organization Act of 1977 established EIA as the federal government authority on energy statistics and analysis in 1974 following the oil market disruption of 1973. The EIA is a part of the US Department of Energy (DOE), which is concerned with the United States' policies regarding energy and safety in handling nuclear material. But the department has a number of other responsibilities in the field of energy sources such as the nation's nuclear weapons program, nuclear reactor production for the US Navy, energy conservation, energy-related research, radioactive waste disposal, and domestic energy production. On the US level, the EIA provides huge information about petroleum and other liquids, natural gas, electricity, consumption, coal, renewable and alternative fuels, and nuclear energy. The agency also presents comprehensive data summaries, comparisons, analysis, and projections integrated across all energy sources. The map-based applications illustrated in Figs. 3.1 and 3.2 are available on the Web page: http://www.eia.gov/maps/.

The IEA is autonomous agency established in the framework of the Organisation for Economic Co-operation and Development (OECD) in 1974 after the oil crisis in 1973. The IEA resides in Paris and acts as a policy adviser to its member states. The agency also collaborates with nonmember countries such as China, India, and

U.S. Energy Mapping System
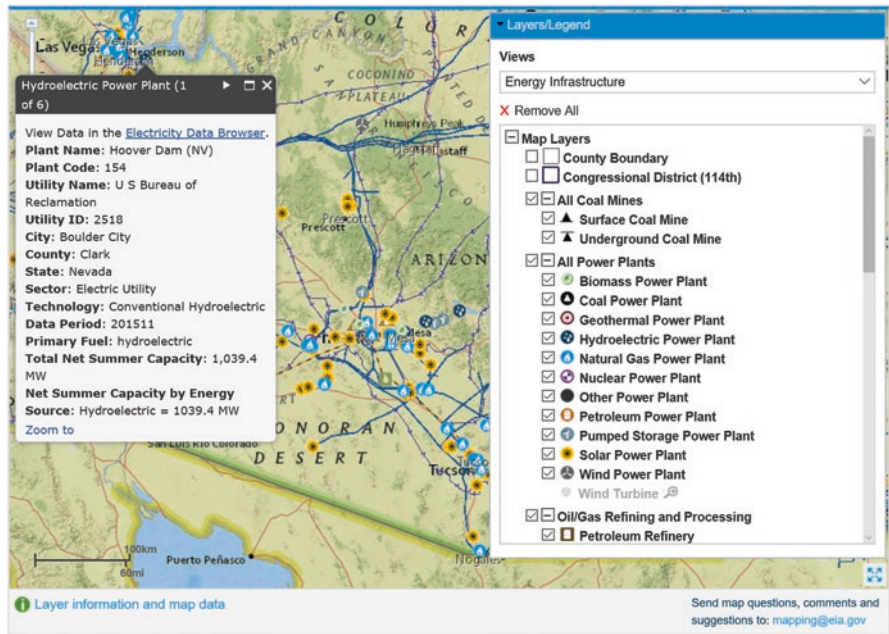
Fig. 3.2 US EIA online mapping: State energy information about renewable energy sources (an example dealing with mapping of renewable energy sources in the United States). Source: EIA, 2016

Russia. Its mandate has broadened to focus on energy policy from the view of energy security, economic development, and environmental protection. The IEA promotes alternate energy sources and multinational energy technology cooperation. Its staff consists of energy analysts, data managers, statisticians, modelers, and operative workers. The IEA produces around 20 priced publications and around 70 free publications a year. The main topics include energy sources, clean energy technologies, energy efficiency, energy security, transport, and climate change. Data- and map-based applications available through the Web page http://www.iea.org/statistics/ are shown in Figs. 3.3 and 3.4.

Publications and data are available. The EEA is an agency of the European Union (EU), which provides information services on the environment in order to adopt, implement, and evaluate environmental policy. EEA is governed by a management board that consists of representatives of the governments of the EU member states, a European Commission representative, and two scientists appointed by the European Parliament. The EEA was established by the European Economic Community Regulation 1210/1990 and became operational in 1994. The agency also cooperates closely with other non-EU member states in the framework of European environmental and observation network: Eionet. Many datasets are available on the Web page http://www.eea.europa.eu/data-and-maps and on the particular Web pages of individual EU projects (Fig. 3.5).

Fig. 3.3 An IEA spreadsheet application: Headline energy data saved in the Excel and presented by an interactive pivot chart (an example of time series of total energy production in ktoe in the United States). Source: IEA, 2016
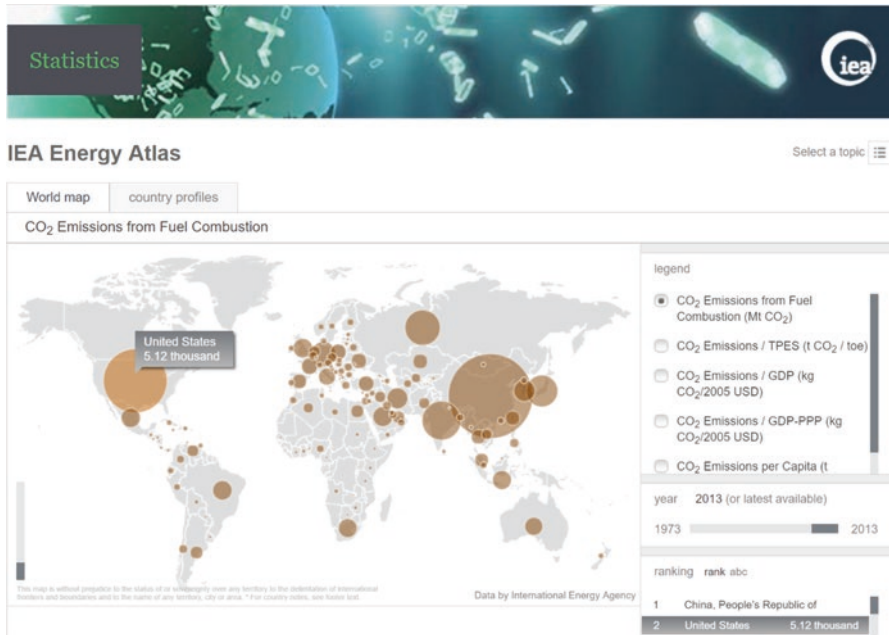
Fig. 3.4 IEA online mapping: Presentation of CO_2 emissions from fuel combustion in Energy atlas (an example presenting CO_2 emissions from fuel combustion across the whole world). Source: IEA, 2016

The BP Public limited company is one of the world's major oil and gas companies founded by a group of British geologists discovered large oil deposits in Iran in 1908. The company operates in all areas of the oil and gas industry, including exploration and production, refining, distribution and marketing, petrochemicals, power generation, and trading. The company has operations in more than 70 countries worldwide with the main headquarters in London. It is organized into two main business segments upstream and downstream (Fig. 3.6). The upstream sector deals with searching for potential underground or underwater crude oil and natural gas fields, drilling, and operating the wells. The downstream sector includes the refining of petroleum crude and the processing of raw natural gas, as well as distribution of derived products. In a long time period, BP ranks among the largest oil and gas companies by revenue (revenue 2015: 222.8 US$ billion). Since 1951, the company has annually published its Statistical Review of World Energy, which can be considered an energy industry benchmark. The BP statistical review provides globally consistent data on world energy markets that can give information for long-term trends in both the demand and supply of energy. The review contains globally consistent data on world energy market mainly focused on primary energy consumptions and fossil fuels such as oil, natural gas, and coal in the period of a few decades. Other highly valued information is about nuclear energy, hydroelectricity, and renewables. It helps to consider how the energy market might evolve over the next decades. In addition to data tables and graphs, the interactive energy charting tool
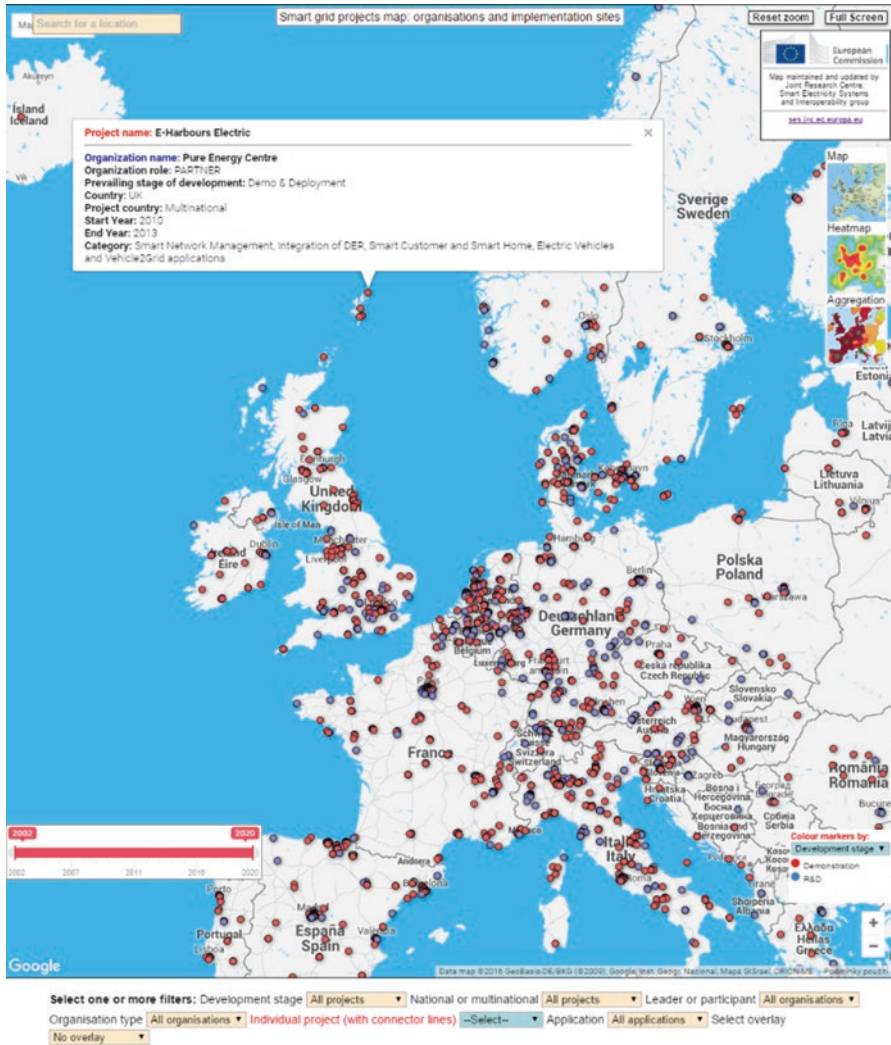
Fig. 3.5 EEA online mapping: The smart grid projects map (an example with organizations and implementation sites from a database of smart grid projects for electricity across the EU member states). Source: EEA, 2016

can give a more complex information about energy reserves and consumption. An example focused on a basic overview of energy market complemented by labels is illustrated in Fig. 3.7.

The international institutions and companies are used to be provided annual world energy outlooks that contain global energy projection and analysis. It enables energy market projections, exploratory statistics, and model predictions. Based on reference scenarios, decision-makers can evaluate their current path, alternative scenarios, and environmental impacts. The outlooks are usually focused on pressing issues such as prospects for oil and gas production and climate scenarios.
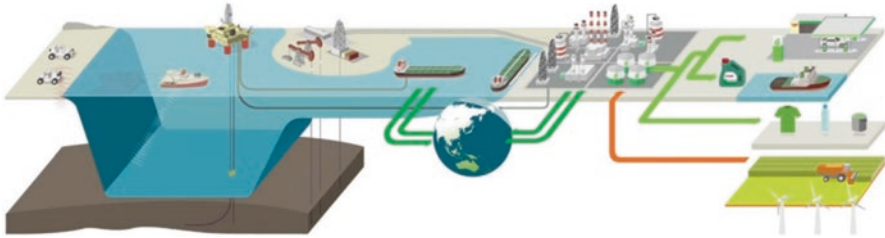
Fig. 3.6 The BP business model that spans everything from exploration to marketing across resource types, geographies, and businesses and adaptable to prevailing conditions. Source: BP, 2016
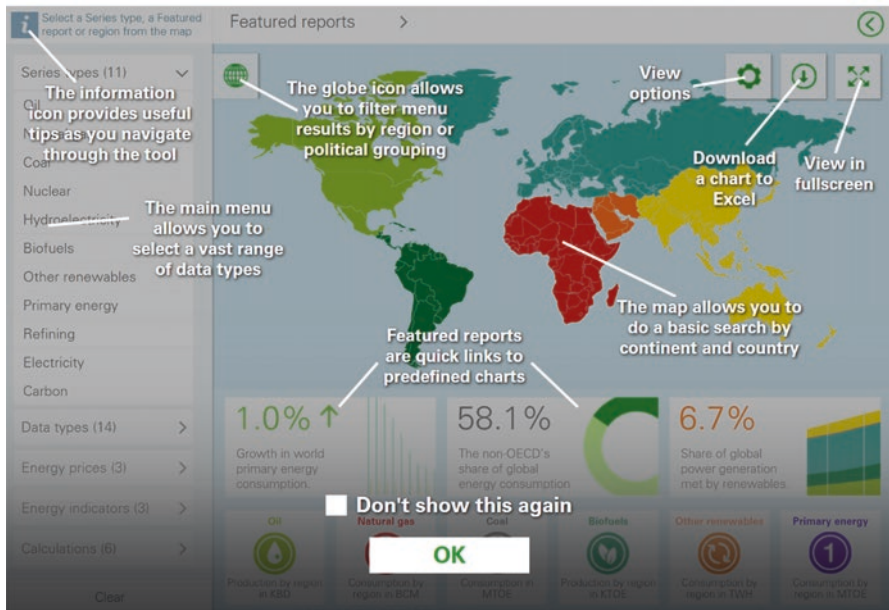
Fig. 3.7 The BP online energy charting tool: International energy information provided by energy charting tools (an example focused on a basic overview of energy market complemented by labels). Source: BP, 2016

3.1.1 The Energy Outlook from EIA

The outlooks from EIA actually include a wide range of information from the United States such as reporting hourly electricity data, incorporating more timely export data in weekly petroleum statistics, releasing energy consumption data, extending energy by rail data, and enhancing mid-term and international energy modeling capabilities. The reports analysis and projections are published as short-term energy outlooks, monthly energy reviews, and annual energy outlooks.

U.S. primary energy consumption by source and sector, 2015

Total = 97.7 quadrillion British thermal units (Btu)
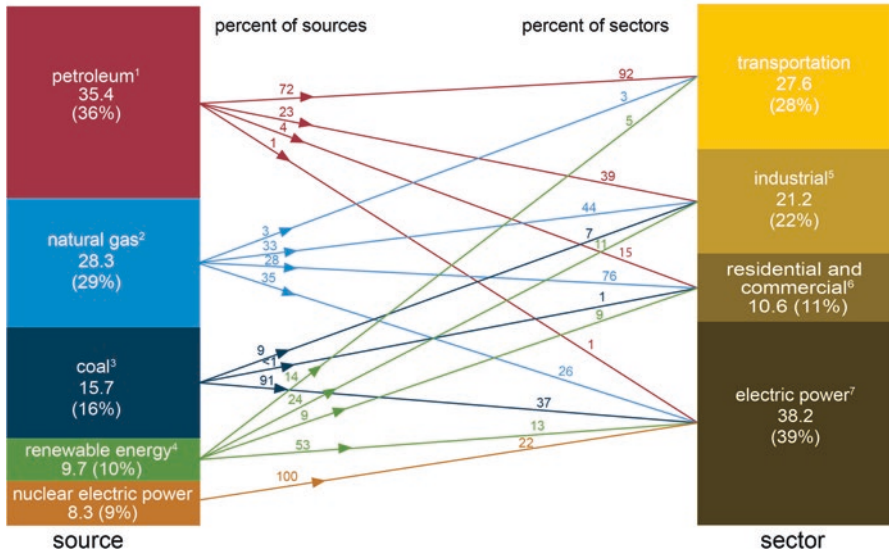
Fig. 3.8 The redistribution of US primary energy consumption by source and sector in 2015 (*1*. Biofuels are included in "renewable energy"; *2*. exclude supplemental gaseous fuels; *3*. include less than −0.02 quadrillion Btu of coal coke net imports; *4*. include conventional hydroelectric power, geothermal, solar/photovoltaic, wind, and biomass; *5* include industrial combined-heat-and-power and industrial electricity-only plants; *6* include commercial combined-heat-and-power and commercial electricity-only plants; *7* electricity-only and combined-heat-and-power plants whose primary business is to sell electricity, or electricity and heat, to the public; include 0.2 quadrillion Btu of electricity net imports not shown under "source"). Source: EIA monthly energy review, April 2016

All the outlooks are available via Web page of the EIA: www.eia.gov . The redistribution of US primary energy consumption by source and sector in 2015 is illustrated in Fig. 3.8, which covers the total transfer of 97.7 quadrillion Btu. It shows the dominant role of two pressing issues: primary energy sources of petroleum and natural gas. In order to illustrate a more complex energy redistribution, Sankey diagrams are used to visualize energy flow by the width of the arrows, which is shown proportionally to the flow quantity. A comparison of estimated energy redistribution between sources and consumers in 2011 and 2015 is shown in Fig. 3.9. Both the schemas are based on Sankey diagrams that show the relative size of primary energy sources and consumers in the United States, with fuels compared on a common energy unit basis. Flow diagrams have been created from publicly available data and estimates of state-level energy use patterns. Each flowchart for US energy sources contains vast quantities of data from the EIA of the Department of Energy. It also includes solar, wind, biomass, and geothermal sources besides nuclear, natural gas, coal, and petroleum sources. About 40% of the total resources are used for production of electricity, which supplies industry, agriculture, transport, residential districts, and other services. Nearly all nuclear energy and many coal resources go toward
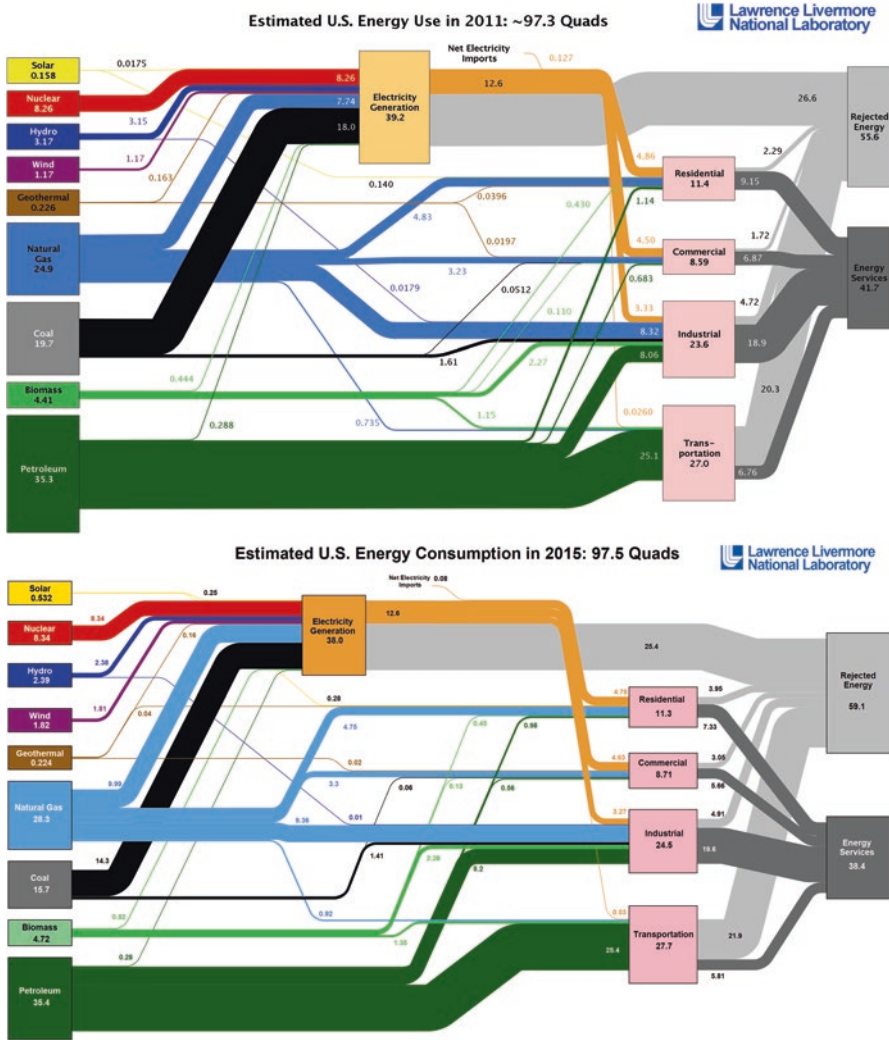
Fig. 3.9 A comparison of estimated energy redistribution between sources and consumers in 2011 and 2015 (Distributed electricity represents only retail electricity sales and does not include self-generation; EIA reports consumption of renewable resources for electricity in BTU-equivalent values by assuming a typical fossil fuel plant "heat rate." The efficiency of electricity production is calculated as the total retail electricity delivered divided by the primary energy input into electricity generation. End use efficiency is estimated as 65% for the residential and commercial sectors 80% for the industrial sector and 21% for the transportation sector. Totals may not equal the sum of components due to independent rounding.) Source: Lawrence Livermore National Laboratory and the Department of Energy; Estimated US Energy Use in 2011 is based on DOE/EIA-0384 (2011); Estimated US Energy Use in 2015 is based on DOE/EIA MER (2015)

electricity generation as well. Petroleum, which represents more than 30% of total energy inputs, is primarily used to fuel cars, planes, and other transportation devices. The use of natural gas is more varied.

Other related schemas for energy redistribution and consumption illustrate US carbon dioxide emissions presented by flowcharts in Fig. 3.10. Carbon dioxide is emitted from the use of three major energy resources: natural gas, coal, and petroleum. Approximately 5749 million metric tons of carbon dioxide was emitted throughout the United States for use in electricity generation and in industrial, transportation, commercial, and residential applications in 2001. In 2014, the chart diagram indicated a slight decrease of carbon dioxide emissions by fossil fuels such as petroleum and coal, which can be caused by propagation of renewable energy sources in the framework of projects focused on improving national energy security and surety while reducing environmental impacts. The innovating science and technology solutions are focused on reduction of greenhouse gases, adding significant amounts of intermittent renewable energy and loads, development of conventional fossil sources in an environmentally sensitive manner, and adapting smart grid technologies in order to stabilize the electric grid.

Energy consumption and carbon dioxide emissions predictions are presented in the annual energy outlooks, which contain scenarios in dependence on implementation of various technological, demographic, and environmental plans. The actual US EIA outlooks assume implementation of the Clean Power Plan (CPP) through mass-balanced standards that establish limits on carbon dioxide emissions from fossil-fired generators. The accuracy of prediction is highly dependent on data, methodologies, model structures, and their final setting and reading of the results. The implementation of new technologies must reflect current laws and regulations, and demographic trends. Implementation of the CPP using a mass-based approach assumes reduction of electricity-related carbon dioxide emissions between 1550 and 1590 million metric tons in the period 2030–2040. Share of total electricity generation from coal (50% in 2005 and 33% in 2015) should fall to 21% in 2030 and to 18% in 2040. The mass-based approach with the strong growth in wind and solar generation spurred by tax credits may lead to a temporal decline in natural gas-fired generation, which is planned to be by far the largest generation source. Even without CPP, electricity-related carbon dioxide emissions remain well below their 2005 level in 2030 and 2040. It reflects both low load growth and generation mix changes driven by the extension of renewable tax credits, reduced solar photovoltaic capital costs, and low natural gas prices. Both the scenarios are illustrated in Fig. 3.11, which contains predictions of the total US primary energy consumption. It grows slowly in both cases, with slightly higher growth in the No CPP case. Total petroleum and other liquids consumption declines in the period 2020–2031 as increases in vehicle fuel economy offset growth in transportation activity and increased industrial use. Natural gas consumption increases throughout the projection period with slower growth in natural gas consumption in the electric power sector for the No CPP case. Coal consumption declines throughout the projection period, mostly before 2030 because of the CPP, but retains a larger market in the No CPP case. The renewable share of total energy consumption (including liquid biofuels) increases, with the significant growth occurring in the electric power sector. Nuclear power generation remains on its current level as the impact of new plant additions is offset by retirements. Reductions in energy intensity largely offset impact of gross domestic product (GDP) growth, leading to slow projected growth in energy use.
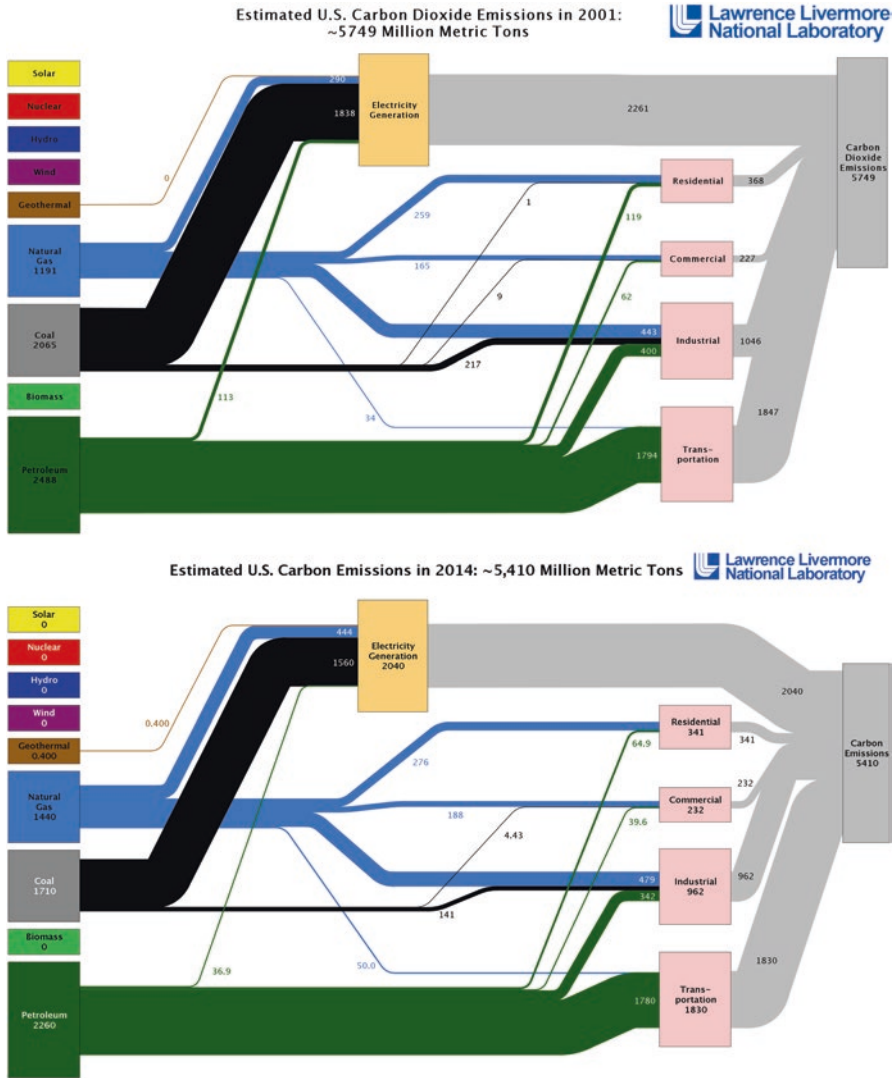
Fig. 3.10 A comparison of estimated carbon dioxide emissions in 2001 and 2014 (Carbon emissions are attributed to their physical source and are not allocated to end use for electricity consumption in the residential, commercial, industrial, and transportation sectors. Petroleum consumption in the electric power sector includes the nonrenewable portion of municipal solid waste. Combustion of biologically derived fuels is assumed to have zero net carbon emissions – the life cycle emissions associated with producing biofuels are included in commercial and industrial emissions. Totals may not equal the sum of components due to independent rounding errors.) Source: Lawrence Livermore National Laboratory and the Department of Energy. Estimated US Carbon Emissions in 2001 are based on DOE/EIA-0384 (2007). Estimated US Carbon Emissions in 2014 are based on DOE/EIA-0035 (2015)

U.S. primary energy consumption
quadrillion Btu
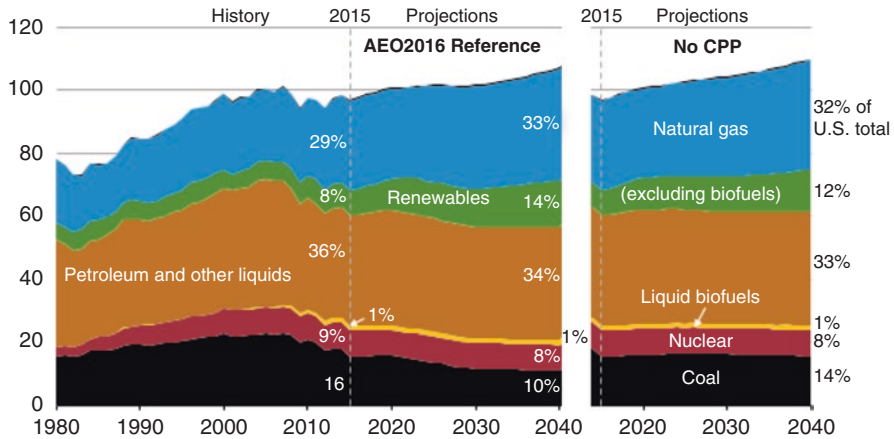
Fig. 3.11 Prediction of the total US primary energy consumption that grows slowly in both cases, with slightly higher growth in the No CPP case. Source: EIA, 2016

3.1.2 The Energy Outlook from IEA

Complex predictions of future energy trends in the world are provided by advanced analysis and models. Since 1993, the IEA uses for medium- and long-term projections World Energy Model (WEM), which is the principal tool used to generate detailed sector-by-sector projections for world energy scenarios. The WEM consists of a few sections:

– Final energy consumption including residential, services, agriculture, industry, transport, and nonenergy use
– Energy transformation including power generation and heat, refinery, and other transformation
– Fossil fuel and bioenergy supply

The current version WEM 2015 covers energy development up to 2040 in 25 regions with 12 countries being modeled on an individual country basis (Brazil, Canada, Chile, China, India, Indonesia, Japan, Korea, Mexico, Russia, South Africa, and the United States). The 25 WEM regions are grouped in a few units (Africa, Caspian, developing countries, Eastern Europe/Eurasia, European Union, G-20, Latin America, Middle East, non-OECD Asia, North Africa, OECD, OECD Americas, OECD Asia Oceania, OECD Europe, Organization of the Petroleum Exporting Countries (OPEC), Southeast Asia, sub-Saharan Africa). Information about energy supply, transformation and demand, as well as energy prices is mostly obtained from the IEA's own databases of energy and economic statistics (http://www.iea.org/statistics). The time horizon of the WEM 2015 goes out to 2040 with
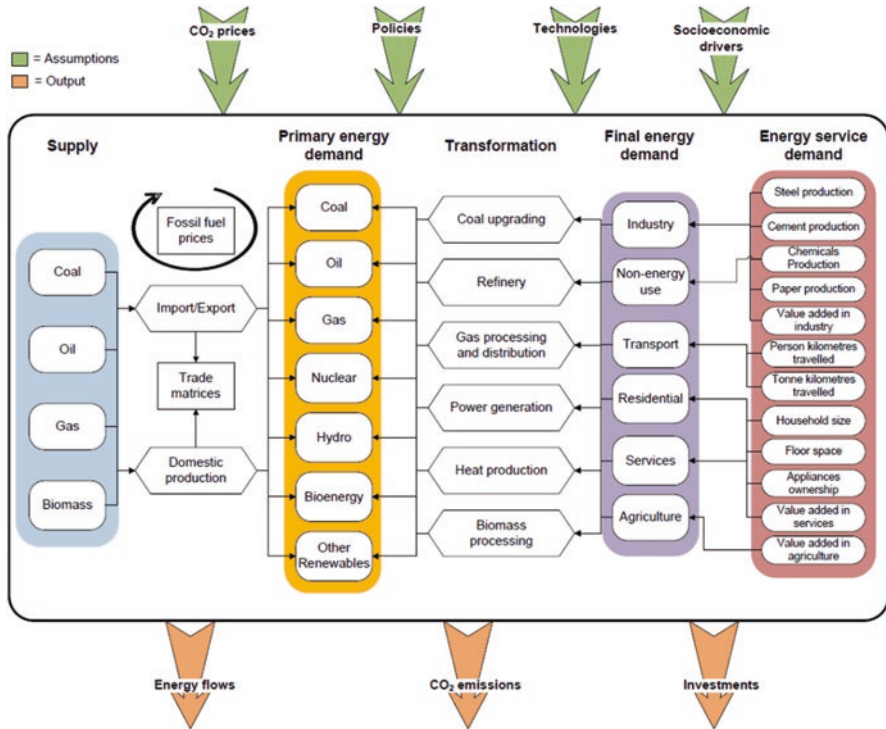
Fig. 3.12 WEM overview. Source: http://www.worldenergyoutlook.org/

annual steps in between. The model is each year recalibrated to the latest available data point. WEM overview is illustrated in Fig. 3.12. The model covers energy supply, energy transformation, and energy demand. The majority of the end-use sectors are based on stock models to characterize the energy infrastructure. Energy-related carbon dioxide emissions and investments related to energy developments are specified besides modeled fuel consumption. More detailed information is published in the IEA WEM documentation 2015, which also includes information about new features of an actual version. The scenarios developed to examine future energy trends are summarized in Table 3.1.

The presented scenarios demonstrate the impact of the policy choices made by governments where rates of growth in energy use and the types of fuels supplied are markedly different across those scenarios. In the New Policies Scenario, which takes into account both existing and planned policies, world primary energy demand is projected to increase on average by 1.1% per year between 2012 and 2040, reaching almost 18,300 Mtoe (an increase of around 4900 Mtoe or 37%) (Fig. 3.13). Demand expands much more rapidly in the Current Policies Scenario, in which no new government policies are assumed, rising at an average rate of 1.5% per year to a level in 2040 that is 50% higher than in 2012. In the 450 Scenario, in which policies are assumed to be introduced to bring the world onto an energy trajectory

Table 3.1 Definitions and objectives of the WEO-2015 scenarios

	Current Policies Scenario	New Policies Scenario	450 Scenario (concentration of greenhouse-gases 450 ppm CO_2-eq)
Definitions	Government policies that had been enacted or adopted by mid-2014 continue unchanged	Existing policies are maintained and recently announced commitments and plans, including those yet to be formally adopted, are implemented in a cautious manner	Policies are adopted that put the world on a pathway that is consistent with having around a 50% chance of limiting the global increase in average temperature to 2 °C in the long term, compared with preindustrial levels
Objectives	To provide a baseline that shows how energy markets would evolve if underlying trends in energy demand and supply are not changed	To provide a benchmark to assess the potential achievements (and limitations) of recent developments in energy and climate policy	To demonstrate a plausible path to achieve the climate target

Source: IEA WEM documentation, 2015
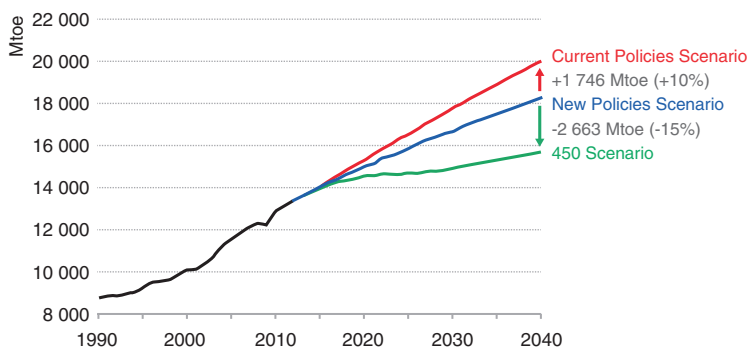
Fig. 3.13 World total primary energy demand by scenario. Source: IEA World Energy Outlook 2014

that provides a 50% chance of constraining the long-term average global temperature increase to 2 °C, global energy demand grows on average by only 0.6% per year (in 2040, demand is 17% up on 2012). The gap in 2040 between demand in the different scenarios is substantial. Taking the New Policies Scenario as the base, demand is 10% higher in the Current Policies Scenario and 15% lower in the 450 Scenario.

The proportion of fossil fuels in the overall primary fuel mix (broadly constant over the past three decades) falls in all three scenarios, though they remain dominant in 2040. Their proportion falls from 82% in 2012 to 80% in the Current Policies Scenario, to 74% in the New Policies Scenario, and to below 60% in the 450 Scenario (Table 3.2). The range of outcomes is widest for coal and non-hydro renewable energy (excluding traditional use of solid biomass), because these energy

Table 3.2 World primary energy demand by fuel and scenario (Mtoe)

			Current Policies Scenario		New Policies Scenario		450 Scenario	
Year	2000	2013	2020	2040	2020	2040	2020	2040
Coal	2343	3929	4228	5618	4033	4414	3752	2495
Oil	3669	4219	4539	5348	4461	4735	4356	3351
Gas	2067	2901	3233	4610	3178	4239	3112	3335
Nuclear	676	646	827	1036	831	1201	839	1627
Hydro	225	326	380	507	383	531	384	588
Bioenergy[a]	1023	1376	1537	1830	1541	1878	1532	2331
Other renewables	60	161	296	693	316	937	332	1470
Total	10,063	13,559	15,041	19,643	14,743	17,934	14,308	15,197

Source: IEA World Energy Outlook, 2015
aIncludes the traditional use of solid biomass and modern use of bioenergy

sources are affected most by environmental, energy security, and climate policies. Coal demands rise by more than half between 2012 and 2040 in the Current Policies Scenario, but fall by one-third in the 450 Scenario. Trends in the use of modern renewable energy run in the opposite direction (use is highest in the 450 Scenario and lowest in the Current Policies Scenario). The variation across scenarios is smallest for hydropower, as its use is to a large degree determined by the extent of technically exploitable resources. Among final fuels, the outlook for electricity is constant with demand growing steadily in each scenario.

In September 2014, the World Meteorological Organization reported that the concentration of carbon dioxide in the atmosphere increased to 142% of the preindustrial era. Because the energy sector causes for around two-thirds of all greenhouse-gas emissions, it will play a full part in effective implementation of the outcome. Global energy-related emissions of carbon dioxide reached 31.6 gigatonnes in 2012, which represents an increase of around 400 megatonnes (1.2%) compared with 2011 (coal contributes around 44% of total emissions, oil 36%, and gas the remaining 20%). While emissions of carbon dioxide fell in the United States (−4.1%) and the European Union (−1.2%), these emissions increase in China (3.1%), India (6.8%), Middle East (4%), Brazil (8%), Russia (0.3%), and Japan (3.4%). An increasing demand for coal in power generation is the primary cause in China and India or a result of the nuclear shutdown in Japan.

Emissions and climate impact in the New Policies Scenario are accepted by many governments, which are in the process of formulating policies to address climate change, directly or indirectly. It mainly includes additional measures to reduce air pollution from the use of coal and improve energy efficiency. The sobering news is that it is sufficient to discontinue the increase of carbon dioxide and other greenhouse gases overall. In addition to modeled factors, other increase of temperature by the greenhouse effect could result from irreversible changes such as slowly melting permafrost. Even in the New Policies Scenario, coal remains the principal source of
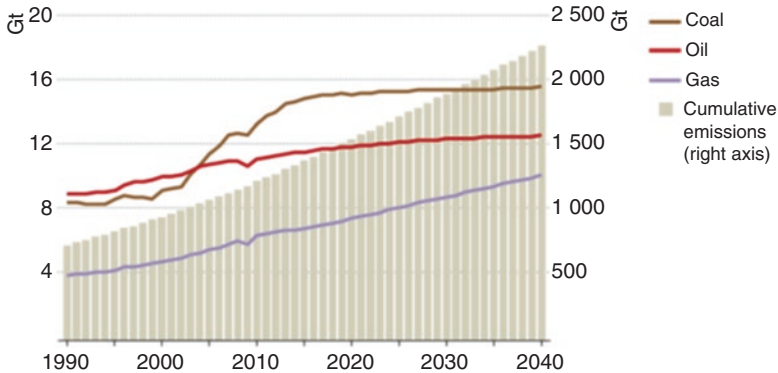
Fig. 3.14 Global emission of carbon dioxide related to global fossil fuel energy and total cumulative emissions of carbon dioxide in the New Policies Scenario. Source: IEA World Energy Outlook 2014

global energy, but coal-dependent emissions can be reduced by carbon capture and storage on a relatively limited scale before 2030. Emissions from natural gas and oil continue to increase. The strong rise in gas demand will make this fuel the largest contributor to emissions. But the lower carbon content of gas means that emissions from this source will be still lower than those of coal in 2040 (Fig. 3.14).

In the 450 Scenario, the reductions in emissions, relative to the New Policies Scenario, result from the assumption of much stronger government policies that preserve economic growth and that are adopted after the 2015 United Nations Climate Change Conference.

The detailed energy redistribution between sources and consumers in 2013 is illustrated in Fig. 3.15 for OECD countries and in Fig. 3.16 for non-OECD countries. The attached graphs show an export of fossil fuels, which is higher in non-OECD countries. Declining oil export indicates limited resources and increasing use in OECD countries.

An example of energy redistribution between sources and consumers in 2013 is shown in Fig. 3.17 for China. Now the export of fossil fuels is highly reduced due to increasing demands of the industry and public sectors. It also shows the high consumption of coal, which contributes significant emissions of carbon dioxide in the world scale. Other example represents redistribution between sources and consumers in 2013 for the Russian Federation with a high export of fossil fuels (Fig. 3.18). The attached graph illustrates an increasing level of a coal export.

3.1.3 The Energy Outlook from EEA

The EU is still dependent on fossil fuels such as oil, natural gas, and coal, but the share of fossil fuels in the total gross inland energy consumption decreased at an annual rate of 0.4% to 73.8% in 2013 (83% in 1990). The decreasing trend of fossil fuel
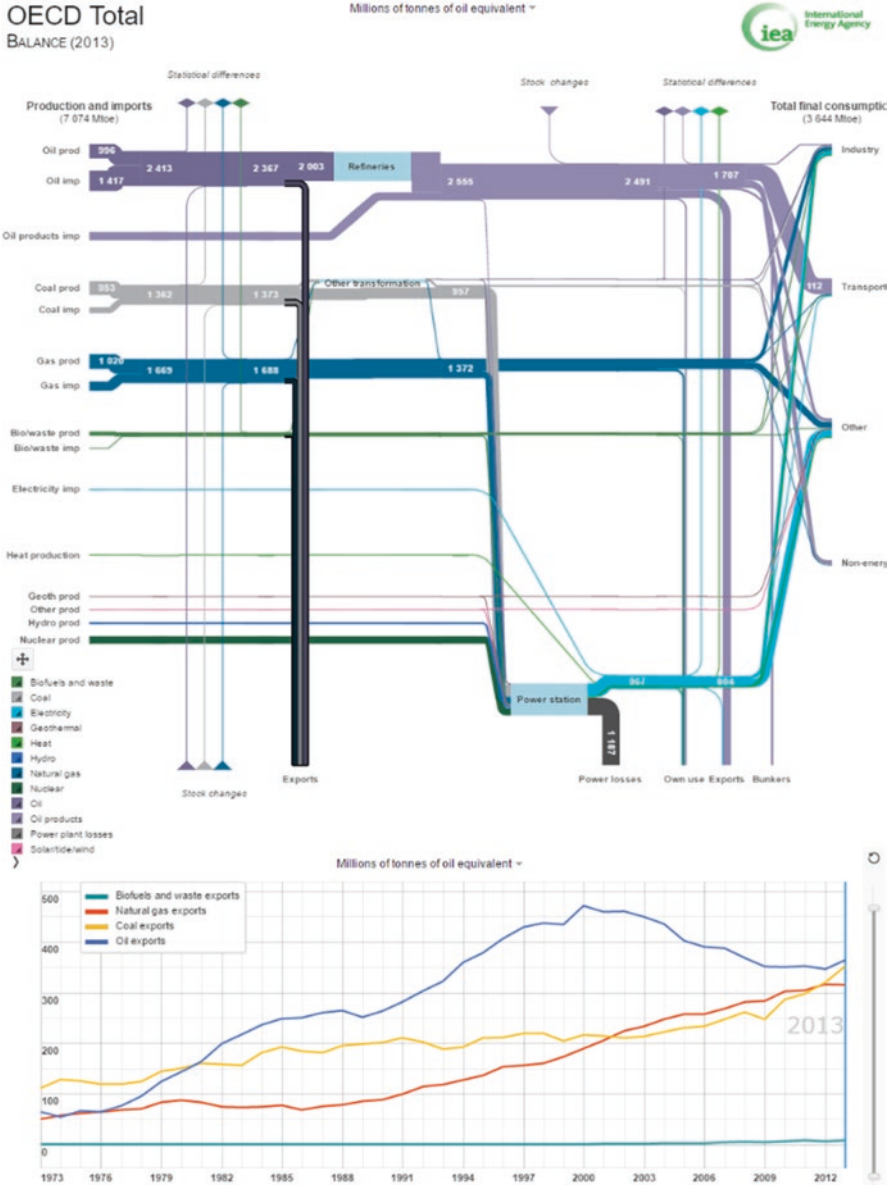
Fig. 3.15 Energy redistribution between sources and consumers by energy flow diagram for OECD countries

consumption has been caused by improving the efficiency of conventional thermal power plants and by expansion of the renewables for a few last decades. The renewables accounted for just about 11.8%. The EU is increasingly relying on imported fossil fuels from other countries. The share of net-imported fossil fuels in total gross
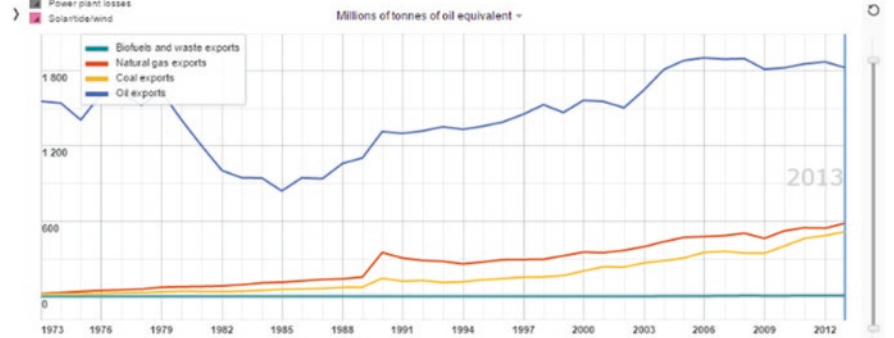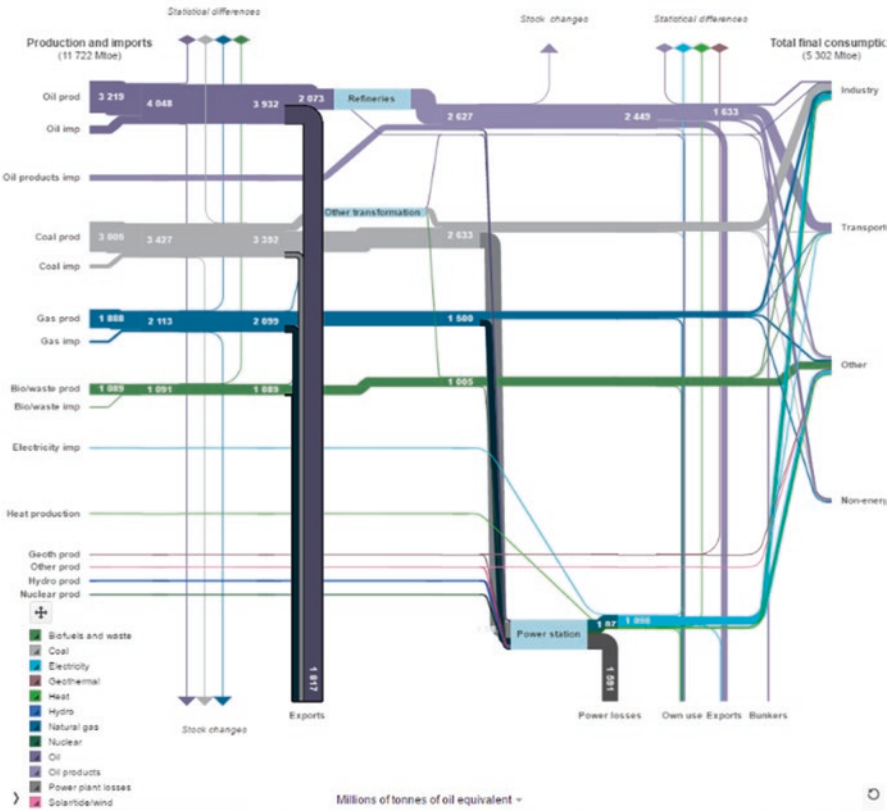
Fig. 3.16 Energy redistribution between sources and consumers by energy flow diagram for non-OECD countries

inland energy consumption increased to 53.2% in 2013 (44% in 1990). The main fossil fuel in total net imports was oil (58%) following by gas (28%) and solid fuels (14%) in 2013. The dependence on imports of fossil fuels remained stable between 2005 and 2013, at around 53% (as a share of total gross inland energy consumption) (Fig. 3.19). Now the EU relies more on imported fuels in comparison with 1990.
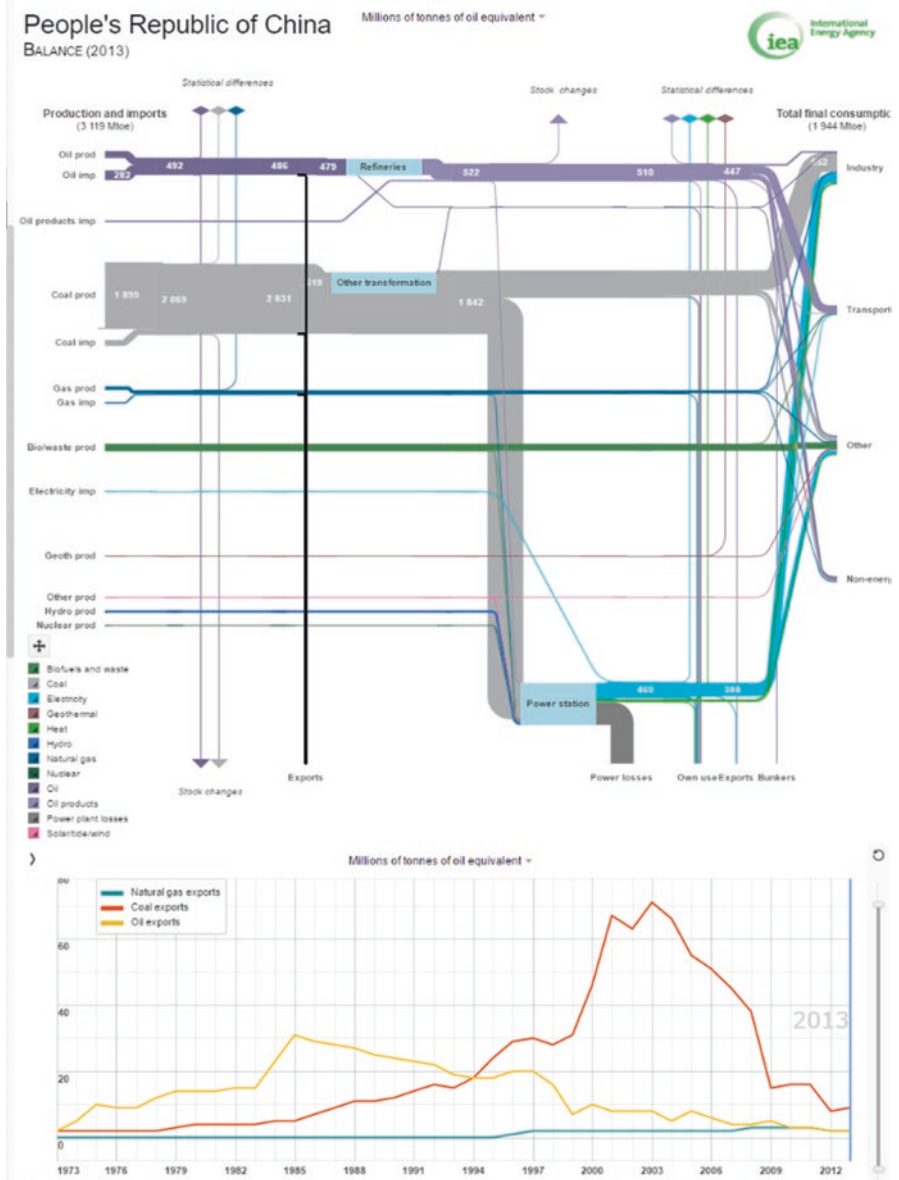
Fig. 3.17 Energy redistribution between sources and consumers by energy flow diagram for China

The EU also imports uranium for its nuclear power industry, which accounted approximately 38% of the world's civil nuclear power generation in 2013 (27% from Russia, 17% from Canada, 13% from Niger, 12% from Australia, 12% from Kazakhstan, and the reminder from other countries).
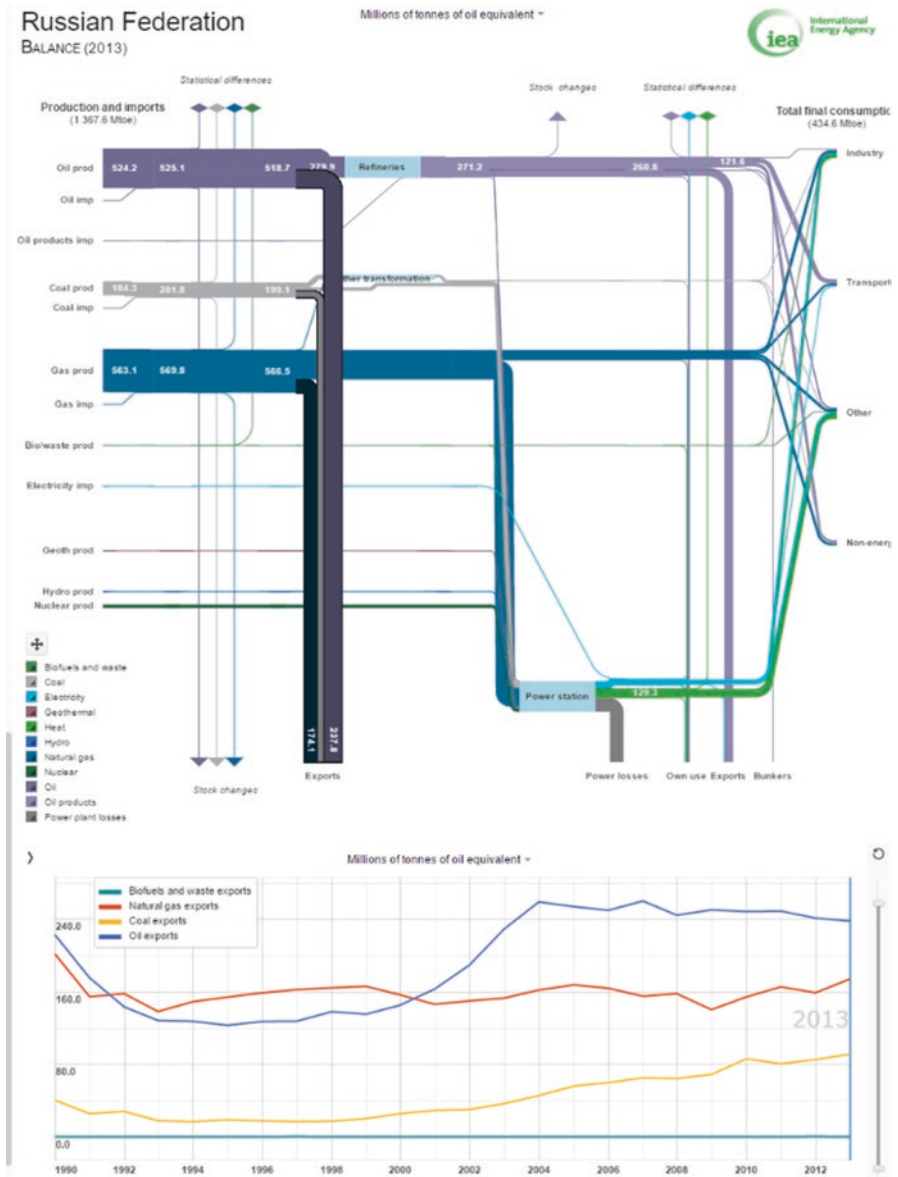
Fig. 3.18 Energy redistribution between sources and consumers by energy flow diagram for the Russian Federation

Fossil fuels are still important for the electricity mix, being responsible for almost one half of all gross electricity generation in the EU in 2012. Nuclear energy sources came second, contributing more than one quarter of all gross electricity generation in 2012. The share of electricity generated from renewable
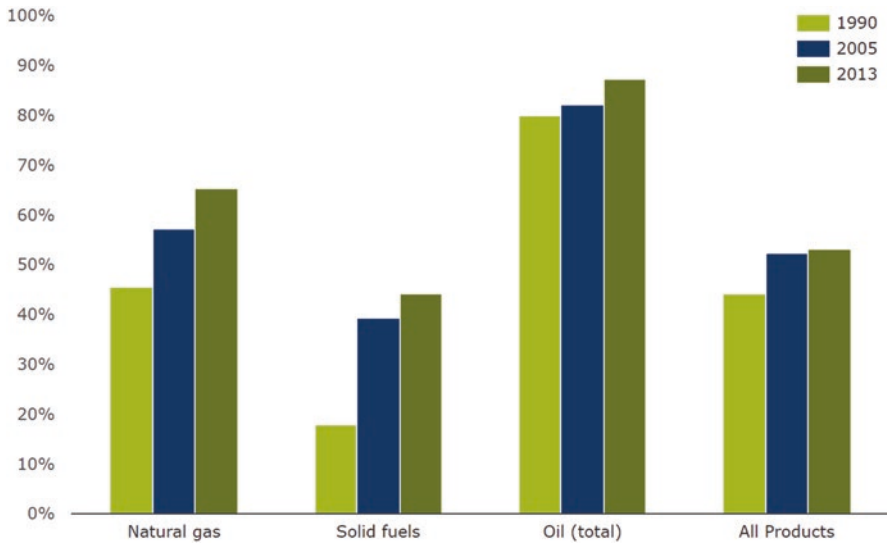
Fig. 3.19 Net imports of fuel types as a percentage of fuel-specific gross inland consumption ("All products" is the sum of net imports of solid fuels, gas, and total petroleum products as a percentage of the total gross inland consumption of all products.) Source: EEA, 2016

sources reached almost one quarter of all gross electricity generation in 2012. Final electricity consumption increased by 29% in the EU28 since 1990, at an average rate of around 1.2% per year. The strongest growth was observed in the services sector (3.0%/year), followed by households (1.4%/year) and industry (0.9%/year).

The key energy flows (in million tonnes of oil equivalent) for the EU based on Eurostat data are displayed in Fig. 3.20. On the left side, the diagram shows the gross inland consumption with the net amount of energy imported compared with that produced indigenously. These energy inputs are converted to heat, electricity, and manufactured fuels, through transformation plants such as power stations, district heating, oil refineries and other utilities, and the associated conversion losses. On the right side, the diagram shows the final mix of energy consumption by energy users such as industry, transport, domestic, other final consumers, and nonenergy use. In the flow energy diagram, the renewables in transport include all biofuels whether sustainable or not. Due to distribution losses and use in the energy sector, there are many diversions and losses incurred before energy reaches the final consumers. The largest losses are caused by conversion, where a proportion of the chemical energy in the fuel is not embodied in the power or heat leaving the generating plant, but is lost as unused waste heat. Fuels are also partially diverted for nonenergy purposes, for example, the use of natural gas as a chemical feedstock in the chemical industry for nonenergy purposes. Moreover, once generated, some of the power and heat is consumed by the plant operator and distributor for the purpose of running auxiliary equipment and distribution to the end users.
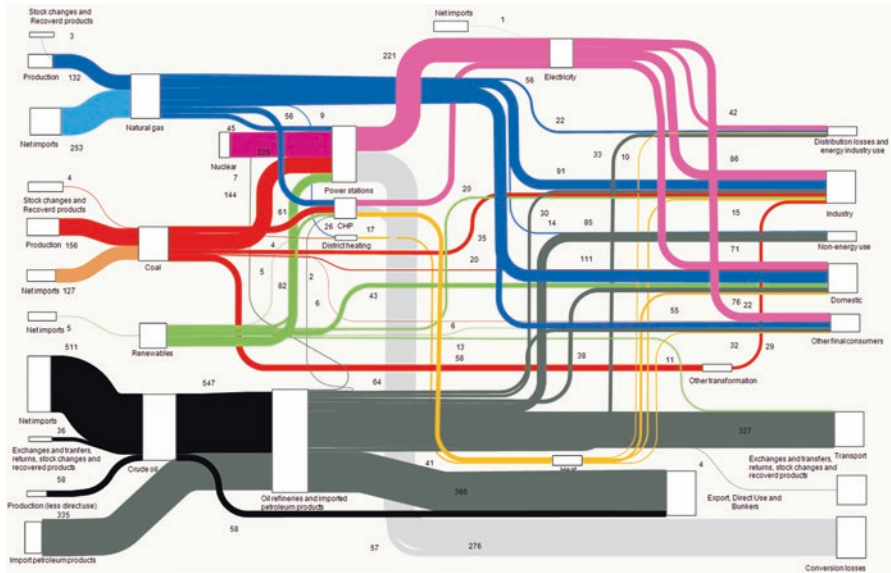
Fig. 3.20 The energy flows illustrated the composition of the primary energy entering the energy system of the EU in 2013, the conversion including, and the consumption by specific sectors of the economy in Mtoe. Source: EEA, 2016

3.2   Oil, Natural Gas, and Coal

World primary energy demand is estimated to increase by more than 30% between 2013 and 2040 (32% from 2013 to 2040 in the New Policies Scenario, which takes account of existing and planned government policies). The slowdown in demand growth can be mainly due to energy efficiency gains and structural changes in the global economy. In the next decades, oil, natural gas, and coal should be partly replaced by low-carbon fuels (mainly nuclear power and renewable energy) making up the rest. Oil will remain the single largest energy source, but concentrated mainly in sectors of transport and petrochemicals where substitution is most challenging. Mostly, the growth in energy demand will come from non-OECD countries. The energy markets will successively shift away from the Americas and Europe to Asia. Evidently China and India will be the dominant force behind global demand growth for the next decades. Despite energy use per capita in non-OECD countries will rise strongly over next decades, in 2040, it will be still below the level that was reached in OECD countries in the early 1970s. Technological progress and improved energy efficiency facilitate a higher level of demand for energy services to be satisfied per unit of energy.

From the view of sectoral trends, the energy demand grows most quickly in industry. In 2040 it is expected the increase by more than 40% in the IEA New Policies Scenario, which could exceed 4900 Mtoe (Fig. 3.21). The strongest growth
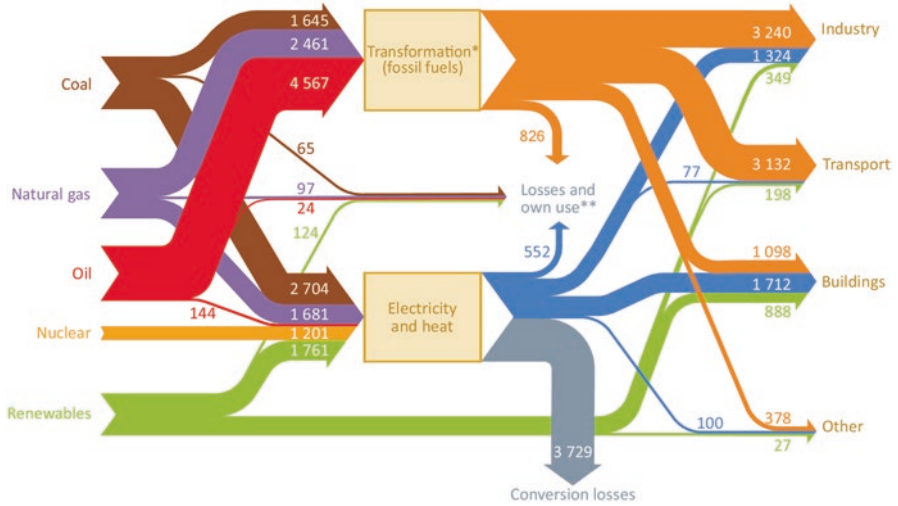
Fig. 3.21 World energy demand by fuel and sector in the New Policies Scenario, 2040 (Mtoe). Source: IEA World Energy Outlook 2015

of the industrial demand is expected in electricity and natural gas due to expansion of infrastructure in many developing countries. There is also expected a shift in fuel use in China's industrial sector, with coal consumption declining and natural gas and electricity increasing to fill the gap. India, one of the most populous countries of the world, has also the rising industrial demand, which is expected to overtake China as the world's largest consumer of coal in industry. Primary energy demand for transport should reach 3400 Mtoe in 2040 (with 85% being met by oil), where the road transport sector remains the leading source of global oil demand growth in the New Policies Scenario. Primary energy demand in the buildings sector will increase by nearly one-quarter in 2040 to nearly 3700 Mtoe due to higher incomes, a growing population, and demographic changes. Globally, energy demand for household appliances more than doubles in the New Policies Scenario with the significant increase in non-OECD markets. In consideration of growing demand for electricity, the power sector accounts for 55% of the growth in primary energy demand in 2040, and its share of the overall energy mix will increase to 42% in the New Policies Scenario.

Extraction of fossil fuels includes multiple uncertainties caused by economics and policy of particular countries. Resource owners must adopt their strategies to manage the risk and opportunities appropriately. But a profound challenge to a fossil fuel-dominated energy sources and the industry is climate change, which requires to proceed to a scenario consistent with meeting a 2 °C target such as 450 Scenario (Fig. 3.22). Even if the countries will move decisively toward the demand and emissions trajectory implied by this scenario, large-scale investment in a mining sector and manufacturing industry will remain an essential component of secure transition to low-carbon future. Government policies play a powerful role in creating the
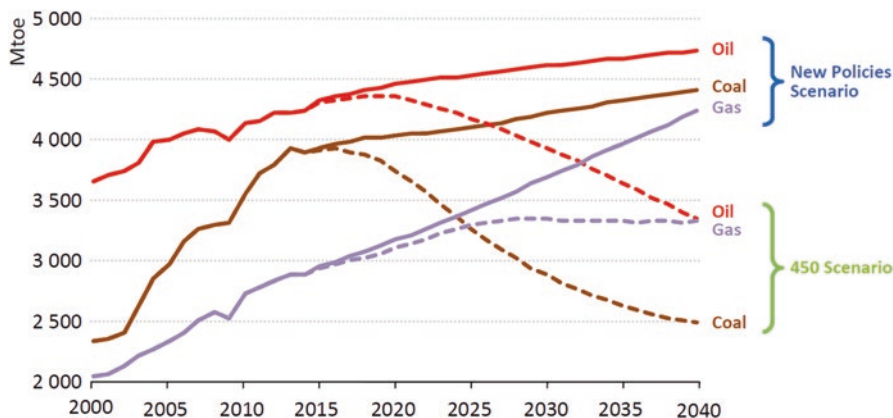
Fig. 3.22 Global fossil fuel demand in the 450 Scenario relative to the New Policies Scenario. Source: IEA World Energy Outlook 2015
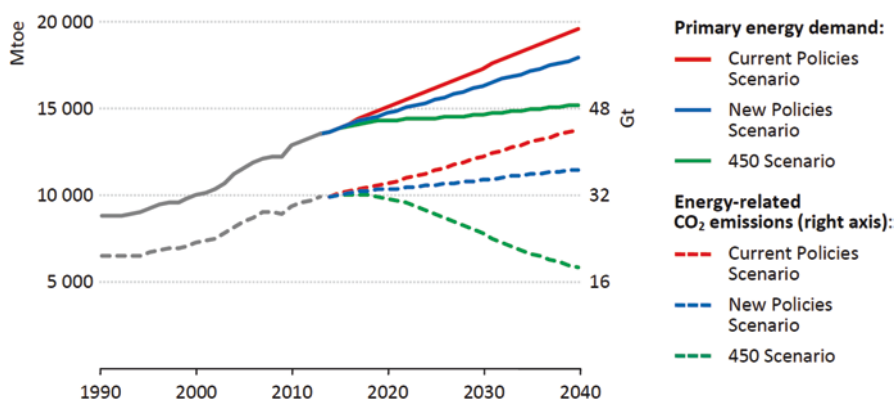
Fig. 3.23 World primary energy demand and carbon dioxide emissions by scenario. Source: EIA World Energy Outlook 2015

degree of growth to which energy-related emissions decouple from energy use. Overall, new energy and climate policies serve to restrain the pace at which energy demand grows in order to weaken the link between growth in energy demand and energy-related emissions (Fig. 3.23). Despite efforts to decarbonize the world's energy system, the share of fossil fuels in the global energy mix has changed little over the last 30 years. Renewables increase significantly, but their growth only partially substitutes the growing energy demand in the global energy mix.

World oil supply is estimated to rise to over 100 millions of barrels per day in 2040 in the New Policies Scenario in dependence on timely investments in the Middle East, the future major source of global supply growth (Table 3.3). The net growth in oil demand will come from non-OECD countries. China will become the

Table 3.3 Oil and total liquids demand by scenario (million barrels per day)

	2014	New Policies Scenario		Low oil price		Current Policies Scenario		450 Scenario	
		2020	2040	2020	2040	2020	2040	2020	2040
OECD	40.7	39.4	29.8	39.9	31.3	40.1	34.4	38.8	20.5
Non-OECD	42.9	48.9	63.6	49.4	65.4	49.7	71.4	47.7	46.7
Bunkers[a]	7	7.6	10	7.7	10.4	7.8	11.2	7.3	6.9
World oil	90.6	95.9	103.5	97	107.2	97.5	117.1	93.7	74.1
Share of non-OECD	47%	51%	62%	51%	61%	51%	61%	51%	63%
World biofuels[b]	1.5	2.1	4.2	1.9	3.3	1.9	3.6	2.1	9.4
World total liquids	92.1	98	107.7	98.9	110.4	99.5	120.7	95.8	83.4

Source: IEA World Energy Outlook 2015 (www.worldenergyoutlook.org/weomodel/)
[a]Includes international marine and aviation fuels
[b]Expressed in energy-equivalent volumes of gasoline and diesel

Table 3.4 Natural gas demand by major region and scenario (billion cubic meters)

	2000	2013	New Policies Scenario		Current Policies Scenario		450 Scenario	
			2020	2040	2020	2040	2020	2040
OECD	1413	1657	1704	1870	1744	2125	1684	1354
Non-OECD	1102	1850	2139	3258	2170	3491	2080	2662
World[a]	2515	3507	3849	5160	3914	5617	3770	4073

Source: IEA World Energy Outlook 2015
[a]The world numbers include the use of LNG as a marine bunker fuel

largest oil-consuming country in next decades, but it is expected that higher efficiency and decreasing growth in industrial activity will equalize oil demand after 2040. Meeting long-term demand will depend increasingly on the large OPEC resource holders in the Middle East, which is partially placed at risk renewed turmoil in the Middle East and North Africa. The refining sector will follow the new geography of oil demand and supply. By 2040, two out of every three barrels of crude oil traded internationally are expected to be destined for Asia in comparison with less than half today. The economic implications of low oil prices are good for oil consumers and importers. Oil producers and exporters are worse off, as the volume gains from higher output are more than offset by the effect of lower prices. Due to the low oil prices, energy-related CO_2 emissions are slightly higher, and efficiency improvements of some crucial low-carbon technologies are slowed when the policy considerations that underpin support for renewables do not change.

Natural gas indicates the fastest growing among the fossil fuels (Table 3.4). The proposed demand of 5.2 trillion cubic meters in 2040 brings gas toward main fossil fuels with coal and oil in the global energy mix. China and the Middle East are going to be the main consumers, which cause gas demand growth. Within the OECD, North America is the only region where gas demand expands significantly. LNG (liquefied natural gas, predominantly methane), which can be converted to

Table 3.5 Coal demand, production, and trade by scenario (million tonnes of oil equivalent)

				New Policies Scenario		Current Policies Scenario		450 Scenario	
		2000	2013	2020	2040	2020	2040	2020	2040
Demand	OECD	1573	1470	1307	878	1413	1289	1152	523
	Non-OECD	1774	4143	4454	5428	4627	6737	4208	3041
	World	3347	5613	5762	6306	6040	8026	5360	3565
	Steam coal	2590	4379	4523	5266	4784	6835	4175	2813
	Coking coal	452	940	929	785	941	851	903	601
	Lignite[a]	304	295	309	254	315	341	282	151
Production	OECD	1380	1361	1255	1042	1391	1505	1134	627
	Non-OECD	1875	4362	4507	5263	4648	6521	4226	2938
Trade[b]	World	471	1084	1143	1291	1221	1780	1038	594
	Steamcoal	310	814	847	984	913	1447	759	373
	Cokingcoal	175	272	299	311	310	337	284	229
Share of world demand	Non-OECD	53%	74%	77%	86%	77%	84%	79%	85%
	Steamcoal	77%	78%	79%	84%	79%	85%	78%	79%
	Trade	14%	19%	20%	20%	20%	22%	19%	17%

Source: IEA World Energy Outlook 2015
[a]Includes peat
[b]Total net exports for all WEO regions, not including intra-regional trade

liquid form for ease of storage or transport, is increasing more rapidly than pipeline gas. But deferred investment in LNG supply brings a risk of tighter markets in a low oil price environment, which can threaten the long-term competitiveness of gas in many importing markets. Besides carbon dioxide, the oil and gas sector is also the largest industrial source of methane emissions that is a potent contributor to climate change. In the absence of robust policy action including a systematic effort of measurement, reporting and monitoring in this area can represent a major missed opportunity to tackle near-term warming.

Global coal demand growth has seen a marked slowdown over the last years (Table 3.5). Coal demand in the global steel industry is levelling off. Thus, future growth hinges mainly on the power sector in non-OECD countries, especially Southeast Asia. Despite coal losing out to renewables as the source of electricity generation, it is estimated by the New Policies Scenario that it still accounts for 30% of global electricity output by 2040. Although coal use in China's power sector flattens and industrial coal demand falls markedly as the economy rebalances away from heavy industry, China still remains a key force in world coal markets. In the next decades, the second largest coal consumer and producer is estimated to be India as its demand nearly triples and production grows more than in any other country. In the United States, the actual world's second-largest coal market, demand peaked in 2005 and has since declined by 23%, primarily due to competition from abundant unconventional gas. Despite new developments in climate and local pollution policies, global trade in coal grows 20%. In the 450 Scenario, world coal demand peaks in the

current decade and then declines by 33% to return to the level of use in the early 2000s. This large reduction in coal uses results from the policies that governments worldwide must adopt toward setting the energy system to keeping long-term increase in the average global temperature to below 2 °C. Today all major producing countries are affected by coal production cuts to some degree. It is expected that, since the end of 2012, between 280 and 330 million tonnes per annum of production capacity has been removed from the global market, mainly in China with the bulk of the reduction about 180–200 million tonnes per annum. Finally, coal prices are also largely dependent on transport costs of coal, of which oil can be a significant component.

3.3   Nuclear Energy

After hydropower, nuclear energy is the world's second largest source of low-carbon electricity generation accounted for 11% (392 GW) of electricity generation. But this share has decreased since 1996, when it was almost 18%. OECD countries operate about 80% of nuclear capacity, but more than three-quarters is over 25 years old. It raises the question about replacement of obsolete equipment to new technology with higher safety and more efficient systems. In the last several decades, the nuclear sector has been focused on improving security and capacity factors, and construction starts on new reactors that have been very slow. The risk in constructing and operating new plants influenced by a combination of public attitudes to nuclear power is critical to its future development. The economics of nuclear power is dependent on many factors such as regulatory and policy conditions in particular regions, external costs in dependence on implemented safety systems, external benefits in avoiding carbon dioxide emissions, and its significant contribution to energy security. In the last decade, the nuclear capacity under construction (about 76 GW) has been mainly in non-OECD countries (40% in China). Also around half of the capacity in non-OECD countries (excluding Russia) operates less than 15 years.

Construction of nuclear plants accelerated during the 1960s and peaked after the oil price shock of 1973–1974. During this period, nuclear power has become a significant feature of the global energy mostly in Europe and the United States (Fig. 3.24). But the accident at Three Mile Island in the United States in 1979 slowed license approvals around the world, and the accidents at Chernobyl in Ukraine in 1986 and at Fukushima in Japan further depressed activity in Europe and Japan. Some countries changed their focus in alternative energy sources such as combined-cycle gas turbines or renewables. Also flatten electricity demand and electricity glut in many countries have forced investments cuts in new nuclear plants. A resurgence in new nuclear plants has been driven mainly by China since the late 2000s, in order to meet growing electricity demand and to reduce air pollution. Key nuclear power statistics by region is shown in Table 3.6, which shows basic information about operational reactors, installed capacity, electricity generation, share of electricity generation, and reactors that are under construction in the end 2013. Japan's nuclear reactors have largely been idled since the accident at Fukushima Daiichi in March 2011.
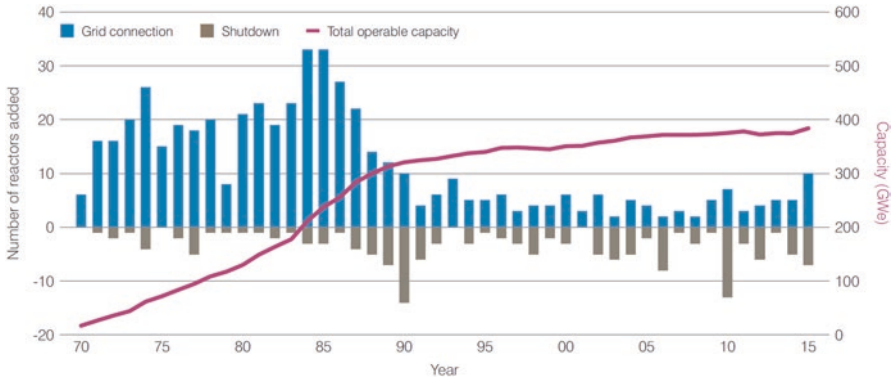
Fig. 3.24 Reactor construction starts and timeline of events. Source: WNA World Nuclear Performance Report 2016

Table 3.6 Key nuclear power statistics by region at the end of 2013

	Operational reactors	Installed capacity (GW)	Electricity generation (TWh)	Share of electricity generation	Under construction (GW)
OECD	324	315	1961	18%	20
United States	100	105	822	19%	6.2
France	58	66	424	74%	1.7
Japan	48	44	9	1%	2.8
Korea	23	22	139	26%	6.6
Canada	19	14	103	16%	0
Germany	9	13	97	15%	0
United Kingdom	16	11	71	20%	0
Other	51	41	297	11%	2.7
Non-OECD	110	78	517	4%	56
Russia	33	25	171	16%	9.1
China	20	17	117	2%	32
Ukraine	15	14	83	44%	2
India	21	5.8	32	3%	4.3
Other	21	16	113	2%	9.5
World	434	392	2478	11%	76

Source: IEA World Energy Outlook 2014 (International Atomic Energy Agency: Power Reactor Information System)

In the New Policies Scenario, nuclear power capacity is increased by almost 60% (from 392 GW in 2013 to 624 GW in 2040). It is estimated that the growth in nuclear energy to 2040 accounts for 46% in China, while India, Korea, and Russia collectively make up a further 30%. Nuclear generation may increase by 16% in the United States and rebounds in Japan to the lower levels before the accident at Fukushima. In the European Union, nuclear power may decline will by 10%, due to shifts in policy and limited lifetime extensions. Nearly half of the European Union
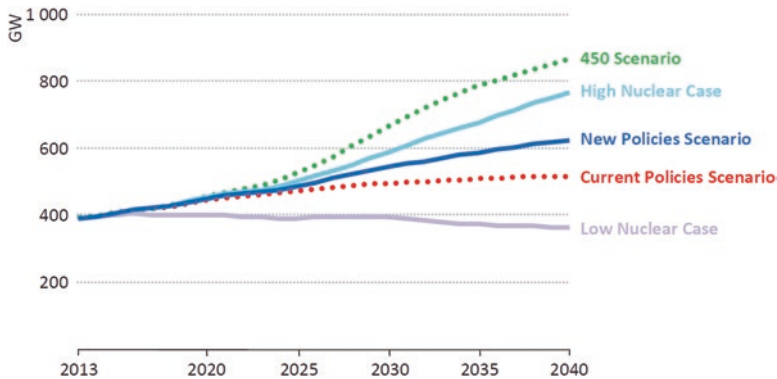
Fig. 3.25 Global nuclear power capacity by scenario and case. Source: IEA World Energy Outlook 2014

is retired in the period to 2040. If there are no substantial new capacities for those reactors that are replaced, nuclear capacity of the European Union would fall to 5% of current levels by 2040. Worldwide retirements of aging nuclear reactors represent almost 200 of the 434 reactors operating at the end of 2013 in the period to 2040 with the majority in the European Union, the United States, Russia, and Japan. Due to a combination of economic, political, and social factors, an idea of the low nuclear case estimates nuclear power capacity declining to 366 GW in 2040 (the nuclear share of generation declining to 7%). By contrast in the high nuclear case, capacity rises to 767 GW (the nuclear share of generation rising to 14%), as greater value is attributed to nuclear power's contribution to carbon abatement and baseload output. In 450 Scenario, the nuclear capacity is even higher, about 862 GW in 2040, in order to meet ambitious climate targets (Fig. 3.25).

New mines will need to be open as early as the 2020s, because uranium production at existing facilities declines. But the resources of uranium are sufficient to provide fuel to satisfy any of proposed scenarios. Recently identified resources can support consumption at current rates of use to over 120 years. If potential undiscovered resources are included, it can even extend to over 250 years. The world's largest uranium resource-holder with 29% of the total identified uranium resources is Australia (29%) followed by Kazakhstan (12%). Other countries, which are larger uranium resource-holders, have less than a 10% share of total identified resources as a single country. Total uranium production was estimated about 60,000 tonnes in 2013. Kazakhstan is the world's largest producer, with 36% of total production, followed by Canada, Australia, Niger, and Namibia. These world's largest producers account for approximately four-fifths of total output.

The initial costs to build new nuclear plants and to finance other supporting utilities are extremely high, but they can offer economic benefits by adding stability to energy systems. Nuclear power is one of a limited number of options that can reduce carbon dioxide emissions in energy mix. It is estimated that nuclear power plants have avoided the release about 56 Gt of carbon dioxide since 1971, which is close to 2 years of emissions at current rates.

3.4 Hydroelectricity

Electricity generated by hydropower represented 16.6% of the world total electricity in 2015 and is estimated to increase about 3.1% each year for the next decades. Hydropower helped avoid about 64 Gt of carbon dioxide emissions globally in the period 1971–2013, which is more than nuclear power or any other low-carbon technology. The majority of hydropower was in Europe and the United States up to 1980, which accounted for about 40% of global hydropower capacity. The new projects constructing a new capacity of 76 GW (leading by the Itaipu dam, installed capacity 14 GW, completed in 1984) moved a leading position to Latin America in the period 1980 to 2000. Since 2014, China has become the world leader in hydropower with about 300 GW of installed capacity (leading by the Three Gorges dam, installed capacity 22.5 GW, completed in 2012, when the last main generator finished its final test). Top ten of the largest hydroelectric producers are shown in Table 3.7, where the annual hydroelectric production and installed capacity is complemented by the capacity factor, the ratio between annual average power, and installed capacity rating. The countries such as Brazil, Canada, Norway, and Venezuela have a majority of the internal electric energy production from hydroelectric power. Other countries such as Switzerland, Austria, New Zealand, and Paraguay have also this majority. Many countries export their seasonal surplus hydroelectric power to their neighboring countries.

Large reservoirs and pumped storage can also provide flexibility to meet fluctuations in electricity load, which are becoming more acute with the rapid growth of renewables such as wind power and photovoltaic power plants. On the other side, the fluctuations by changes in rainfall and average temperatures in output in Latin America and China indicate that hydropower has the highest annual variation of any renewable energy technology. It can be more significant due to further changes resulting from the effects of global climate change, with greater rainfall and hydropower output in some regions and less in others.

Based on New Policies Scenario estimates, hydropower installed capacity by region is illustrated in Fig. 3.26. Hydropower continues to expand in most parts

Table 3.7 Top ten of the largest hydroelectric producers

Country	Annual hydroelectric production (TWh)	Installed capacity (GW)	Capacity factor	% of total production
China	920	194	0.37	16.90%
Canada	392	76	0.59	60.10%
Brazil	391	86	0.56	68.60%
United States	290	102	0.42	6.70%
Russia	183	50	0.42	17.30%
India	142	40	0.43	11.90%
Norway	129	31	0.49	96.10%
Japan	85	49	0.37	8.10%
Venezuela	84	15	0.67	67.80%
France	76	25	0.46	13.20%

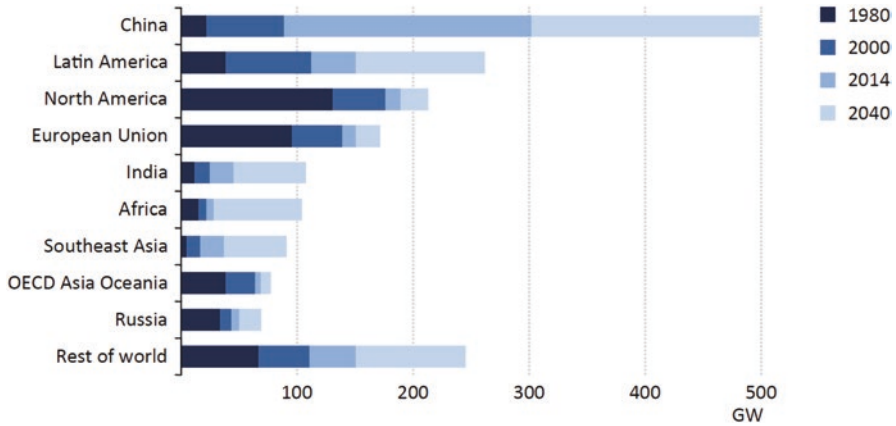Source: IEA Key World Energy Statistics, 2015

Fig. 3.26 Hydropower-installed capacity by region in the New Policies Scenario in the period from 1980 to 2040. Source: IEA World Energy Outlook 2015

around the world through to 2040, but environmental concerns and social considerations may limit its growth. China extends its lead in hydropower capacity by projects that tap large river systems. Also Latin America extends its hydropower capacity in spite of social and environmental concerns that drive a technological shift from reservoir hydropower to run-of-river designs. In OECD countries, hydropower capacity increases only moderately. Canada is planning a number of large-scale projects. The United States restrict new projects and limit expansion of existing sites. In Europe, the majority of hydropower potential has already been exhausted, and other forms of renewable energy are explored to fulfil energy supply and climate goals. India expects to double its hydropower capacity to 2040. In dependence on geography, Africa has large hydropower potential remaining mainly Congo and Ethiopia. Other countries in Asia excluding China and India expand hydropower capacity substantially. The mentioned hydropower capacity is mainly based on large projects, which can supply over 10 MW. These large hydropower plants represent about 94% of global installed hydropower capacity in 2014. They will dominate in China, Latin America, and Africa. In many countries over the world and especially in Europe, there is potential for small-scale projects that require shorter authorization processes and are less politically sensitive. These projects are without large reservoirs to smooth out variability in river flow and are more vulnerable to weather variability, but in the mix of other renewables can help to supply regional electricity consumption.

3.5 Renewable Energy

Renewables, energy sources capable of being replaced by natural ecological cycles or sound management practices (Merriam Webster), include wind power, hydropower, solar energy, geothermal energy, bioenergy, and other tools that can

complement these systems such as energy storage tools and advanced control systems. Hydropower used to be often classified separately due to constructing "nonrenewable" large hydroelectric dams and reservoirs in case of conventional hydroelectric power stations. Renewables accounted for 85% of the increase in total electricity generation in 2014 compared to 2013. Over the last decade, there has been the significant increase in hydropower (318 GW), wind power (304 GW), and solar photovoltaics (173 GW). The New Policies Scenario supports using of renewables in the total primary energy demand from 14% in 2014 to 19% in 2040. It represents global capacity additions of renewables totaling about 3600 GW over 2015–2040. Recently, nearly three-quarters of renewable generation mainly from hydropower is competitive without subsidies. But it is expected that the fully competitive share of non-hydro renewables doubles to one-third in 2040. In case of solar photovoltaics, the solar industry in Asia dominates the global market and continues its dominance with rising demand for solar photovoltaics and low production costs. Thus, the majority of added solar photovoltaics in the United States and European Union is imported from Asia. Renewables may avoid nearly 135 Gt of carbon dioxide over 2014–2040. Power generation from new renewable installations can avoid 50 Gt to 2040 (carbon dioxide related to their production may be about 1.3Gt). In order to reduce energy-related emissions, each scenario continues to expand renewables in dependence on local conditions and upon the strength of government policies. The principal scenarios (Current Policies Scenario, New Policies Scenario, and 450 Scenario) are shown in Table 3.8, which summarized primary demand, electricity generation, heat, biofuels, and traditional use of solid biomass. The Current Policies Scenario assumes the implementation of existing government policies, which results in 15% of the share of renewables in global total primary energy demand throughout the period to 2040. The New Policies Scenario, the most expected scenario, assumes implementation of cautious policies and predicts increasing of the share of renewables to 19% in 2040. The 450 Scenario (achieves an emission trajectory consistent with a 50% probability of limiting the average global temperature increase to the international goal of 2 degrees Celsius) estimates the share of renewables 29%, which means that the share of renewables in total primary energy demand quadruples in the United States, nearly triples in the European Union, and doubles in China.

The traditional use of solid biomass in the developing world is projected to decline in all scenarios due to economic growth that enables greater access to modern energy services. In the New Policies Scenario, it may decline from 40% in 2013 to 18% in 2040. The 450 Scenario expects falling to just 13%.

In the power sector, electricity generation from renewables is expected to increase by 2.5 times in the New Policies Scenario in the period from 2013 to 2040. Renewables also make up for the declining share of coal and surpass natural gas becoming the second-largest source of electricity, trailing only coal in total generation. In case of continued policy support and environmental restriction for coal-fired power plants, renewables will become the largest source of electricity in the next decades. Over two-thirds of the global increase in renewables generation is expected in non-OECD countries, as they have to supply demand that more than doubles

Table 3.8 World renewables consumption by scenario

		New Policies		Current Policies		450 Scenario	
	2013	2025	2040	2025	2025	2025	2040
Primary demand (Mtoe)	1863	2507	3346	2423	3030	2687	4388
United States	147	217	323	201	286	258	499
European Union	209	292	378	277	342	309	457
China	331	448	589	430	517	485	808
Share of global TPED	14%	16%	19%	15%	15%	19%	29%
Electricity generation (TWh)	5105	8784	13,429	8202	11,487	9549	17,816
Bioenergy	464	902	1454	865	1258	973	2077
Hydropower	3789	4951	6180	4854	5902	5083	6836
Wind	635	1988	3568	1701	2778	2344	5101
Geothermal	72	162	392	143	299	197	541
Solar photovoltaics	139	725	1521	593	1066	862	2232
Concentrating solar power	5	50	262	41	147	83	937
Marine	1	6	51	5	37	7	93
Share of total generation	22%	29%	34%	26%	27%	34%	53%
Heat (Mtoe)[a]	364	492	691	484	653	510	834
Industry	206	264	357	271	373	267	378
Buildings* and agriculture	158	227	334	213	279	243	456
Share of total final demand*	10%	13%	16%	12%	14%	14%	22%
Biofuels (mboe/d)[b]	1.4	2.6	4.2	2.3	3.6	4	9.4
Road transport	1.4	2.6	4.1	2.3	3.5	3.6	7.6
Aviation[c]	–	0.02	0.1	0.02	0.1	0.4	1.8
Share of total transport fuels	3%	4%	6%	4%	5%	7%	18%
Traditional use of solid biomass (Mtoe)	759	722	600	727	611	711	574
Share of total bioenergy	55%	44%	32%	45%	33%	41%	25%
Share of renewable energy use	41%	29%	18%	30%	20%	26%	13%

Source: IEA World Energy Outlook 2015
[a]Excludes traditional use of solid biomass in households
[b]Expressed in energy-equivalent volumes of gasoline and diesel
[c]Includes international bunkers. Notes: TPED = total primary energy demand; mboe/d = million barrels of oil equivalent per day

from 2013 to 2040. One-quarter of the global increase in renewables-based generation will be realized in followed by India and Latin America (Fig. 3.27). Hydropower will dominate in non-OECD countries, and other renewables such as wind power and solar PV will make large gains, rising their electricity generation to 15% by 2040. In OECD countries, renewables will account for less than one-third of the global increase in the next decades, in order to reduce the consumption of fossil fuels in large part. Despite the limited electricity demand growth, renewables will raise their share in total generation to nearly 40% by 2040, to a higher level than in non-OECD countries. In the United States, the increased volume of power generation from renewables is similar to Europe; renewables are expected to remain in
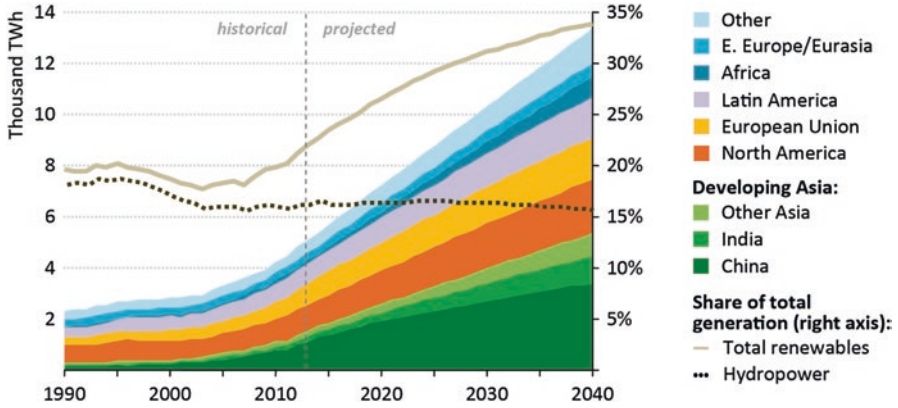
Fig. 3.27 Renewables-based electricity generation by region in the New Policies Scenario. Source: IEA World Energy Outlook 2015

total generation less than 30%. But applied research and implementation in global and regional scales is highly dependent on policies that provide financial support such as direct payments, fixed remuneration, tax rebates, dedicated auctions, green certificates, and facilitated financing conditions. Thus, the use of renewables is highly dependent on initial cost reductions and innovative policy approaches that can help renewables to make inroads into new markets.

3.6 Environmental Effects

Environmental pollution is highly dependent on energy production and use of poorly regulated or inefficient fuel combustion. In the global scale, air pollution is one of major public health risks. The most important man-made sources of air pollution emissions are particulate matter, sulfur oxides, and nitrogen oxides. The mentioned pollutants are responsible for widespread impacts, either directly or once transformed into other pollutants via chemical reactions in the atmosphere. In developing countries, air pollutants are emitted mainly as a result of cooking and lighting by more than 2.7 billion people who using the wood and other solid fuels. In developed countries, air pollutants originate from fossil fuel-intensive development and urbanization, where cities become pollution hotspots with high concentration of people, energy use, construction activity, and traffic. Concentration of air pollutants is measured in the local and global scale, in order to put aggregate global emissions of the main pollutants on a slowly declining trend. As an example, the animation based on the Goddard Earth Observing System Model (GEOS-5) is illustrated in Fig. 3.28, where the GEOS-5 system is used with the GOCART module of AeroChem to make real-time estimates and forecasts of aerosols and CO and CO_2 tracers in support of NASA field campaigns from August 2006 through April 2007.
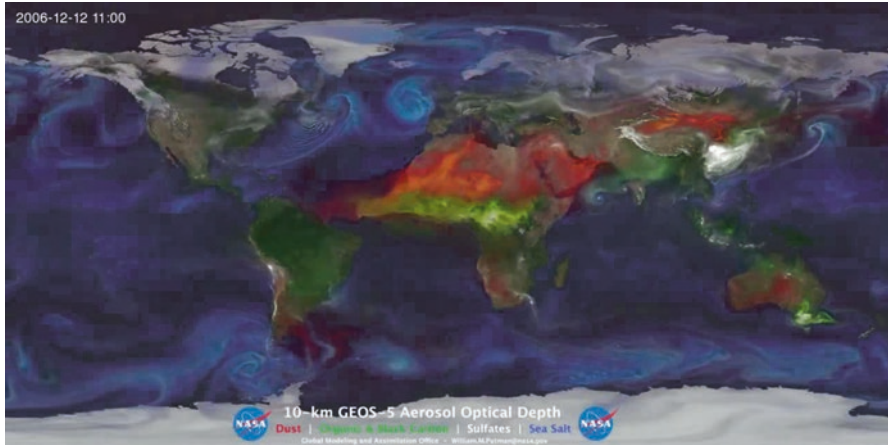
Fig. 3.28 The extinction optical thickness of aerosols from a free running 10 km GEOS-5 nature run including dust (*red*), sea salt (*blue*), black and organic carbon (*green*), and sulfate (*white*) are depicted from August 2006 through April 2007. Source: http://gmao.gsfc.nasa.gov/research/aerosol/

Air pollution is caused by many pollutants that may occur naturally (wildfires and volcanoes) or artificially (by human activity), stay in the atmosphere from minutes to years, and affect the environment in local, national, regional, or global scales. Primary pollutants are emitted directly as a result of natural and human activities, while secondary pollutants are derived from primary pollutants and other reacting compounds. The main air pollutants from human activity include:

– Sulfur oxides SO_x (in particular sulfur dioxide SO_2) are released at combustion such as in power generation or industrial processes to the atmosphere and linked to environmental effects, as well as being a precursor to the formation of secondary pollutants such as secondary particulate matter.
– Nitrogen oxides NO_X (in particular nitrogen oxide NO and nitrogen dioxide NO_2) are released from high-temperature combustion, mainly in transport and power generation. NO_2 is a toxic pollutant that can lead to the formation of secondary pollutants such as secondary particulate matter and ozone.
– Particulate matter (PM) is a mix of solid and liquid, organic and inorganic substances classified by their diameter (e.g., PM_{10} and PM2.5 with the diameter less than 10 μm and 2.5 μm, respectively), as natural or artificial pollutants are formed by the incomplete combustion of fossil fuels and bioenergy and are short-lived climate pollutants. Finer particles are particularly harmful to health as they can penetrate deep into the lungs.
– Carbon monoxide (CO) is a toxic gas that comes from the incomplete combustion of road transport fuels, natural gas, coal, or wood.
– Volatile organic compounds (VOCs) are released from artificial chemicals as well as natural sources as they evaporate or sublimate into the surrounding air and have negative health effects.

– Methane (CH_4) is the main component of natural gas and is often considered separately from other VOCs.
– Ammonia (NH_3) is released in relation to agricultural and waste management activities and reacts with oxides of nitrogen and sulfur to form secondary particles in the atmosphere.
– Ground-level ozone (O_3) is formed from NO_X and VOCs in the presence of sunlight and, at high concentrations, has negative health effects.
– Other air pollutants include heavy metals such as lead emitted from industry, power generation, and waste incineration; mercury originated mainly from industry.

The sources of air pollution are widespread over the world. Some pollutants disperse only locally, while others are moved large distances in the atmosphere and can have regional and even global impacts. The composition and level of energy-related air pollution in each country is also related to climatic conditions and stage of economic development. In developing countries at low-income levels, households tend to be reliant on solid biomass the combustion of which can lead to undesirable exposure to particulate matter. In developed countries with industrialized economy, societies massively use fossil fuels in power generation and industry, which results to high emissions of sulfur dioxide and other pollutants. Agriculture is based on intensified farming and the use of chemical fertilizers and pesticides, which can result in higher levels of air pollution, as well as having other environmental impacts. Other demands for more energy services, including electricity for appliances and oil for transport, result in higher emissions of sulfur oxides, nitrogen oxides, and other pollutants. Continuing industrialization and urbanization bring demographic changes and can also boost and concentrate energy-related air pollution in large cities. The energy sector becomes the largest source of air pollution emissions from human activity. The emissions come primarily from the combustion of fossil fuels and bioenergy. Other sources of emissions represent mining industry and industrial activities that have to be used for processing of coal, transportation of coal and natural gas, oil refining, as well as non-exhaust emissions from the transport sector. Selected primary air pollutants and their sources are illustrated in Fig. 3.29. The key pollutants include sulfur dioxide, nitrogen oxides, and particulate matter. The emissions from these pollutants are mainly caused by energy production and use over the whole world, but their occurrence of mentioned pollutants is dependent on regional conditions such as local economic activity, population size, the energy mix, and geographic and meteorological conditions that affect pollutant dispersion in the atmosphere. In many countries, existing and planned policies are not sufficient to reduce the impacts of air pollution. Pollutant emissions are expected to rise as energy demand grows as economies develop, with the result of declining the environment and impacting the human health. Thus, an alternative scenario, the Clean Air Scenario, has been developed by IEA to achieve through stronger policy action, delivering a significant reduction in pollutant emissions and the consequent
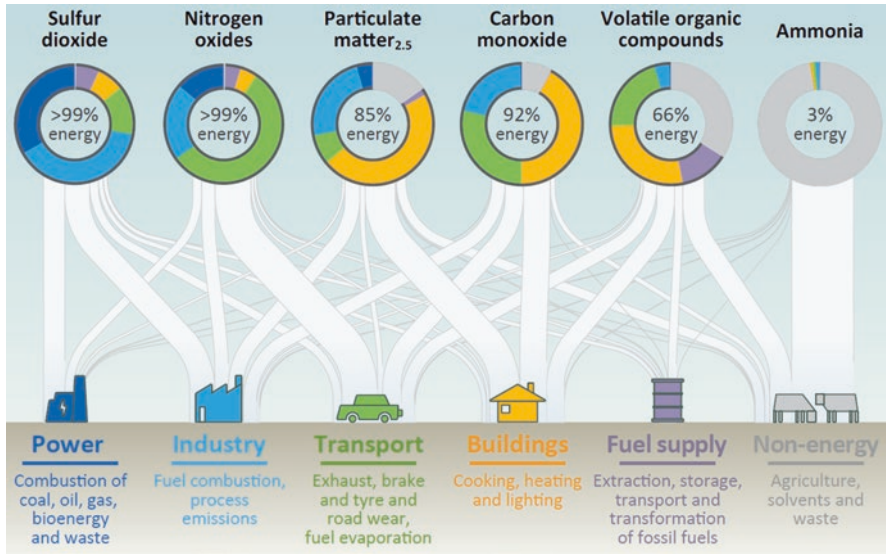
Fig. 3.29 Selected primary air pollutants and their sources, 2015. Source: IEA World Energy Outlook Special Report 2016

impacts on human health. It does offer a pragmatic agenda for change by efficiency improvements in existing technologies that are known and proven already today. The policies are categorized into two ways: those that avoid pollutant emissions and those that reduce emissions and their impacts (Table 3.9). Each country can approach these policy goals from a different starting point. Countries with well-developed regulatory frameworks are in a position to go faster. For other countries, full implementation of these policies requires a concerted effort over an extended period of time. Regulations include increasing energy efficiency, reducing the use of the least efficient coal-fired power plants, increasing investment in research, and implementation of renewable energy technologies.

The degree to which environmental protection including air quality is adopted in the New Policies Scenario differs by country, depending on its status of development and its structure of the energy mix. In the New Policies Scenario, global primary energy demand increases by one-third to 2040 driven by population and economy growth. The main contribution to satisfying total global energy demand growth is expected from energy sources that emit little amounts of air pollutants during normal operations such as nuclear, hydropower, wind, and solar energy. Although global energy demand continues to grow in the New Policies Scenario, energy-related air pollutant emissions decline in many countries from 2015 to 2040 (SO_2 by 20%, NO_X by 10%, and $PM_{2.5}$ by 7%) (Fig. 3.30).

Table 3.9 Clean Air Scenario

Policy pillars to avoid air pollutant emissions	Policy pillars to reduce air pollutant emissions
Strong push for industrial and power sector efficiency: For industry, the introduction or strengthening of existing minimum energy performance standards for electric motor-driven systems. In the power sector, reduced use of inefficient coal-fired power plants (typically subcritical) and a ban on new inefficient coal-fired power plants	Stringent emission limits for new and existing combustion plants: For plants above 50 MW$_{th}$ (megawatts thermal) using solid fuels, emission limits are set at 30 mg/m^3 for PM and 200 mg/m^3 for NO$_X$ and SO$_2$. Existing plants need to be retrofitted within 10 years. Emission limits for smaller plants (below 50 MW$_{th}$) depending on size, fuel, and combustion process[a]. Industrial processes required to be fitted with the best available techniques in order to obtain operating permits[b]
Strong efficiency policies for appliances and buildings: Introduction or strengthening of existing minimum energy performance standards for appliances, lighting, heating, and cooling. Introduction of mandatory energy conservation building codes	Stringent controls for biomass boilers in residential buildings: Emissions limits for biomass boilers set at 40–60 mg/m^3 for PM and 200 mg/m^3 for NO$_X$[c]
Higher fuel-efficiency standards: Adoption or strengthening of fuel-economy standards for road vehicles, including for both light- and heavy-duty vehicles.	Higher vehicle emissions standards: For light-duty diesel vehicles: limits as low as 0.1 g/km for NO$_X$ and 0.01 g/km for PM. For heavy-duty diesel vehicles and machinery: limits of 3.5 g/km for NO$_X$ and 0.03 g/km for PM. For all vehicles, full on-road compliance by 2025. A ban on light-duty gasoline vehicles without three-way catalysts and tight evaporative controls and a phaseout of two-stroke engines for two- and three-wheelers
Increased support to nonthermal renewable power generation: Increased investment in renewable energy technologies in the power sector	Fuel switching to lower emissions fuels: Increased coal-to-gas switching and use of low-sulfur fuels in maritime transport
Better public transport, urban planning, and support to alternative transport fuels: Promotion of public transport, a switch to electric two- and three-wheelers, electric commercial vehicles, and natural gas buses	Improved fuel quality: Maximum sulfur content of oil products capped at 1% for heavy fuel oil, 0.1% for gasoil, and 10 ppm for gasoline and diesel
Access to electricity/clean cooking facilities: Enhanced provision of electricity and clean cooking access based on renewable technologies	Access to electricity/clean cooking facilities: Enhanced provision of improved cook stoves and modern fuels for cooking
Support avoid and/or reduce via a change in economic incentives	
Phaseout fossil fuel consumption subsidies: Pricing reforms that remove the incentives for wasteful consumption of fossil fuels	

Source: policy pillars to avoid or reduce air pollutant emissions. Source: IEA World Energy Outlook Special Report 2016

Notes: MWth =megawatts thermal; mg/m^3 = micrograms per cubic meter; g/km = grams per kilometer; ppm = parts per million

[a]The Medium Combustion Plants Directive of the European Union and the revised US Clean Air Standards from 2015 provided the guidelines for achievable emission limit values in these cases

[b]The BAT Reference Documents of the Industrial Emissions Directive of the European Union and the New Source Performance Standards in the United States are important sources for best available techniques

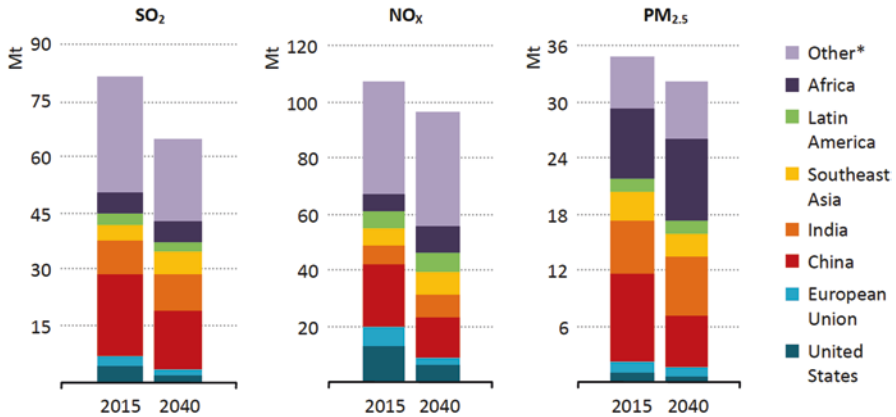[c]The EU's EcoDesign Directive provides a guide for implementation

Fig. 3.30 Air pollutant emissions from the energy sector by region in the New Policies Scenario. Source: IEA World Energy Outlook Special Report 2016

3.7   Mapping Energy Sources Using GIS

World energy extraction, transport, appropriate transformation, distribution, and consumption can be explored and analyzed by a number of software tools. Besides mapping and exploring energy sources by GIS, there are also needs to display redistribution of energy between sources and consumers over large regions or local areas. The Sankey diagrams are used to be selected for this reason. In case of spreadsheets, macros can be developed to extent existing functionality in order to manage and display data by Sankey diagrams. Another possibility on how to visualize the datasets is implemented in Google Charts with a simple JavaScript that embedded in the Web page. An example based on IEA data for world final consumption in 2013 (http://www.iea.org/sankey/) is illustrated in Fig. 3.31. It shows redistribution of fossil fuels, renewables, and electricity by industry, transport, and other services to target consumers. As expected, oil products are mainly used by transport and in the road traffic, while fossil fuels as a whole dominate in industry and other services to support production and final consumption. The Sankey diagram depicts a flow from one set of values to another. The items being connected are called nodes, and their connections are called links. A code in JavaScript using Google Charts library for rendering of the diagram in the browser is shown in Table 3.10. In order to create more than two levels of connections, the multilevel Sankey diagram was created, but the tools in Google Charts will add additional levels as needed, laying them out automatically. Information about the source and destination labels are in the square brackets. The third parameter indicates the strength of that connection and is reflected in the width of the path between the labels. The Sankey diagram uses default colors, but both nodes and links can be given custom color palettes using their colors options. Other configuration options can control brightness and transparency, create a border around the links, customize labels, adjust the position of the labels relative to the nodes, and set the width and distance of the nodes. In order to simplify a code, the configuration settings are minimized, and the default options are used mostly for rendering of this Sankey diagram.
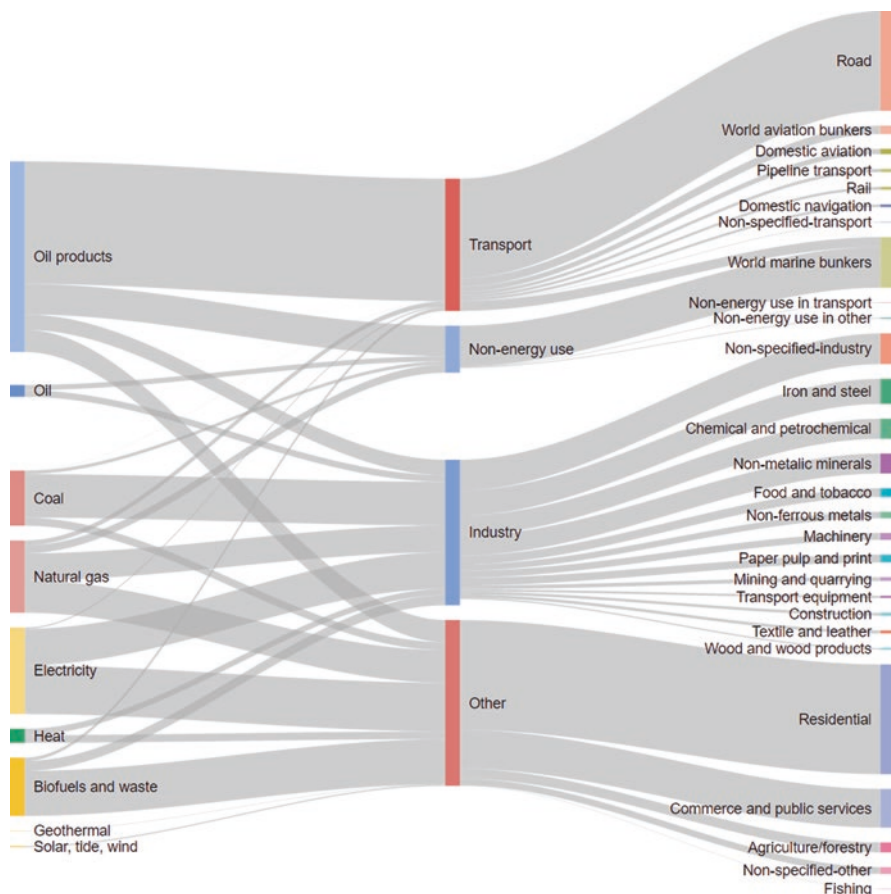
Fig. 3.31 An example of the Sankey diagram that is based on IEA data for world final consumption in 2013 (the diagram was rendered in the browser using Google Charts with a simple JavaScript). Source: http://www.iea.org/sankey/, https://developers.google.com/chart/interactive/docs/gallery/sankey

3.7.1 Geodatabase Data Management

Geodatabase design include a number of steps that are focused on identification of thematic map layers, specification of data elements and their relationships, dataset preparation in terms of their processing and visualization, and finally, testing and refining through a series of initial implementations. The final phase includes documentation of the created geodatabase design. In order to demonstrate the geodatabase design, an example has been created to explore energy consumption together with electricity production and carbon dioxide emissions over the world. The geodatabase design is dealing with selected data from IEA (Headline Global Energy Data, 2015 edition, http://www.iea.org/statistics/) about total final consumption, electricity output production, and total CO_2 emissions from final consumption. The selected datasets contain time series 1971–2013 for OECD countries, non-OECD countries,

Table 3.10 The code in JavaScript for rendering of world final consumption in 2013 by Sankey diagram with Google Charts (the repeated source labels are omitted in order the shorten the code, which is marked by …)

```
1   <html>
2   <body>
3   <script type="text/javascript" src="https://www.gstatic.com/charts/loader.js"></script>
4   <div id="sankey_multiple" style="width: 900px; height: 600px;"></div>
5   <script type="text/javascript">
6       google.charts.load("current", {packages:["sankey"]});
7       google.charts.setOnLoadCallback(drawChart);
8       function drawChart() {
9           var data = new google.visualization.DataTable();
10          data.addColumn('string', 'From');
11          data.addColumn('string', 'To');
12          data.addColumn('number', 'Weight');
13          data.addRows([
14              [ 'Oil', 'Industry', 130 ],
15              ...
16              [ 'Coal', 'Industry', 844 ],
17              ...
18              [ 'Natural gas', 'Industry', 521 ],
19              ...
20              [ 'Biofuels and waste', 'Industry', 194 ],
21              ...
22              [ 'Geothermal', 'Industry', 1 ],
23              ...
24              [ 'Solar, tide, wind', 'Other', 26 ],
25              [ 'Electricity', 'Industry', 709 ],
26              ...
27              [ 'Heat', 'Industry', 123 ],
28              ...
29              [ 'Industry', 'Iron and steel', 487 ],
30              ...
31              [ 'Transport', 'Road', 1929 ],
32              ...
33              [ 'Other', 'Residential', 2128 ],
34              ...
35              [ 'Non-energy use', 'World marine bunkers', 791 ],
36              ...
37          ]);
38          // Set chart options
39          var options = {width: 600};
40          // Instantiate and draw our chart, passing in some options.
41          var chart = new google.visualization.Sankey(document.getElementById('sankey_multiple'));
42          chart.draw(data, options);
43      }
44  </script>
45  </body>
46  </html>
```

Source: http://www.iea.org/sankey/, https://developers.google.com/chart/interactive/docs/gallery/sankey

world, and, in particular, the United States. These datasets were imported into the geodatabase as data tables together with feature datasets of countries in selected regions (Fig. 3.32). The geodatabase OECD.gdb consists of feature classes and data tables. The feature class COUNTRIES contains feature datasets with countries of selected regions. The feature class ENERGY contains the same feature classes like feature class COUNTRIES, but the attributes of each country are extended by data from data tables, which are recalculated and linked as the values per capita.

3.7.2 Spatial and Temporal Analysis

An example for testing and refining of the proposed geodatabase is illustrated in Fig. 3.33. The project contains thematic map layers based on feature datasets from the proposed geodatabase. For each OECD country in the selected region, the total

Fig. 3.32 The geodatabase OECD.gdb consisting of imported data tables and feature classes COUNTRIES, and ENERGY, which contains extended feature datasets by IEA data about countries in selected regions
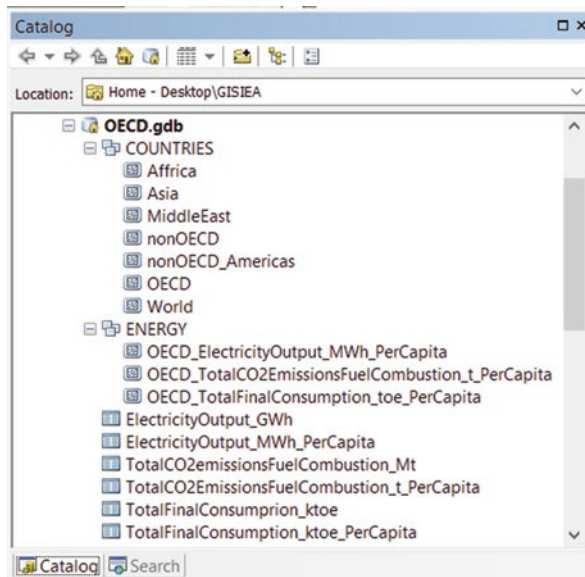
final consumption per capita in 2013 and the electricity output in 2013 are symbolized by a size of the circle (toe per capita) and by a size of the rectangle (MWh per capita), respectively. The total CO_2 emissions from fuel combustion are symbolized by a color gradient on the background. The view is complemented by data tables, which contain the symbolized values in the thematic map layers.

3.7.3 Display of Spatial and Temporal Data

Presentations of the thematic map layers derived from the GIS project are shown in Fig. 3.34 and Fig. 3.36 for the total final consumption and the electricity output, respectively. The presentations are focused on OECD countries in the selected region, and the attached column graphs show the values per capita in 1990, 1995, 2000, 2005, 2010, and 2013. The layers are complemented by a thematic map layer with the total CO_2 emissions from fuel combustion in 2013. The values per capita are symbolized by a gray gradient on the background. The total final consumption and electricity output per capita for OECD countries and selected regions are illustrated in Fig. 3.35 and Fig.3.37, respectively.

The total CO_2 emissions from fuel combustion for OECD countries and other selected regions in a series of years (1990, 1995, 2000, 2005, 2010, and 2013) are in descendent order (2013) in Table 3.11. The non-OECD countries, especially in Asia (including China), represent the significant contribution, which can be increased in dependence on using fossil fuels. The values are in millions of tonnes of CO2. In order to compare various populations living in explored countries and selected regions, the original values are recalculated and expressed as tonnes per capita in all thematic layers and charts. The total CO_2 emissions from fuel combustion per capita
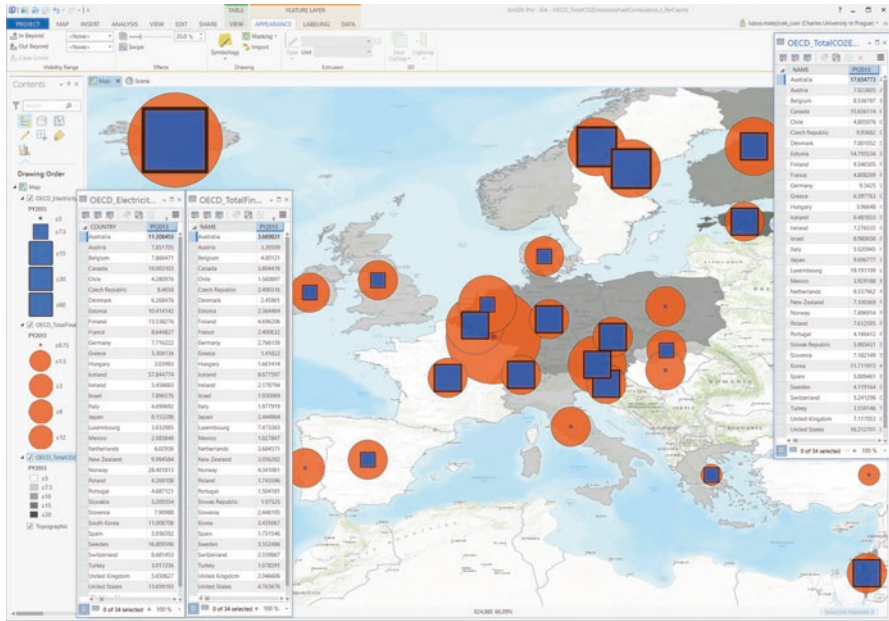
Fig. 3.33 The project containing thematic map layers based on feature datasets from the proposed geodatabase
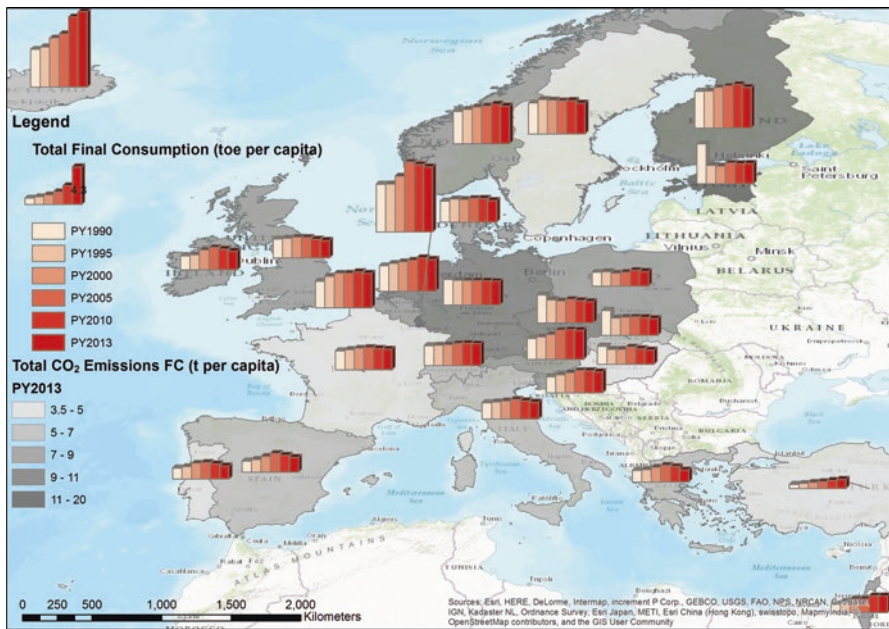

Fig. 3.34 The total final consumption per capita for OECD countries in the selected region in 1990, 1995, 2000, 2005, 2010, and 2013 and corresponding total CO_2 emissions from fuel combustion in 2013
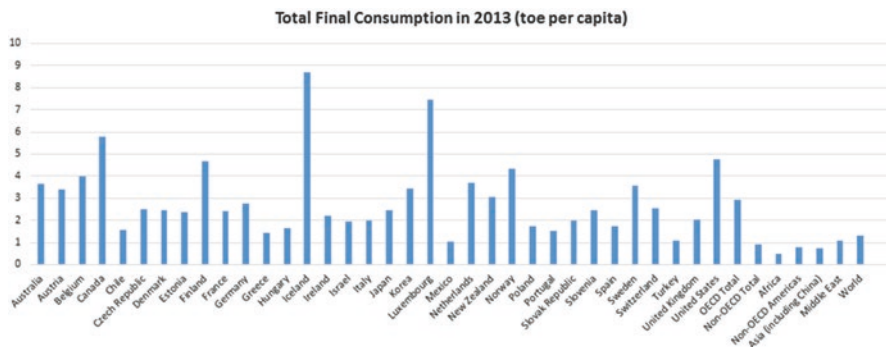
Fig. 3.35 The total final consumption per capita for OECD countries and other selected regions. Source: IEA Headline Global Energy Data, 2015 edition, http://www.iea.org/statistics/

Fig. 3.36 The electricity output per capita for OECD countries in the selected region in 1990, 1995, 2000, 2005, 2010, and 2013 and the corresponding total CO_2 emissions from fuel combustion in 2013

for OECD countries and other selected regions are illustrated in Fig. 3.38. The values in tonnes per capita show different relations, which dominate mostly developed countries, such as the United States, Canada, Australia, and other smaller countries over the world.

The time series of the total final consumption per capita, the electricity output per capita, and the total CO_2 emissions from fuel combustion per capita are illustrated in Figs. 3.39, 3.40, and 3.41, respectively. All the time series indicate increasing

Fig. 3.37 The electricity output per capita for OECD countries and other selected regions. Source: IEA Headline Global Energy Data, 2015 edition, http://www.iea.org/statistics/
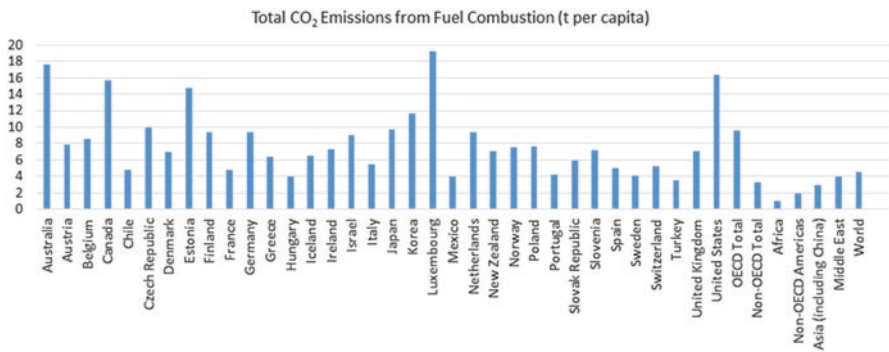
Fig. 3.38 The total CO_2 emissions from fuel combustion per capita for OECD countries and other selected regions. Source: IEA Headline Global Energy Data, 2015 edition, http://www.iea.org/statistics/
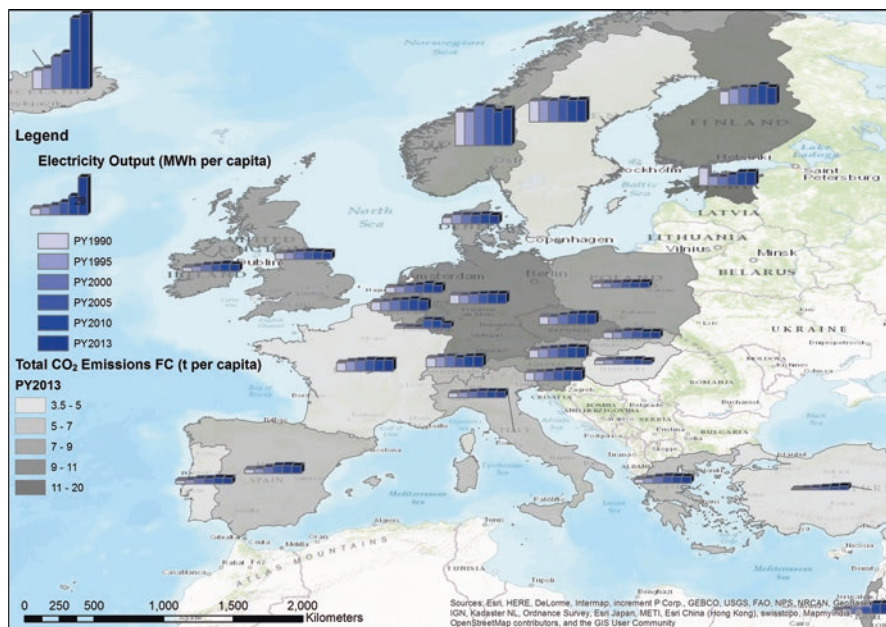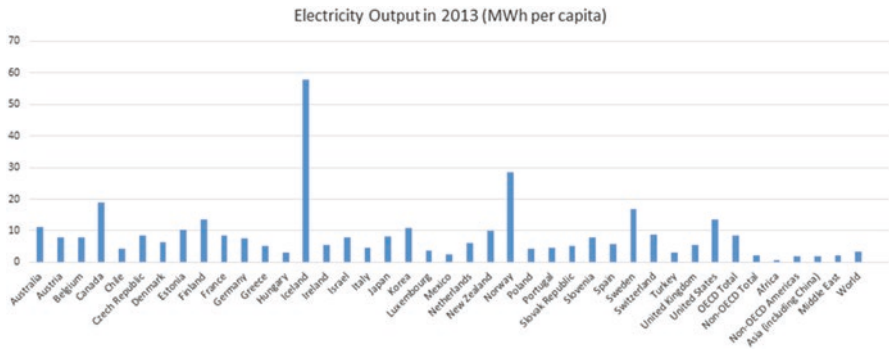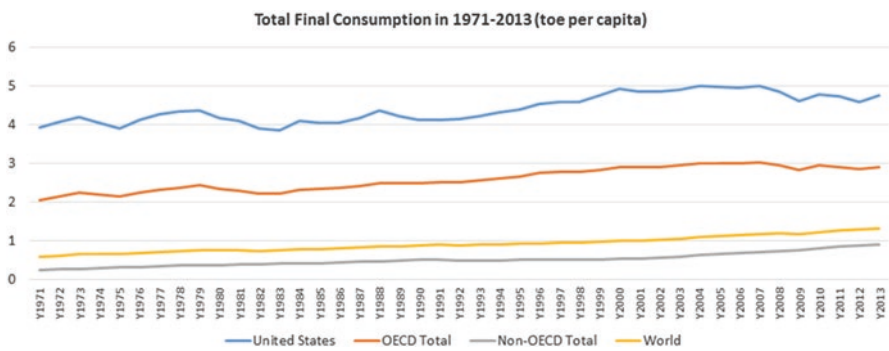

Fig. 3.39 Total final consumption per capita (tonnes of oil equivalent per capita) in 1971–2013 for OECD countries and other selected regions
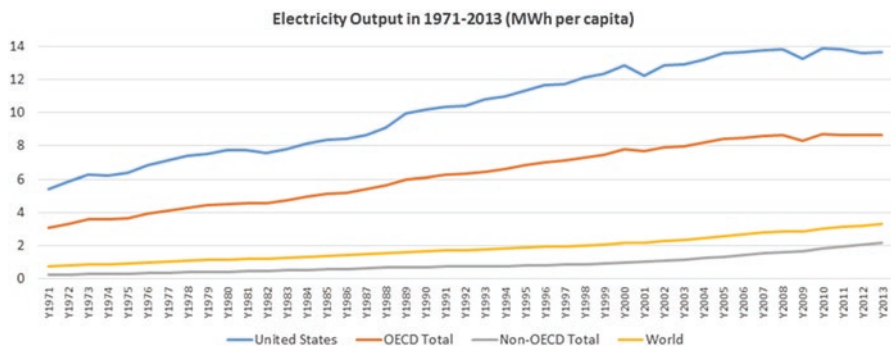
Fig. 3.40 Electricity output per capita (MWh per capita) in 1971–2013 for OECD countries and other selected regions
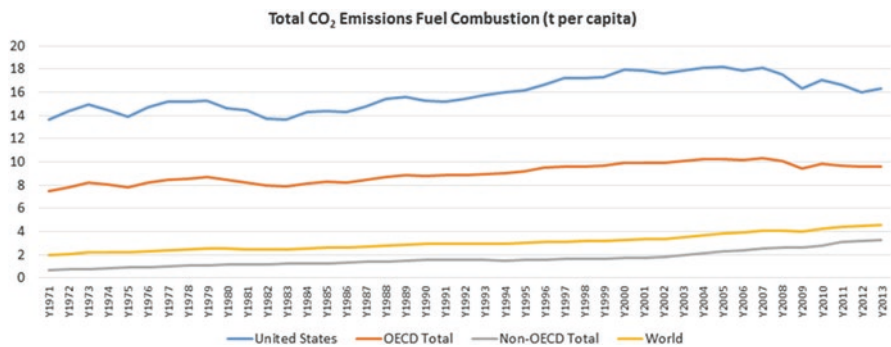
Fig. 3.41 The total carbon dioxide emissions from fuel combustion per capita (tonnes per capita) in 1971–2013 for OECD countries and other selected regions

levels over the whole period, but there are slightly decreasing levels in the total CO_2 emissions from fuel combustion per capita for the United States and OECD countries. It is caused by adopting local policies scenarios in individual countries and by an effort to provide reduction in coal uses, which results from the policies that governments worldwide must adopt toward setting the energy system to keeping long-term increase in the average global temperature to below 2 °C. But based on the time series for the world and non-OECD countries, a higher effort will be needed to improve our environment.

Table 3.11 The total CO_2 emissions from fuel combustion for OECD countries and other selected regions in a series of years (1990, 1995, 2000, 2005, 2010, and 2013) in descendent order (2013)

	Total CO_2 emissions-fuel combustion (Mt of CO_2)					
Country	1990	1995	2000	2005	2010	2013
World	20,623	21,478	23,322	27,048	29,838	32,190
Non-OECD total	8987	9261	10,021	13,229	16,406	19,053
Asia (including China)	3430	4654	5322	7891	10,352	12,630
OECD Total	11,006	11,496	12,447	12,816	12,306	12,038
United States	4802	5073	5643	5702	5355	5120
Middle East	535	744	886	1154	1496	1647
Japan	1049	1122	1157	1196	1126	1235
Non-OECD Americas	553	652	779	855	1022	1128
Africa	529	576	658	858	999	1075
Germany	940	857	812	787	759	760
Korea	232	357	432	458	551	572
Canada	419	448	516	536	515	536
Mexico	260	286	344	382	414	452
United Kingdom	548	514	521	531	477	449
Australia	260	285	335	371	385	389
Italy	389	401	420	456	392	338
France	346	344	365	370	340	316
Poland	345	333	290	296	310	292
Turkey	127	152	201	216	265	284
Spain	203	228	279	334	262	236
Netherlands	145	158	157	163	168	156
Czech Republic	150	123	121	118	111	101
Belgium	106	112	114	107	102	89
Chile	29	37	49	54	69	82
Greece	70	77	88	95	83	69
Israel	33	45	55	59	68	68
Austria	56	59	62	75	70	65
Finland	54	55	54	55	62	49
Portugal	38	47	58	61	48	45
Switzerland	41	41	42	44	43	42
Hungary	66	56	53	55	48	40
Denmark	51	58	51	48	47	39
Sweden	52	57	52	49	46	38
Norway	27	31	32	35	38	35
Ireland	30	33	41	44	39	34
Slovak Republic	55	41	37	37	35	32
New Zealand	22	24	29	34	30	31
Estonia	36	16	15	17	19	19
Slovenia	14	14	14	15	15	14
Luxembourg	11	8	8	11	11	10
Iceland	2	2	2	2	2	2

Bibliography

EIA. (2009). *The National Energy Modeling System: An overview 2009*. Washington, DC: EIA. Retrieved from http://www.eia.gov/forecasts/aeo/nems/overview/index.html

EEA. (2013). *Overview of the European energy system*. Copenhagen: EEA. Retrieved from http://www.eea.europa.eu/data-and-maps/indicators/overview-of-the-european-energy-system-3/assessment

EEA. (2016). *Renewable energy in Europe 2016: Recent growth and knock-on effects*. EEA Report No 4/2016. Luxembourg: Publications Office EU. Retrieved from http://www.eea.europa.eu/publications/renewable-energy-in-europe-2016

EIA. (2016). *Annual Energy Outlook 2016 early release: Annotated summary of two cases*. Retrieved from https://www.eia.gov/forecasts/aeo/er/

EIA. (2016). *Monthly energy review: May 2016*. Washington, DC: . Retrieved from http://www.eia.gov/totalenergy/data/monthly/

IAEA. (2012). *IAEA nuclear energy series no. NP-T-2.7*. Vienna: IAEA. Retrieved from http://www-pub.iaea.org/books/IAEABooks/8759/Project-Management-in-Nuclear-Power-Plant-Construction-Guidelines-and-Experience

IAEA. (2012). *Nuclear power reactors in the world*. Vienna: IAEA. Retrieved from http://www-pub.iaea.org/books/IAEABooks/11079/Nuclear-Power-Reactors-in-the-World

IEA. (2014). *World energy outlook 2014*. Paris: IEA. Retrieved from http://www.worldenergyoutlook.org/weo2014/

IEA. (2015). *Key world energy statistic 2015*. Paris: IEA. Retrieved from http://www.iea.org/publications/freepublications/publication/key-world-energy-statistics-2015.html

IEA. (2015). World Energy Outlook 2015. Paris: IEA, Retrieved from http://www.worldenergyoutlook.org/weo2015/

IEA. (2016). *Energy and air pollution: World energy outlook special report*. Paris: IEA. Retrieved from https://www.iea.org/publications/freepublications/publication/weo-2016-special-report-energy-and-air-pollution.html

IIASA. (2016). *IIASA annual report 2015*. Vienna: IIASA. Retrieved from http://www.iiasa.ac.at/web/home/resources/publications/annual-report/ar.html

REN21. (2016). *Renewables 2016: Global status report*. Paris: REN21. Retrieved from http://www.ren21.net/status-of-renewables/global-status-report/

WNA. (2016). *World Nuclear Performance Report (2016)*. Retrieved from http://www.world-nuclear.org/our-association/publications/online-reports/world-nuclear-performance-report-2016.aspx

Data Sources (Revised in September, 2016)

BP. *Energy Outlook*. Retrieved from http://www.bp.com/en/global/corporate/energy-economics/energy-outlook-2035.html

BP. *Statistical review of world energy*. Retrieved from http://www.bp.com/en/global/corporate/energy-economics/statistical-review-of-world-energy/downloads.html

EEA. *Data and maps*. Retrieved from http://www.eea.europa.eu/data-and-maps

EEA. *Overview of the European energy system*. Retrieved from http://www.eea.europa.eu/data-and-maps/indicators/overview-of-the-european-energy-system-3/assessment

EEA. *Urban atlas*. Retrieved from http://www.eea.europa.eu/data-and-maps/data/urban-atlas

EIA. *International energy analysis*. Retrieved from http://www.eia.gov/beta/international/analysis.cfm

EIA. *International energy data*. Retrieved from http://www.eia.gov/beta/international/data/browser/

EIA. *Maps*. Retrieved from http://www.eia.gov/maps/

Google Charts. *Sankey diagram*. Retrieved from https://developers.google.com/chart/interactive/docs/gallery/sankey

IEA. *Free publications*. Retrieved from http://www.iea.org/publications/freepublications/

IEA. *Sankey diagrams*. Retrieved from http://www.iea.org/Sankey/

IEA. *Statistics*. Retrieved from http://www.iea.org/statistics/

NREL. *The dynamic maps, GIS data and analysis tools*. Retrieved from http://www.nrel.gov/gis/

World Bank Open Data. Retrieved from http://data.worldbank.org/

Chapter 4
Energy from Fossil Fuels: Digital Mapping of Sources and Environmental Issues

At present fossil fuels are the most important sources of energy. In many countries most of the energy is still generated by nonrenewable sources, which are represented by a limited reserve coal, oil, and gas. They will become scarce and therefore prohibitively expensive after a few decades. The choice can be limited by other criteria such as air pollution and climate change. The pollution due to coal power stations depends on the quality of the coal. A coal power station can emit each year a few million tonnes of carbon dioxide, a million tonnes of ash, half a million tonnes of gypsum, and other pollutants such as nitrous oxide, sulfur dioxide, and smaller amounts of other toxic wastes. Besides that coal mining is dangerous, dirty and many miners contract debilitating diseases such as silicosis. Oil became one of the world's leading energy sources. It has a higher caloric value than coal and is more easily transported. Transport and industry are more dependent on oil supply than on the availability of coal. Moreover oil is the basis of petrochemical industries such as plastics, drugs, and paints. Similarly to coal, main oil reserves last for a few decades, and then the production becomes increasingly expensive. The changes can be more rapid in individual countries, which do not have their own oilfields. Since a large fraction of the oil is used for transport, it is imperative to discover new ways of driving cars and ships. The energy supply of gas has risen rapidly. As the rate of consumption is rising, it is unlikely to last longer than oil. In comparison with other fossil fuels, gas is now the cheapest and convenient energy source, but its world's reserve is severely limited.

4.1 Description of Fossil Fuels

Fossil fuels are the residues of dead organic matter, particularly vegetation, trapped for millions of years in sedimentary deposits. Coal forms from geological processes, which involve the burying of plants under anaerobic conditions in swamps. Initially, it becomes peat and is overlain gradually by rock, raising the pressure and

temperature of the organic matter. Oil results from more dispersed organic matter, such as organic sediments on a continental shelf that are buried by geological processes and subjected to a high-pressure cooking deep underground. It can migrate through cracks and form large underground pools. Nongaseous fossil fuels are made up of complicated molecules with backbones of many carbon atoms, which originate from the residues of their plant parents: mostly the light atoms of carbon, hydrogen, sulfur, and phosphorus that constitute carbohydrates. Over the long period, the oxygen content is reduced, and the dominate molecular form becomes a mixture of hydrocarbons. But there is a significant variability in the atomic and molecular composition of these fuels in dependence on geologic deposits in different regions of the Earth's surface. Natural gas is composed on the fewest molecular components, low-molecular-weight hydrocarbons.

The energy role of fossil fuels is in their fuel heating value, which is the amount of heat released during the combustion. The heating value is a characteristic for each fuel and is usually measured in units of energy per unit of mass (kJ/kg, kJ/mol, kcal/kg, or Btu/lb). The heat of combustion for fuels can be expressed as the higher heating value (HHV) or lower heating value (LHV). The HHV is determined by bringing all the products of combustion back to the original pre-combustion temperature and in particular condensing any vapor produced. The LHV is determined by subtracting the heat of vaporization of the water vapor from the HHV. For many fuels, the higher heating value is correct, which is particularly relevant for natural gas, whose high hydrogen content produces much water, when it is burned in condensing boilers and power plants with flue-gas condensation. For the applications, which waste heat by producing unused water vapor, the lower heating value must be used to give a real estimate for the process. The difference between HHV and LHV depends on the chemical composition of the fuel. A relation between HHV to LHV can be expressed by

$$ HHV = LHV + H_v \frac{n_{H_2O,out}}{n_{fuel,in}} \tag{4.1} $$

where H_v is the heat of vaporization of water and $n_{H_2O,out}$ and $n_{fuel,in}$ are the number of moles of water vaporized and fuel combusted, respectively.

Commercially available fossil fuels include coal (anthracite and bituminous, subbituminous, and lignite), liquid petroleum (gasoline, diesel fuel, kerosene, heating fuels), and petroleum gases (natural gas, ethane, propane, butane). The heating values of these fossil fuels are highly variable in dependence on molecular composition and inert components. Besides varied structure of the fossil fuels, the distinction between HHV and LHV is primarily a matter of convention. Sellers like to quote their price in terms of dollars per energy units of HHV, which is a lower price than that per energy units of LHV. On the other hand, producers of energy such as power plants or heating plants prefer to rate their plant efficiency in terms of electrical or heating energy produced per energy unit of LHV, which shows a higher efficiency in comparison with HHV. The heat values (LHV) of selected fuels together with percentage of carbon and carbon dioxide are shown in Table 4.1.

Table 4.1 Heat values of various fuels

Fuel	LHV (MJ/kg)	% Carbon	CO$_2$ (g/MJ)
Hydrogen	121	0	0
Petrol/gasoline	44–46		
Diesel fuel	45		
Crude oil	42–44	89	70–73
Methanol	20	37	
Liquefied petroleum gas (LPG)	49	81	59
Natural gas (UK, United States, Australia)	38–39	76	51
Natural gas (Canada)	37		
Natural gas (Russia)	34		
Natural gas as LNG (Australia)	55		
Hard black coal (IEA definition)	>23.9		
Hard black coal (Australia and Canada)	c 25.5	67	90
Subbituminous coal (IEA definition)	17.4–23.9		
Subbituminous coal (Australia and Canada)	c 18		
Lignite/brown coal (IEA definition)	<17.4		
Lignite/brown coal (Australia, electricity)	c 10	25	1.25 (kg/kWh)
Firewood (dry)	16	42	94
Natural uranium, in LWR (normal reactor)	500 (GJ/kg)	0	0
Natural uranium, in LWR with U and Pu recycle	650 (GJ/kg)	0	0

Source: World Nuclear Association, 2010
Notes: % carbon is by mass; mass CO$_2$ = 3.667 mass C; one tonne of oil equivalent (toe) is equal to 41.868 GJ

4.1.1 Coal as an Energy Source

Coal as a variety of solid organic fuels refers to a wide range of sedimentary rock materials spanning a continuous quality scale for combustion. This continuous series is used to be divided into two main categories such as hard coal and brown coal. Hard coal contains two subcategories such as anthracite and bituminous coal (coking coal and other bituminous coal). Also brown coal contains two subcategories that is subbituminous coal and lignite. But coal categories vary in the classification system in dependence on national and international specifications such as caloric value, volatile matter content, fixed carbon content, and other criteria. Fuel combustion and emissions are also affected by the degree of dilution by moisture and ash and contamination by sulfur and other trace elements. Thus the International Coal Classification of the Economic Commission for Europe (UNECE) recognizes two broad categories, which are determined by a gross caloric value that accounts for water in the exhaust leaving as vapor, and includes liquid water in the fuel prior to combustion and basic composition. The category hard coal is characterized as coal of gross calorific value not less than 5700 kcal/kg (23.9 GJ/t) on an ash-free but moist basis and with a mean random reflectance of vitrinite of at least 0.6.

Fig. 4.1 Coal surface mine with mining equipment such as excavators and conveyors

The category brown coal is non-agglomerating coal with a gross calorific value less than 5700 kcal/kg (23.9 GJ/t) containing more than 31% volatile matter on a dry mineral matter-free basis.

Small-scale coal mining has been existing for thousands of years. But the exponential expansion of international trade began in industrial revolution in Britain in the eighteenth century. The new mines were created in continental Europe and North America and then over the whole world in order to power steam engines. The methods of coal extraction depend on the depth and quality of the seams, the geology, and environmental factors. The two basic methods represent surface mining and deep underground mining. Seams close to the surface, at depths less than approximately 50 m, are used to be surface mined using open cut mining methods. Opencast coal mining recovers a greater proportion of the coal deposit than underground methods. Opencast mines often cover large areas of many square kilometers (Fig. 4.1) and use very large pieces of equipment such as excavators and conveyors. The extraction of coal by an excavator in a detail view is shown in Fig. 4.2. An example of a fossil fueled power station is shown in Fig. 4.3.

Coal is mostly used as a solid fuel to produce heat and electricity through combustion. World coal consumption increased to 8285 million of tones in 2011, but then shows slight declining. Consumption increased in Asia, while Europe has declined. Coal consumption trends 1980–2012 in the world, EU-27, OECD, non-OECD, and selected countries such as the United States, China, and Russia (former USSR to 1991) are shown in Fig. 4.4 and in Table 4.2 in millions of short tonnes (1 short tonne equals 907.18470 kg). Total coal consumption in 2005–2012 in top ten countries with the highest coal consumption in 2012 and their coal reserves in 2011 are shown in Table 4.3. Many countries have to import coal, because their reserves and production are negligible in comparison to their consumption.

The world's leading coal producer and consumer has been China since 1985 with a small decline in 2012. Other countries with notable declines of coal production in 2014

Fig. 4.2 (**a**) Coal extraction in a surface mine with an excavator. (**b**) The extraction of coal by an excavator in a detail view

included Ukraine (−24.1 Mt. due to turmoil in the Eastern Oblasts of Donetsk and Luhansk in the second half of 2014), Indonesia (−16.9 Mt. partly due to current weaker demand for Indonesian coals in China), and Serbia (−10.4 Mt. due to flooding of mines). While production of coking coal reached a new record high of 1064.8 Mt. in 2014, it was unable to counter decreases in production of steam coal and lignite. The following shows Table 4.4, which excludes other specific minor items such as peat, oil shale, and oil sands.

Generally, global production of all primary coal types passed 4 gigatons (Gt) in 1983 (3 Gt in 1972), 5 Gt in 2003, and 8 Gt in 2013. Annual coal production has

Fig. 4.3 (**a**) Fossil-fueled power station for production of electricity and for central heating of neighbor residential sites. (**b**) Temporary coal storage of the fossil fueled power station
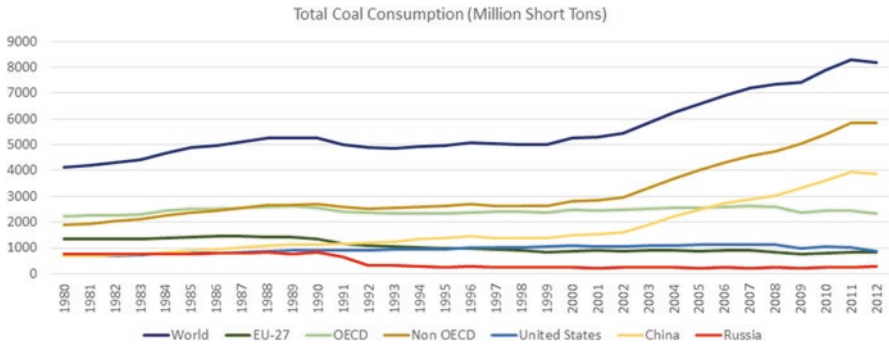
Fig. 4.4 Total coal consumption trends in 1980–2012 in the world, EU-27, OECD, non-OECD, and selected countries such as the United States, China, and Russia (former USSR to 1991). Source: EIA International Energy Statistics, 2016

increased by more than four billion tonnes in the last 30 years and more than twice the level achieved in 1983. Coal will continue to be primarily used for the production of electricity and commercial heat. The percentage of this use in OECD countries was 49.9% in 1971 with the rapid growth to 67.5% in 1983 as replacements for oil after the oil shocks in the 1970s (IEA Coal Information-excerpt, 2015).

In 2012 global emissions of carbon dioxide from fuel combustion increased by 390 Mt. to reach 31.7 Gt. Coal remained the largest source of emissions with an increase 172 Mt. to reach 13.9 Gt in the global emission inventory. OECD coal-based emissions increased from 3.91 to 3.95 Gt in 2013. Extra emissions could be explained as a result of a severe winter, especially in the United States in 2013. It also includes an increase of emissions in Japan as a result of limited electricity generation from nuclear power in 2013. Overall since 1971, coal-related emissions of carbon dioxide have increased from 5.2 to 13.9 Gt in 2012 (passing 8.3 Gt in 1990). Since 2004, coal is the leading source of global carbon dioxide emissions, outstripping those from oil and natural gas and other sources (IEA Coal Information-excerpt, 2015).

4.1.2 Oil as an Energy Source

Oil (petroleum) consists of hydrocarbons and other organic compounds, which are commonly refined into various types of fuels. The name petroleum covers both naturally occurring unprocessed crude oil and petroleum products that are made up of refined crude oil. Crude oil is a fossil fuel, and it exists in liquid form in underground pools, in tiny spaces within sedimentary rocks, and near the surface in tar sands. Petroleum is recovered by oil drilling, which is carried out after structural geology explorations. The pumpjack pumping an oil well and an oil platform in the sea is illustrated in Fig. 4.5. Subsequently, it is refined and separated by distillation, into a large number of final products, from gasoline and kerosene to asphalt and chemical reagents used to make plastics and pharmaceuticals.

Table 4.2 Total coal consumption in the world, EU-27, OECD, non-OECD, and selected countries such as the United States, China, and Russia (former USSR to 1991)

Country group	Total coal consumption (millions of short tonnes)												
	1980	1985	1990	1995	2000	2005	2006	2007	2008	2009	2010	2011	2012
World	4123	4888	5262	4961	5279	6575	6900	7187	7336	7416	7885	8285	8186
EU-27	1335	1439	1333	986	890	886	896	903	851	777	786	825	838
OECD	2230	2530	2559	2320	2482	2574	2578	2631	2577	2363	2457	2432	2348
Non-OECD	1893	2359	2702	2641	2797	4001	4322	4557	4750	5043	5419	5843	5838
United States	703	818	904	962	1084	1126	1112	1128	1121	997	1049	1003	889
China	679	911	1123	1382	1493	2484	2722	2890	3017	3321	3606	3954	3887
Russia[a]	751	779	848	270	253	233	240	230	250	204	244	246	274

Source: EIA International Energy Statistics, 2016

[a]Russia after disintegration of former USSR in 1991, the higher value in 1980–1990 include total coal consumption of former USSR

Table 4.3 Total coal consumption in 2005–2012 in top ten countries with the highest coal consumption in 2012 and estimates of coal reserves in 2011

	Total coal consumption (millions of short tonnes)								Coal reserves
Country	2005	2006	2007	2008	2009	2010	2011	2012	2011
China	2484	2722	2890	3017	3321	3606	3954	3887	126,215
United States	1126	1112	1128	1121	997	1049	1003	889	258,619
India	505	539	587	619	687	699	720	745	66,800
Russia	233	240	230	250	204	244	246	274	173,074
Germany	271	271	281	268	248	256	262	269	44,697
Japan	196	198	208	204	181	206	193	202	383
Australia	153	155	155	154	158	152	147	151	84,217
Poland	150	155	150	149	141	148	153	147	6024
South Korea	88	90	98	111	114	127	140	138	139
Turkey	85	92	109	109	109	106	112	108	9592

Source: EIA International Energy Statistics, 2016

Table 4.4 Total world coal production in dependence on target consumption in 2012–2014 (it excludes other specific minor items such as peat, oil shale, and oil sands)

	Total world coal production in dependence on target consumption		
	2012	2013	2014
Steam coal	5901	6203	6147
Coking coal	976	1038	1065
Lignite	887	835	811
Subtotal	7764	8076	8023

Source: IEA Coal Information-excerpt, 2015

Oil has been used since ancient times. Now it is important across economy, politics, and technology due to the invention of the internal combustion engine and the importance to industrial organic chemistry. Access to oil has been a major factor in several military conflicts for last centuries. During the early twentieth century, oil exploration in North America led to the United States becoming the leading producer, but in the 1960s the United States was surpassed by Saudi Arabia and the Soviet Union. The top oil-producing countries are Russia, Saudi Arabia, and the United States, but about 80% of the world's accessible reserves are located in the Middle East (Saudi Arabia, the United Arab Emirates, Iraq, Qatar, and Kuwait). A portion of the world's reserves exists as unconventional sources, such as bitumen in Canada and extra heavy oil in Venezuela. Oil extraction from oil sands, particularly in Canada, requires large amounts of heat and water, making its net energy content quite low relative to conventional crude oil. Oil sands near the Birch Mountains in Alberta, Canada, are illustrated in Fig. 4.6. The proportion of light hydrocarbons in oil constitution significantly varies among different resources. It ranges from 97% by weight in the lighter oils to 50% in the heavier oil and bitumen oil. Hydrocarbons in crude oil are mostly alkanes (paraffins, 15–60%), naphthenes (30–60%), aromatics

Fig. 4.5 A pumpjack pumping an oil well and an oil platform in the sea. Source: www.pixabay. com

(3–30%), and asphaltics (more than 6%). Other organic impurities contain nitrogen, oxygen, sulfur, and trace amounts of metals such as iron, nickel, copper, and vanadium, but the exact molecular composition varies widely from formation to formation.

The production of crude oil is generally classified by the petroleum industry in dependence on its geographic location, API (American Petroleum Institute) gravity, and sulfur content. The geographic location affects transportation costs to the refinery. From the view of API gravity, light crude oil is more desirable than heavy oil since it produces a higher yield of gasoline. In case of sulfur content, sweet oil commands a higher price than sour oil because it has fewer environmental problems and requires less refining to meet sulfur standards. Each crude oil has unique constitution which is understood by the use of crude oil assay analysis in petroleum laboratories. It is used as pricing references for barrels throughout the world. Examples of the common reference crudes are West Texas Intermediate (a very high-quality oil delivered at Cushing, Oklahoma, for North American oil), Brent Blend (comprising 15 oils from fields of the North Sea), Dubai-Oman (used as benchmark for Middle East sour crude oil), Tapis (from Malaysia, used as a reference for light Far East oil), Minas (from Indonesia, used as a reference for heavy Far East oil), the OPEC Reference Basket (a weighted average of oil blends from various OPEC), Midway-Sunset

Fig. 4.6 Oil (tar or bituminous) sands near the Birch Mountains in Alberta, Canada. Source: Google Earth 2016

Fig. 4.7 Oil refining and transporting with oil tankers. Source: www.pixabay.com

Heavy (used for pricing of heavy oil in California), and Western Canadian Select (benchmark crude oil for emerging heavy, high TAN acidic crudes). The production of crude oil by petroleum industry involves the global processes of exploration, extraction, refining, transporting with oil tankers and pipelines, and marketing (Figs. 4.7 and 4.8).

Consumption of crude oil in the last decades has been significantly pushed by automobile growth and, partly, by industry. But in the future, a lower growth of demand can be indicated by emerging economies concerns, especially in non-OECD countries like China, because oil products are also in competition with alternative

Fig. 4.8 The Houston Ship Channel in Texas with a number of oil transport utilities. Source: pixabay CC0
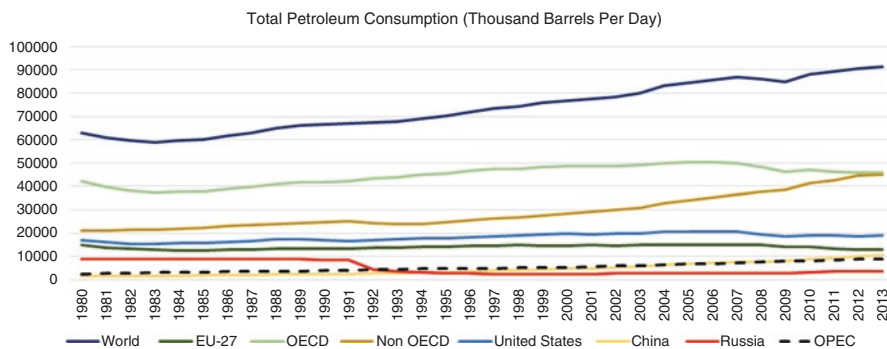

Fig. 4.9 Total petroleum consumption trends in 1980–2013 in the world, EU-27, OECD, non-OECD, OPEC, and selected countries such as the United States, China, and Russia (former USSR to 1991). Source: EIA International Energy Statistics, 2016

cheaper sources, mainly coal and natural gas. Petroleum consumption trends in 1980–2013 in the world, EU-27, OECD, non-OECD, OPEC, and selected countries are shown in Fig. 4.9 and in Table 4.5. Total petroleum consumption in 2005–2012 in top ten countries with the highest petroleum consumption in 2013 and their total oil supply in 2014 are shown in Table 4.6.

   The environmental impacts of petroleum are negative due to its toxicity in almost all forms of life. Oil products such as crude oil are closely linked to all aspects of

Table 4.5 Total petroleum consumption in the world, EU-27, OECD, non-OECD, OPEC, and selected countries such as the United States, China, and Russia (former USSR to 1991)

| Country group | Total petroleum consumption (thousand barrels per day) | | | | | | | | | | |
	1980	1985	1990	1995	2000	2005	2010	2011	2012	2013
World	63,122	60,083	66,541	70,258	76,928	84,588	88,216	89,127	90,392	91,253
EU-27	14,873	12,569	13,387	14,233	14,607	15,079	14,005	13,559	13,067	12,829
OECD	42,032	37,697	41,754	45,401	48,506	50,416	46,998	46,345	45,923	45,994
Non-OECD	21,090	22,386	24,786	24,858	28,422	34,172	41,219	42,783	44,469	45,165
United States	17,056	15,726	16,988	17,725	19,701	20,802	19,180	18,882	18,490	18,961
China	1765	1885	2296	3363	4796	6795	8938	9504	10,175	10,480
Russia	8995	8950	8392	2976	2578	2785	3135	3422	3445	3493
OPEC	2510	3327	3983	4730	5351	6707	8248	8376	8827	9011

Source: EIA International Energy Statistics, 2016

Table 4.6 Total petroleum consumption in 2005–2013 in top ten countries with the highest petroleum consumption in 2013 and their oil supply in 2014

Country	Total petroleum consumption (thousand barrels per day)									Total oil supply
	2005	2006	2007	2008	2009	2010	2011	2012	2013	2014
United States	20,802	20,687	20,680	19,498	18,771	19,180	18,882	18,490	18,961	14,021
China	6795	7263	7480	7697	8070	8938	9504	10,175	10,480	4598
Japan	5298	5168	5009	4770	4363	4429	4439	4697	4557	137
India	2550	2702	2888	2957	3068	3305	3461	3618	3660	1011
Russia	2785	2803	2885	2982	2889	3135	3422	3445	3493	10,847
Brazil	2171	2197	2297	2441	2459	2699	2777	2923	3003	2966
Saudi Arabia	1964	2020	2094	2237	2436	2580	2761	2882	2961	11,624
Germany	2624	2636	2407	2533	2434	2467	2392	2389	2435	159
Canada	2296	2294	2389	2317	2230	2326	2357	2403	2374	4383
South Korea	2191	2180	2240	2142	2188	2269	2259	2322	2328	79

Source: EIA International Energy Statistics, 2016

present society, especially for transportation and heating. When burned, petroleum releases carbon dioxide and together with coal is the largest contributor to the increase in atmospheric carbon dioxide. Increasing of carbon dioxide in the atmosphere causes global warming and ocean acidification by the uptake of carbon dioxide from the atmosphere. Also oil spills from tanker ship accidents have damaged natural ecosystems in many parts of the world such as Alaska, the Gulf of Mexico, and other places. Even small oil spills have a great impact on ecosystems due to their spreading for hundreds of miles in a thin oil slick in comparison with oil spills on land that can be rapidly bulldozed around the spill site before most of the oil escapes.

4.1.3   Natural Gas as an Energy Source

Natural gas is one of the cleanest fossil-based fuels that will continue making significant contribution to the world energy economy. Natural gas is plentiful and flexible, which is useful for power generation technologies and local heating systems. The exploration, development, and transport of gas require significant upfront investment and close coordination between investment in the gas and power infrastructure. Natural gas is often informally referred to simply as "gas," especially when compared to other energy sources such as oil or coal.

Natural gas is a mixture consisting primarily of methane with varying amounts of other higher alkanes. Sometimes it contains a small percentage of carbon dioxide, nitrogen, hydrogen sulfide, or rare gases (Table 4.7). Natural gas like oil and coal is essentially derived from the remains of plants and animals that lived millions of years ago. It is formed when layers of decomposing plant and animal matter are exposed to intense heat and pressure supplied by existing under the surface of the Earth over millions of years. The energy stored in the form of chemical bonds originates from the energy that the plants and animals obtained from the sun through the food chain. Before natural gas can be used for power generation or local heating, it must be processed to remove impurities, including water, to meet the specifications of marketable natural gas.

Table 4.7 Typical composition of natural gas

Methane	CH_4	70–90%
Ethane	C_2H_6	0–20%
Propane	C_3H_8	
Butane	C_4H_{10}	
Carbon dioxide	CO_2	0–8%
Oxygen	O_2	0–0.2%
Nitrogen	N_2	0–5%
Hydrogen sulfide	H_2S	0–5%
Rare gases	A, He, Ne, Xe	Trace

Source: http://naturalgas.org/overview/background/, 2016

Fig. 4.10 Remote natural gas well. Source: https://www.flickr.com/photos/25069384@N03/8743405319, 2016

Natural gas deposits are often located near oil deposits, and the gas is mostly extracted by drilling from the Earth's surface. An illustration of the natural gas well is shown in Fig. 4.10. The amount of natural gas is measured in cubic meters or standard cubic feet. In 2009, the US EIA estimated that the world's proven natural gas reserves are around 6289 trillion cubic feet (tcf). Most of the reserves are in the Middle East (40% of total world reserves). Russia has the second-highest amount of proven reserves. The United States has just over 4% of the world's natural gas reserves. After natural gas is extracted, it is transported through pipelines (from 2 to 60 in. in diameter). For example, the continental United States has more than 210 pipeline systems including about 490,850 km (305,000 miles) of transmission pipelines that transfer gas to all states. This system is complemented by more than 1400 compressor stations to ensure that the gas continues on its path, 400 underground storage facilities, 11,000 locations to deliver the gas, and 5000 locations to receive the gas. Natural gas can also be cooled to about −162 °C (−260 °F) and converted into liquefied natural gas (LNG). In this form, natural gas takes up only 1/600 of the volume of its gaseous state and can be transported by specialized insulated tankers to sites that do not have pipelines.

Natural gas is utilized in countless ways for industrial, residential, and transportation purposes. An example of mobile gas turbine used to generate electricity is shown in Fig. 4.11. Natural gas can be also used as an alternative fuel for vehicles that are running cleaner and cheaper to refuel then gasoline or diesel vehicles.

Fig. 4.11 Mobile gas turbine used to generate electricity. Source: www.pixabay.com

Other promising technology is represented by fuel cells where the energy from natural gas is also used to generate electricity. It produces water, heat, and electricity without any other by-products or emissions.

Global production and consumption of natural gas has increasing trend for last decades. While consumption in the OECD rose by a few percent (driven by the United States and Canada), consumption in non-OECD rose more significantly in the last years. The natural gas consumption trends in 1980–2013 in the world, EU-27, OECD, non-OECD, OPEC, and selected countries such as the United States, China, and Russia are illustrated in Fig. 4.12 and Table 4.8. Natural gas consumption in 2005–2013 in top ten countries with the highest natural gas consumption in 2013 and their natural gas production in 2014 is shown in Table 4.9. Besides the price on the market, demand for natural gas was also influenced by mild weather in Europe and by effects of the escalating conflicts between Russia and Ukraine.

4.2 Mapping of Fossil Sources with GPS and GIS

Exploration of local sites with mobile GIS can assess energy sources in a more accurate way and collaborate in both field and office environments. Using mobile GIS enables to improve efficiency and accuracy of field operations and provides
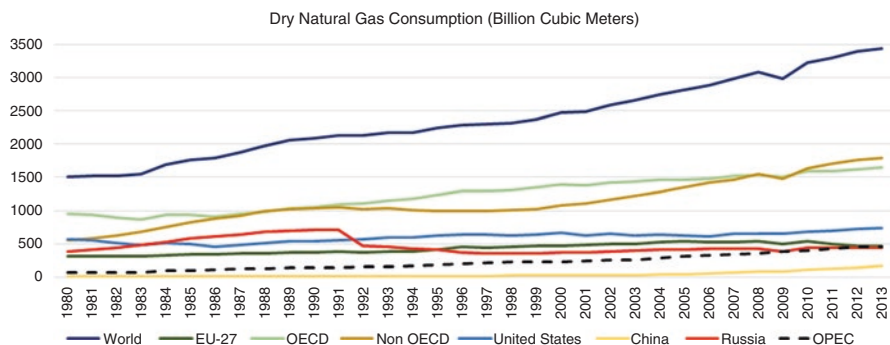
Fig. 4.12 Dry natural gas consumption trends in 1980–2013 in the world, EU-27, OECD, non-OECD, OPEC, and selected countries such as the United States, China, and Russia (former USSR to 1991). Source: EIA International Energy Statistics, 2016

Table 4.8 Dry natural gas consumption in the world, EU-27, OECD, non-OECD, OPEC, and selected countries such as the United States, China, and Russia (former USSR to 1991)

Country group	Dry natural gas consumption (Billion cubic meters)									
	1980	1985	1990	1995	2000	2005	2010	2011	2012	2013
World	1499	1761	2083	2238	2471	2817	3224	3296	3390	3437
EU-27	311	339	363	418	473	533	534	492	475	469
OECD	950	936	1050	1239	1388	1461	1590	1595	1626	1647
Non-OECD	550	824	1033	999	1082	1356	1634	1701	1764	1790
United States	563	489	*543*	629	661	623	682	693	723	741
China	14	13	14	16	25	47	107	131	144	163
Russia	377	575	705	411	370	406	438	434	445	442
OPEC	67	100	141	178	232	314	395	421	453	459

Source: EIA International Energy Statistics, 2016

Table 4.9 Dry natural gas consumption in 2005–2013 in top ten countries with the highest dry natural gas consumption in 2013 and dry natural gas production in 2014

Country	Dry natural gas consumption (Billion cubic meters)									Production
	2005	2006	2007	2008	2009	2010	2011	2012	2013	2014
United States	623	615	654	659	649	682	693	723	741	729
Russia	406	431	430	432	382	438	434	445	442	579
China	47	56	71	77	89	107	131	144	163	122
Iran	105	109	113	119	141	145	153	157	157	(in 2013) 161
Japan	88	97	106	104	103	109	126	127	127	5
Canada	89	93	86	83	85	80	86	100	104	151
Saudi Arabia	71	73	74	80	78	88	92	99	100	102
Germany	91	93	89	92	86	94	86	85	88	10
United Kingdom	96	91	92	95	88	94	81	78	77	39
Italy	86	84	85	85	78	83	78	75	70	7

Source: EIA International Energy Statistics, 2016

rapid data collection and seamless data integration. Field mapping and data collection are supported by a number of mobile computing tools, which are used to be extended by high-sensitivity GPS receivers, cameras, and professional laser rangefinders, which can measure slope distance, inclination, and azimuth and calculate horizontal and vertical distance. Mobile GIS includes capabilities for capturing, editing, and displaying of thematic map layers. Its GIS extensions can manage GPS data and data from optional sensors. There is also geodatabase connectivity through mobile networks in the mobile GIS environment. Thus, mobile GIS can be a part of an enterprise GIS solution in order to perform reliable field data collection with internal and external sensors, share enterprise data for rapid decision-making, increase the accuracy and validity of geodatabase, and improve the productivity of field research (Table 4.10).

Table 4.10 A list of selected mobile GISs and other related software tools

GIS	Description and the key features	Website and development
ArcPad (ESRI) [commercial]	Mobile field mapping and data collection software, which includes advanced GIS and GPS capabilities for capturing, editing, and displaying geographic information. It can manage external sensors and enables data synchronization with ArcGIS Server 10.x and ArcGIS Online feature services	http://www.esri.com/software/arcgis/arcpad Mobile GIS is supported by Windows Mobile (5.0, 6.0, 6.1, and 6.5), Windows Tablets (8.1 and 10), and Windows Desktop (XP, Vista, 7, 8.1, and 10) All customizations for ArcPad can be performed on the Windows Desktop with ArcPad Studio, and deployed with ArcPad on the mobile device
ArcGIS for Windows Mobile (ESRI) [commercial]	An application that delivers GIS capabilities and data from centralized servers to a range of mobile devices. It supports simplified mapping, spatial query, sketching, limited tools for GIS editing, and basic GPS functionality	http://www.esri.com/software/arcgis/arcgismobile Mobile GIS is supported by Windows Embedded Handheld (6.0, 6.1, and 6.5) and Windows Desktop (XP, Vista, 7, 8.1, and 10). It comes with a ready-to-deploy application and a software development kit. NET SDK for building custom applications
Apps for smartphones and tablets (ESRI) [commercial]	A few applications for sharing public maps (Explorer for ArcGIS, Web AppBuilder, AppStudio), sharing maps within an organization (Explorer for ArcGIS), and geographic data editing in the field (Collector and Web AppBuilder for ArcGIS, ArcGIS web application templates)	http://www.esri.com/software/arcgis/arcgis-app-for-smartphones-and-tablets Mobile applications are supported by smartphones and tablets running on various software platforms. Then installations also support a number of languages and national data formats. More detail information is available on ESRI Web pages
QGIS (previously known as Quantum GIS) [open source]	A free and open-source geographic information system, which offers geospatial data management. Limited functionality is also supported on mobile platform	http://www.qgis.org/en/site/ QGIS is freely available on Windows, Linux, MacOS X, BSD, and android. Binary packages (installers) for current versions can be downloaded from http://www.qgis.org/en/site/forusers/download.html

Using mobile GIS on field computers with GPS advanced tools can benefit from availability of a computing system, GPS data collection, and sharing data with other external sensors such as laser rangefinders and cameras. It can be helpful for terrain exploration of the fossil fuels and their environmental effects during the extraction and remediation. Using new computing devices with GPS technology and internal laser rangefinders is setting new mapping and GIS industry standards with real-time decimeter level positioning accuracy. Programming capabilities enable to create a number of analytical functions and modeling tools that are best fitted to the area of interest. New developments in the mobile GIS have enabled the geodatabases to be taken into the field as digital maps providing field access to enterprise geographic information. It offers terrain researches to add real-time information to their database and analytical applications, speeding up analysis, display, and decision-making by using actual, more accurate spatial and temporal data. Thus, the mobile GIS can support online field mapping, asset inventories, inspections, incident reporting, and a wide range of GIS methods recently processed in the desktop GIS environment. It is expected that feature powerful mobile GISs with more accurate sensors will be able to provide even more complex data analysis.

The global navigation satellite system enables high accuracy positioning using satellite signals that meet the requirements of real-time accuracy, continuity of signal, and signal coverage as wide as possible. The system is very useful for mineral prospecting and mining besides road, rail, air, and maritime transport and other areas such as telecommunications, geodesy, agriculture, and environmental Earth observation. The market is growing, and it is expected that in 2020 will be operating for about three billion satellite navigation receivers.

Global Positioning System (GPS) managed by the United States is at present the only one fully operating satellite navigation system. It provides users with positioning, navigation, and timing services. This system consists of three segments: the space segment, the control segment, and the user segment. The US Air Force develops, maintains, and operates the space and control segments. The space segment consists of a constellation of satellites transmitting radio signals to users. The United States is committed to maintaining the availability of at least 24 operational GPS satellites, 95% of the time. To ensure this commitment, the Air Force has been flying more operational GPS satellites. GPS satellites fly in medium Earth orbit at an altitude of approximately 20,200 km, and their constellations are arranged into six equally spaced orbital planes surrounding the Earth. Each satellite circles the Earth twice a day. As of June, 2016, the GPS constellation is a mix of old and new satellites with 31 operational satellites. The GPS control segment consists of a global network of ground facilities that track the GPS satellites, monitor their transmissions, perform analyses, and send commands and data to the constellation (Fig. 4.13). The user segment consists of the GPS receiver equipment, which receives the signals from the GPS satellites and uses the transmitted information to calculate the user's three-dimensional position and time. GPS satellites provide service to civilian and military users. The civilian service is freely available to all users on a continuous, worldwide basis. The military service is available to US and allied armed forces as well as approved government agencies. The generations of

GPS Control Segment
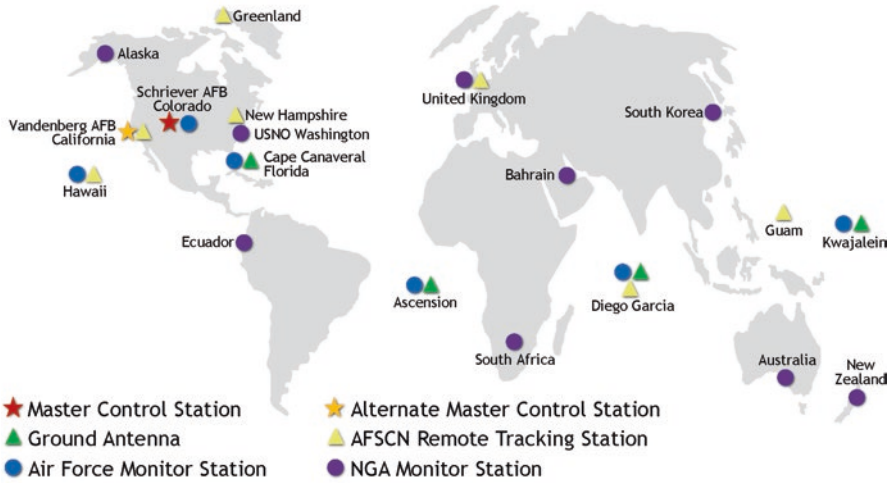
Updated April 2016

Fig. 4.13 The map schema of the GPS control segment. Source: www.gps.gov, 2016

Fig. 4.14 GPS IIF in production phase (on the left side) and GPS IIF in the operational phase (on the right side). Source: Boeing media-room, 2016

GPS satellites consist of legacy satellites (BLOCK IIA, 0 operational; BLOCK IIR, 12 operational) and modernized satellites (BLOCK IIR-M, 7 operational; BLOCK IIF, 12 operational; GPS III: in production). A satellite BLOCK IIF is in production phase and the operational phase is illustrated in Fig. 4.14.

EGNOS (European Geostationary Navigation Overlay Service) is a European project that provides a form of differential correction signal for GPS. Corrections are provided for the territory of Europe in order to eliminate errors by differential signal processing in receivers, which gives more precision to positioning. The system is composed of 34 ground Ranging and Integrity Monitoring Station (RIMS), which are located in Europe and continuously monitors the data transmitted from satellites in the GPS. The received result is continuously transmitted through a secure data network to one of the Master Control Centers (MCC), where the data is used to estimate errors caused by the state of Earth's atmosphere. The resulting information is then transmitted through the three networks of broadcasters to three satellites in geostationary orbit. These satellites return data back to Earth, where the receiver corrects them according to data received from GPS satellites. In practice, the error should be at least 99% measuring less than 1.5 m. The system is being developed and managed by the European Space Agency (ESA), European Commission (EC), and European Organization for the Safety of Air Navigation (EUROCONTROL).

GLONASS (Global Navigation Satellite System) managed by the Russian Federation Government is analogy to the US GPS. Both systems share the same principles in the data transmission and positioning methods. The operational space segment of GLONASS consists of 21 satellites in three orbital planes, with three on-orbit spare ones. Its active satellites continuously transmit coded signals, which can be received by users anywhere on the Earth's surface to identify their position and velocity in real time based on ranging measurements.

GALILEO Global Navigation Satellite System is planned as an autonomous European Global Navigation Satellite System (GNSS), which should be similar to the US GPS. Its development is actually ensured by the European Union (EU), represented by the European Commission (EC) and European Space Agency (ESA). System Galileo was originally planned to be operational by 2010, but its start was postponed several times. The fully deployed Galileo system consists of 30 satellites (27 operational + 3 active spares), positioned in three circular medium Earth orbit (MEO) planes at 23,222 km altitude above the Earth and at an inclination of the orbital planes of 56° with reference to the equatorial plane. Once this is achieved, the Galileo navigation signals will provide good coverage even at latitudes up to 75° north. It will provide five basic services:

– Open service will provide free of charge superior position and timing performance.
– Safety of life service will be offered and guaranteed to the critical transport community, such as aviation and maritime, delivering enhanced performance that includes the provision of the integrity function including a warning of system malfunction that will reach the user in a given alarm time.
– Commercial service will provide access to two additional encrypted signals to enable users improving of accuracy.
– Public regulated service will provide positioning and timing to specific users requiring a high continuity of service, with controlled access.
– Search and rescue service will represent Europe's contribution of to the international COSPAS-SARSAT cooperative effort on humanitarian search and rescue activities.

All services will have great potential especially in transport, but still offers a wide range of use in other areas where it will increase security, accuracy, and comfort such as energy industry, environmental protection, banking, and agriculture.

BeiDou Navigation Satellite System (Compass) is a Chinese project of a satellite navigation system that is created as independent system consisting of two project generations: BeiDou 1 and BeiDou 2. BeiDou 1 has been working since 2000 and provides services in China and adjacent countries. The next project, BeiDou 2, is still under construction and should be finished in 2020. It will use five geostationary orbit satellites and 30 low orbit satellites in order to provide signal all around the world.

RNSS (Indian Regional Navigational Satellite System) is managed by Indian Space Research Organization as a fully civilian system under control of Indian government. The project was launched in 2006. The complete configuration will consist of seven satellites (three satellites in geostationary orbit).

QZSS (Quasi-Zenith Satellite System) is a proposed three-satellite regional time transfer system as an enhancement for existing GPS within Japan. The system was launched in 2010. The satellites would be placed in a periodic highly elliptical orbit.

4.3 Mapping of Fossil Sources with Remote Sensing and GIS

Remote sensing is defined as collecting and interpreting information about the environment and the surface of the Earth from distance, primarily by sensing radiation that is naturally emitted or reflected by the Earth's surface or from the atmosphere or by sensing signals transmitted from a device and reflected back to it. Remote sensing is used to be divided into active and passive methods. Active methods include systems such as radar and LiDAR (Light Detection and Ranging) that produce electromagnetic radiation and measure its reflection back from a surface. Passive methods deal with satellite imaging and aerial photography that detect energy naturally reflected or emitted by objects.

Particularly the remote sensing systems deployed on satellites can provide a repetitive view of the Earth's surface, which is invaluable for exploration of long-term land cover changes. In case of passive methods, the optical regime from visible spectrum through thermal spectrum of the electromagnetic radiation depends on two source of radiation: the Sun and the Earth. The radiation collected in the visible to shortwave infrared spectrum originates from the Sun. A part of this radiation is reflected at the Earth's surface, and a part is scattered by the atmosphere, without reaching the Earth. The radiation collected in the thermal infrared spectrum is emitted directly by the Earth's surface. A number of applications in remote sensing have been developed in the context of research projects dealing with climate change, land cover dynamics, and environmental risk assessment. It began when the Landsat Multispectral Scanner System (MSS) provided a consistent set of high-resolution Earth images to the scientific community. Now the Landsat project represents the world's longest continuously acquired collection land remote sensing data. Four decades of imagery give a unique resource for research in those who work in geology,

Fig. 4.15 A timeline of the Landsat missions. Source: USGS, 2016, http://landsat.usgs.gov

forestry, agriculture, regional planning, and assessment of energy sources. As a joint initiative between the US Geological Survey (USGS) and NASA, the Landsat project and the data it collects support government, commercial, industrial, civilian, military, and educational communities throughout the United States and worldwide. More detailed information is on Web pages: http://landsat.usgs.gov. A timeline of Landsat missions is shown in Fig. 4.15. The first civilian Earth observation satellite ERTS-1 (Earth Resources Technology Satellite) was launched in 1972. The ERST-1 was later renamed Landsat 1, and the launches of Landsat 2, Landsat 3, and Landsat 4 followed in 1975, 1978, and 1982, respectively. Landsat 5 was launched in 1984 and delivered high-quality, global data of Earth's land surfaces for more than 28 years. It gives an opportunity to explore land cover changes captured by identical sensors in long-term period. The next satellite Landsat 6 failed to achieve orbit in 1993, but the Landsat program continued by Landsat 7 (successfully launched in 1999) and Landsat 8 (launched in 2013), which continue to provide daily global data. Now images from Landsat satellites are provided free to the public by the Department of the Interior's US Geological Survey. Landsat images also provide standards for a number of new applications such as Timelapse powered by Google, or ChangeMatters Viewer, which is a commercial product of ESRI. Both applications can utilize the global time-lapse video showing changes to our planet visible from Landsat satellite imagery.

The latest Landsat 8's Operational Land Imager (OLI) improves on past Landsat sensors and preserves measurement compatibility with previous Landsat missions, in order to have comparable images for long-term land cover studies. The OLI instrument uses a new sensor, which aligns the imaging detector arrays along Landsat 8's focal plane allowing it to view across the entire swath, 185 km cross-track field of view. The OLI collects data from nine spectral bands, where seven of them are consistent with the Thematic Mapper (TM) and Enhanced Thematic Mapper Plus (ETM+) sensors in earlier Landsat satellites. The Thermal Infrared Sensor (TIRS) conducts thermal imaging and is registered to OLI data to create radiometrically, geometrically, and terrain-corrected datasets. The TIRS only provides Landsat data continuity with one band, band 10. Visual comparison of Landsat spectral bands from all missions is shown in Fig. 4.16, which includes spectral bands

* MSS bands 1–4 were known as bands 4–7, respectively, on Landsats 1–3
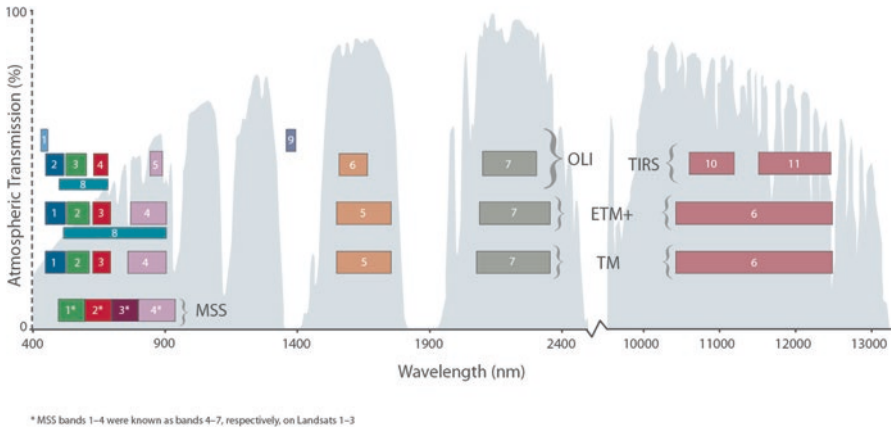
Fig. 4.16 Visual comparison of Landsat spectral bands for Landsat Multispectral Scanner (MSS) on Landsat 1–3, Thematic Mapper (TM) on Landsat 4–5, Enhanced Thematic Mapper Plus (ETM+) on Landsat 7, and OLI together with TIRS on Landsat 8 (atmospheric transmission values were calculated using the model MODTRAN for a summertime mid-latitude hazy atmosphere). Sources: NASA, 2016, http://landsat.gsfc.nasa.gov/

Table 4.11   Landsat 8 Operational Land Imager (OLI) bands and Thermal Infrared Sensor (TIRS) bands

OIL and TIRS spectral bands	Wavelength (μm)	Useful for mapping
Band 1—coastal aerosol	0.43–0.45	Coastal and aerosol studies
Band 2—blue	0.45–0.51	Bathymetric mapping, distinguishing soil from vegetation and deciduous from coniferous vegetation
Band 3—green	0.53–0.59	Emphasizes peak vegetation, which is useful for assessing plant vigor
Band 4—red	0.64–0.67	Discriminates vegetation slopes
Band 5—near infrared (NIR)	0.85–0.88	Emphasizes biomass content and shorelines
Band 6—shortwave infrared (SWIR) 1	1.57–1.65	Discriminates moisture content of soil and vegetation; penetrates thin clouds
Band 7—shortwave infrared (SWIR) 2	2.11–2.29	Improved moisture content of soil and vegetation and thin cloud penetration
Band 8—panchromatic	0.50–0.68	15 m resolution, sharper image definition
Band 9—Cirrus	1.36–1.38	Improved detection of cirrus cloud contamination
Band 10—TIRS 1	10.60–11.19	100 m resolution, thermal mapping and estimated soil moisture
Band 11—TIRS 2	11.5–12.51	100 m resolution, improved thermal mapping and estimated soil moisture

Source: USGS 2016, http://landsat.usgs.gov/best_spectral_bands_to_use.php

from Landsat Multispectral Scanner (MSS) on Landsat 1–3, Thematic Mapper (TM) on Landsat 4–5, Enhanced Thematic Mapper Plus (ETM+) on Landsat 7, and OLI together with TIRS on Landsat 8. The detailed information about all Landsat bands are shown in Tables 4.11, 4.12 and 4.13.

Table 4.12 Landsat 4–5 Thematic Mapper (TM) and Landsat 7 Enhanced Thematic Mapper Plus (ETM+)

TM and ETM+ spectral bands	Wavelength (μm)	Useful for mapping
Band 1—blue	0.45–0.52	Bathymetric mapping, distinguishing soil from vegetation and deciduous from coniferous vegetation
Band 2—green	0.52–0.60	Emphasizes peak vegetation, which is useful for assessing plant vigor
Band 3—red	0.63–0.69	Discriminates vegetation slopes
Band 4—near infrared	0.77–0.90	Emphasizes biomass content and shorelines
Band 5—shortwave infrared	1.55–1.75	Discriminates moisture content of soil and vegetation; penetrates thin clouds
Band 6—thermal infrared	10.40–12.50	Thermal mapping and estimated soil moisture
Band 7—shortwave infrared	2.09–2.35	Hydrothermally altered rocks associated with mineral deposits
Band 8—panchromatic (Landsat 7 only)	0.52–0.90	15 m resolution, sharper image definition

Source: USGS 2016, http://landsat.usgs.gov/best_spectral_bands_to_use.php

Table 4.13 Landsat Multispectral Scanner (MSS) and its utilization on Landsat 1, 2, and 3 and Landsat 4 and 5

Landsat MSS 1,2, and 3 spectral bands	Landsat MSS 4 and 5 spectral bands	Wavelength (μm)	Useful for mapping
Band 4—green	Band 1—green	0.5–0.6	Sediment-laden water, delineates areas of shallow water
Band 5—red	Band 2—red	0.6–0.7	Cultural features
Band 6—near Infrared	Band 3—near infrared	0.7–0.8	Vegetation boundary between land and water and landforms
Band 7—near infrared	Band 4—near infrared	0.8–1.1	Penetrates atmospheric haze best, emphasizes vegetation, boundary between land and water, and landforms

Source: USGS 2016, http://landsat.usgs.gov/best_spectral_bands_to_use.php

The National Satellite Land Remote Sensing Data Archive (NSLRSDA) at the US Geological Survey (USGS) Earth Resources Observation and Science (EROS) Center holds the rich collection of Landsat data in the world. Currently it holds more than three million Landsat scenes that Landsat satellites have acquired from across the globe for more than four decades. As examples, geographical presentations of scenes that are archived at the EROS are shown in Fig. 4.17 for Landsat 1 MSS in 1973 and for Landsat 8 OLI and TIRS in 2014. The complete presentation of the USGS Landsat Global Archive is available on the Web page: http://landsat.usgs.gov/USGSLandsatGlobalArchive.php. The images are sorted by date and then satellite and then sensor, because most years have multiple maps associated with several
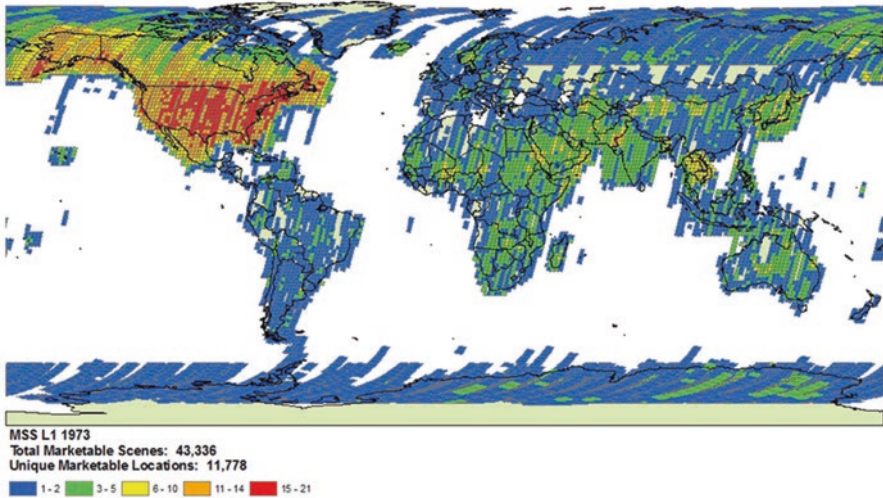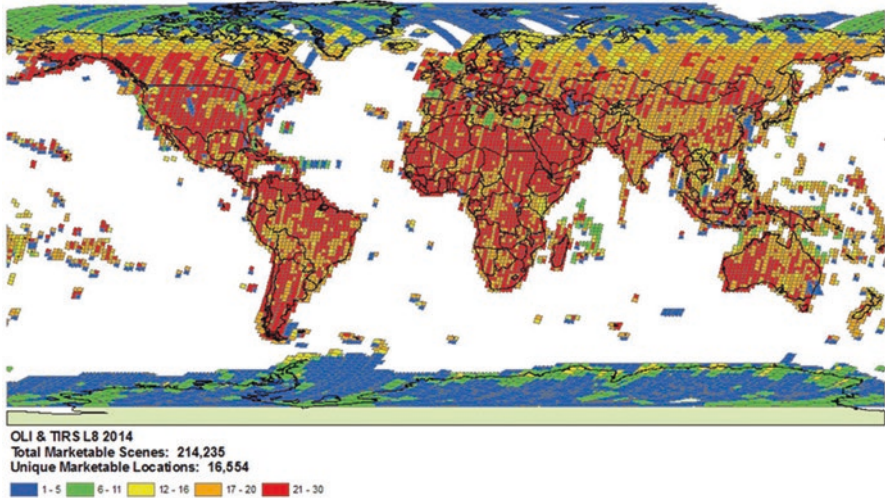
Fig. 4.17 Geographical presentations of scenes that are archived at the EROS for Landsat 1 MSS in 1973. Source: USGS, 2016, http://landsat.usgs.gov/documents/StateOfTheArchive_web.pdf

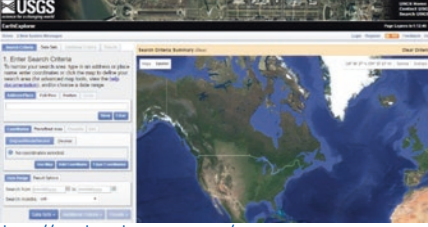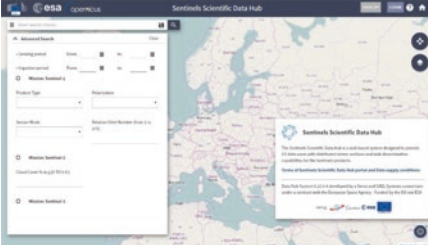satellites and sensors. It shows only images held at the USGS EROS Center at time of file creation, but other images can be completed from International Ground Stations that downlinked Landsat data over the years. The Landsat Global Archive Consolidation (LGAC) program started in 2010. Its goal is to consolidate the Landsat archives of all stations worldwide into the USGS EROS Archives (Fig. 4.18).

Landsat images play an important role in identifying and assessment of new energy sources and mitigating the human and environmental impact of energy development. The archive data including more than 40 years of imagery can support decision-makers to monitor the environmental impact of mining and energy generation and track ecological recovery after operations end. The infrared and visible measurements together assist energy companies in identifying minerals on the surface. Farmers can estimate the health of biofuel crops and natural vegetation near dams and mining sites. Scientists and managers from around the world can use data from the archives for a variety of applications and research programs. Besides the USGS EROS Archives, there are many other data sources dealing with satellite imagery, aerial photographs, and LiDAR/radar data over the world. A list of selected satellite imagery data sources is shown in Table 4.14.

Preprocessing of remote sensing data is dealing with feature extraction, radiometric and atmospheric correction, and geometric transformation. But each project requires specific attention and individual preprocessing decisions in dependence on source images and target applications. While the feature extraction depends on a source of images, radiometric and atmospheric correction includes a set of techniques related to the sensitivity of the sensor, topography and sun angle, and atmospheric scattering

OLI & TIRS L8 2014
Total Marketable Scenes: 214,235
Unique Marketable Locations: 16,554

1 - 5   6 - 11   12 - 16   17 - 20   21 - 30

Fig. 4.18 Geographical presentations of scenes that are archived at the EROS for Landsat 8 OLI and TIRS in 2014. Source: USGS, 2016, http://landsat.usgs.gov/documents/StateOfTheArchive_web.pdf

and absorption. The geometric transformation is used to provide spatial correction by a digital terrain model and to bring an image into registration with selected map coordinates. Because preprocessing changes original data, it is recommended to use only those methods that are essential to obtain target results.

After an initial stage of preprocessing data, advanced methods for image classification are mostly applied to explore remote sensing data. Images can be classified based on many distinguishable cover types that are specified by the user such as land cover classes based on geology, major vegetation types, vegetation condition, disturbed areas, or land-use changes. By comparing pixels to one another and to pixels of known identity, the classifier can assemble groups of similar pixels into classes that are associated with explored categories. These classes create regions on an image, which are transformed into a mosaic of uniform parcels, each identified by a color. The pixels in each class are spectrally more similar to one another than they are to pixels in other classes. Image classification techniques in remote sensing are used to be divided into supervised and unsupervised classification.

In the unsupervised classification, pixels are grouped based on their spectral properties into clusters. The user selects the digital image bands, the number of clusters to generate, and the classification algorithm such as K-means or ISODATA. With this information, the unsupervised classification algorithm generates clusters that have to be manually attached to land cover classes. This classification is commonly used when no sample sites exist.

In the supervised classification, the user selects representative samples and training sites, for each land cover class in the digital image. This information is used by

Table 4.14 A list of selected satellite imagery data sources

Data sources	The key features	Website
Earth Explorer (USGS)	-access to Landsat satellite data (the USGS EROS Archives), -ASTER image data, -Shuttle Radar Topography Missions global Digital Elevation Models, -Hyperion's hyperspectral data, -MODIS & AVHRR land surface reflectance and disperse Radar data.	http://earthexplorer.usgs.gov/
Sentinel Mission (ESA)	-Sentinel 1 day and night radar imaging for land and ocean services (Sentinel 1A, Sentinel 1B), -Sentinel 2 high-resolution optical imaging for land services (Sentinel 2), -Sentinel 3 ocean and global land monitoring services (Sentinel 3A), (a number of Sentinels are planned to be lunched in the future).	https://scihub.copernicus.eu/dhus/ .
CLASS (NOAA)	-POES, DMSP, GOES, MetOp, Jason-2 data, and selected reanalysis data, -it will archive data collections from the NPP, JPSS (formerly NPOESS), GOES-R, Jason-3, and planned Earth-based observing systems include NEXRAD products.	http://www.class.ngdc.noaa.gov/saa/products/welcome
Reverb (NASA)	-data from Aqua, Terra, Aura, TRMM, Calipso, NASA DC, JASON, ENVISAT, ALOS, METEOSAT, GOES, ICESAT, GMS, Landsat, NIMBUS, SMAP, RADARSAT, NOAA satellites.	http://reverb.echo.nasa.gov/reverb/
DigitalGlobe (DigitalGlobe)	-the largest commercial satellite data supplier in the world with downloadable: -data samples from the newly launched satellites, -data samples in fields such as exploration, engineering, land management and simulation, -huge amount of technical information.	http://www.digitalglobe.com/

the supervised classification algorithm to identify the land cover classes in the image. The supervised classification of land cover is based on the spectral signature defined in the training set. The digital image classification software determines each class on what it resembles most in the training set. The mostly used supervised classification algorithms are maximum likelihood and minimum distance classification.

Described pixel-based classification techniques generate groups of square classified pixels. New object-based image classification is different in that it generates objects of different shape and scale. This process is called multiresolution segmentation, which creates homogenous image objects by grouping pixels. These objects are more meaningful than the standard pixel-based segmentation because they can be classified based on texture, context, and geometry. The object-based techniques are favored for very high spatial resolution images, where objects are made up of several pixels. In addition, object-based image classification can take advantage of both spectral and contextual information in the remotely sensed imagery, which brings higher accuracy to classification.

Satellite and aerial imagery can provide even more answers for assessment of energy sources, environmental change, weather forecasting, disaster management, and other remote sensing applications. Remote sensing software processes images and provides solutions to local or global issues. Applications in geology include bedrock and lithological and structural mapping, where multispectral spectral reflectance has provided valuable information on rock composition while radar has also been useful in studying surface roughness. Other applications deal with extracting mineral deposits with hyperspectral remote sensing, where having more spectral bands gives potential to map more minerals in dependence on their chemical composition. Many applications are focused on detecting land cover/use types for decision-making and monitoring the environment for protection.

4.4 Environmental Effects of Fossil Fuel Use

Fossil fuels such as coal, oil, and gas are currently the world's primary energy source, which have increasingly fueled global economic development for a few last centuries. Fossil fuels are finite resources, and their combustion irreparably harms the environment and is responsible for greenhouse gas emissions. These gases can insulate the planet and may cause catastrophic changes in the Earth's climate. Recently, there are only partial solutions for reduction of greenhouse gas emissions over the world such as energy efficiency, nuclear energy as a zero-carbon alternative for electricity generation, renewable energy, and carbon capture and storage.

The energy supply industry is the largest contributor to global greenhouse gas emissions. It attributed approximately 35% of total anthropogenic emissions in 2010 and accelerated from 1.7% per year in 1990–2000 to 3.1% in 2000–2010. The higher demand for power, heat, and transport services followed by a higher share of coal in the global fuel mix were the main contributors to this trend. The energy supply industry converts over 75% of the total primary energy into other forms such as

electricity, heat, refined oil products, coke, and natural gas. Including non-energy use, the industry consumes 84% of final use of coal and peat, 26% of petroleum products, 47% of natural gas, 40% of electricity, and 43% of heat. Transportation consumes 62% of liquid fuels final use. The building sector is responsible for 46% of final natural gas consumption, 76% of combustible renewables and waste, 52% of electricity use, and 51% of heat. Energy losses assessed as the difference between the energy inputs and outputs are estimated more than 29% of total primary energy supply, which also includes the relatively low average global efficiency of energy conversion, transmission, and distribution processes, 37% efficiency for fossil fuel power production and 83% for fossil fuel district heat generation. Between 2000 and 2010, the total primary energy supply grew by 27% globally, 2.4% per year, while for the regions it was 79% in Asia, 47% in Middle East and Africa, 32% in Latin America, and 13% in economies in transition. It was nearly stable for the countries of the OECD. After 2010, the growth was slower, about 2% per year over 2010–2012 in Asia, Middle East and Africa, and Latin America and even declining in economies in transitions and OECD countries (Fig. 4.19) (IPCC, 2014: Climate Change 2014).

The energy market in Asia differs considerably from other markets. This region accounted a high increment for fossil fuels in the last decades. In particular, China doubled the total primary energy supply between 2000 and 2010 and became the
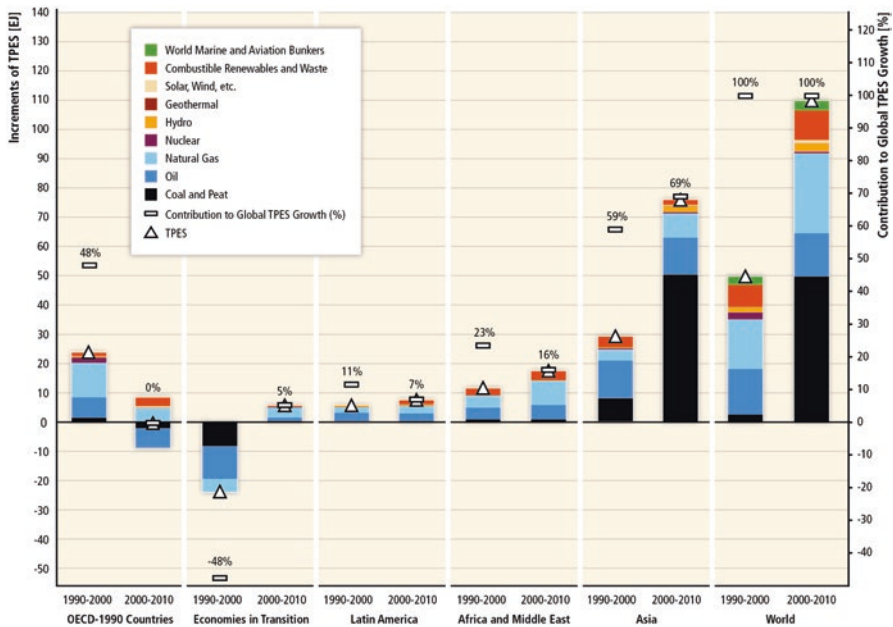
Fig. 4.19 Contribution of energy sources to regional and total primary energy supply (TPES) increments (modern biomass contributes 40% of the total biomass share). Source: IPCC, 2014: Climate Change 2014

leading energy-consuming nation and coal producer. Thus, power generation remains the main global coal renaissance driver in China (47% of world 2012 production), followed by the United States, Australia, Indonesia, India, and other countries. The energy supply industry accounts for 49% of all energy-related greenhouse gas emissions, while remaining energy-related emissions occur in the consumer sectors in 2010. According to emission database EDGAR (Emission Database for Global Atmospheric Research, which provides global past and present-day anthropogenic emissions of greenhouse gases and air pollutants by country and on spatial grid), global greenhouse gas emissions from energy supply industry increased by more than 35% in 2000–2010 and grew on average 1% per year, which was faster than global anthropogenic greenhouse gas emissions (Fig. 4.20). In addition to the predominant carbon dioxide emissions, other emitted emissions involved methane, of which 31% comes from coal and gas production and transmission, and indirect nitrous oxide, of which 9% comes from coal and fuelwood.

Oil is the world's primary fuel source for transportation and chemical industry. Besides the environmental degradation caused by oil spills and extraction, combustion of its products is a major source of greenhouse gas emissions. Also release of fine particulates can lead to serious respiratory problems. Heavier crude oils, especially those extracted from tar sands and shale, require the use of extra energy-intensive methods that result in more emissions and larger environmental degradation in comparison to conventional oil. Unfortunately, extraction of crude oils expands,
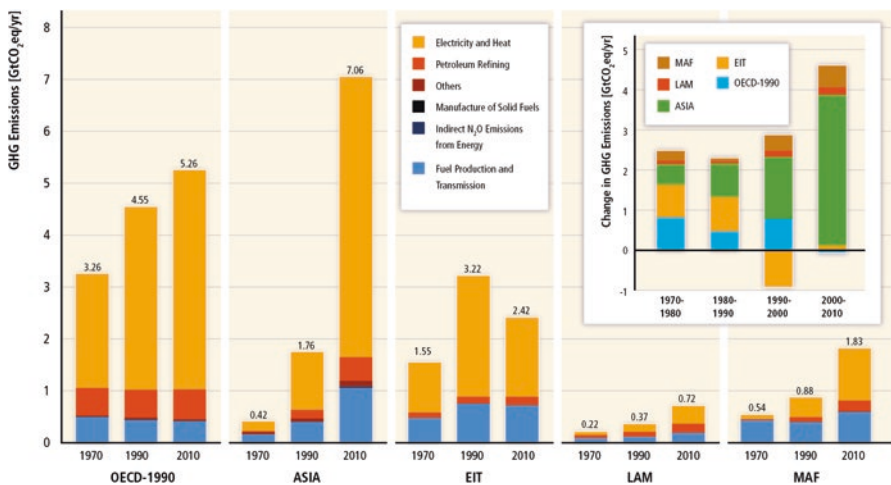
Fig. 4.20 Energy supply industry greenhouse gas (GHG) emissions by subsectors and regions: OECD countries, Asian countries, economies in transition (EIT), Africa and the Middle East (MAF), and Latin America (LAM). The graph on the right side shows contribution of different regions to decadal emissions increments. Source: IPCC, 2014: Climate Change 2014; Emissions Database EDGAR; IEA

because conventional oil from underground reservoirs runs out, and more oil producers have to turn to unconventional sources such as tar sands and oil shale.

Combustion of natural gas is cleaner than coal and oil, with almost zero sulfur dioxide emissions and far fewer nitrogen oxide and particulate emissions. Natural gas releases almost 30% less carbon dioxide than oil and 43% less than coal. Like other fossil fuels, also natural gas is responsible for approximately 27% of greenhouse gas emissions. Natural gas is primarily composed of methane, which is a greenhouse gas that is more than 20 times as potent as carbon dioxide. Thus, capturing and burning the gas, which is also generated by the decomposition of municipal waste in landfills and manure from livestock production, prevent the methane from being released into the atmosphere directly.

Based on the emissions database EDGAR, the global carbon dioxide emissions per region from fossil fuel use and cement production is shown in Fig. 4.21. Carbon dioxide emissions from fossil fuel use and cement production in the top five emitting countries and the EU are illustrated in Fig. 4.22. Finally, the combustion of coal and partially oil releases air pollutants such as acid rain-inducing sulfur dioxide, nitrogen oxides (NOx), and mercury. The extraction is used to be very damaging to the environment, often resulting in the destruction of vegetation and topsoil and potentially contamination of rivers and streams by mine wastes. Technology focused on carbon capture and storage (CCS), where carbon is separated from coal and injected underground for long-term storage, could theoretically be used to mitigate the coal industry's greenhouse gas emissions. It is proven as a way to reduce greenhouse gas emissions from commercial power plants.
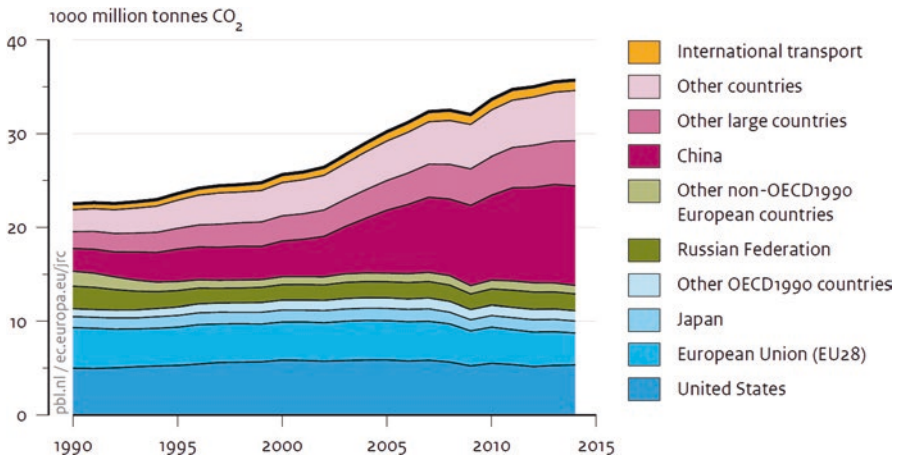
Fig. 4.21 Global carbon dioxide emissions per region from fossil fuel use and cement production. Source: Trends in global carbon dioxide emissions: 2015 Report of the Netherlands Environmental Assessment Agency
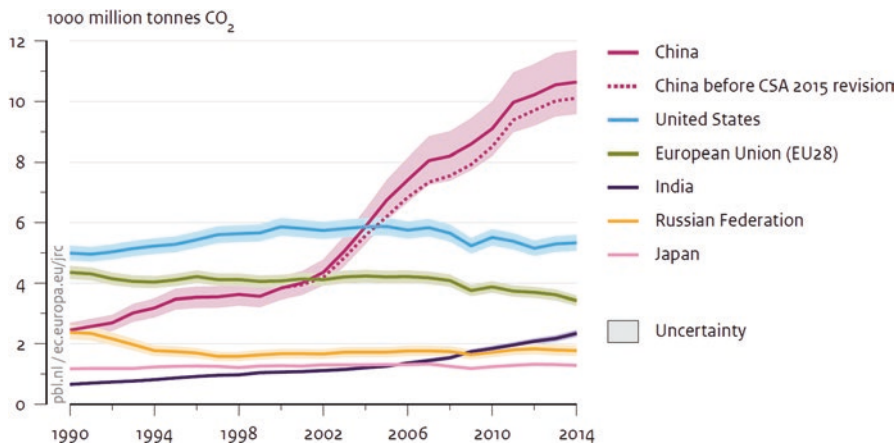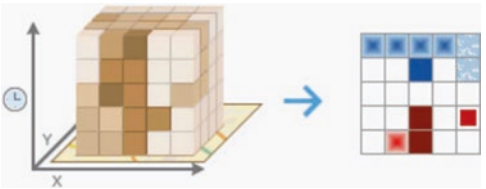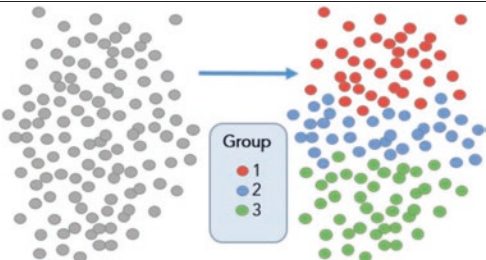
Fig. 4.22 Carbon dioxide emissions from fossil fuel use and cement production in the top five emitting countries and the EU. Source: Trends in global carbon dioxide emissions: 2015 Report of the Netherlands Environmental Assessment Agency

4.5   Integration of Spatial and Temporal Data in GIS

Spatial-temporal analysis in assessment of energy sources offers additional insight into environmental processes at a variety of scales. Hypotheses at the landscape level can now be generated and tested by combining spatial-temporal analyses and models. Advanced methods are necessary for changes in spatial patterns to be identified. These methods are mostly implemented in new versions of GIS software such as Hot Spot Analysis (Getis-Ord Gi* statistic), Cluster and Outlier Analysis (Anselin Local Moran's I statistic), Emerging Hot Spot Analysis, and Grouping Analysis in ArcGIS Pro (Table 4.15). The spatial statistical tools contain a number of other statistical methods for analyzing spatial distributions, patterns, processes, and relationships. Unlike traditional nonspatial statistical methods, they incorporate space (proximity, area, connectivity, and/or other spatial relationships) directly into their mathematics. In addition, for those tools written with Python, the source code can be modified and extended in order to share these and other analysis tools with others. Besides GIS tools also widely implemented in open-source software, a number of special applications are dealing with space and time such as Web-based tools of US EIA, IEA, BP, and EEA. A list of selected Web-based tools for display of spatial and temporal data related to fossil fuels is shown in Table 4.16. Other applications have been created in the framework of research projects in the last years. As examples, FFDAS (Fossil Fuel Data Assimilation System) focused on estimates of carbon dioxide emissions is illustrated in Fig. 4.23, and monitoring of methane with satellites ENVISAT and GOSAT is shown in Fig. 4.24 (Table 4.17).

Table 4.15 A list of selected methods focused on space-time cluster analysis

Method	Description	Principal schema
Hot Spot Analysis (ArcGIS Pro)	Identifies statistically significant hot spots and cold spots using the Getis-Ord Gi* statistic by given a set of weighted features.	http://pro.arcgis.com/en/pro-app/tool-reference/spatial-statistics/hot-spot-analysis.htm
Cluster and Outlier Analysis (ArcGIS Pro)	Identifies statistically significant hot spots, cold spots, and spatial outliers using the Anselin Local Moran's I statistic by given a set of weighted features	http://pro.arcgis.com/en/pro-app/tool-reference/spatial-statistics/cluster-and-outlier-analysis-anselin-local-moran-s.htm
Emerging Hot Spot Analysis (ArcGIS Pro)	Identifies trends in the clustering of point densities (counts) or summary fields in a space-time cube created using the Create Space Time Cube tool. Categories include new, consecutive, intensifying, persistent, diminishing, sporadic, oscillating, and historical hot and cold spots.	http://pro.arcgis.com/en/pro-app/tool-reference/space-time-pattern-mining/emerginghotspots.htm
Grouping Analysis (ArcGIS Pro)	Groups features based on feature attributes and optional spatial or temporal constraints.	http://pro.arcgis.com/en/pro-app/tool-reference/spatial-statistics/grouping-analysis.htm

4.6   Spatial and Temporal Modeling with GIS

Environmental models are used to be developed to understand spatial and temporal phenomena of environmental processes and to optimize their environmental impacts. In case of fossil fuels, these models can support impact assessment of extraction, treatment, transportation, and combustion together with environmental pollution and disturbance of landscape patterns. Recently, there have been several different contexts for the term modeling in the environmental sciences.

In the traditional environmental dynamic modeling, the models are used to be representations of processes that are believed to occur in the real world, mainly from the geosphere, the hydrosphere, and the atmosphere and also from the biosphere. Thus, the huge variety of phenomena and approaches can be studied in the

Table 4.16 A list of selected Web-based tools for display of spatial and temporal data related to fossil fuels
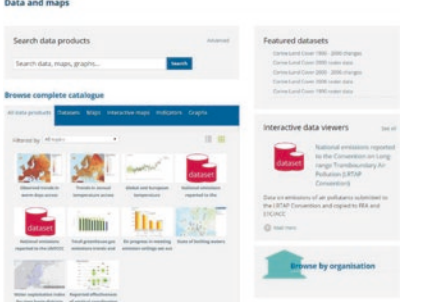
Organization	Description	Website
U.S. EIA (Energy Information Administration)	The EIA provides a wide range of information and data products covering energy production, stocks, demand, imports, exports, and prices. EIA also prepares analyses and special reports on topics of current interest. Mapping applications are focused on energy view of petroleum, natural gas, renewable energy power plants, coal, biomass, solar, geothermal, fossil fuel resources, energy infrastructure, electricity, wind and hydroelectric issues. Example: Mapping of petroleum production over the world ->	http://www.eia.gov/beta/international/
IEA (International Energy Agency)	The IEA is made up of 29 member countries. The IEA examines the full spectrum of energy issues and advocates policies that will enhance the reliability, affordability and sustainability of energy in its 29 member countries and beyond. Example: Total final consumption of coal in 2013 ->	http://www.iea.org/statistics/statisticssearch/
BP (British Petroleum)	The BP provides fuel for transportation, energy for heat and light, lubricants to keep engines moving and petrochemicals used to make everyday items. The BP energy charting tool allows to interrogate data, create charts and download reports from the Statistical Review of World Energy. Example: Consumption of coal in a few part of the world ->.	http://www.class.ngdc.noaa.gov/saa/products/welcome
EEA (European Environment Agency of the European Union)	The EEA provides sound, independent information on the environment. The EEA is a major information source for those involved in developing, adopting, implementing and evaluating environmental policy, and also the general public. Example: a list of data products focused on environmental mapping ->.	http://reverb.echo.nasa.gov/reverb/

Fig. 4.23 Mapping the surface coal mine with 3D laser scanner HDS3000 (on the left side) and GPS (on the right side)
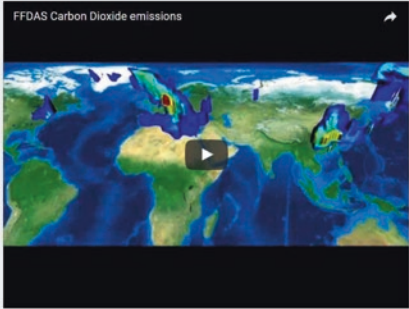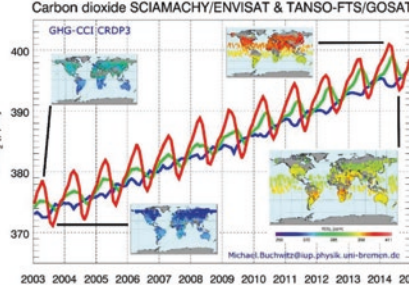

Fig. 4.24 Mapping the surface coal mine with 3D laser scanner HDS3000 (on the left side) and GPS (on the right side)

framework of environmental systems and their models. Dynamic modeling can be deterministic or stochastic in dependence on nature of the environmental processes that are described by physical, chemical, or biological laws and rules. It includes processes of diffusion, dispersion, advection, sorption, and other basic phenomena. There are models that can simulate global processes of the entire globe or local phenomena of the mass and energy transport. The description of the processes and phenomena is based on the mathematical approach, which deals with the changes of variables, such as pollutant concentration or species density, in space and time. Now, the solution of mathematical models can be made by computer programs that assist in time-consuming numerical calculations of multidimensional problems and spatial and temporal analysis of the results.

In spatial modeling by GISs, the models are considered as a template into which the spatial datasets needed for a particular application can be fitted. Thus, data models

Table 4.17 A list of applications created in the framework of research projects

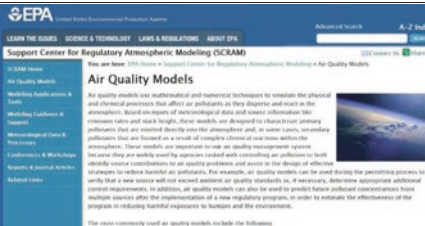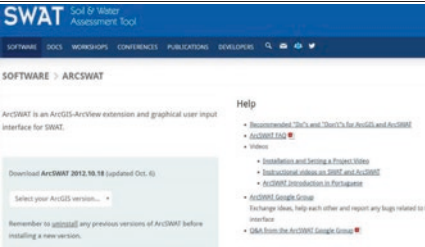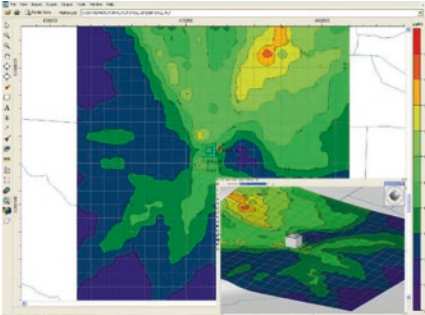| Organization	Description	Website
FFDAS project (Fossil Fuel Data Assimilation System**)**	The subsets of the FFDAS include fossil fuel carbon dioxide emissions data focused on: - an electricity production sector - other sectors (all other fossil fuel, emissions excepting shipping and aviation), - EDGAR shipping – international and domestic shipping, - EDGAR aviation – international and domestic aviation, -uncertainty values associated with the total emissions. The FFDAS v2.0 visualization and data for download are available at FFDAS web pages ->	http://hpcg.purdue.edu/FFDAS/index.php?page=media http://hpcg.purdue.edu/FFDAS/Map.php
GHG-CCI project (ESA)	Satellite observations (SCIAMACHY on ENVISAT in 2002 - 2012) and TANSO on GOSAT) combined with modelling help to improve our knowledge on carbon dioxide and methane sources and sinks as required for better climate prediction. GHG-CCI aims at delivering the high quality satellite retrievals needed for this application. Other satellite instruments will be used to provide constraints for upper layers such as IASI, MIPAS and ACE-FTS ->	http://www.iea.org/statistics/statisticssearch/ http://www.esa-ghg-cci.org/?q=image_gallery
CDIAC (Carbon Dioxide Information Analysis Center)	CDIAC serves the climate change-related data and information needs of users worldwide. CDIAC includes estimates of carbon dioxide emissions from fossil-fuel consumption and land-use changes; records of atmospheric concentrations of carbon dioxide and other radiatively active trace gases and other related information ->.	http://cdiac.ornl.gov/ http://cdiac.ornl.gov/trends/emis/meth_reg.html
EUROSTAT (European Commission)	Eurostat's task is to provide the European Union with statistics at European level that enable comparisons between countries and regions. GISCO (Geographic Information System of the Commission) can localize, analyze, visualize environmental data ->.	http://ec.europa.eu/eurostat/web/main http://ec.europa.eu/eurostat/web/gisco/overview

based on geodatabase design, mostly preferred for large datasets, can be also used for smaller data amounts. But the GIS data models implemented in the geodatabases share universal concepts that are important for data sharing and building of more complex spatial and temporal analyses. For example, land cover classes can be represented by polygons with their boundaries and share a geometry set of rules. Roads, railways, or rivers are represented by their centerlines, which are connected at the endpoints, and the topological connection in a geometric network enables tracing and interconnection based on a set of rules. In addition to the geometric representation, all these features have a commonly used set of attributes and relationships to tax their rolls. All datasets are used to be stored in the geodatabase that can manage spatial features and their topology together with the support of spatial and temporal model tasks such as landscape disturbance or environmental modeling. For example, risk assessment focused on environmental pollution can be supported by a number of geostatistical tools, such as exploratory spatial data analysis (ESDA), semivariogram modeling, threshold mapping, model validation and diagnostics, or surface prediction using cokriging.

In the framework of the both concepts, the models provide abstractions that simplify in communicating ideas from scientists to less scientifically informed public. The visual tools have become one of the most important ways of presenting environmental problems to a wide range of interests. Thus, GIS represents a powerful medium for communicating of spatial and temporal models in a wide variety of disciplines and from many different perspectives such as energy assessment of fossil fuels and their environmental impacts.

Complex monitoring systems and data management systems for large datasets are needed for development of environmental models that are used to support decision-making processes. The systematic assessment of environmental characteristics, such as air quality or climatic changes, based on regular measurements together with model predictions, can help to optimize living environment and improve public health. Considering to the huge amount of data, many studies, research reports, and other specific documents are published to inform research society and public about environmental problems. The impact assessment studies are mostly carried out by measurements in areas where the level of landscape disturbance and environmental pollution reaches the upper assessment thresholds.

A number of environmental datasets, analysis, and models are available on US EPA (Environmental Protection Agency) Web pages: https://www3.epa.gov/. Many environmental tools were created in the framework of research projects focused on environmental monitoring, analysis, and modeling. A number of modeling tools have been implemented in software packages, which offer user-friendly environment and advanced data management. These software tools also include data exchange methods, which support data formats managed by GIS and Web-based applications. A list of selected software tools for environmental management and impact assessment is shown in Table 4.18.

Table 4.18 A list of selected software tools for environmental management and impact assessment

Subject	Description	Website
U.S. EPA (Environmental Protection Agency)	The EPA's Air Quality Modeling Group (AQMG) conducts modeling analyses to support policy and regulatory decisions in the Office of Air and Radiation (OAR) and provides the full range of air quality models and other techniques used in assessing control strategies and source impacts. Documentation, guidelines, models and data are available on the website ->	 https://www3.epa.gov/ https://www3.epa.gov/ttn/scram/
USGS (U.S. Geological Survey)	The water resources Groundwater software and related material (data and documentation) are made available to be used in the public interest and the advancement of science. As an example, the MODFLOW (3D finite-difference groundwater model for prediction of groundwater conditions and interactions is selected for the website presentation ->	 https://www.usgs.gov/ http://water.usgs.gov/software/lists/groundwater
SWAT Soil and Water Assessment Tool, public domain model jointly developed by USDA ARS (Agricultural Research Service) and Texas A&M (AgriLife Research, a part of The Texas A&M University	It is a small watershed to river basin-scale model to simulate the quality and quantity of surface and ground water and predict the environmental impact of land use, land management practices, and climate change. It can be used for regional management in watersheds. As an example, ArcSWAT (ArcGIS-ArcView extension and graphical user input interface for SWAT) is selected for the website presentation ->	 http://swat.tamu.edu/ http://swat.tamu.edu/software/arcswat/
AERMOD View (Scientific Software Group)	It is a complete air dispersion modeling package which incorporates the U.S. EPA models into one interface: AERMOD, ISCST3 (Industrial Source Complex - Short Term), and ISC-PRIME (Industrial Source Complex - Plume RIse Model Enhancements). These models are used to assess pollution concentration and deposition from a wide variety of emission sources. AEROMOD is an air dispersion model designed for short-range dispersion of air pollutant emissions from stationary industrial sources ->	 http://www.scisoftware.com/environmental_software/ https://www3.epa.gov/ttn/scram/dispersionindex.htm

4.7   Case-Oriented Studies

Assessment of energy sources dealing with fossil fuels includes a wide range of operations. The attached examples are focused on environmental research using advanced computing tools such as mobile GIS, GPS, remote sensing data, and environmental modeling. Environmental research requires to manage a wide range of terrain measurements, remote sensing images, existing datasets, and inputs/outputs of mathematical models. Thus, GISs are often used to process datasets from terrain research, remote sensing, and a wide variety of other monitoring and modeling tools. In order to demonstrate the integration of spatial and temporal data together with methods related to spatial and dynamic modeling, a few case studies are presented for assessment of energy sources dealing with environmental research and risk assessment of opencast coal mining sites.

4.7.1   Using GPS and Mobile GIS for Mapping of Fossil Fuels in a Local Scale

An attached case study is focused on estimates of mineral dust impacts on the neighborhood of an opencast coal mine. Mapping of the potential emissions sources is complemented by measurements of wind flows with a few local meteorological stations. In the local scale, the wind flows are highly dependent on terrain morphology, which causes difficulties in estimating the dust transport. In addition to wind flows, physical processes in soils predetermine the conditions of primary dust dispersion. These processes are affected by variable natural factors, such as meteorology, soil state, and surface roughness. In cases of opencast coal mines, potential emission sources are temporary storage sites, coal sorting, excavators, conveyors, and moving vehicles. A temporary coal storage site with coal sorting excavators and erosion of slopes are illustrated in Fig. 4.23. Coal sorting causes dust emissions, which are spread by wind flows over an opencast mine and its neighbor areas. Erosion can form gullies that carry large volumes of water resulting in even greater erosion.

The GIS mapping of the mine is based on 3D surface laser scanning, GPS measurements, and existing digital thematic maps. The 3D laser scanners provided an efficient method for local 3D point cloud acquisition of the surface and its associated industrial installations. Complete coverage with point cloud data is created from multiple standpoints. Four scans with an average grid size of 0.2 m were performed with a Leica HDS 3000 3D laser scanner. While the 3D surface laser scanning was used for mapping of continuous parts, a few GPS instruments were used to assist in the capturing of breaklines of the slopes, boundaries of the temporary storage sites, and locations of other surface objects such as transport routes, potential emission sources, and the local meteorological stations. The accuracy of the GPS measurements was improved in the postprocessing phase using data from the nearest reference stations in the country. The final accuracy of the GPS spatial

data after the postprocessing phase was 0.5 m. The 3D laser scanner Leica HDS3000 making point cloud acquisition and terrain data collection with GPS are shown in Fig. 4.24. The datasets created by laser scanning and GPS were imported into the GIS datasets in order to provide integrated data management, processing, analysis, and modeling. A part of the surface visualized by Leica Geosystems HDS Cyclone software is illustrated in Fig. 4.25a, which shows an overview of a slope visualized by merged 3D point clouds from the acquisition phase. A detailed view on a temporary coal storage site is shown in Fig. 4.25b. The 3D point cloud provides the detailed scan of the mining equipment with an average grid size of 0.2 m. Both the scans were created with a filtered and reduced data in order to optimize response time of the visualization functions.
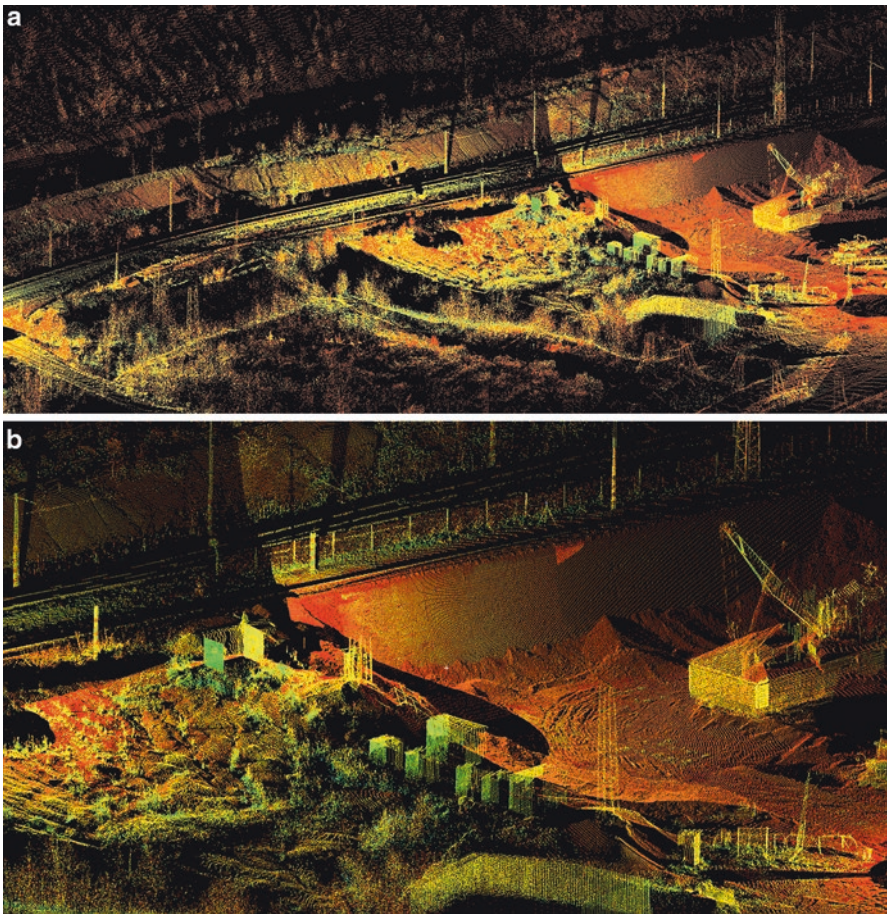
Fig. 4.25 (**a**) Visualization of a point cloud with the Leica Cyclone 3D point cloud processing software: an overview. (**b**) Visualization of a point cloud with the Leica Cyclone 3D point cloud processing software: a detail view

4.7.2   Mapping Surface Coal Mines in a Regional Scale with Landsat Images

A case study is focused on using the Landsat 8 image for environmental mapping of opencast mines, which are located in the Northwestern Czech Republic. The selected Landsat scene and an area of interest are illustrated in a map schema of Europe in Fig. 4.26. The area of interest in visible spectrum, thermal spectrum, and combination of visible and near infrared spectrum is shown in Figs. 4.27, 4.28 and 4.29, respectively.

The Landsat bands offer to explore surface by indexes. As an example, the normalized difference vegetation index (NDVI) is used to estimate the relative biomass. The chlorophyll absorption in red band and relatively high reflectance of vegetation in near infrared band can assist in estimating landscape disturbance by the opencast mine, Fig. 4.30. The NDVI shows the relative biomass by positive value and rocks and bare soil by values close to zero. The disturb landscape with mineral extraction sites and dump sites is shown in Fig. 4.31. The next image captured by Landsat 5 shows the opencast mines in 1988 (Fig. 4.32) and 2009 (Fig. 4.33), respectively. The seasonal changes in vegetation are illustrated by Landsat 8 images for spring season (Fig. 4.34) and autumn season (Fig. 4.35).
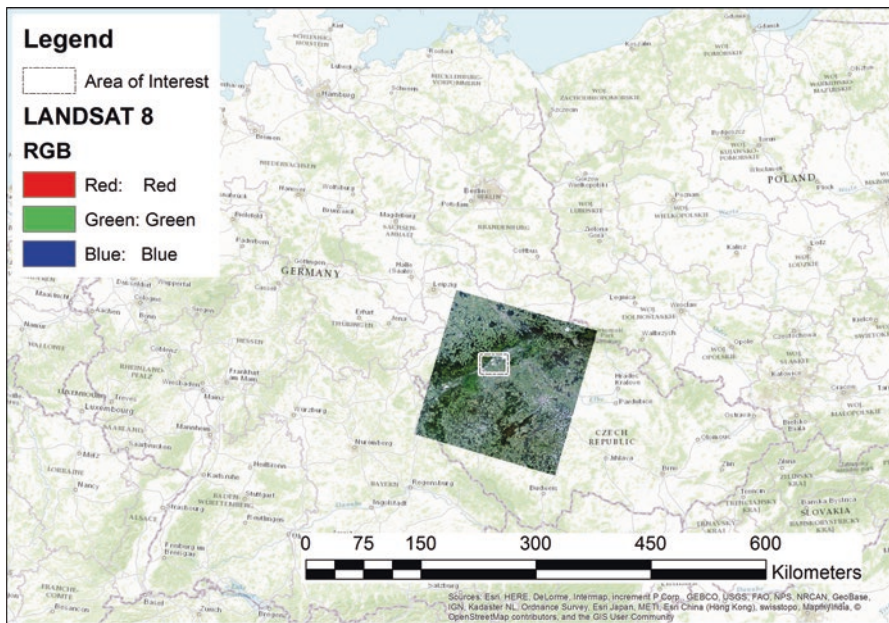

Fig. 4.26 The selected Landsat 8 scene (June 24, 2016) and an area of interest in the Northwestern Czech Republic

Fig. 4.27 Landsat 8 image (June 24, 2016) in visible spectrum (OLI band: 4, 3, 2), mines are indicated by light sites
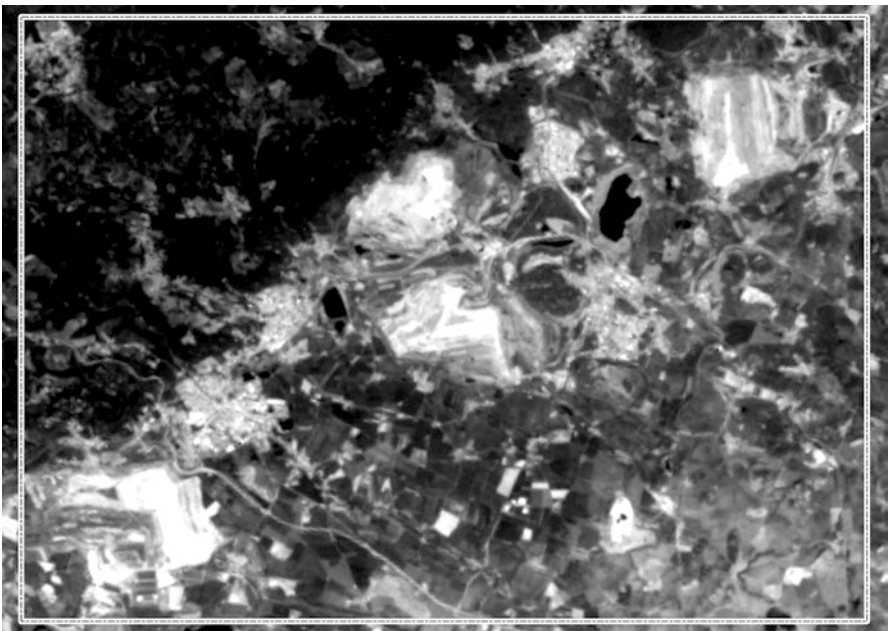

Fig. 4.28 Landsat 8 image (June 24, 2016) in thermal spectrum (TIRS: band 11), mines are indicated by light sites
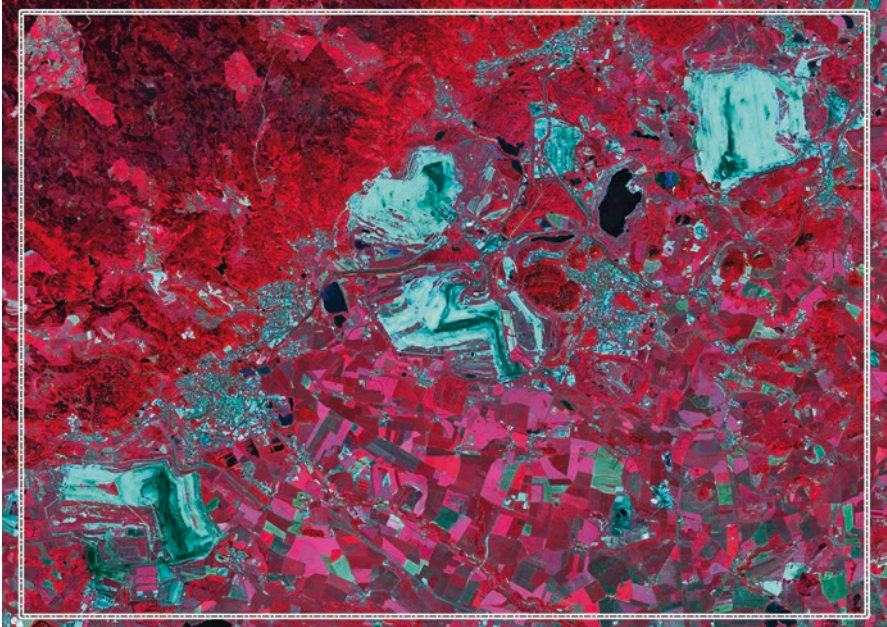
Fig. 4.29 Landsat 8 image (June 24, 2016) in visible and near infrared spectrum (OLI band: 5, 4, 3)
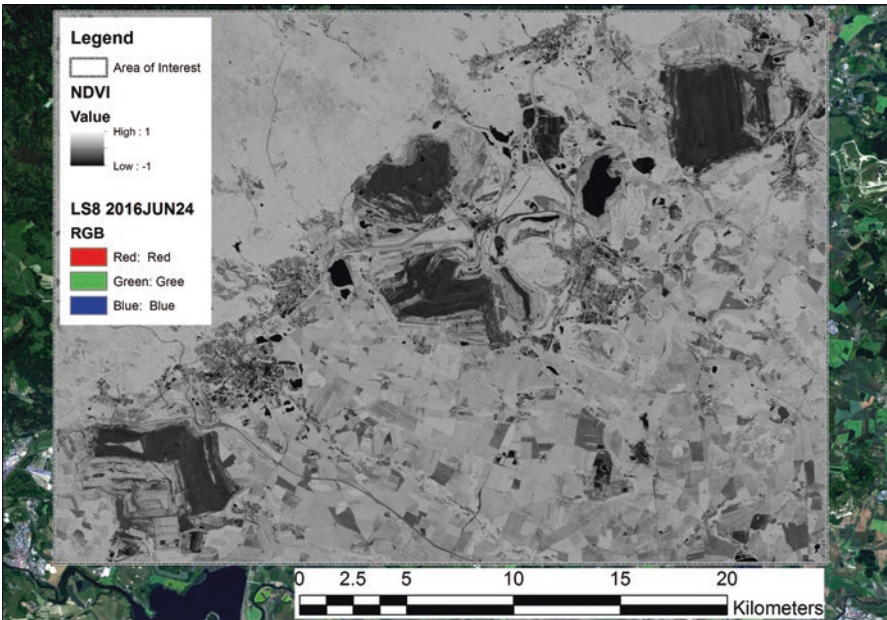

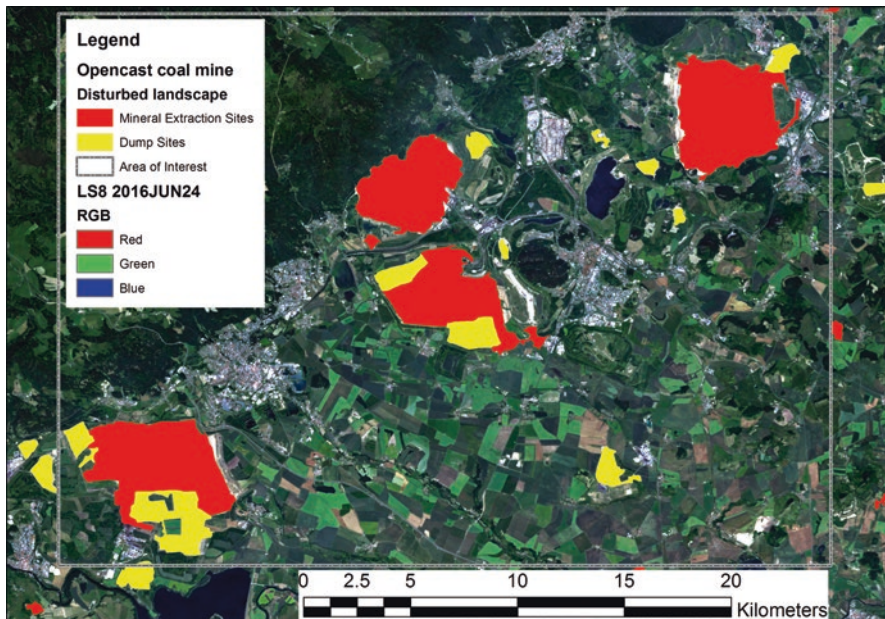**Fig. 4.30** NDVI (June 24, 2016): biomass is indicated by positive value and rocks and bare soil by values close to zero

Fig. 4.31 The opencast coal mines: mineral extraction sites and dump sites (June 24, 2016)

Fig. 4.32 Landsat 5 image (August 14, 1988, an initial image) in visible spectrum (TM band: 3, 2, 1)

Fig. 4.33 Landsat 5 image (August 24, 2009, an image captured after 21 years) in visible spectrum (TM band: 3, 2, 1)

Fig. 4.34 Landsat 8 image (March 18, 2015, spring season) in visible spectrum (OLI band: 3, 2, 1)

Fig. 4.35 Landsat 8 image (October 12, 2015, autumn season) in visible spectrum (OLI band: 3, 2, 1)

4.7.3 Modeling of Coal Dust Dispersion in a Local Scale

Estimates of dust dispersion can be provided either by measurements or by modeling, but it is often a combination of the both procedures, where model predictions are used to provide data for areas, in which monitoring data are lacking. Model predictions include a number of methods such as spatial interpolations, regression-based techniques, numerical modeling, and aerodynamic research in wind tunnels. Integration of data flows is seen as a central task for using of combined research. Complex processing of environmental data for spatial modeling, air dispersion numerical models, and aerodynamic research in wind tunnels include many steps, which are illustrated in Fig. 4.36.

The input datasets into the preprocessing phase include spatial data for the digital terrain model (DEM), emission sources for thematic maps dealing with location of emission sites and pollutant amounts, regular sampling of air pollution for validation of numerical models, and regular meteorological data (wind speed and direction and other variables such as temperature, humidity, precipitation, and solar). After the preprocessing stage, the created spatial and temporal datasets are integrated into the GIS and managed by the geodatabase, which can be complemented by other data, such as satellite images, aerial photographs, thematic maps, and historical records. These datasets are used by spatial modeling, air dispersion numeri-
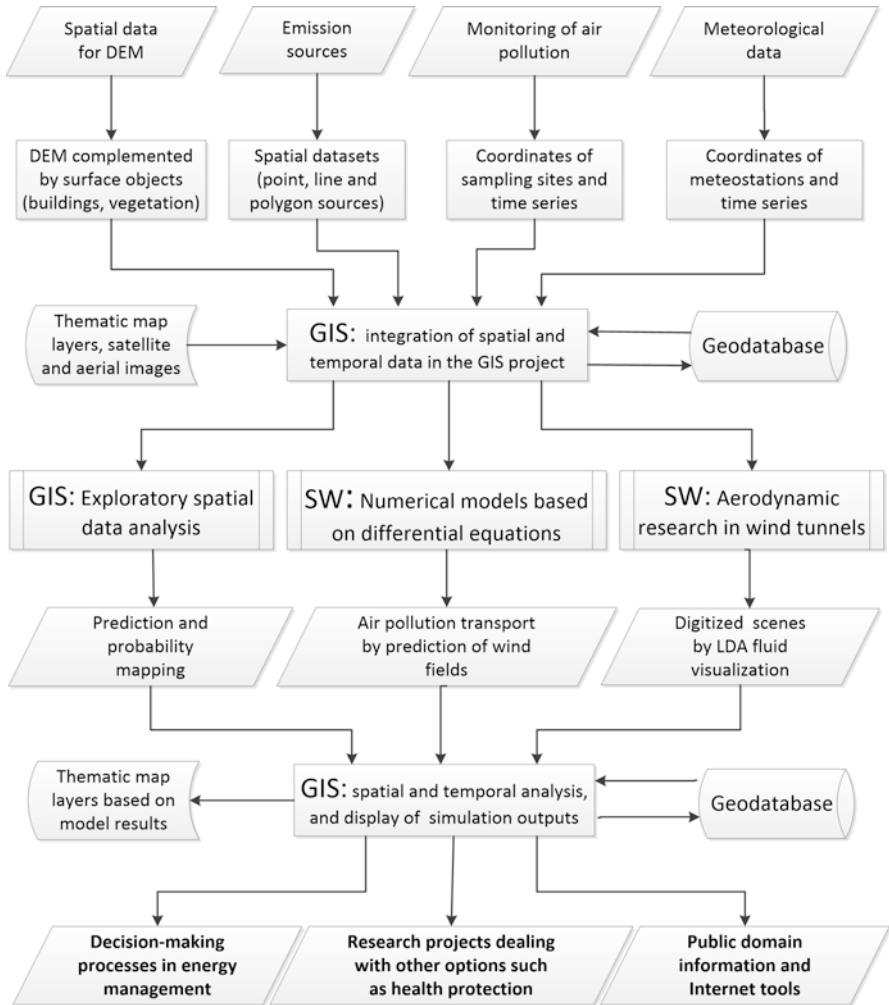
Fig. 4.36 Data flows in the processing of environmental data for spatial modeling, air dispersion numerical models, and aerodynamic research in wind tunnels designated for decision-making processes in energy management and related projects that are focused on health protection and information in the public domain

cal models, and aerodynamic research in wind tunnels to provide model predictions and validation and optimization of the explored processes in order to minimize health effects and other environmental risks. As an example a part of the DEM for numerical modeling and aerodynamic research is shown in Figs. 4.37 and 4.38. The DEM is complemented by localization of sites for monitoring of air pollution and collection of meteorological data. The standard color palette is used for symbolizing of various heights in altimetry of the opencast mine in the GIS environment.
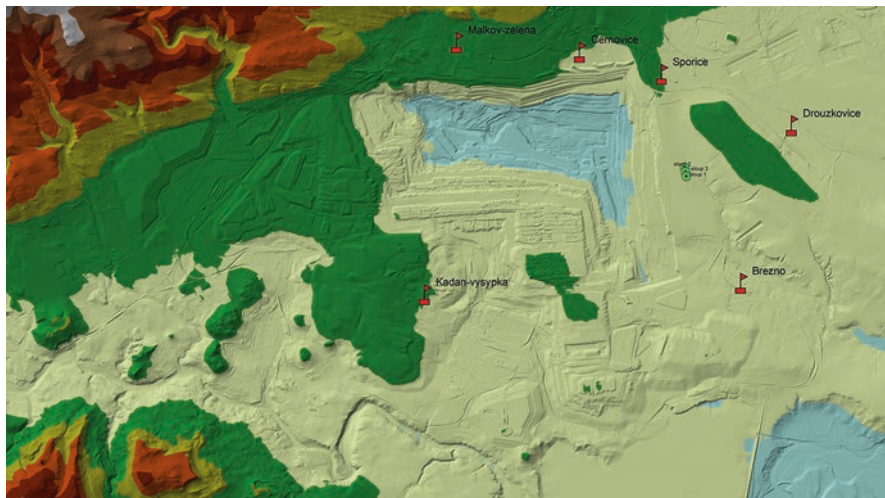
Fig. 4.37 Opencast coal mine: a part of the DEM in the GIS environment for numerical modeling and aerodynamic research complemented by localization of sites for monitoring of air pollution and regular collection of meteorological data (a predefined color palette is used for symbolizing of altimetry)
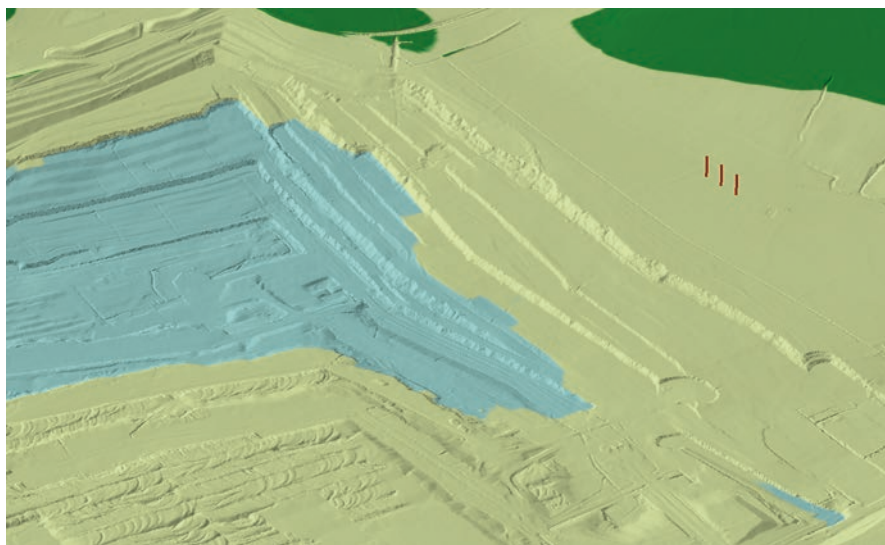

Fig. 4.38 Opencast coal mine: a 3D detail of the DEM in the GIS environment for numerical modeling and aerodynamic research complemented by localization of sites with three poles on the right site for monitoring of air pollution and collection of meteorological data (a predefined color palette is used for symbolizing of altimetry)

In case of dust dispersion, spatial modeling deals with deterministic and geostatistical interpolation methods, probability mapping, and geographically weighted regression (GWR). The interpolation and probability mapping are based on point samples. They are used for continuous surface layers that predict the values of air pollutant concentrations for every location in the area of interest. The probability maps can assess the probability that a critical concentration threshold value has been exceeded. GWR is used to provide a local model by fitting regression equations containing the dependent variable, concentration of air pollutant, and explanatory variables, such as potential sites of pollutant emissions, local wind speed, and surface temperature or humidity.

The numerical models based on the Navier-Stokes equations and other mathematical expressions are solved by standalone software tools, because GIS mostly supports only basic tasks in dispersion modeling. Additional procedures are needed to export data to the required data inputs of various numerical models. The initial tests were performed with Gaussian plume air dispersion models, such as AERMOD, ISCST3, and ISC-PRIME. The numerical models utilized data from the digital elevation model (DEM), extended by simplified 3D buildings, datasets containing air pollution sources and sampling points/receptors, as well as records of meteorological data. The output datasets are extracted and imported into the GIS by other software tools and GIS functions. These air dispersion numerical models employ hourly meteorological data records to define the conditions for plume rise, transport, diffusion, and deposition. The concentration or deposition values are estimated for each hour of input meteorology. The model outputs, user-selected, short-term averages of the concentrations at each receptor location, are exported into GIS for analysis and visualization, together with the existing spatial data, Fig. 4.39.

An alternative approach to numerical modeling is represented by aerodynamic research that uses wind tunnels to study the effects of air moving past models of a surface. The size of a model on a scale of about 1:9000 is 1.5 m x 1.5 m. The measurements are visualized by two-dimensional optical fiber laser Doppler anemometry (LDA). After capturing the scenes, the experimental data are imported into the computer system for other processing. The plastic models are produced using computer numerical control (CNC) machine tools. The data inputs are derived from DEMs created in GIS. The DEMs are based on a large dataset of points (1500 x 1500 points for the 1.5 m x 1.5 m model).

The inputs into the postprocessing phase represent continuous surface layers from spatial modeling, user-selected short-term averages of concentrations at each receptor location from numerical models and captured images of flow fields from aerodynamic research in wind tunnels. The postprocessing phase employs import of simulation results into the GIS project to integrate new datasets together with existing data in the geodatabase. The spatial and temporal analysis and visualization are used to create thematic maps of environmental impacts for decision-making processes, related research projects that are focused on health protection and information in the public domain. As an example of landscape disturbance, the changes in terrain heights in 2010–2014 are illustrated by a 3D view in Fig. 4.40, which compare two DEMs related to the stage of mining in 2010 and 2014. The difference of
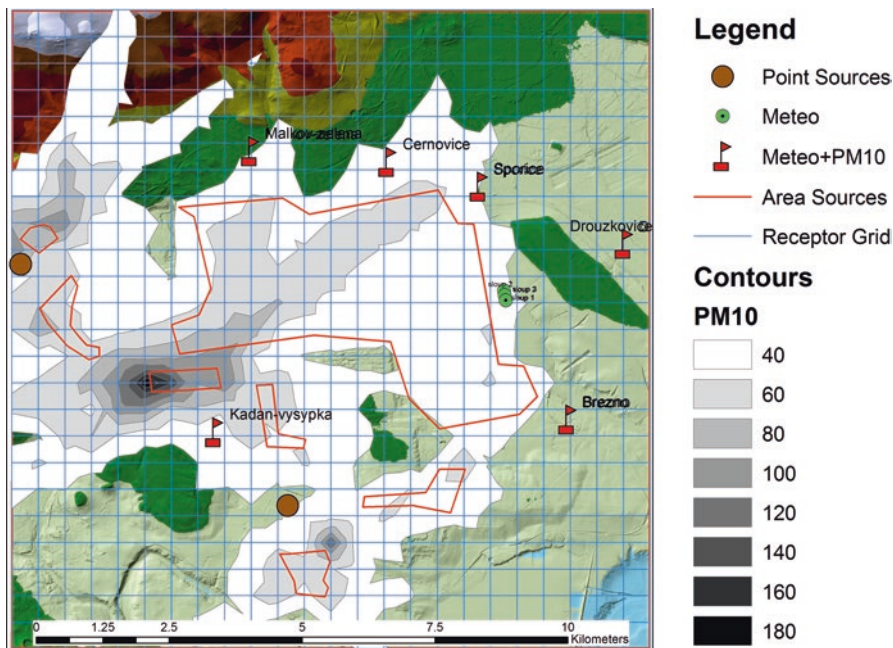
Fig. 4.39 The model outputs for a year period: user-selected short-term averages of concentrations at each receptor location in the regular grid. The isolines of PM_{10} concentrations are complemented by a DEM layer and by other features, such as monitoring stations and a receptor grid
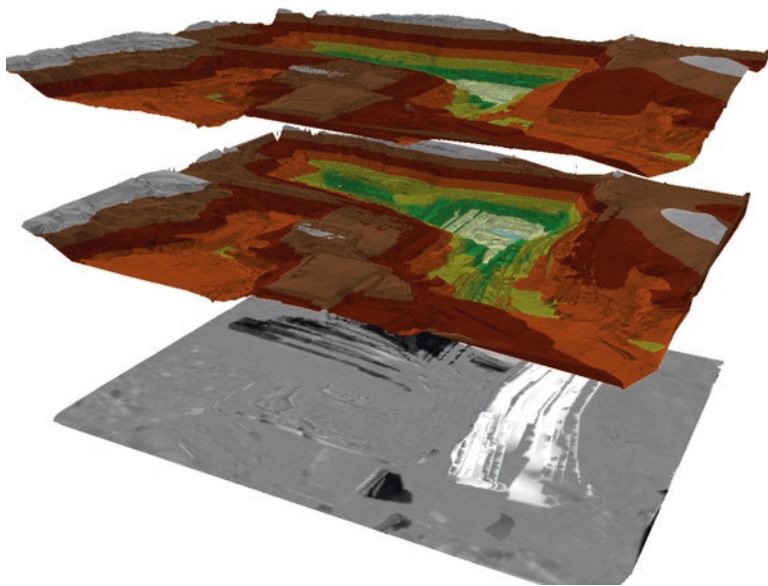

Fig. 4.40 A 3D view for visualization of the altimetry in the opencast mine in 2010–2014; the height difference on the surface of the mine between 2014 and 2010 is indicated with an attached layer by light pixels for decreasing by extraction and by gray pixels for increasing by accumulation

heights is indicated on the attached layer by light pixels for decreasing in elevations by extraction and by gray pixels for increasing in elevations by accumulation.

This case study focused on modeling of coal dust dispersion in a local scale in the GIS environment offers a wide range of spatial and temporal analyses. It is a way how to share data and methods dealing with spatial modeling, air dispersion modeling, and aerodynamic research in wind tunnels. Also it can explore the influence of terrain changes caused by mining activities on wind flows and air pollution dispersion, which is useful for decision-making processes related to reducing the environmental impacts of surface coal mining. The simulation of appropriate manmade barriers and different flow conditions enables to test the most suitable solution for reducing the environmental impacts of mining activities. The results can facilitate prediction of air pollution above the area of interest in the surface coal mine and its neighboring areas.

Bibliography

EIA. (2016). *International Energy Outlook 2016*. Retrieved from http://www.eia.gov/forecasts/ieo/pdf/0484(2016).pdf

IAEA. (2015). *Annual report 2014*. Retrieved from https://www.iaea.org/sites/default/files/gc59-7_en.pdf

IEA. (2015). *CO_2 emissions from fuel combustion highlights 2015*. Retrieved from http://www.iea.org/publications/freepublications/publication/CO2EmissionsFromFuelCombustionHighlights2015.pdf

IEA. (2016). *Coal information—2016 edition—Excerpt—Key coal trends*. Retrieved from http://www.iea.org/publications/freepublications/publication/KeyCoalTrends-1.pdf

IEA. (2016). *Oil information—2016 edition—Excerpt—Key oil trends*. Retrieved from http://www.iea.org/publications/freepublications/publication/KeyOilTrends.pdf

IEA. (2016). Natural gas information—2016 edition—Excerpt—Key natural gas trends. Retrieved from http://www.iea.org/publications/freepublications/publication/KeyNaturalGasTrends-1.pdf

IEA. (2016). *Tracking clean energy progress 2016*. Retrieved from https://www.iea.org/publications/freepublications/publication/TrackingCleanEnergyProgress2016.pdf

IEA. (2016). *World energy statistics 2016*. Retrieved from http://www.iea.org/bookshop/723-World_Energy_Statistics_2016

IPCC. (2014). Climate change 2014: mitigation of climate change. Contribution of Working Group III to the Fifth Assessment Report of the Intergovernmental Panel on Climate Change. Cambridge University Press, Cambridge. Retrieved from https://www.ipcc.ch/pdf/assessment-report/ar5/wg3/ipcc_wg3_ar5_full.pdf

Netherlands Environmental Assessment Agency. (2015). *Trends in global CO_2 emissions: 2015 report*. Retrieved from http://edgar.jrc.ec.europa.eu/news_docs/jrc-2015-trends-in-global-co2-emissions-2015-report-98184.pdf

Dictionaries and Encyclopedia

EIA. (2016). *Energy explained: Your guide to understanding energy*. Retrieved from http://www.eia.gov/energyexplained/index.cfm

Data Sources (Revised in January, 2016)

CLASS (NOAA). *Satellite imagery data sources*. Retrieved from http://www.class.ngdc.noaa.gov/saa/products/welcome

Digital Globe (Digital Globe). *Satellite imagery data sources*. Retrieved from http://www.digital-globe.com/

Earth Explorer (USGS). *Satellite imagery data sources*. Retrieved from http://earthexplorer.usgs.gov/

EIA. *International Energy Statistics*. Retrieved from http://www.eia.gov/cfapps/ipdbproject/IEDIndex3.cfm

European Global Positioning System. Retrieved from http://gnss-centre.cz/en/

Mobile GIS. *ArcPad*. Retrieved from http://www.esri.com/software/arcgis/arcpad

Mobile GIS. *ArcGIS for Windows mobile*. Retrieved from http://www.esri.com/software/arcgis/arcgismobile

Mobile GIS. *Apps for smartphones and tablets*. Retrieved from http://www.esri.com/software/arcgis/arcgis-app-for-smartphones-and-tablets

Mobile GIS & GIS. *QGIS*. Retrieved from http://www.qgis.org/en/site/

Reverb (NASA). *Satellite imagery data sources*. Retrieved from http://reverb.echo.nasa.gov/reverb/

Sentinel Mission (ESA). *Satellite imagery data sources*. Retrieved from https://scihub.copernicus.eu/dhus/

USGS Landsat Global Archive. Retrieved from http://landsat.usgs.gov/USGSLandsatGlobalArchive.php

U.S. Global Positioning System. Retrieved from http://www.gps.gov/

Chapter 5
Hydropower: Assessment of Energy Potential and Environmental Issues in the Local and Global Scales

Hydropower has been used for energy supply for many centuries. Now it accounts for about a few percent of world energy production. Hydropower is described as a renewable source, but it is slightly different, because it occupies large areas of land and can disrupt the local ecosystems. The dam prevents the upstream migration of aquatic animals, which can be overcome by building fish ladders. The areas below the dam are deprived of silt that causes lower yield in organic farming. Hydroelectric power is widely utilized by mountainous countries like Austria, Norway, and Switzerland. Nowadays, the expansion is limited in many developed countries, because most of the suitable sites have already been used. The hydroelectric potential can be increased by the concept of distributed generation from small hydro plants that are connected to conventional electrical distribution networks as a source of low-cost renewable energy. Also small hydro projects may be built in isolated areas, where there is no national electrical distribution network. Since small hydro projects generating capacity of 1–20 megawatts have minimal civil construction work, they are seen as having a relatively low environmental impact compared to large hydro plants.

5.1 Description of Hydropower Sources

Hydropower is electricity generated by using the energy of moving water. Conventional hydroelectric power plants must be located on or near a water source, because the source of hydroelectric power is water. Hydropower became a source for generating electricity in the late nineteenth century. The first hydroelectric power plant was built at Niagara Falls in 1879. In 1881, the hydropower powered street lamps in the city of Niagara Falls. In 1882, the world's first hydroelectric power plant began operating in the United States in Appleton, Wisconsin. Other milestone in construction of dams is represented by Hoover Dam, a concrete arch-gravity dam in the Black Canyon of the Colorado River in the United States (Fig. 5.1). It was

Fig. 5.1 Hoover Dam, a concrete arch-gravity dam in the Black Canyon of the Colorado River in the United States. It was constructed between 1931 and 1936, the height of the dam is 221.4 m, and the installed power capacity is 2080 MW. Hoover Dam impounds Lake Mead, the largest reservoir in the United States by the total capacity 35,200 km³

constructed between 1931 and 1936 with the height of the dam of 221.4 m. Hoover Dam impounds Lake Mead, the largest reservoir in the United States by the total capacity of 35,200 km³. The installed capacity of the power station is 2080 MW. The dam's generators provide power utilities in Nevada, Arizona, and California. Hoover Dam is also a major tourist attraction in a region.

In the last years, hydropower was produced in 150 countries with the Asia Pacific region generating about one-third of global hydropower in 2013. Now China is the largest hydroelectricity producer and dominates the market for new development and total installed capacity. The world installed hydropower capacity by country at the end of 2015 and estimated new hydropower capacity added by region in 2015 is in Figs. 5.2 and 5.3, respectively.

Hydropower continues to grow around the world. In 2015, an estimated new hydropower capacity added into operation was about 33 GW, including pumped storage about 2.5 GW. An increase in demand for electricity and other related reservoir services are crucial drivers for hydropower in developing countries. In developed countries, a new development of hydropower is more influenced by looking for reliable, clean, and affordable power. There still remains significant undeveloped hydropower potential across the world, particularly in regions such as Asia, Africa, and Latin America. The adoption of UN Sustainable Development Goals also includes a specific goal related to energy, which calls for a substantial increase in the share of renewables by 2030, in order to reduce anthropogenic greenhouse
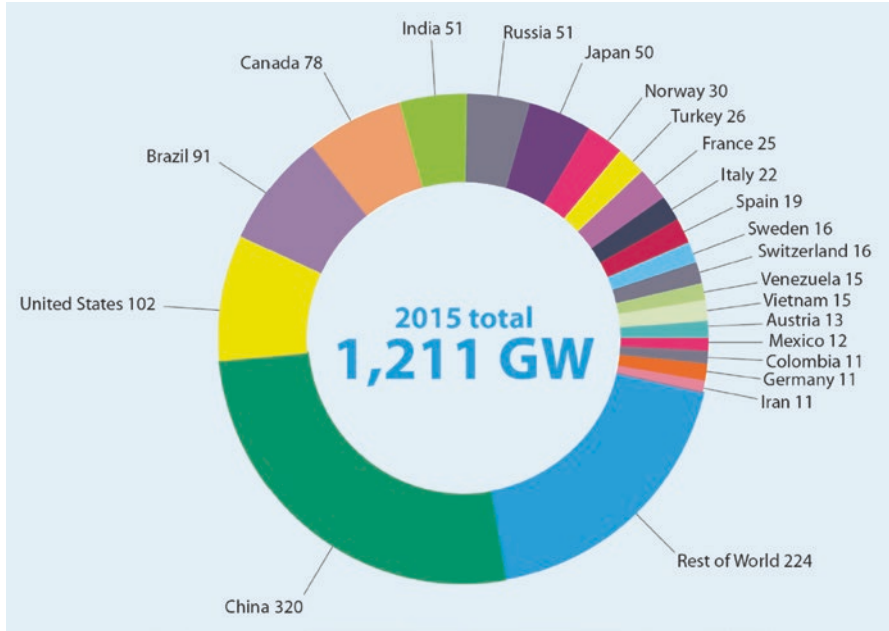
Fig. 5.2 World installed hydropower capacity in GW by country at the end of 2015, including pumped storage about 145 GW. Source: IHA 2016 Key Trends in Hydropower, 2016
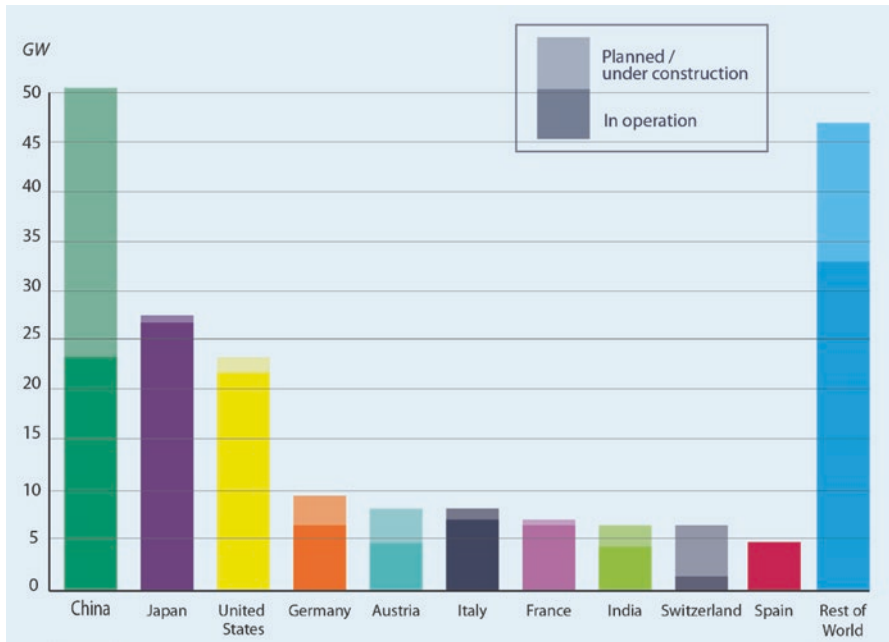

Fig. 5.3 An estimated new hydropower capacity added by region in 2015 in GW (33 GW including pumped storage about 2.5 GW). Source: IHA 2016 Key Trends in Hydropower, 2016
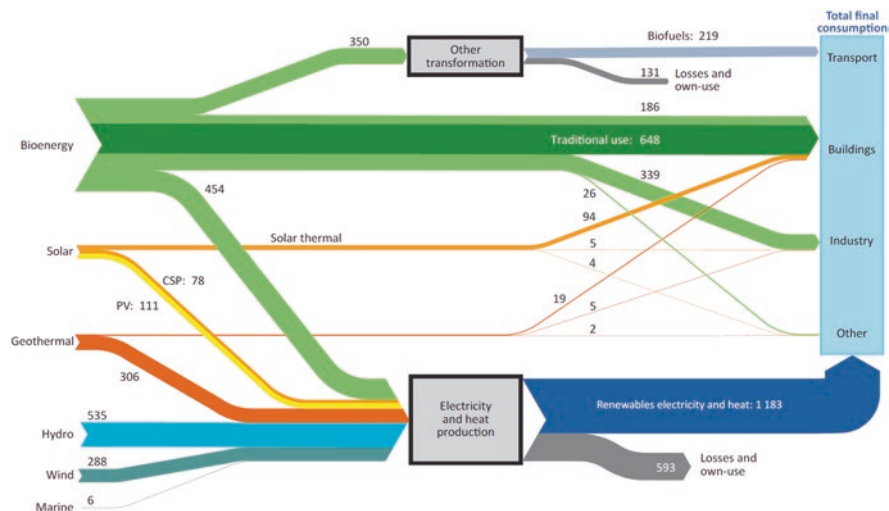
Fig. 5.4 Hydropower included in the grid of world renewable energy balances in the New Policies Scenario. Source: IEA World Energy Outlook 2014

gas emissions as soon as possible. It also drives further growth in the hydropower sector, especially in emerging and developing economies.

Other actual factor for hydropower development represents advanced hydropower control technologies for renewable hybrids, which can minimize the real-time variations of power provided from renewables to the grid. For example, China completed Phase II of the Longyangxia Solar Park, raising capacity from 320 to 850 MW. The Solar System is coupled directly to one of four turbines at the nearby 1280 MW hydro station, and the advanced control system allows the turbine to regulate the variable supply from the Solar System before dispatching firm power to the grid. It minimizes the grid's need for reserve capacity, frequency control, and voltage regulation and maximizes photovoltaic utilization and conserves water. The similar systems for wind-hydro hybrids are in development. Hydropower majority in storage accounts for over 97% of global energy storage capacity, and the additional growth is expected in the both developed and developing countries. Hydropower included in the grid of world renewable energy balances in the New Policies Scenario (IEA World Energy Outlook 2014) is illustrated in Fig. 5.4, where renewable energy consumed in the power sector accounts for one-third of total renewable energy supply in 2012, rising to more than one-half in 2040. Renewable energy in the power sector should more than triple, also with large increases coming from hydropower including electricity generation from marine. Also the uses of bioenergy shift markedly. Traditional ways of the use for cooking and heating in poor households in developing countries will be declining, while the use of bioenergy for the production of biofuels used in transport and energy sector will significantly increase. Taking into account the retirement of almost 890 GW of older installations that need to be replaced, total renewables capacity should increase by 2850 GW to about 4550 GW in 2040. The average share

of renewables in total global capacity should reach 42% in 2040, up from 29% today, which is slightly higher in the OECD countries at 46%, and slightly lower at 40% in non-OECD countries (IEA World Energy Outlook 2014). Cumulative renewable capacity additions by region and source based on the New Policies Scenario are in Table 5.1.

5.2   Potential Sources of Hydropower

Hydropower is linked to the hydrological cycle, which provides the movement of water on Earth. The mass of water remains constant over time, but its partitioning into the major reservoirs of ice, fresh water, saline water, and atmospheric water is variable in dependence on a wide range of climatic factors.

Simplified description of hydrological cycle for hydropower can be based on a few steps:

– Solar energy heats water on the Earth surface, which causes its evaporation.
– Water vapor condenses into clouds and falls as precipitation or snowing on the Earth surface.
– Water flows through streams to rivers back into the oceans.

The amount of precipitation that drains into river basins determines the amount of water available for producing hydropower. Seasonal variations in precipitation and long-term changes in precipitation patterns, such as droughts and floods, have significant impacts on hydropower production. Flows of water over and beneath the Earth are also a key component of other biogeochemical cycles. Runoff is responsible for transport of eroded sediments from land to waterbodies. The salinity of the oceans is derived from erosion and transport of dissolved salts from the land. Both runoff and groundwater flow play significant roles in transporting nutrients from the land to waterbodies.

In case of a conventional hydroelectric dam illustrated in Fig. 5.5, the power output available from falling water can be estimated by the term:

$$P = \eta \cdot \rho \cdot g \cdot h \cdot Q, \tag{5.1}$$

where P is power output in watts (W), η is the efficiency of the turbine (−), ρ is the density of water in kilograms per cubic meter (kg m^{-3}), g is the acceleration due to gravity (m·s^{-2}), h is the height difference between inlet and outlet in meters (m), and Q is the volume flow in cubic meters per second (m^3·s^{-1}). The power output depends on the product $h\,Q$, which means that a high dam with a large h and a small Q can have the same power output as a run-of-river installation with a small h and large Q. For example, the power output of a dam with the height difference of 50 m and volume flow of 20 m^3·s^{-1} (assume $\eta = 0.9$, $\rho = 1000$ kg m^{-3}, g = 10 m·s^{-2}) is (Fig. 5.6):

$$P = \eta \cdot \rho \cdot g \cdot h \cdot Q = 0.9 \cdot 1000 \cdot 10 \cdot 50 \cdot 20 = 90000000\,\text{W} = 9\,MW.$$

Table 5.1 Cumulative renewable capacity additions by region and source based on the New Policies Scenario (GW)

Region/country	2014–2025						2026–2040						2014–2040
	Hydro	Bio	Wind	PV	Other[a]	Total	Hydro	Bio	Wind	PV	Other[a]	Total	Total
OECD	84	39	237	167	21	548	90	59	450	285	57	940	488
Americas	34	18	87	55	12	207	36	26	189	98	18	367	574
United States	19	14	64	49	9	155	20	20	148	85	12	286	441
Europe	40	16	129	59	4	249	40	25	223	123	26	436	685
Asia Oceania	10	5	21	52	5	93	14	8	39	63	13	137	230
Japan	7	3	7	44	2	64	10	5	16	49	6	86	150
Non-OECD	338	59	266	203	19	885	341	92	476	366	86	1360	2245
E. E./Eurasia	21	3	8	3	1	36	32	11	20	8	2	73	109
Russia	12	2	3	1	1	18	19	8	6	1	2	36	54
Asia	212	46	231	170	7	666	188	59	371	269	35	921	1587
China	123	32	184	126	3	467	51	29	251	143	22	496	964
India	36	6	37	32	1	112	69	12	78	93	6	258	370
Southeast Asia	22	5	4	8	3	42	34	9	14	18	6	83	124
Middle East	7	1	4	8	3	23	5	3	45	36	19	109	131
Africa	30	4	8	15	6	63	52	7	18	39	25	140	203
Latin America	68	5	15	7	1	97	64	11	22	15	5	118	214
Brazil	38	4	13	5	-	59	36	8	16	7	2	69	128
World	422	98	503	370	40	1433	431	151	926	650	143	2301	3734
EU	31	15	120	58	4	229	29	24	209	121	25	408	637

Source: IEA World Energy Outlook 2014

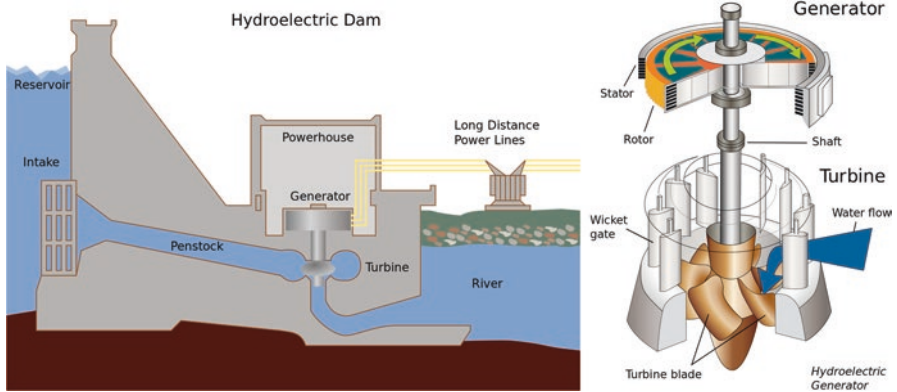[a]Other includes geothermal, concentrating solar power and marine

Fig. 5.5 A schema of a dammed-hydro facility, the most common type of hydroelectric power generation, and a view on the Kaplan turbine connected to an electricity generator. Source: Wikipedia, 2016
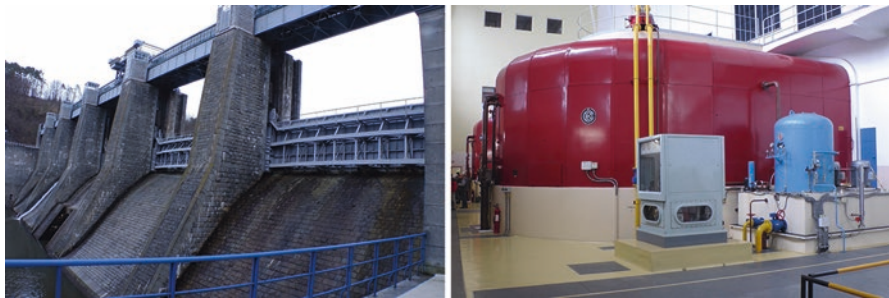

Fig. 5.6 A smaller dammed-hydro facility and an electricity generator complemented with control systems

5.2.1   Storage Hydropower

The described hydropower by dammed-hydro facility represents storage hydropower, which is mostly a large system that uses a dam to store water in a reservoir, and electricity is produced by releasing water from the reservoir through a turbine connected to an electricity generator. Storage hydropower provides base load as well as the ability to be shut down and started up at short notice according the demands of the system such as peak loads. In dependence on storage capacity, it can operate independently of the hydrological inflow for many weeks or even months. The list of top 20 largest hydropower stations in the world in terms of installed electrical capacity is in Table 5.2. It includes nonrenewable power stations running on fossil fuels such as coal, fuel oils, natural gas, and nuclear fuel, as well as renewable power stations running on biomass, hydro and solar energy, geothermal heat, and wind energy. Storage

Table 5.2 Top 20 largest power stations in the world in terms of installed electrical capacity

Power station	Country	Capacity (MW)	Annual generation (TWh)	Type
Three Gorges Dam	China	22,500	98.8 (2014)	Hydro
Itaipu Dam	Brazil, Paraguay	14,000	98.63 (2013)	Hydro
Xiluodu	China	13,860	55.2 (2015)	Hydro
Guri	Venezuela	10,235	47 (average)	Hydro
Tucuruí	Brazil	8370	21.4 (1999)	Hydro
Kashiwazaki-Kariwa	Japan	7965	60.3 (1999)	Nuclear (Susp. in 2011)
Grand Coulee	United States	6809	21 (2008)	Hydro
Xiangjiaba	China	6448	30.7 (2015)	Hydro
Longtan	China	6426	18.7	Hydro
Sayano-Shushenskaya	Russia	6400	24.9 (2013)	Hydro
Bruce	Canada	6300	45 (2013)	Nuclear
Krasnoyarsk	Russia	6000	23.0 (2014)	Hydro
Hanul	South Korea	5881	48.16	Nuclear
Hanbit	South Korea	5875	47.62	Nuclear
Nuozhadu Dam	China	5850	23.9 (estimate)	Hydro
Zaporizhia	Ukraine	5700	48.16 (average)	Nuclear
Robert-Bourassa	Canada	5616	26.5	Hydro
Shoaiba	Saudi Arabia	5600		Fuel oil
Surgut-2	Russia	5597	39.85 (2013)	Natural gas
Taichung	Taiwan	5500	42 (average)	Coal

Source: Wikipedia, 2016

hydropower stations dominate in the list in view of the fact that they are attached to mighty rivers. There is also the dominance of hydropower stations in timeline of the largest power plants in the world, which is listed in Table 5.3.

5.2.2   Pumped-Storage Hydropower

The ability to be shut down and started up at short notice according the demands of the system such as peak loads is the main property of this type of hydro facilities. Harnessing water is cycled between a lower and upper reservoir by pumps which use surplus energy from the system at times of low demand. When electricity demand is high, water is released back to the lower reservoir through turbines to produce electricity (Figs. 5.7 and 5.8). The list of largest operational/under construction pumped-storage stations in the world in terms of installed electrical capacity is in Table 5.4. The tables list the power-generating capacity in megawatts like for storage hydropower stations, but the other important parameter is the overall energy storage capacity in megawatt hours, which depends on the volume of reservoirs.

Table 5.3 Timeline of the largest power stations in the world

| Held record | | Name of power station | Capacity | Country |
From	To			
1922	1924	Sir Adam Beck Hydroelectric Generating Stations	450	Canada
1924	1939	Wilson Dam	663	United States
1939	1949	Hoover Dam	705	United States
1949	1960	Grand Coulee Dam	2280	United States
1960	1966	Volga Hydroelectric Station	2300–2563	Russia
1966	1971	Bratsk Hydroelectric Power Station	4515	Russia
1971	1979	Churchill Falls Generating Station	5428	Canada
1979	1986	Grand Coulee Dam	5585–6809	United States
1986	1989	Guri Dam	10,235	Venezuela
1989	2007	Itaipu Dam	10,500–14,000	Brazil, Paraguay
2007	present	Three Gorges Dam	14,100–22,500	China

Source: Wikipedia, 2016
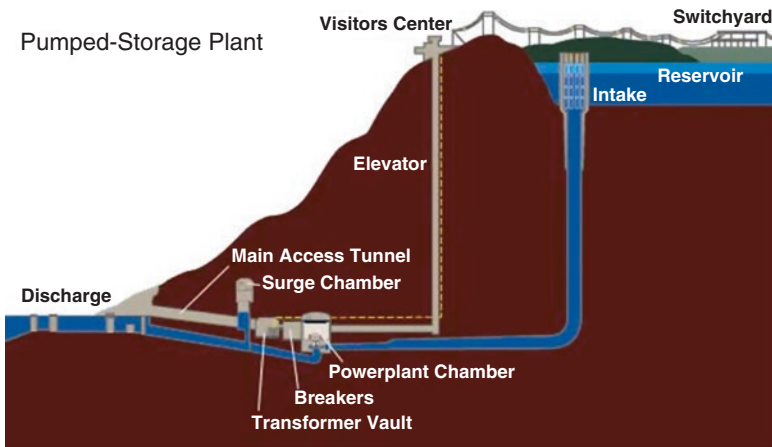
Fig. 5.7 A schema of a pumped-storage plant connected to a lower and upper reservoir. Source: Wikipedia, 2016

The full list of projects including new projects under construction is available in the US Department of Energy's Global Energy Storage Database (GESDB), which is a free-access database of energy storage projects and policies (Fig. 5.9).

5.2.3   Run-of-River Hydropower

It is a facility whereby little or no water storage is provided. It channels flowing water from a river through a canal to a turbine. Run-of-river provides a continuous supply of electricity on the base load, with some flexibility of operation for daily

Fig. 5.8 A view on lower and upper reservoir of a pumped-storage plant. Source: Google Earth, 2016

Table 5.4 The largest operational/under construction pumped-storage stations in the world in terms of installed electrical capacity

Operational station	Country	Location	Capacity (MW)
Bath County Pumped Storage Station	United States	38°12′32″N 79°48′00″W	3003
Guangdong Pumped Storage Power Station	China	23°45′52″N 113°57′12″E	2400
Huizhou Pumped Storage Power Station	China	23°16′07″N 114°18′50″E	2400
Okutataragi Pumped Storage Power Station	Japan	35°14′13″N 134°49′55″E	1932
Ludington Pumped Storage Power Plant	United States	43°53′37″N 86°26′43″W	1872
Fengning Pumped Storage Power Station	China	41°40′40″N 116°29′47″E	3600 (year 2019)
Kannagawa Hydropower Plant	Japan	36°00′18″N 138°39′09″E	2820 (year 2020)
Dniester Pumped Storage Power Station	Ukraine	48°30′49″N 27°28′24″E	2268 (year 2017)
Jixi Pumped Storage Power Station	China	30°11′07″N 118°46′57″E	1800 (year 2018)
Huanggou Pumped Storage Power Station	China	45°22′42″N 129°37′44″E	1200 (year 2019)

Source: Wikipedia, 2016

Fig. 5.9 A search view of the Global Energy Storage Database (GESDB), a free-access database of energy storage projects and policies. Source: DOE GESDB, http://www.energystorageex-change.org/projects.html, 2016

Fig. 5.10 A screw turbine (reverse Archimedes' screw): the hydropower plant and a detailed view on the screws

fluctuations in demand through water flow, which is regulated by the facility. Turbines used for this type of hydropower are similar to storage hydropower such as Pelton, Francis, and Kaplan turbines, but construction details are site specific. For low hydropower potential, brooks are used as micro hydro plants (installations from 5 kW to 100 kW of electricity) or pico hydro plants (installations below 5 kW). Another type of turbine is illustrated in Figs. 5.10 and 5.11, which is a screw turbine (reverse Archimedes' screw). This hydropower is suitable for streams or rivers that can sustain a minimum flow or those regulated by a lake or reservoir upstream. In contrast with storage hydropower that stores enormous quantities of water in reservoirs flooding large areas of land, run-of-river projects do not have most of the disadvantages associated with dams and reservoirs. Thus, they are often considered environmentally friendly. Micro hydro systems can also complement renewables, because in many areas, water flow is used to be highest in the winter when solar energy is at a minimum.

Fig. 5.11 Screw turbines at a small hydropower complemented by a weir and a fish ladder. This construction is considered to be friendly to aquatic wildlife (labeled as "fish friendly")

The significant energy potential of providing a substantial amount of new renewable energy around the world represents actually a less-established but growing group of marine technologies that use energy carried by tides, ocean waves, salinity, and ocean temperature differences. The movement of water in the world's oceans creates a vast store of kinetic energy, which can be harnessed to generate electricity to power industry, transport, and homes.

5.2.4   Tidal Hydropower

The combined attraction and movement of the Moon and the Sun together with the rotation of the earth provides the dynamic framework driving the tides. The respective positions of the Moon and Sun in relation to the Earth cause the cycle of monthly variations. When aligned, their influences are reinforced; when at a right angle, they are reduced. Unlike other renewables such as wind and wave energy, tidal variations are predictable, which is a very attractive feature of tidal energy. Tidal variations are associated with tidal currents that can be also harvested by turbines placed in the stream. The tidal variations can be described by superimposing harmonic components using constants known as the tidal "constituents":

$$z(t) = z_0 + \sum_{i=1}^{M} A_i \cos\left(\omega_i t - \phi_i\right), \qquad (5.2)$$

where z_0 is the mean surface value and A_i, ω_i, and φ_i represent the amplitude, frequency, and phase lag, respectively,

for each of the *M* tidal constituents. Principal semidiurnal (twice daily) constituents are represented by M2 (principal lunar, twice daily, period 12.42 h), S2 (principal solar, twice daily, 12.00 h), K1 (lunisolar diurnal, once daily, 23.93 h), and O1 (principal lunar diurnal, once daily, 25.82 h). The values of the constituents vary depending on local conditions as indicated with colors in Fig. 5.12 for M2 and K1 tidal waves. Due to the Moon, the main component of the tide (wave M2) is the dominant component in many regions. It is observed that regions with an increase in tide variations are, in particular, near the coasts on the North Atlantic. Other factors, which significantly affect tides and can amplify the effects, are the seabed topography and the shape of the coastline. There are many sites suitable for construction of tidal power plant over the world. For example, operational installations are in the bays of Mont St Michel in France and Fundy in Canada (Fig. 5.13).
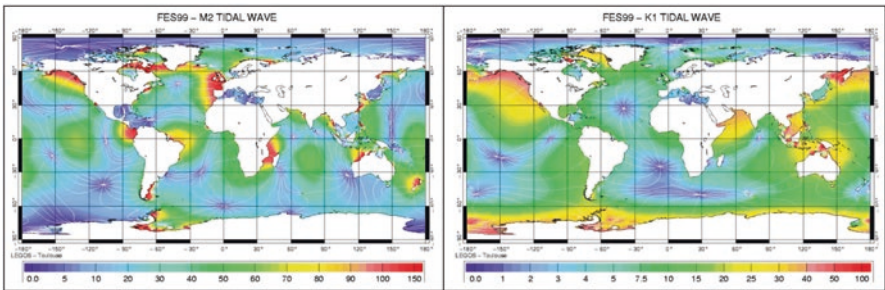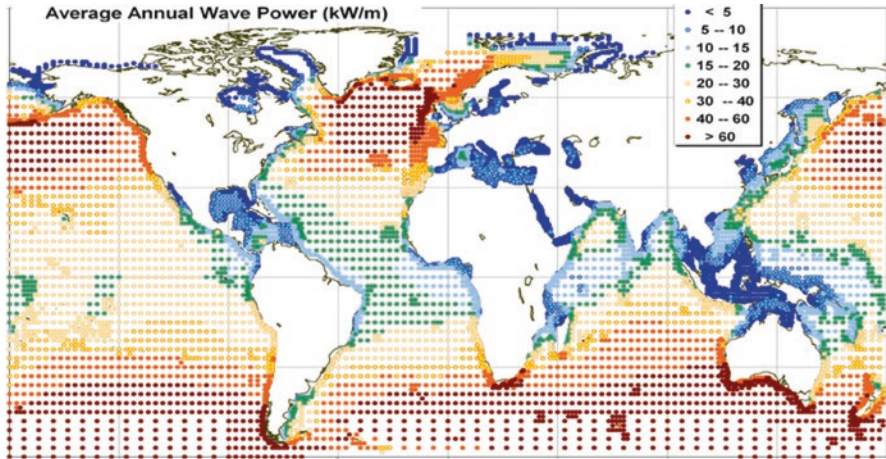

Fig. 5.12 Variation of tidal components M2 and K1 with location. Source: K. Nielsen (2010). Report T02-0.0 Development of Recommended Practices for Testing and Evaluating Ocean Energy Systems, OES-IA Annex II Extension Summary Report

Fig. 5.13 The Annapolis Tidal Power Plant (20 MW) with a daily output of roughly 80–100 MWh, depending on the tides. Source: Google Earth, 2016

Fig. 5.14 Variation of tidal components M2 and K1 with location. Source: K. Nielsen (2010). Report T02-0.0 Development of Recommended Practices for Testing and Evaluating Ocean Energy Systems, OES-IA Annex II Extension Summary Report

5.2.5   Wave Hydropower

It originates from ocean waves that are created by the winds blowing over the surface of the ocean. Waves are oscillations that transport energy from one location to the other without any net transport of the sea water. The potential wave power is indicated in Fig. 5.14, which shows annual average values. Wave power values are dependent on location conditions and range from 5 to more than 60 kW. The more energetic seas are located toward the poles in the Northern and Southern hemisphere. Coastlines exposed to higher wave power are located at the southern part of Chile, South Africa, Australia, New Zealand, and Northern Canada and the west coast of the Scotland and Ireland. But wave energy is highly variable due to climate changes that rise temperatures and make wave energy predictions less reliable.

5.2.6   Hydropower Based on Temperature and Salinity Gradients

Besides described types of marine hydropower, there are a number of projects focused on temperature and salinity gradients. The temperature gradient between the sea surface and deep water can be harnessed using different ocean thermal energy conversion (OTEC) processes. Some projects dealing with OTEC are tested in tropical regions, where surface water can be much warmer than deep water. The United States became involved in OTEC research in 1974 with the establishment

of the Natural Energy Laboratory of Hawaii Authority. The salinity gradients can be found at the mouth of rivers, where freshwater mixes with saltwater. Energy associated with the salinity gradient can be harnessed using the pressure-retarded reverse osmosis process and associated conversion technologies. The prototype of an osmotic power plant is located at Tofte in Hurum in Norway. The tests of power production began on 24 November 2009. It operates with a water usage of 10 liters of fresh water and 20 liters of salt water per second, which gives a power output of between 2 and 4 kW. It is assumed that the power for a similar plant can be increased to about 10 kW by using better membranes.

5.3 Environmental Effects of Hydropower Installations

Hydropower installations include both massive hydroelectric dams or large tidal hydropower systems and small run-of-river hydropower or other particular hydropower installation on the ocean. Large-scale hydroelectric dams continue to be built in many parts of the world where the hydropower capacity remains. In many developed countries over the world, the hydropower capacity is nearly utilized, and the future of hydroelectric power will likely involve increased capacity at current dams and new smaller run-of-river projects. The hydropower installations in the ocean such as tidal, wave, and other new technologies are mostly in trial stages with the absence of internationally assessment guidelines and standards. Despite the fact that hydropower is mostly included into renewables, environmental impacts, particularly large-scale hydroelectric dams or tidal systems, are significant and need environmental social risk assessment.

Most of new hydropower projects must undergo an Environmental and Social Impact Assessment (ESIA). It provides a baseline understanding of the pre-project conditions, estimates potential impacts, and puts in place management plans to mitigate or compensate for impacts. Environmental assessments may be governed by rules of administrative procedure regarding public participation and documentation of decision-making and are a subject to judicial review. The purpose of the assessment is to ensure that decision-makers consider the environmental impacts. The International Association for Impact Assessment (IAIA) defines an environmental impact assessment as the process of identifying, predicting, evaluating, and mitigating the biophysical, social, and other relevant effects of development proposals prior to major decisions being taken and commitments made. Environmental Impact Assessment (EIA) is unique in that it deals with decision-makers to account for environmental values in their decisions and to justify those decisions in light of detailed environmental studies and public comments on the potential environmental impacts. Engineering and consulting companies represent the contractors that can prepare an EIA study but most importantly get these studies approved by each country government offices prior to the execution of a project. The Hydropower Sustainability Assessment Protocol is another instrument, which is used to promote and guide more sustainable hydropower projects.

It deals with a methodology used to audit the performance of a hydropower project across many environmental, social, technical, and economic topics. A protocol assessment provides a synoptic sustainability health check, but it does not replace the ESIA, which takes place over a much longer period of time, and is usually a mandatory regulatory requirement.

An overall evaluation of environmental impacts of hydropower can be based on a few criteria such as land use, wildlife impacts, and life cycle global warming emissions. Other criteria may cover local environmental conditions, historical aspects and social traditions, or economy and politics.

5.3.1 Land Use

Flooding land for a hydropower reservoir has significant environmental and social impacts that destroy forest, wildlife habitat, agricultural land, scenic lands, and local communities including industry transport and residential sites. The size of the reservoir created by a hydropower project varies widely, depending on the hydropower capacity, installed power of the hydroelectric generators, and the topography of the land. Hydroelectric plants in flat areas tend to cover much more land than those in hilly areas or canyons where deeper reservoirs hold more volume of water in a smaller area. A few image views in Figs. 5.15, 5.16, 5.17, and 5.18 demonstrate land use flooding in case of four largest power stations in the world such as Three Gorges Dam, Itaipu Dam, Guri Dam, and Balbina Dam, which dominates by its flooded area (about 2360 km^2).

Fig. 5.15 Three Gorges Dam: China, 30°49′15″N 111°00′08″E, capacity 22,500 MW (creates Three Gorges Reservoir, total capacity 39.3 km^3, catchment area 1000,000 km^2, surface area 1084 km^2, max. length 600 km, normal elevation 175 m). Source: Google Earth, 2016

Fig. 5.16   Itaipu Dam: Brazil-Paraguay, 25°24′31″S 54°35′21″W, capacity: 14,000 MW (creates Itaipu Reservoir, total capacity 29 km^3, catchment area 1350,000 km^2, surface area 1350 km^2, max. length 170 km, max. width 12 km). Source: Google Earth, 2016

Fig. 5.17   Guri Dam: Venezuela, 07°45′59″N 62°59′57″W, 10,200 MW (creates Guri Reservoir, total capacity 135 km^3, surface area 4250 km^2. Source: Google Earth, 2016

5.3.2   *Wildlife Impacts*

The reservoirs of storage hydropower plants are used for multiple purposes, such as agricultural irrigation, flood control, and recreation. However, hydroelectric facilities have significant impacts on aquatic ecosystems. Apart from direct contact by turbine devices, there are wildlife impacts both within the dammed reservoirs and

Fig. 5.18 Balbina Dam: Brazil, 01°55′02″S 59°28′25″W, capacity 250 MW (creates Balbina Reservoir, total capacity 17.54 km^3, catchment area 16,502 km^2, surface area 2360 km^2, max. water depth 30 m). Source: Google Earth, 2016

downstream from the facility. Reservoir water is used to be more stagnant than normal river water. As a result, the reservoir can have higher amounts of sediments and nutrients, which cultivates an excess of algae and other aquatic weeds that can crowd out other aquatic life. Water evaporation is higher in dammed reservoirs than in flowing rivers, and water temperature of the river downstream from the reservoir is influence by a level of the intake that delivers water from the reservoir to the turbine due to the water temperature stratification in the reservoir. Released water is colder than normal river water and low in dissolved oxygen, which can negative impact downstream plants and animals. To reduce these impacts, aerating extra turbines can be installed to increase dissolved oxygen, and regulated multilevel water intakes can control that water released from the reservoir comes from all levels of the reservoir, rather than just the bottom with the lowest temperature dissolved oxygen.

5.3.3   Life Cycle Global Warming Emissions

Global emissions are mainly produced during the construction and dismantling of hydroelectric power plants, but recent research suggests that other emissions of carbon dioxide and methane are released by decomposed vegetation and soils in the flooded areas. Such emissions vary greatly depending on the size of the reservoir and the nature of the land that was flooded by the reservoir. It is higher in tropical areas or temperate peatlands. The exact amount of emissions depends greatly on site-specific characteristics.

5.4   Risk Assessment of Hydropower Plants with GIS

Climate aspects have increased influence on project design, construction, and administration of hydropower plants. Potential climate change impacts disturb decision-making processes for hydropower owners and operators. The European Bank for Reconstruction and Development (EBRD), which used to be cofinancing these projects, is trying to make model predictions of hydrological flows under various scenarios to identify the most suitable design. Besides energy efficiency, power and energy, and natural resources, the EBRD finances projects in a number of other sectors such as agribusiness, financial institutions, manufacturing, and public works.

In the regional scale, the water flow in a stream can vary from season to season. The development of a hydropower site requires analysis of flow records for a few decades, in order to estimate the reliable annual energy supply. Storage hydropower with dams and reservoirs provides a more dependable source of power by smoothing seasonal changes in water flow. The design of the dam must account for the worst case, such as a flood season, that can be expected at the site. The dam is for this reason complemented by the spillway to bypass flood flows around the dam. The computer models of the hydraulic basin completed by rainfall and snowfall records are used to predict the extreme conditions. A number of computing tools are used for spatial and dynamic modeling.

GIS can assist in spatial modeling for delineation and definition of stream networks. It includes a number of steps, where some are required, while others are optional depending on the characteristics of the input datasets. Identification of flow across a surface is based on the steepest downslope direction in the grid of cells. Once the direction of flow out of each cell is known, it is possible to determine which and how many cells flow into any given cell. This information can be used to define watershed boundaries and stream networks. A basic concept is illustrated in a flowchart that shows the process of extracting hydrologic information, such as watershed boundaries and stream networks, from a digital elevation model (DEM) (Fig. 5.19).
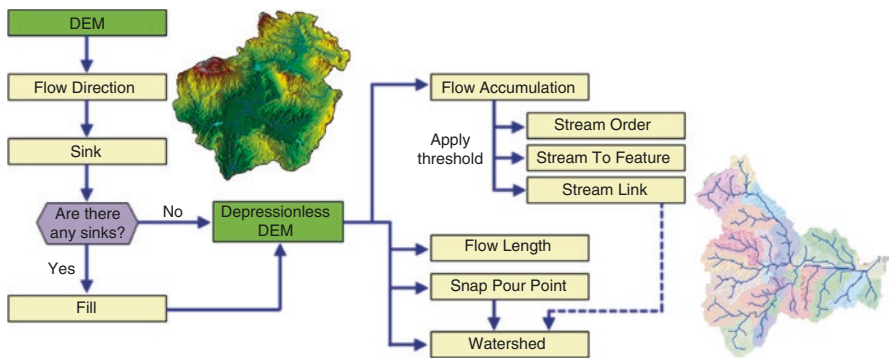

Fig. 5.19   A flowchart for watershed delineation that is based on extracting hydrologic information from the DEM. Source: ESRI ArcGIS Resource Center

Table 5.5 The hydrology tools that can be applied individually or used in sequence to create a stream network or delineate watersheds
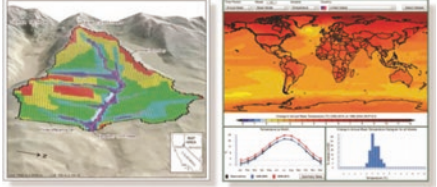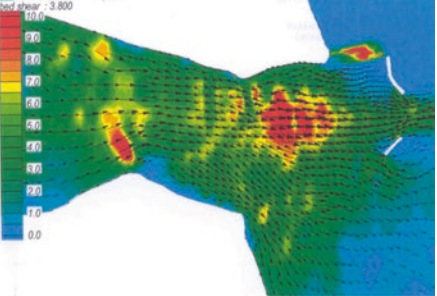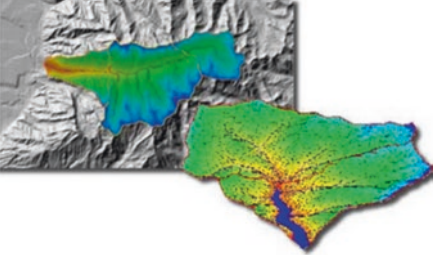
Tool	Description
Basin	Creates a raster delineating all drainage basins
Fill	Fills sinks in a surface raster to remove small imperfections in the data
Flow accumulation	Creates a raster of accumulated flow into each cell; a weight factor can optionally be applied
Flow direction	Creates a raster of flow direction from each cell to its steepest downslope neighbor
Flow length	Calculates the upstream, downstream, or weighted distance, along the flow path for each cell
Sink	Creates a raster identifying all sinks or areas of internal drainage
Snap pour point	Snaps pour points to the cell of highest flow accumulation within a specified distance
Streamlink	Assigns unique values to sections of a raster linear network between intersections
Stream order	Assigns a numeric order to segments of a raster representing branches of a linear network
Stream to feature	Converts a raster representing a linear network to features representing the linear network
Watershed	Determines the contributing area above a set of cells in a raster

Source: ESRI ArcGIS Resource Center

The elevation model is used to determine the flow direction. If there are depressions in the elevation model, there may be some cell locations that are lower than the surrounding cells. These depressions, called sinks, are identified, and the hydrologic analysis tools allow to fill them. The result is a depression-less elevation model that is used to determine the flow direction on this depression-less elevation model. In the next stage, the watershed is created for each stream segment between stream junctions. After calculation of the flow accumulation for each cell location, the stream network is defined. Besides identification of the direction water flows from cell to cell, water flow identification through the stream network is complemented, and watershed is created. The list of hydrological methods, which are implemented ArcGIS, is in Table 5.5. The list of other computing tools dealing with hydrological modeling is in Table 5.6.

Besides environmental modeling dealing with watershed, reservoirs, and coastal areas, other modeling approach is also focused on hydropower generation such as proper modeling of the dynamic aspect of flowing water, gate controlling, and electricity generation. The latter generation of models often adopts simulation approach with MATLAB/Simulink software. The MATLAB platform based on the language for technical computing is optimized for solving engineering and scientific problems. Built-in graphic tools make it easy to explore and visualize data. A vast library of prebuilt toolboxes offers many tools for hydropower and automatic control simulations. Other example of modeling tools is represented by COMSOL Multiphysics, which provides interfaces for electrical, mechanical, fluid flow, and chemical applications. Any number of modules can be seamlessly combined to handle challenging of hydropower applications.

Table 5.6 A list of selected software tools for environmental management and impact assessment

| Subject	Description	Website
U.S. EPA (Environmental Protection Agency)	The EPA Center for Exposure Assessment Modeling (CEAM) distributes computer models and database software for quantify movement and concentration of contaminants in lakes, streams, estuaries, and marine environments. Models, such as BASINS, HSPF, AQUATOX were developed by the U.S. EPA in conjunction with other institutions. Models can be downloaded and used for non-commercial purposes ->	https://www.epa.gov/exposure-assessment-models
USGS (U.S. Geological Survey)	Ground-water and Surface-water FLOW (GSFLOW) has been recently developed to model coupled ground-water and surface-water resources -> The Global Climate Change Viewer (GCCV) is designed to visualize future temperature and precipitation changes simulated by global climate models in the Coupled Model Intercomparison Project Phase 5 (CMIP5) ->	https://www.usgs.gov/ http://water.usgs.gov/ogw/gsflow/index.html http://regclim.coas.oregonstate.edu/gccv/index.html
MIKE-DHI (the global organization dedicated to solving challenges in water environments worldwide)	MIKE is a range of software products that enable you to accurately analyze, model and simulate any type of challenge in water environments. It contains a number of products designed to water resources, coast and sea, cities, groundwater and porous media, decision support and operational forecasting. As an example, an applications of Coastal Tech is used to illustrate works on restoration and enhancement of coastal resources and property ->	http://www.coastaltechcorp.com/mike21.php https://www.mikepoweredbydhi.com/
WMS, Watershed Modeling System (Scientific Software Group)	It is a modeling environment for watershed hydrology and hydraulics. It includes automated basin delineation, geometric parameter calculations, GIS overlay computations, and cross-section extraction from terrain data. It supports hydrologic modeling with HEC-1 (HEC-HMS), TR-20, TR-55, Rational Method, NFF, MODRAT, HSPF, and GSSHA, which are managed with the graphical tools ->	http://www.scisoftware.com/environmental_software/ https://www.epa.gov/exposure-assessment-models
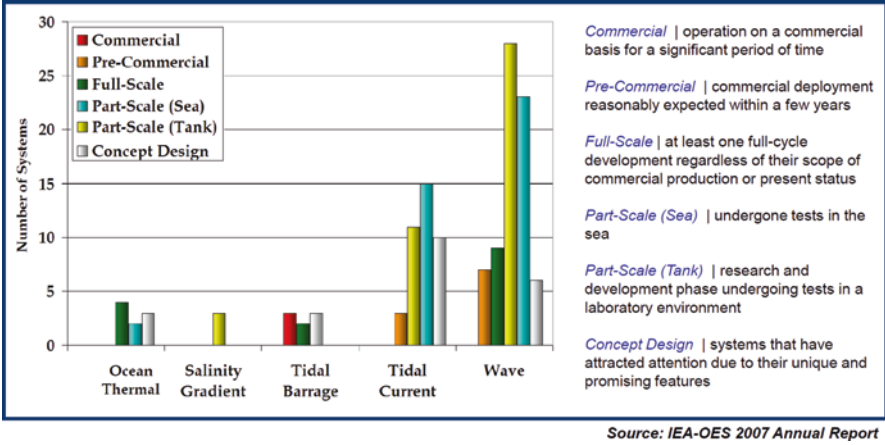
Fig. 5.20 Ocean energy systems: status of technology development. Source: IEA-OES 2007 Annual Report

As opposed to the terrestrial hydropower including mainly large storage hydropower plants, ocean hydropower still represents great challenges for new technology and its commercial implementation. A status of technology development in ocean energy systems is illustrated in Fig. 5.20. Despite the fact that marine hydropower has a high energy potential, there are a number of barriers and limits in the expansion over the world. Tidal hydropower has significant impact on local ecosystems due to the disruption of tidal cycles. In ocean wave hydropower, a number of technologies have been developed worldwide; some of them are near full-scale development and undergoing sea trials. Hydropower based on temperature and salinity gradients is in the stage of development. Also appropriate government policy mechanisms are required to bring these conversion technologies to commercial stage. The barriers and challenges may be lack of experience from a larger number of full-scale sea trials on performance and environmental impacts, prolonged licensing and permitting of the projects, the absence of internationally recognized performance including assessment guidelines, and electrical grid connection and capacity constraint challenges.

5.5 Case-Oriented Studies

Assessment of hydropower sources is currently in the process of sustainable development of many countries. It addresses many issues related to energy systems, industry development, and environmental and social factors. The GIS can assist in decision-making processes. Through the integration of spatial data and other information, it can provide multi-criteria analysis in order to rational decisions.

5.5.1   Processing of Data About Hydropower Sources in GIS

A case study is focused on using remote sensing data, particularly from Landsat 8 for environmental mapping of a large storage hydropower plant: Itaipu Dam. The satellite image is in Fig. 5.21, and the detailed views are in Fig. 5.22, which shows a part of the image in natural colors, in a combination of natural colors (green and red band) and an infrared band, in NDVI levels of vegetation density, and in a few classes of unsupervised classification.

5.5.2   Mapping Potential Sources for Small Hydropower Plants in the Basin

Small hydroelectric plants with a capacity to 20 MW (or up to 50 MW in the United States, Canada, and China) are a valuable market of the hydro industry, providing local power in underdeveloped countries and sources of new capacity in established energy systems. These hydropower plants are used to be further subdivided into mini hydro (100–1000 kW), micro hydro (5–100 kW), and even pico hydro (below 5 kW), which can usually provide electricity for smaller communities, or single families. Small hydro plants may be connected to conventional electrical distribution networks as a source of renewable energy. Since small hydropower plants have negligible reservoirs and other construction work, they are seen as environmental friendly. Plants with small reservoir can control electricity contribution, which helps to balance local energy grids. Such plants can complement at the regional level renewable energy sources. The proposed case study is focused on a local mapping of small potential hydropower sources at the sites of weirs. Examples of suitable sites are illustrated in Fig. 5.23. The GIS project dealing with mapping of potential hydropower sources in location of weirs is in Fig. 5.24. Integration of spatial datasets, meteorological observations, and rate of flows is in Fig. 5.25.

Integration of spatial and temporal data in the GIS project improves data management for exploratory analysis and modeling tasks. A number of modeling tools can be used to provide prediction of water flows, environmental risk assessment, and market predictions. An example focused on comparison of land cover changes of the selected basin and other neighbor basins in a few decades is illustrated in Fig. 5.26. The Landsat images captured in 1990, 2000, and 2006 together with the CORINE Land Cover inventory are used to evaluate land use changes and their influence on nutrient flows in the basin with ArcSWAT, an ArcGIS extension and graphical user input interface for soil and water assessment tool (SWAT). Besides a few presented Landsat images, the GIS project has been extended by a series of other Landsat images captured since 1985. Thus, the long time period for a few decades and short time seasonal period can be explored in the view of land cover changes, water flows, and nutrient transport. The final steps mostly deal with presentation of results.

Fig. 5.21 The satellite image of Itaipu Dam on the border between Brazil and Paraguay (surface area 1350 km², max. Length 170 km, max. Width 12 km) captured from Landsat 8 (August 11, 2016)
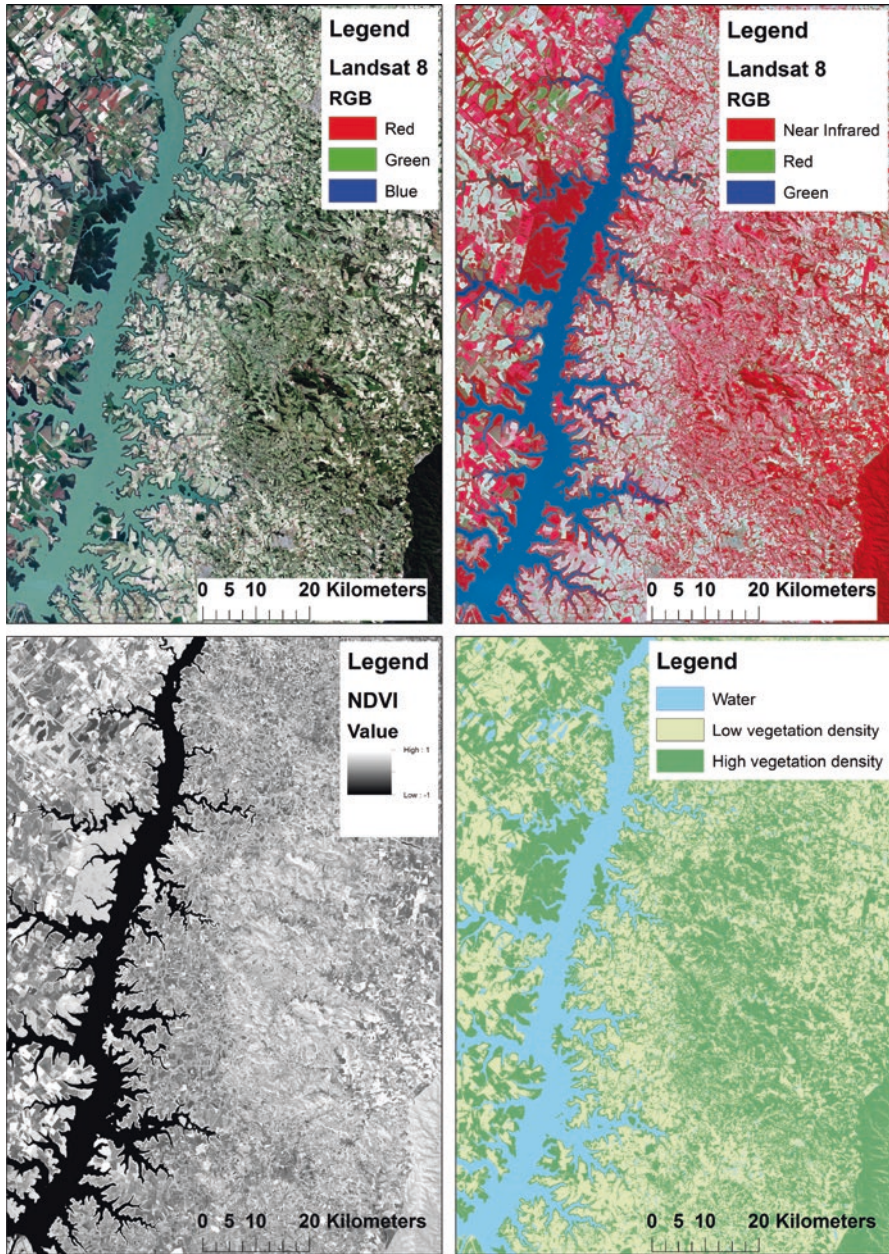
Fig. 5.22 A part of the Landsat image in natural colors, in a combination of natural colors (green and red band) and an infrared band, in NDVI levels of vegetation density, and in a few classes of unsupervised classification

Fig. 5.23 Examples of two weirs on a downstream part of the basin. Source: Google Earth, 2016
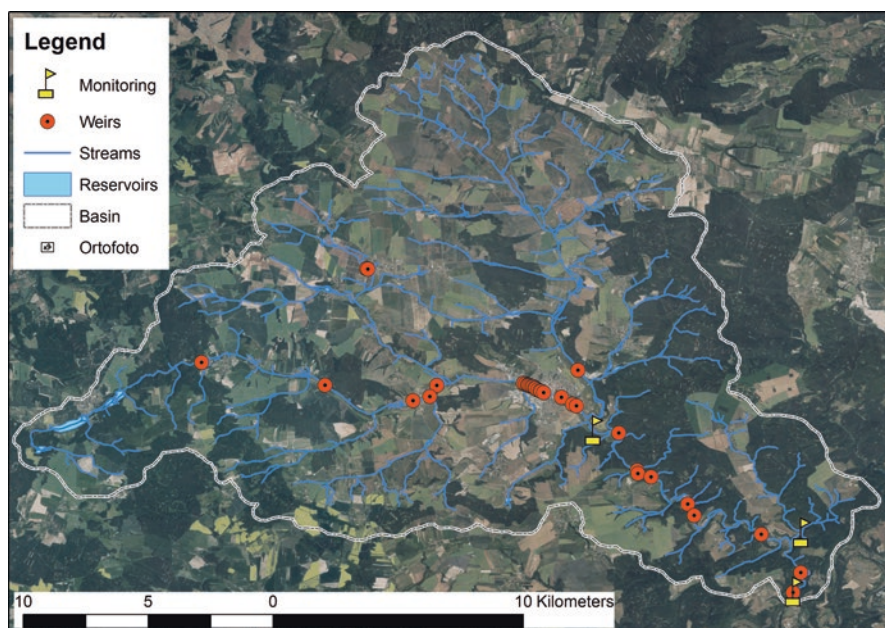
Fig. 5.24 The GIS project with map layers focused on mapping of potential power sources in location of weirs

GIS tools can use visualization methods to show map layers in a 3D view. An example in Fig. 5.27 shows the DEM complemented by other thematic map layers such as sites for monitoring, location of weirs, reservoirs, and stream network.
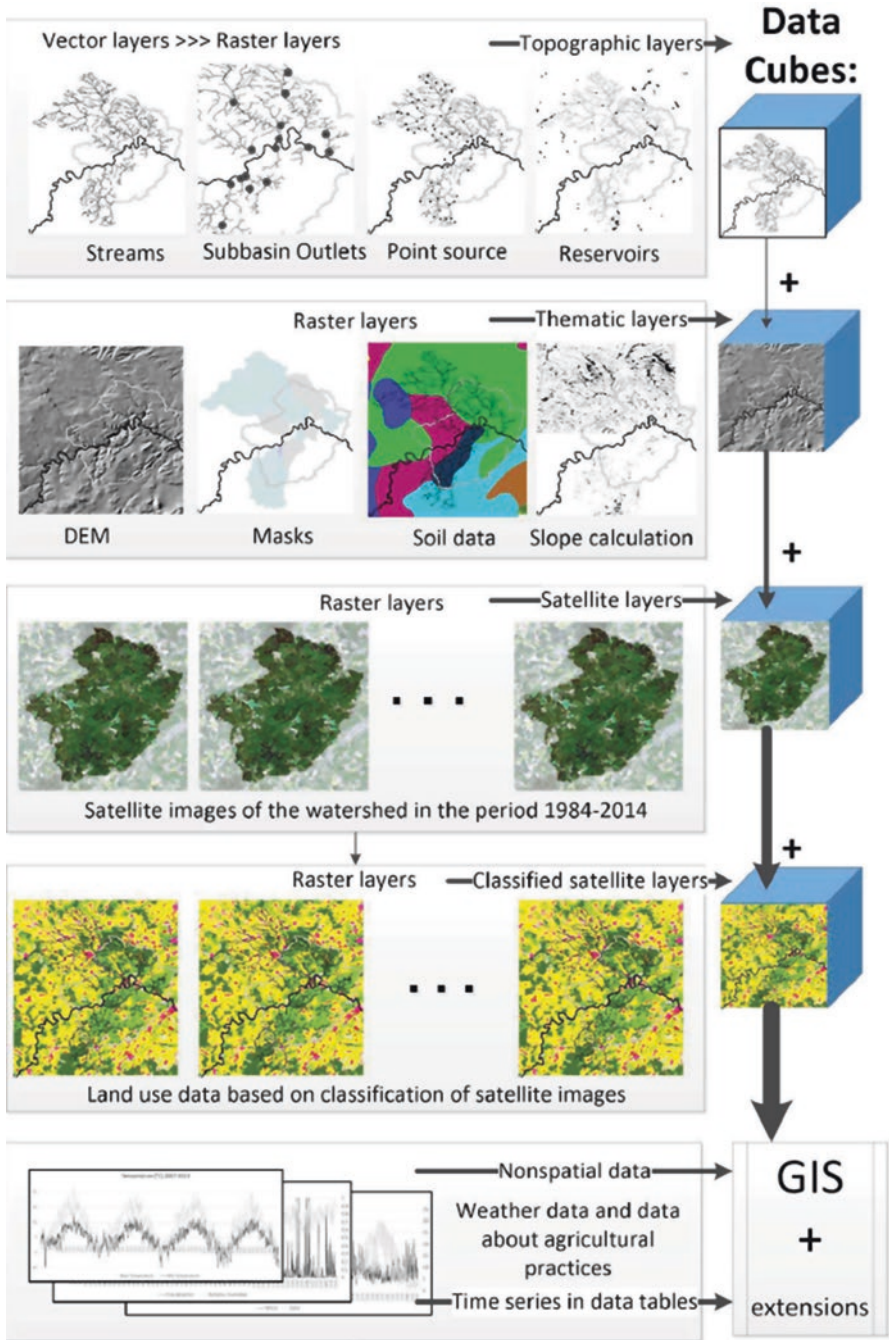
Fig. 5.25 Integration of spatial datasets, meteorological observations, and rate of flows in the framework of environmental risk assessment study. Source: Matejicek, L., 2014. Integration of simulation models for watershed management and data from remote sensing in geographic information systems. In: Ames, D.P., Quinn, N.W.T., Rizzoli, A.E. (Eds.), Proceedings of the 7th International Congress on Environmental Modelling and Software, June 15-19, San Diego, California, USA
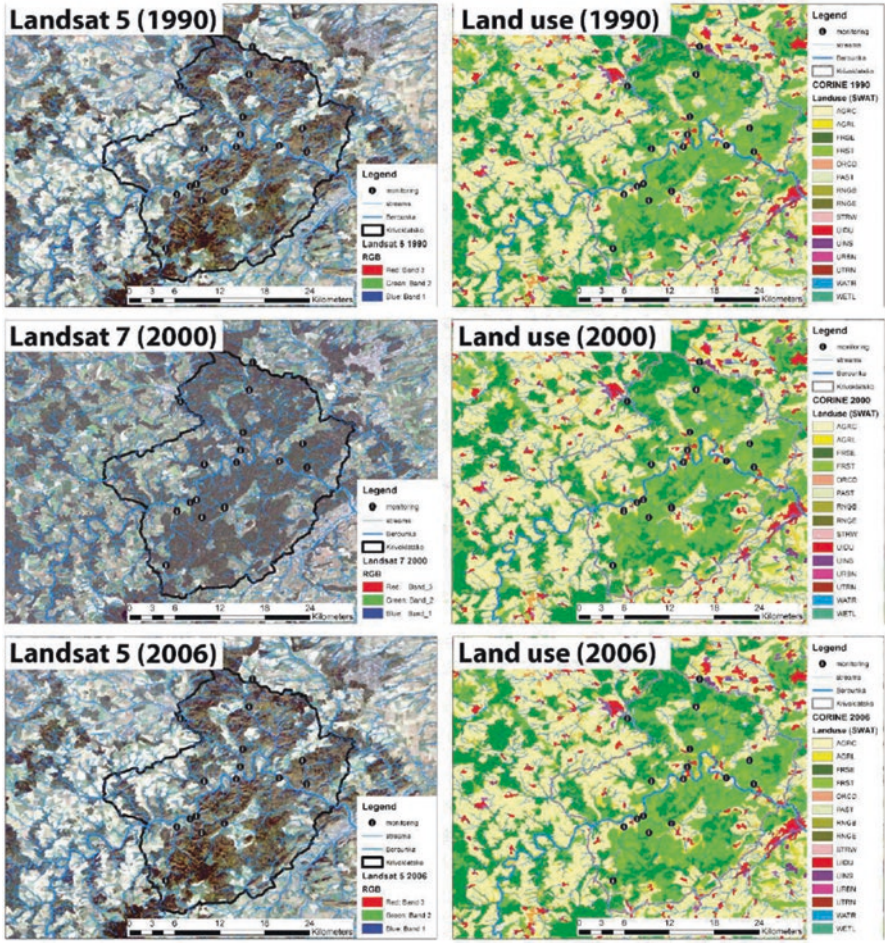
Fig. 5.26 An example focused on comparison of land cover changes of the selected basin in 1990, 2000, and 2006 together with the CORINE Land Cover inventory. Source: Matejicek, L. (2014). Integration of simulation models for watershed management and data from remote sensing in geographic information systems. In: Ames, D. P., Quinn, N. W. T., Rizzoli, A. E. (Eds.), Proceedings of the 7th International Congress on Environmental Modelling and Software, June 15–19, San Diego, CA, USA
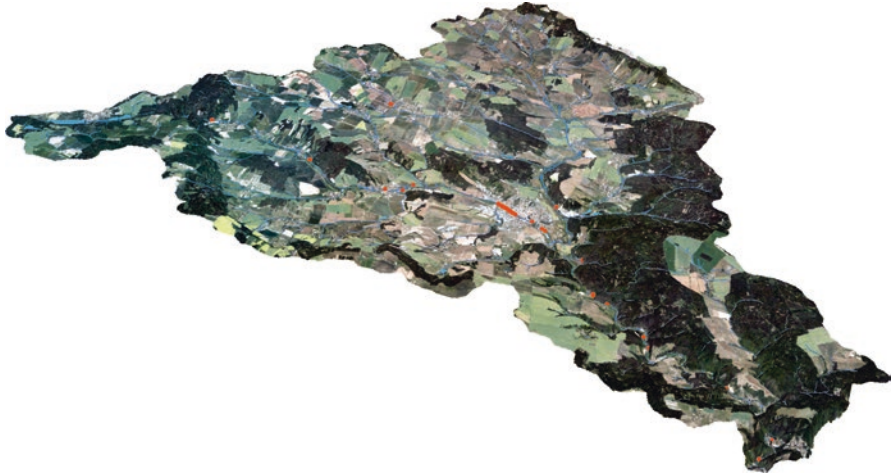
Fig. 5.27 A 3D view of the DEM, which is complemented by other thematic map layers such as sites for monitoring, location of weirs, reservoirs, and stream network (vertical exaggeration: 5)

Bibliography

EIA. (2016). *International Energy Outlook 2016*. Retrieved from http://www.eia.gov/forecasts/ieo/pdf/0484(2016).pdf

IEA. (2016). *World Energy Statistics 2016*. Retrieved from http://www.iea.org/bookshop/723-World_Energy_Statistics_2016

International Hydropower Association. *2016 Hydropower status report*. Retrieved from https://www.hydropower.org/2016-hydropower-status-report

Ocean Energy Systems. Retrieved from https://report2014.ocean-energy-systems.org/statistical-overview-of-ocean-energy-in-2014/open-sea-testing/

Tidal Energy Today. Retrieved from http://tidalenergytoday.com/2015/04/10/overview-of-tidal-and-wave-activities-in-2014/

Dictionaries and Encyclopedia

EIA. (2016). *Energy explained: Your guide to understanding energy*. Retrieved from http://www.eia.gov/energyexplained/index.cfm

Data Sources (Revised in January 2016)

EIA. *International Energy Statistics*. Retrieved from http://www.eia.gov/cfapps/ipdbproject/IEDIndex3.cfm

USGS Landsat Global Archive. Retrieved from http://landsat.usgs.gov/USGSLandsatGlobalArchive.php

Renewable Energy World. Retrieved from http://www.renewableenergyworld.com/hydropower/tech.html

Chapter 6
Wind Power: Estimates of Energy Potential and Environmental Issues

Wind power plants have been indicated great progress for last decades. They consist of large propeller blades driving turbines mounted on high towers. Hundreds of wind power plants are approximately needed to equal the output of one coal power station. The energy output of wind turbines is highly variable, because it is proportional to the cube of the wind velocity. The wind power plants are mostly grouped into the wind farms that occupy large areas of land, so many of them are often being built offshore. It results in the highly variable output power that can oscillate during an hour. In many countries, the subsidies for wind power are on the low level, which causes stopping further the development. Wind power is useful on remote windy sites where the electricity demand is insufficient for the development of large power stations and the transport of electrical power is uneconomical.

6.1 Description of Wind Power Sources

Wind energy originated from Sun radiation, which is primarily absorbed by the surface of the land and the sea. The different absorption of radiation by these materials in turn heats the surrounding air with diverse temperature gradients, which cause convection and pressure changes resulting in winds. On an Earth scale, the higher radiation at the equator than elsewhere causes warm air to rise up from the equator and cooler air to flow in from the north and south. It is estimated that up to 0.5% of the incident solar power of 1.37 kW/m^2 can be converted into wind energy. It is estimated that the total wind power converted from surface radiation of the Earth can be about 10^{15} W (10^6 GW), which is many times more than the total energy demand in the world. However, the wind power is a diffuse variable source in time and in location, and only a small fraction can be practically harnessed. The spatial variability of wind power is also determined by the effect of the rotation of the Earth, which is noticeable in the global scale. An example of global atmospheric modeling, which also enables to study wind flows and weather within Earth's
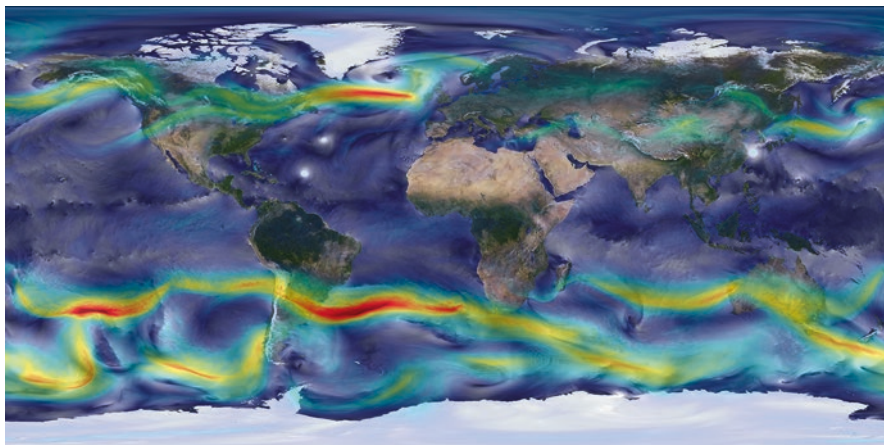
Fig. 6.1 Visualization of global winds from a GEOS-5 simulation using 10 km resolution. Surface winds (0–40 m/s) are shown in *white* and *trace features* including Atlantic and Pacific cyclones. Upper-level winds (250 hectopascals) are colored by speed (0–175 m/s), with *red* indicating faster. Source: William Putman/NASA Goddard Space Flight Center, http://www.nasa.gov/content/a-portrait-of-global-winds

climate system, is in Fig. 6.1. It shows global winds from the NASA's Goddard Earth Observing System Model (GEOS-5) that is capable of simulating worldwide weather at resolutions as fine as 3.5 km.

The use of wind power for pumping water and grinding grain was recorded in the Mediterranean, Near East and China even in antique. In middle ages, horizontal-axis windmills started to appear in European countries, such as England, France, and Holland, and spread rapidly over the continent. The use of windmills peaked around the eighteenth century after which they were displaced by coal-powered steam engines, which could be continuously available and more adaptable to the local energy requirements. Since the late nineteenth century, a number of wind machines, wind turbines, have been developed for generating electricity. Obsolete construction of old windmill was replaced by new devices based on advanced technologies (Fig. 6.2). In the 1970s, environmentalists also promoted the development of renewable energy both as a replacement for the eventual depletion of fossil fuels and for an escape from dependence on fossil fuels.

The majority of current wind turbines for production of electricity is represented by the horizontal-axis wind turbines (HAWTs), which is illustrated in Fig. 6.3. It consists of a tower on top which is mounted the nacelle and mostly three wind turbine blades mounted to the rotor hub. Inside the nacelle are the bearings for the turbine rotor, the gearbox (optionally), and the generator. The turbine rotor with blades is oriented by a yaw control mechanism into the wind, typically upwind of the tower to avoid the tower shielding the blades from the wind. Contemporary blades are made from aluminum and steel. Also new composite materials are increasingly used because of their mechanical properties and longer lifetime.

Fig. 6.2 The old windmill and a number of modern wind turbines grouped into a wind farm. Source: www.pixabay.com, 2016
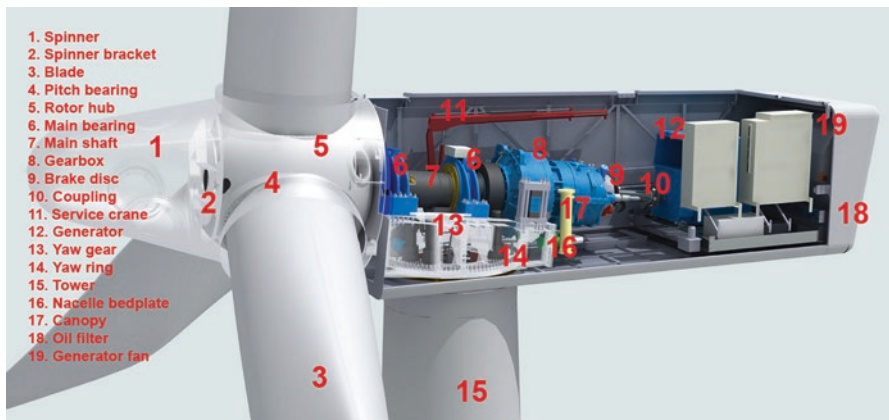

Fig. 6.3 A schema of the modern horizontal-axis wind turbines (HAWTs). Source: London Array Limited: How a turbine works, 2016, http://www.londonarray.com/how-a-turbine-works/

The size of wind turbines was increased from typical turbines with rated power about 80 kW (rotor diameter 20 m, hub height 30 m) in 1985 to 5 MW modern turbines (rotor diameter 125 m, hub height 90 m) with the capacity factor 0.2–0.4 in 2011. The rated power is the maximum continuous power, which the turbine is designed to produce. The capacity factor is the ratio of the annual energy yield to that which would be produced at the rated power.

Location of wind turbines is dependent on wind conditions and requires long-term regular measurements. Onshore wind turbine installations in hilly regions tend to be on ridgelines, which can exploit the topographic acceleration, a few kilometers inland from the nearest shoreline. This is done to exploit the topographic acceleration as the wind accelerates over a ridge. Experience has shown that onshore installations require an average wind speed greater than 6.5 m/s. An example of onshore

Fig. 6.4   The onshore wind farm in a hilly region on ridgelines. Source: www.pixabay.com, 2016

wind turbines grouped into a wind farm is in Fig. 6.4. Grouping of wind turbines requires in dependence on local conditions a spacing of about 3–10 rotor diameters for the reduced wind speed downwind and from the surroundings by gaining wind speed energy. From a turbine to have been brought up to its original speed by gaining, an array energy loss is about 5–10% and is highly dependent on local topography, the distribution of wind direction and wind speed, and spacing of the turbines. But costs for the wind farm installation, operation, and connection to the electrical grid is used to be lower than for widespread individual devices.

Offshore wind turbine installations, usually in the wind farms, are often located on the continental shelf to harvest wind power with stronger wind speeds compared to on land. However, offshore wind farms are relatively more expensive due to marine environment and connection to the electrical grid. An example of the offshore wind farm is in Fig. 6.5, which shows a part of London Array containing 175 Siemens 3.6 MW wind turbines (rotor diameter 120 m, hub height 87 m) aligned according to the prevailing southwesterly wind and covering an area of 100 km^2. The fiberglass blades have its own independent pitching mechanism capable of changing the angle of the blade. These turbines start generating electricity when wind speeds reach 3 m/s and achieve full power from 13 m/s. For safety reasons, the turbines start shutting down if the wind speed becomes greater than 25 m/s. The rotor shaft goes into a three-stage gearbox to increase speed before the generator converts the rotational energy into electrical energy. The electricity produced then passes through the turbine's transformer and is stepped up to 33 kV for export to the offshore substations. An example of connection to the electrical grid and its installation is in Fig. 6.6. The turbines are designed to run for more than 20 years.

Europe is the world leader in offshore wind turbine installations. The first offshore wind farm (Vindeby) was installed in Denmark in 1991. By January 2014, 69

Fig. 6.5 A part of London Array containing 175 Siemens 3.6 MW wind turbines (rotor diameter 120 m, hub height 87 m), floating crane is used for installation of blades (on the *left side*). Source: London Array Limited: How a turbine works, 2016, http://www.londonarray.com/how-a-turbine-works/

Fig. 6.6 An example of connection to the electrical grid and its installation (on the *left side*). Source: London Array Limited: How a turbine works, 2016, http://www.londonarray.com/how-a-turbine-works/

offshore wind farms had been constructed in Europe with an average annual rated capacity of 482 MW in 2013. The United Kingdom has by far the largest capacity of offshore wind farms with 3681 MW followed by Denmark with 1271 MW and Belgium with 571 MW.

In addition to horizontal-axis wind turbines (HAWTs), vertical-axis turbines (VAWTs) and other spatial type of wind power devices have been used since antiquity. The VAWT devices do not need to be pointed into the wind to be effective,
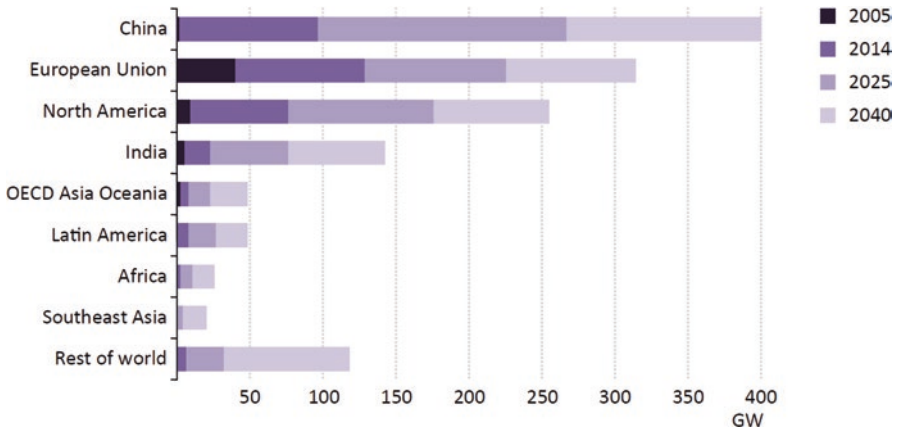
Fig. 6.7 Wind power installed capacity by region in the New Policies Scenario. Source: IEA World Energy Outlook 2014

which is an advantage on sites where the wind direction is highly variable. Also, the generator together with gearbox can be placed near the ground, using a direct drive from the rotor assembly. The disadvantages include the relatively low rotational speed with higher pulsating torque, which needs higher cost of the drive train and the lower power coefficient.

Total installed capacity of wind power reached 350 GW in 2014, in which the European Union, China, and the United States account for more than 80% and India about 10% (Fig. 6.7). The European Union has been the leader in wind power, steadily increasing the annual new installations from 5.0 GW per year on average from 2000 to 2004 to 8.2 GW per year from 2005 to 2009 and 10.7 GW per year from 2010 to 2014. Also the United States has supported the wind power for more than two decades, but the variable support mechanism caused erratic annual capacity additions, which ranged between 0.9 GW and 13.4 GW in 2009–2014, with an average of 6.7 GW. China started to deploy wind power on a commercial scale in the last 10 years, and India has been steadily installing new wind turbines.

It is expected that the top wind power markets such as the European Union, the United States, China, and India remain dominant through to 2040, with China taking the lead before 2020. The energy and climate package drives will continue to create a challenging investment environment due to state-level renewable portfolio standards, and mainly by required carbon dioxide emission reductions under the Clean Power Plan, which provides long-term direction for suppliers and developers, helping them to develop more efficient supply chains. As a result, wind power capacity should increase from 23 GW in 2014 to over 140 GW in 2040.

Initially, wind turbines were built onshore due to availability of viable sites for development. Recent technological improvements in construction of wind turbines also enable to utilize a wider range of wind regimes, including relatively low wind speed environments. Compared with offshore wind installations, onshore projects

are still easier to build and less expensive. But offshore wind power sites mostly offer higher capacity factors, due to more consistent wind conditions, which looks set to play a significant role in the future. The European Union is one of regions in which offshore projects have been deployed at commercial scale with 8 GW of installed capacity by 2014. Based on the long-term predictions and technological progress, it is expected that these projects will exceed to 65 GW in 2040. Similarly, the China market with more than 0.5 GW of offshore wind power installations in 2014 could reach 50 GW in 2040.

6.2   Potential Sources of Wind Power

The maximum power output of a wind turbine can be estimated by the kinetic energy of the air passing through the effective disk area of the rotor blades multiplied by power coefficient 0.59, which is the maximum fraction of the kinetic energy that is extracted by the turbine:

$$P = 0.59 \cdot EAv = 0.59 \cdot \frac{1}{2} \rho v^2 Av = 0.59 \cdot \frac{1}{2} A\rho v^3 \tag{6.1}$$

where P is power output in watts (W), E is power per volume flow, the term Av is the volume flow in cubic meters per second (m³/s) expressed by Av of the air flowing through the area A (m²) with wind speed v (m/s), and ρ is the density of air in kilograms per cubic meter (kg/m³). The theoretical maximum efficiency of 0.59 known as the Betz limit is caused by residual wind energy, which is carried downstream of the turbine in order to maintain air flow. But the resulting output power is additionally decreased by aerodynamic efficiency, mechanical losses, and efficiency of the electrical generator and transport line to the electrical grid. For example, the power output of the air flowing with wind speed of 5 m/s on a rotor blades of 100 m diameter (assume $\rho = 1.2$ kg/m³) is:

$$P = 0.59 \cdot \frac{1}{2} A\rho v^3 = 0.59 \cdot \frac{1}{2} \cdot \pi \cdot \left(\frac{100}{2}\right)^2 \cdot 1.2 \cdot 5^3 \approx 0.35 \, MW,$$

but the power will significantly change if the wind speed increases twice more (from 5 m/s to 10 m/s):

$$P = 0.59 \cdot \frac{1}{2} A\rho (2v)^3 = 8 \cdot 0.59 \cdot \frac{1}{2} A\rho v^3 = 8 \cdot 0.59 \cdot \frac{1}{2} \cdot \pi \cdot \left(\frac{100}{2}\right)^2 \cdot 1.2 \cdot 5^3 \approx 2.8 \, MW.$$

Doubling the wind speed increases the power output by a factor of $2^3 = 8$. The power will increase to $8 \cdot 0.35 = 2.8$ MW, which demonstrates the extreme variability of wind power in dependence on the variability of wind speed.

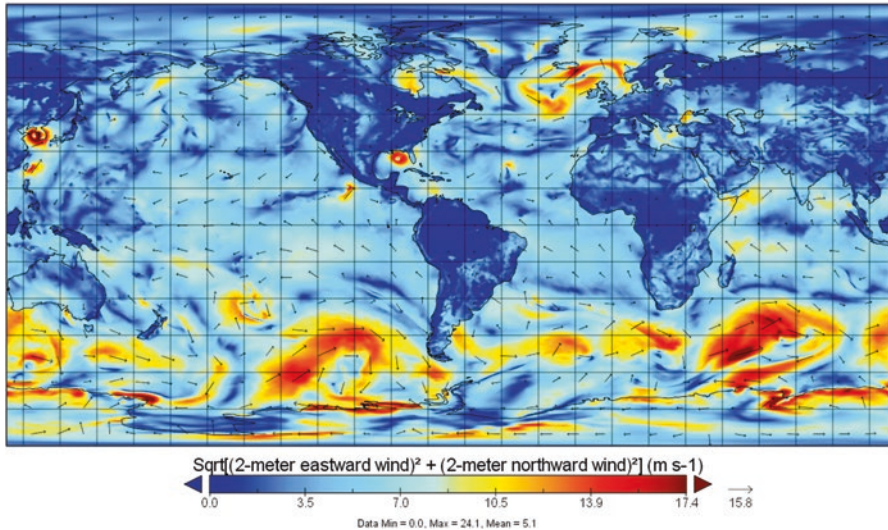MERRA-2 Wind Speed using M2T1NXLSV U2M and V2M on 08/28/2012

Sqrt[(2-meter eastward wind)² + (2-meter northward wind)²] (m s-1)

0.0   3.5   7.0   10.5   13.9   17.4   15.8

Data Min = 0.0, Max = 24.1, Mean = 5.1

Fig. 6.8 An example of a global wind speed map, which is based on the MERRA-2 data files. *Colored fields* with the higher wind speed are mostly located out of consumers in middle parts of ocean on the southern hemisphere. Source: NASA—Global Modeling and Assimilation Office http://disc.sci.gsfc.nasa.gov/datareleases/images/merra2_wind_speed_august_28_2012

Precise and regular measurements are required to determine where to locate a wind turbine or a wind farm. Onshore installations usually require an average wind speed greater than 6.5 m/s, while offshore installations are used to be placed in sites where wind speeds are generally higher with an average wind speeds greater than 9 m/s. Suitable locations can be high altitude plains or coastal areas. Access lines to the electrical grids are very important, because the windiest sites are used to be also some of the most remote. Offshore wind turbines need undersea cables to land, which increases installation costs. An example of a global wind speed map, which is based on the Modern-Era Retrospective analysis for Research and Applications, Version 2 (MERRA-2), data files, is in Fig. 6.8. MERRA-2 data are available at MDISC, managed by the NASA Goddard Earth Sciences (GES) Data and Information Services Center (DISC).

The global growth of installed wind power capacity has been at an average rate of 24% per year since 2000. The aggregate growth of installed wind power capacity for leading countries is in Fig. 6.9. It brought total onshore and offshore capacity to 282 GW in 2012. Among the largest energy projects developed in 2012 were four offshore wind sites (from 216 MW to 400 MW) in the German, United Kingdom, and Belgian waters of the North Sea. Other large-scale offshore projects have started mostly in Europe. By the end of 2012, 5.4 GW had been installed mainly in the United Kingdom (3 GW) and Denmark (1 GW) with other offshore wind power plants installed in Belgium, China, Germany, the Netherlands, and Sweden. In the
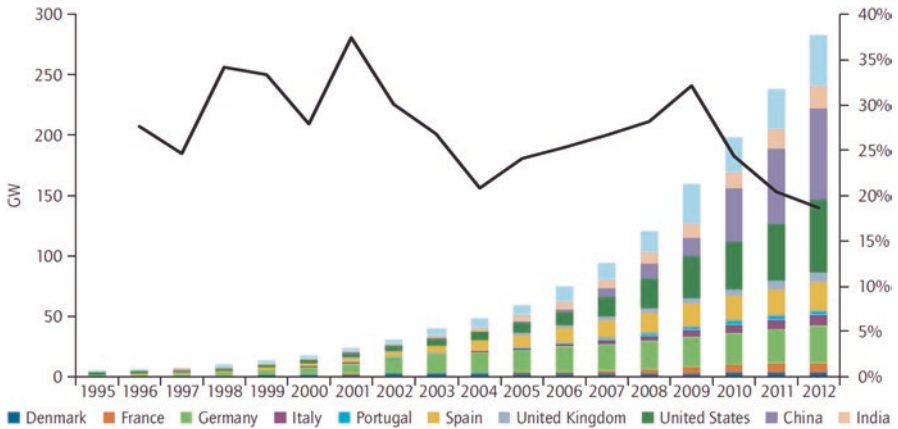
Fig. 6.9 The aggregate growth of installed wind power capacity for leading countries. IEA Wind 2013 Roadmap

United Kingdom, 46 GW of offshore projects are registered, of which around 10 GW have been progressing to consenting, construction, or operation. At the end of 2012, 69 GW of installed capacity were located in cold climate areas in Scandinavia, North America, Europe, and Asia, of which 19 GW were in areas with temperatures below 20 °C. Replacing of old devices (mostly 500 kW, 40 m diameter rotor built in 1990s) with more powerful wind turbines (2 MW and more) is also on the rise. Repowering began in Denmark and Germany and has expanded to other countries such as India, Italy, Portugal, Spain, the United Kingdom, and the United States. For example, in Germany, 325 turbines with installed capacity of 196 MW were replaced with 210 turbines of 541 MW in total in 2012. A global wind map complemented by installed capacity and production for leading countries is illustrated in Fig. 6.10.

A thematic map focused on assessment of surface wind source in the United States, and its coastal zones are in Fig.6.11. The estimates are based on surface wind data, coastal marine data, and upper-air data, where applicable. It also takes into consideration local topographic and meteorological indicators such as mountains summits, sheltered valleys, wind deformed vegetation, and eolian areas with playas and dunes. Evaluation of data is provided at a regional level to produce regional wind resource assessments. The national wind resource assessment is documented in the Wind Energy Resource Atlas of the United States (http://rredc.nrel.gov/wind/pubs/atlas/), which was created for the US Department of Energy in 1986 by the Pacific Northwest Laboratory. Many case-oriented applications and tools focused on assessment of wind power can be provided by NREL Wind Prospector: https://maps.nrel.gov/wind-prospector. An application dealing with mapping wind power plants is illustrated in Fig. 6.12. It is administrated by US EIA (http://www.eia.gov/state/maps.cfm?v=Wind). The locations of wind power devices are complemented by thematic layers linked to onshore 50 m tower wind potential and offshore 50 meter tower wind speed.
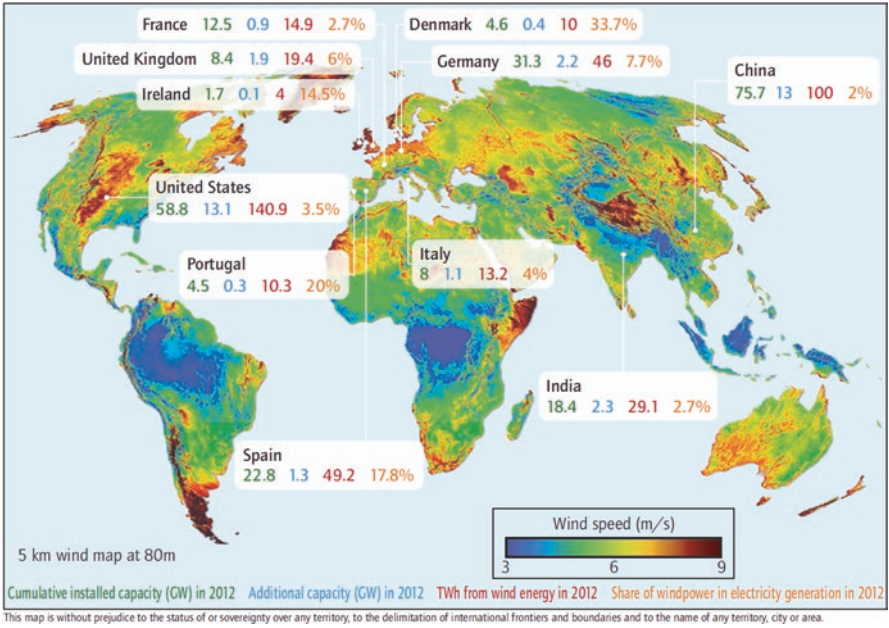
Fig. 6.10 Global wind map complemented by installed capacity and production for leading countries (cumulative and additional capacity in GW, average generation in TWh, and share of wind power in electricity generation in 2012). Source: IEA Wind 2013 Roadmap
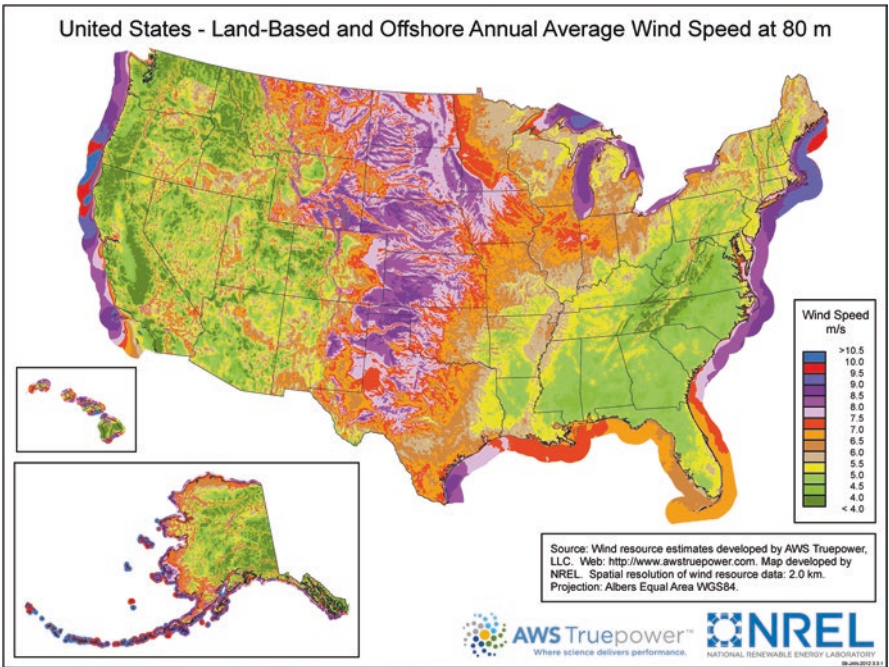

Fig. 6.11 A thematic map focused on assessment of surface wind source in the United States and its coastal zones. NREL (National Renewable Energy Laboratory), 2016. http://www.nrel.gov/gis/wind.html
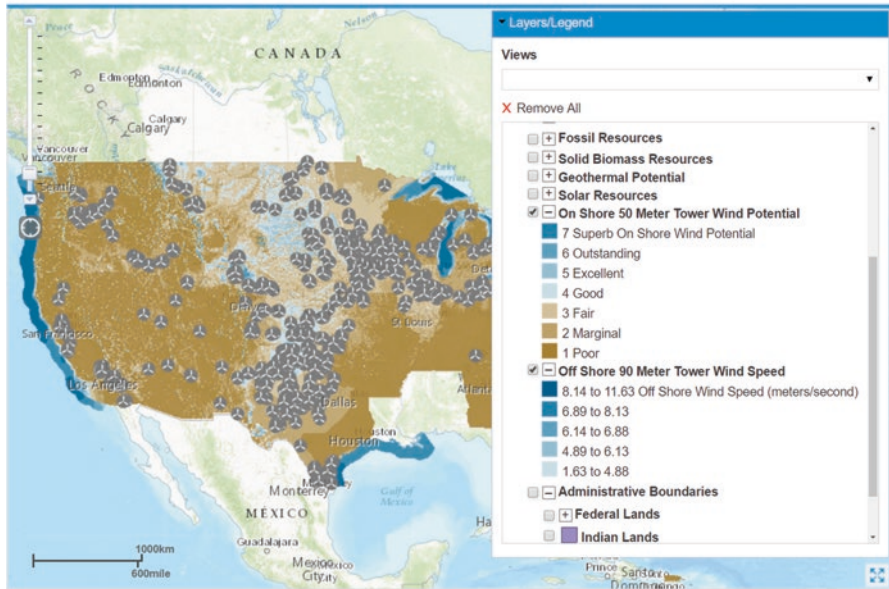
U.S. Energy Mapping System

Fig. 6.12 An application dealing with mapping of wind power plants and thematic layers linked to onshore 50 meter tower wind potential and offshore 50 meter tower wind speed. Source: US EIA Energy Mapping System: http://www.eia.gov/state/maps.cfm?v=Wind, 2016

Maps and resource data for wind power are needed at several stages in the development of wind projects. They can also assist in site prospecting, early-stage feasibility studies, evaluation of alternative project sites, and providing the basis for preliminary or advanced plant design and energy production estimates. Besides international and national institutions, such as Global Wind Energy Council (GWEC), European Wind Energy Association (EWEA), International Energy Agency (IEA), US Energy Information Administration (EIA), and European Environmental Agency (EU EEA), a number of companies can provide resource mapping and modeling. As an example, windNavigator developed by AWS Truepower is illustrated in Fig. 6.13. This application and similar computer tools offer regional resource maps based on mesoscale models for site screening. Local mapping of wind power resource grids can support plant design and energy estimates in more detailed way. Time series files allow better understanding of the wind resource and energy production potential over a few decades.

In 2015, an annual installation crossed the 60 GW for the first time in history. More than 63 GW of new wind power capacity was installed. This growth was mainly powered by new installations in China (nearly 31 GW). Thus, the new global total for wind power was 432.9 GW at the end of 2015. Information about top ten countries with new installed capacity and top ten countries with cumulative capacity in 2015 are in Fig. 6.14. China has been retaining as the largest overall market for wind power since 2009, followed by Europe and North America closing the gap. In the last years, the majority of wind installations globally were outside the OECD
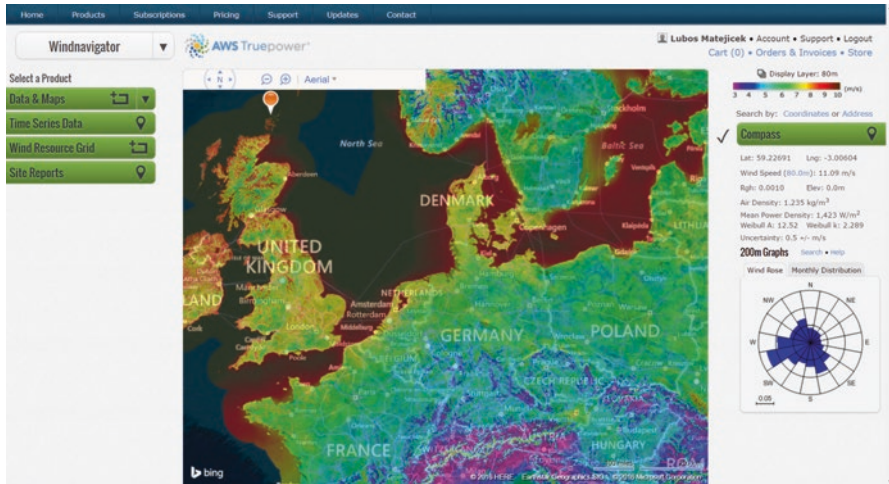
Fig. 6.13 windNavigator offering regional resource maps for wind power sources. It is based on mesoscale models for site screening and local mapping, which can support plant design and energy estimates in more detailed way. The available datasets contain thematic maps, time series data, wind resource girds, and generating final reports. Source: AWS Truepower, https://dashboards. awstruepower.com/wsa, 2016
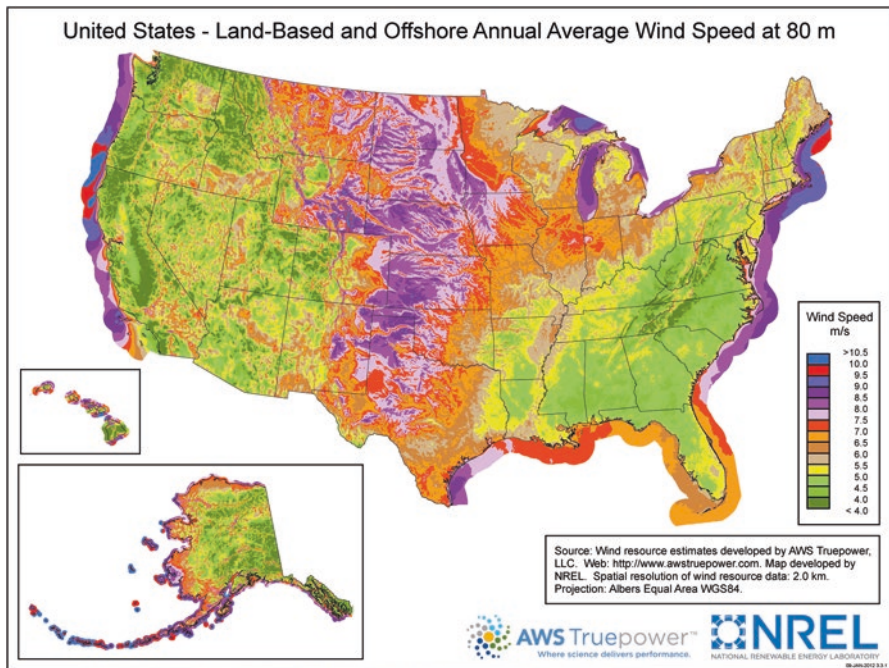

Fig. 6.14 Top ten countries with new installed capacity and top ten countries with cumulative capacity in 2015. Source: GWEC Global Wind Report—Annual Market Update 2015

Table 6.1 Top countries with the total capacity of the wind power plants more than 1000 MW

Country	Continent	Number of wind farms	Total capacity (MW)
United States	North America	1147	80,589
China	Asia	860	63,768
Germany	Europe	4267	45,166
Spain	Europe	984	23,326
United Kingdom	Europe	868	19,009
India	Asia	466	17,918
Canada	North America	240	12,013
France	Europe	912	11,490
Brazil	South America	347	10,950
Italy	Europe	359	9586
Turkey	Asia	130	5419
Denmark	Europe	1517	5266
Sweden	Europe	860	5034
Portugal	Europe	251	4998
Netherlands	Europe	471	4359
Australia	Oceania	57	4262
Mexico	North America	45	4005
Poland	Europe	205	3994
Romania	Europe	61	3131
Japan	Asia	233	2680
Ireland	Europe	174	2453
Belgium	Europe	143	2387
Austria	Europe	225	2331
Greece	Europe	146	2210
South Africa	Africa	25	2034
Chile	South America	31	1501
Uruguay	South America	38	1369
Finland	Europe	160	1170
Norway	Europe	33	1097

Source: The Wind Power Database, 2016, http://www.thewindpower.net

countries. A list of top countries with the total capacity of the wind power plants more than 1000 MW is in Table 6.1. A list of top ten selected large onshore and offshore wind farms is in Tables 6.2 and 6.3, respectively.

In 2015, the European Commission (EC) launched its new vision for a unified energy strategy for the European Union: the Energy Union. The Energy Union means making energy more secure, affordable, and sustainable. It should allow a free flow of energy across borders and a secure supply in every EU country. Also, building renewed infrastructure including renewables, such as wind power, should cut household payments and create new jobs and skills, as companies expand exports and boost growth. The vision is dealing with a sustainable, low carbon, and environmentally friendly economy, putting Europe at the forefront of renewable energy production and the fight against global warming. The EC also launched a consultation in November 2015 for a revised Renewable Energy Directive for the period 2020–2030 (https://ec.europa.eu/priorities/energy-union-and-climate_en).

Table 6.2 Top ten selected large onshore wind farms

Wind farm	Capacity (MW)	Country	Turbines
Gansu Wind Farm	6000	China	
Muppandal Wind Farm	1500	India	
Alta-Oak Creek Mojave	1320	United States	600
Jaisalmer Wind Park	1064	India	
Shepherds Flat Wind Farm	845	United States	338
Roscoe Wind Farm	782	United States	634
Horse Hollow Wind Energy Center	736	United States	421
Capricorn Ridge Wind Farm	662	United States	407
Fântânele-Cogealac Wind Farm	600	Romania	240
Fowler Ridge Wind Farm	600	United States	215

Source: Wikipedia, 2016

Table 6.3 Top five selected large offshore wind farms

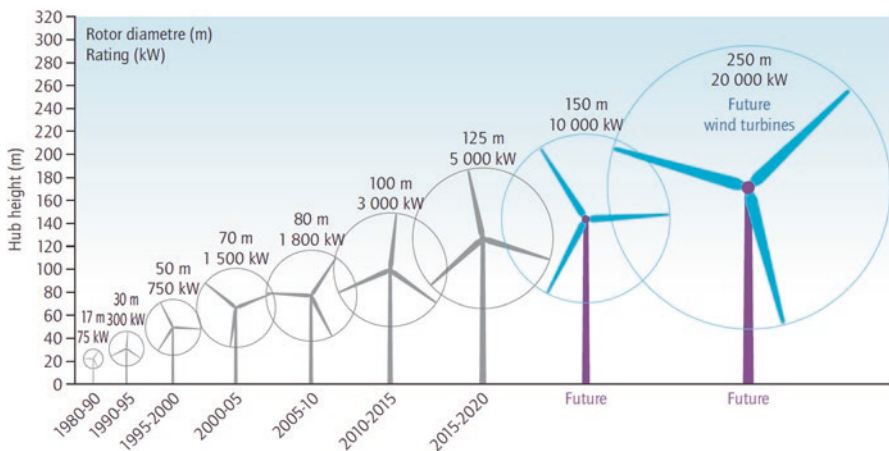| Wind farm	Capacity (MW)	Country	Turbines: model	Commissioned
London Array	630	United Kingdom	175: Siemens SWT-3.6	2012
Gwynt y Môr	576	United Kingdom	160: Siemens SWT-3.6 107	2015
Greater Gabbard	504	United Kingdom	140: Siemens SWT-3.6	2012
Anholt	400	Denmark	111: Siemens SWT-3.6–120	2013
BARD Offshore 1	400	Germany	80: BARD 5.0 turbines	2013

Source: Wikipedia, 2016

Fig. 6.15 Growth in size of horizontal wind turbines since 1980 and its prospects. Source: IEA Technology Roadmap: Wind Energy, 2013 edition

Besides new installations, new system design targets for upscaling of the wind power turbines to 10 MW, or even to 20 MW, which can reduce costs in comparison with installation provided by actual power turbines for 2–5 MW. Optimum size for both onshore and offshore power plants is a new challenge for construction and logistic constrains as well as sound and visibility regulations (Fig. 6.15).

6.3   Environmental Effects of Wind Turbine Installations

The environmental impacts of wind power systems are minor in comparison to the environmental impacts of energy systems based on fossil fuels. By this point of view, wind power can reduce GHG emissions together with the emissions of other air pollutants, by displacing fossil fuel-based electricity generation. Wind energy, like other industrial activities, can produce some detrimental impacts on the environment and on human beings. Thus, local and national governments have established permitting procedures to minimize those impacts.

An indirect environmental impact of wind power arises from the release of air pollutants during the manufacturing, transport, and installation of wind turbines and their subsequent decommissioning. In order to provide full fuel cycle comparisons with other forms of electricity production, life cycle assessment (LCA) procedures based on ISO standards ISO 14040 and ISO 14044 have been used to analyze these impacts. The carbon intensity of wind energy estimated by the studies ranges from 4.6 to 27 gCO_2/kWh. The variability of the results is caused by estimates of the manufacturing stage, which dominates overall life cycle GHG emissions. Energy payback times for the studies suggest that the embodied energy of new wind turbines is repaid from 3 to 9 months of operation.

Potential ecological impacts include bird and bat collision fatalities and more indirect habitat and ecosystem modifications. For offshore power plants, implications for marine life must be considered. Impact of wind power plants on the local climate can be caused by extracting momentum from the air flow and thus reduce the wind speed behind the turbines, and also by increasing vertical mixing by introducing turbulence across a range of length scales. Based on a number of studies, impact of wind energy on local climates remains uncertain. It is recognized that wind turbines are not the only structures to potentially impact local climate variables and that any impacts caused by increased wind energy development should be placed in the context of other anthropogenic climate influences.

Impacts on humans include land and marine usage; visual impacts; proximal impacts such as noise, flicker, health, and safety; and property value impacts. Wind power plants, especially onshore wind farms, operate on large areas (approximately 5–10 MW per km^2), where their supporting roads can disturb from 2% to 5% of the total area encompassed. The installation of wind turbines may be precluded from the residential areas, airports, shipping for offshore installations and some radar installations as well as nature reserves and historical and sacred sites.

Despite the described potential impacts, wind power seems to be widely accepted by the general public. But on the local level, a number of concerns exist that can make barriers for stakeholders toward wind energy, such as land and marine use, and the visual, proximal, and property value impacts. Practical experiences have found that public concern toward wind energy development is greatest directly after the announcement of a wind power plant, but that acceptance increases after construction when actual impacts can be assessed. Regardless of the degree of social and environmental concerns, addressing them directly is an essential part of any successful wind power planning and plant siting process. Also, involving the local community in the planning and siting process has sometimes been shown to improve
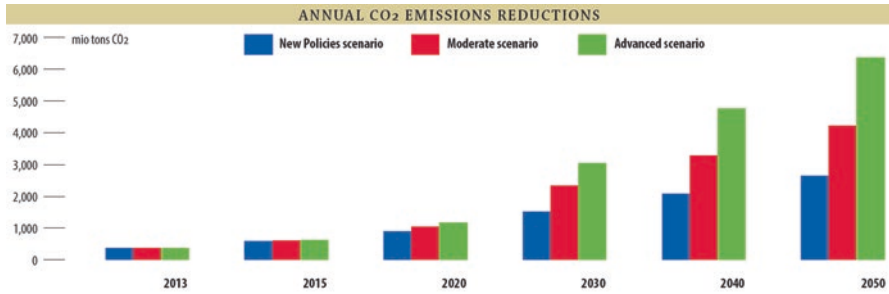
Fig. 6.16 A comparison of annual carbon dioxide (CO_2) emission reductions based on described scenario: IEA New Policies Scenario and GWEC Moderate and Advanced scenarios. Source: GWEC Global Wind Energy Outlook 2014

outcome, as well as co-ownership of local wind power plants can improve public attitudes toward wind energy.

It is estimated that annual reductions in carbon dioxide from existing wind power plants were about 372 million tons in 2013. But the IEA New Policies Scenario expects to raise the reduction to 899 million tons annually by 2020 and even up to 1521 tons per year by 2030. An alternative to the IEA scenarios is presented by the Global Wind Energy Council (GWEC) in its Global Wind Energy Outlook 2014. Its Moderate scenario implies savings of over 1 billion tons of carbon dioxide per annum by 2020 and more than 2.3 billion tons by 2030, while its Advanced scenario would result in even higher savings of nearly 1.2 billion tons of carbon dioxide per annum by 2020, and 3.1 billion tons per annum by 2030 (Fig. 6.16). The alternative scenarios by GWEC include significant reductions in all cases and the extreme speed at which the savings are achieved. But wind power's scalability and its speed of deployment can make it an ideal technology to bring proposed reduction of carbon dioxide into reality. A comparison of annual carbon dioxide emissions reductions based on described scenarios is in Fig. 6.16.

6.4   Risk Assessment of Wind Turbines and Wind Farms with GIS

Using GIS can help to determine the most favorable locations for individual power plants or large wind farms. Spatial modeling tools in GIS enable analysis of terrain, which significantly impacts the quality of wind at particular sites. The results can be used by government decision-makers or by local authorities to provide optimal installations of wind power plants. In the United States, National Renewable Energy Laboratory (NREL) provides updated wind resource maps, which are components of the wind deployment models. GIS can also help to determine the most favorable locations for wind farms based on the cost of transmission, locations of load centers

and wind resources, as well as the layout of the electrical grid. Multi-criteria analysis can examine economic development potential based on strong manufacturing centers and exclude sites such as national parks and wilderness areas, in order to provide policy analysis and implementation analysis. The results of GIS analysis include thematic map layers with voltage of transmission lines and classes of wind speed and wind power. It can be extended by forecasts dealing with expansion of wind farms and their impacts on the environment.

GIS advanced methods and functions, which can assist in spatial analysis, are mostly include in 3D analysis tools, spatial analysis tools, and network analysis tools. For demonstration of GIS capabilities to provide a wide range of tools for assessment of wind power sources, selected ArcGIS methods and functions arranged in case-oriented toolboxes such as 3D Analyst, Spatial Analyst, and Network Analyst are introduced for 3D analysis tools in Table 6.4, for spatial analysis tools in Table 6.5, and for network analysis tools in Table 6.6. The presented tools have the universal use in many GIS tasks, but analysis and spatial modeling for assessment of wind energy systems can benefit from their implementation in the decision-making procedures. The GIS projects by themselves are used to be based on a wider range of operations, which deals with spatial data management, data exchange tools, visualization, map layer creations GIS, and Web-based applications. The described tools dealing with 3D, spatial, and network analyses are mostly optional extensions of the existing GIS software packages, such as ESRI's ArcGIS.

Table 6.4 Selected methods of GIS 3D analysis tools that can be applied individually or used in sequence to create and analyze 3D data, such as digital elevation models (DEMs)

3D analysis tools	Data management, conversion, and analysis on surface models in 3D data represented in raster, terrain, triangulated irregular network (TIN) and LAS dataset formats
3D Features	Evaluate geometric properties and relationships between three-dimensional features
Conversion	Convert feature classes, files, LAS datasets, rasters, TINs, and terrains to other data formats
Data Management	Provide tools for creating and managing terrain, TIN, and LAS datasets
Functional Surface	Evaluate elevation information from raster, terrain, and TIN surfaces
Raster Interpolation	Produce continuous raster surfaces from a given set of sample points
Raster Math	Mathematical operations on raster datasets
Raster Reclass	Reclassification of raster data
Raster Surface	Analyze raster surface properties, such as contours, slope, aspect, hillshade, and difference calculation
Triangulated Surface	Analyze TIN surface properties, such as contours, slope, aspect, hillshade, difference calculation, volumetric computations, and outlier detection
Visibility	Visibility analysis of features, such as surfaces, multipatches (buildings and other 3D feature)

Source: ESRI ArcGIS Resource Center, 2016

Table 6.5 Selected methods of GIS spatial analysis tools that can be applied individually or used in sequence to create, analyze raster and vector data, as well as provide spatial modeling

Spatial analysis tools	A wide range of spatial analysis and modeling methods for both raster (cell-based) and feature (vector) data including map algebra and case-oriented analyses
Conditional	Control the output values based on the conditions placed on the input values and can be applied in queries based on the attributes or the position
Density	Calculate the density of input features within a neighborhood around each output raster cell
Distance	Perform distance analysis with Euclidean (straight line) distance, cost-weighted distance, and paths and corridors between sources with the least cost of travel
Extraction	Extract a subset of cells from a raster by either the cells' attributes or their spatial location
Generalization	Generalize the data to get rid of unnecessary detail for a more general analysis
Interpolation	Create a continuous (or prediction) surface from sampled point values
Local	Combine the input rasters, calculate a statistic on them, or evaluate a criterion for each cell on the output raster based on the values of each cell from multiple input rasters
Map Algebra	Perform spatial analysis by creating expressions in an algebraic language
Multivariate	Multivariate statistical analysis, focused on the exploration of relationships among many different types of attributes, with classification methods or principal component analysis
Neighborhood	Create output values for each cell location based on the location value and the values identified in a specified neighborhood
Overlay	Apply weights to several input layers, combine them into a single output, and subject to specifications of distribution and shape, identify preferred locations within that result. These tools are commonly used for suitability modeling and include methods such as fuzzy membership, fuzzy overlay, locate regions, weighted overlay, and weighted sum
Raster creation	Generate new rasters in which the output values are based on a constant or a statistical distribution
Reclass	Provide a variety of methods that allow you to reclassify or change input cell values to alternative values
Surface	Quantify and visualize a terrain landform represented by a digital elevation model
Zonal	Perform analysis where the output is a result of computations performed on all cells that belong to each input zone. A zone can be defined as being one single area of a particular value, but it can also be composed of multiple disconnected elements, or regions, all having the same value

Source: ESRI ArcGIS Resource Center, 2016

Table 6.6 Selected methods of GIS network analysis tools that can be applied individually or used in sequence to maintain network datasets that model transportation networks

Network analysis tools	Maintain network datasets that model transportation networks and perform route, closest facility, service area, origin-destination cost matrix
Make Closest Facility Analysis Layer	Determine the closest service facility or facilities to an incident based on a specified travel mode
Make Location-Allocation Analysis Layer	Choose a given number of facilities from a set of potential locations such that a demand will be allocated to facilities in an optimal manner
Make OD Cost Matrix Analysis Layer	Provide a matrix of costs going from a set of origin locations to a set of destination locations
Make Route Analysis Layer	Determine the best route between a set of network locations based on a specified network cost
Make Service Area Analysis Layer	Determining the area of accessibility within a given cutoff cost from a facility location

Source: ESRI ArcGIS Resource Center, 2016

6.5 Case-Oriented Studies

Assessment of wind power sources is currently in the focal point. For the investors, the wind farms generate revenue when they sell the energy the turbines generate. In addition, investing in wind energy helps countries meet renewable energy portfolio standards. Using GIS in this market can give developers information for placing wind turbines, in order to work for their power needs and their budgets.

6.5.1 Processing of Data About Wind Power Sources in GIS

A case study is focused on mapping of wind flows in Indiana, a US state located in the midwestern and Great Lakes regions of North America. A map in Fig. 6.17 shows locations of renewables, including wind power plants.

Using of ArcGIS Online for mapping of wind power is illustrated in Fig. 6.18. ArcGIS Online is a complete, cloud-based mapping platform, which can make and share digital maps, and provide a wide range of GIS functionality. As an example, a map layer with the wind power density is linked to the GIS. In order to explore wind
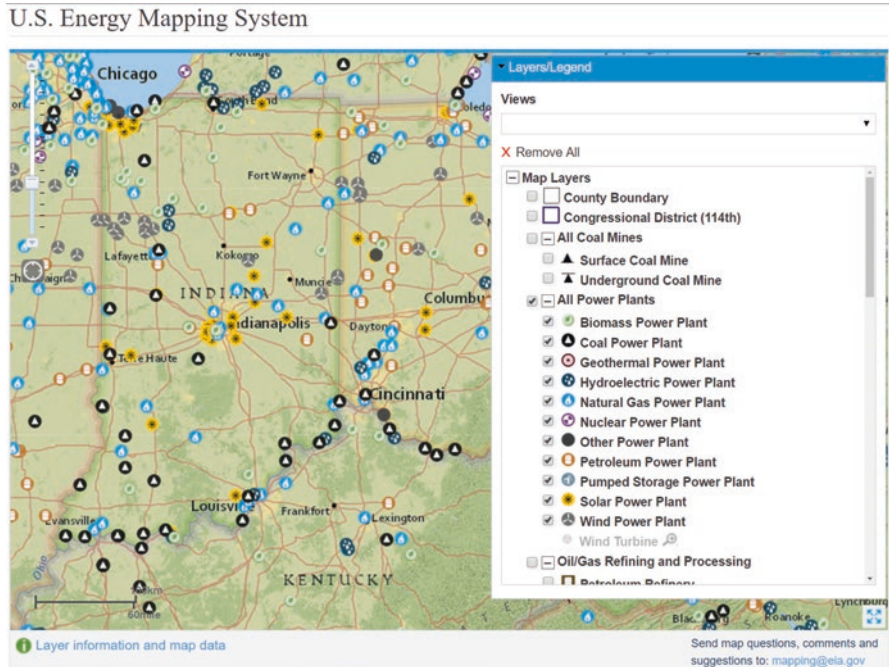
Fig. 6.17 Mapping of renewables in the territory of Indiana by US Energy Mapping System. Source: EIA, 2016
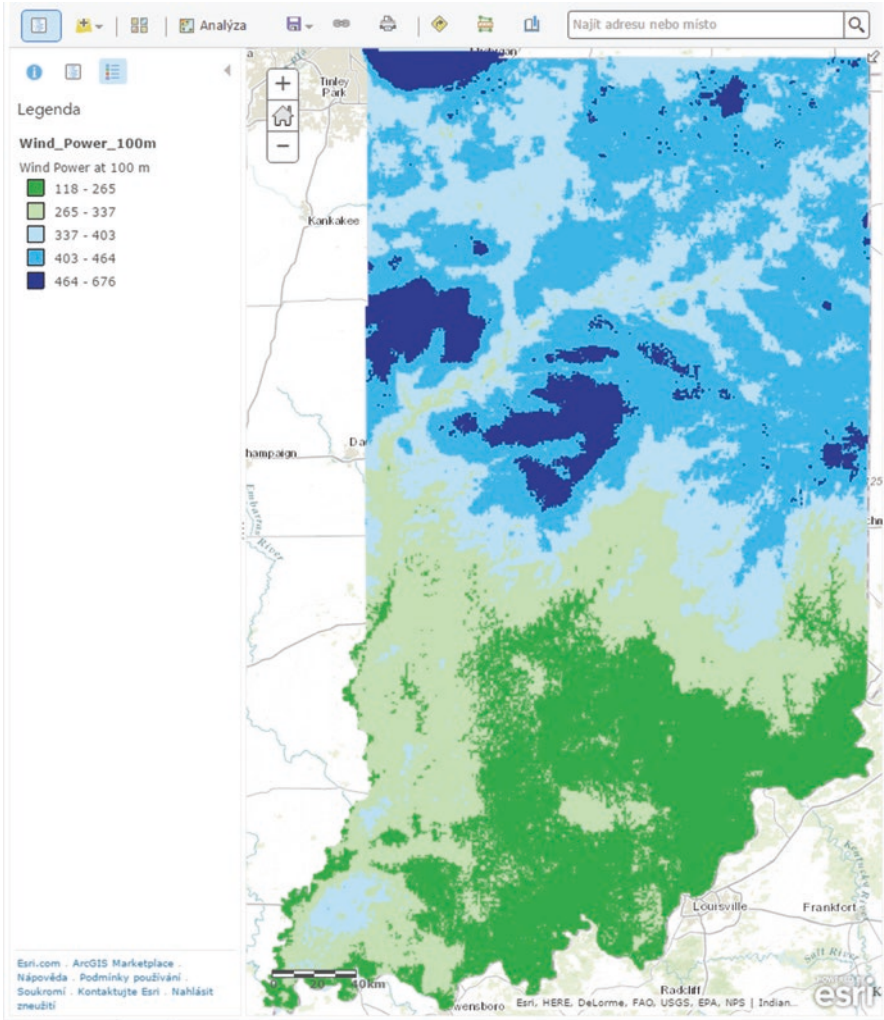
Fig. 6.18 An example of the ArcGIS Online project containing a linked map layer with mean wind power density at height of 100 m above ground in W/m². Source: ESRI ArcGIS Online, 2016; Indiana Department of Commerce, TrueWind Solutions, LLC, National Renewable Energy Laboratory (NREL), 2016

power conditions, a few other layers complement the project. An example of the DEM based on LiDAR data is in Fig. 6.19, and the land cover is in Fig. 6.20, respectively. The linked map datasets can be complemented by other spatial data and analyzed by ArcGIS Online methods and functions. This cloud-based mapping application gives an opportunity to share data with other users such as research/public community, investors, and developers.
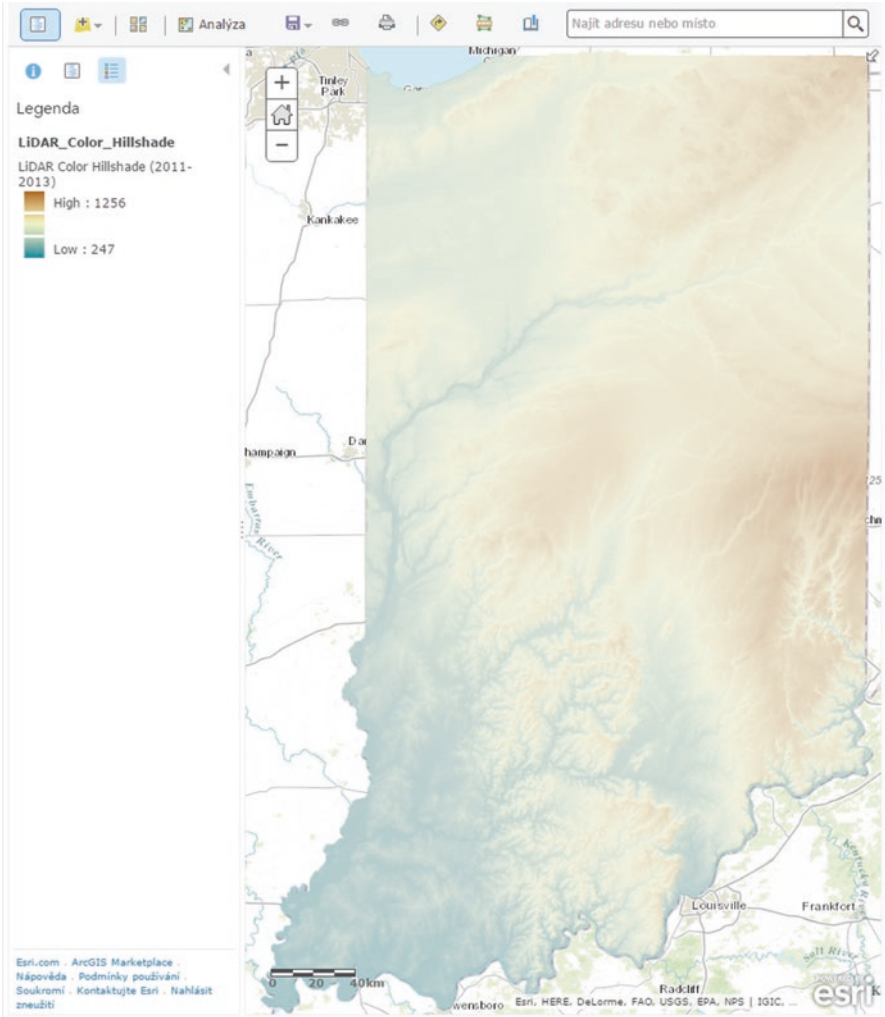
Fig. 6.19 The image layer based on LiDAR data (1.5 m DEMs) created by using the colorized DEM, hillshade, and slope data (last updated on February 14, 2014) in ArcGIS Online. Source: ESRI ArcGIS Online, 2016; Indiana Geological Survey (Indiana Spatial Data Portal, University Information Technology Services, Indiana University), 2016

The linked map layer with mean wind power density at height of 100 m above ground is derived from Mesoscale Atmospheric Simulation System (MASS), which is a numerical weather model that simulates the physics of the atmosphere. MASS is coupled to a simpler wind flow model, Wind Map, which is used to refine the spatial resolution of MASS and account for localized effects of terrain and surface roughness. MASS simulates weather conditions over a region for 366 historical
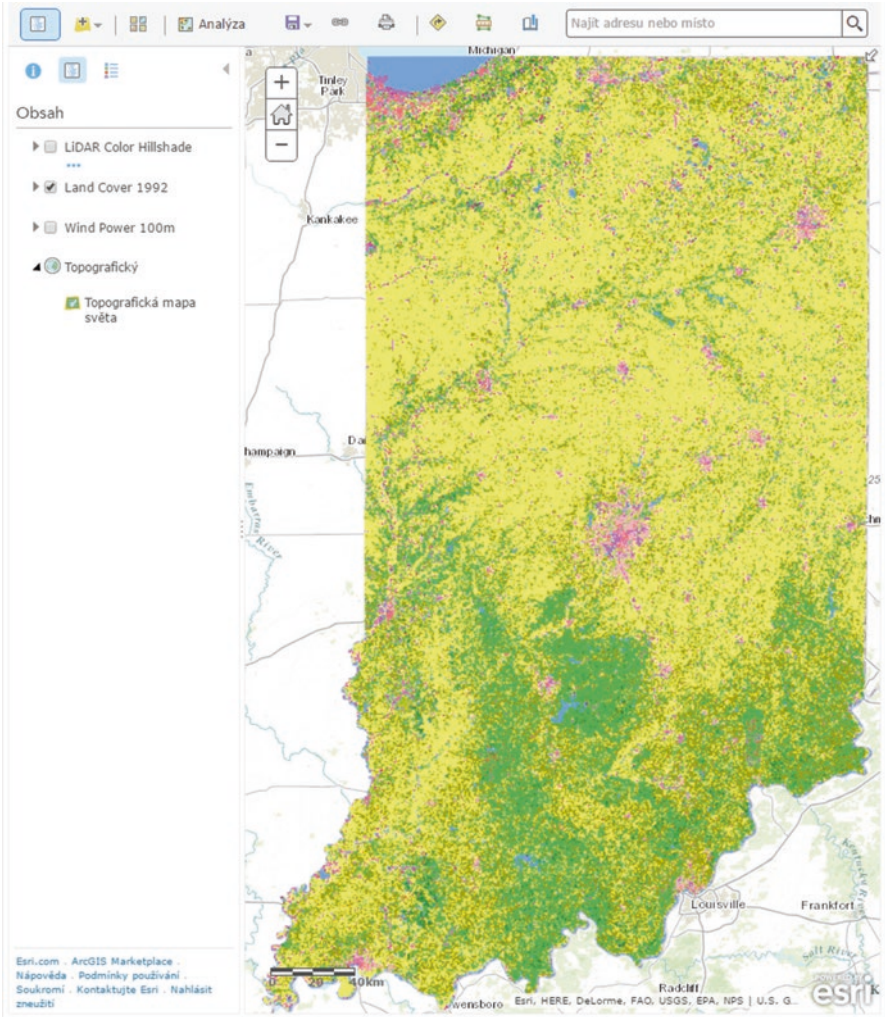
Fig. 6.20 The grid land cover containing 18 categories of land use in Indiana (30 m grid in 1992) in ArcGIS Online. The categories range from water (*blue*), subcategories of forest (*green shades*), agriculture subcategories (*yellow shade*) to residential, industrial, commerce, and transportation categories (*violet shade*). The grid layer is a subset of the National Land Cover Data (NLCD, 1992, Version 06-03-99, of the US Geological Survey). Source: ESRI ArcGIS Online, 2016; US Geological Survey, 2016

days randomly selected from a 15-year period. When the runs are finished, the results are input into Wind Map. In this project, the MASS model was run on a grid spacing of 1.7 km and Wind Map on a grid spacing of 200 m (derived from ArcGIS Online data resources).

    Exploration of wind power density is complemented by the image layer based on
LiDAR data (Indiana Geological Survey, 1.5 m DEMs) and by the grid land cover
layer. An image layer was created by using the colorized DEM, hillshade, and slope
data (last updated on February 14, 2014). The grid land cover shows 18 categories
of land use in Indiana (30 m grid in 1992). The grid layer is a subset of the National
Land Cover Data (NLCD, 1992, Version 06-03-99, of the US Geological Survey).
The sample layers are complemented in the project by topographic map on the
background layer.

6.5.2   *Mapping Potential Sources for Wind Turbines*

Smaller wind farms with a capacity to 50 MW also represent a valuable market of
the wind power industry in the regional scale. This case study is focused on a wind
farm of a capacity 42 MW with estimated production of electricity about 100 GWh.
The wind farm contains 21 turbines, each of a capacity 2 MW. A part of the area
occupied by wind turbines is illustrated in Fig. 6.21. A detailed view on the instal-
lation of a wind turbine is in Fig. 6.22. Again, map layers with spatial datasets for
assessment of local wind power sources are link in the ArcGIS Online. The wind
power density, wind speed, and wind direction were estimated by local long-term
measurements. The linked map layers are represented by an aerial photograph in

Fig. 6.21 A part of the regional wind warm (42 MW, 21 turbines, estimated production 100 GWh).
Google Earth, 2016

Fig. 6.22 A detailed view on the installation of a wind turbine (2 MW). Google Earth, 2016
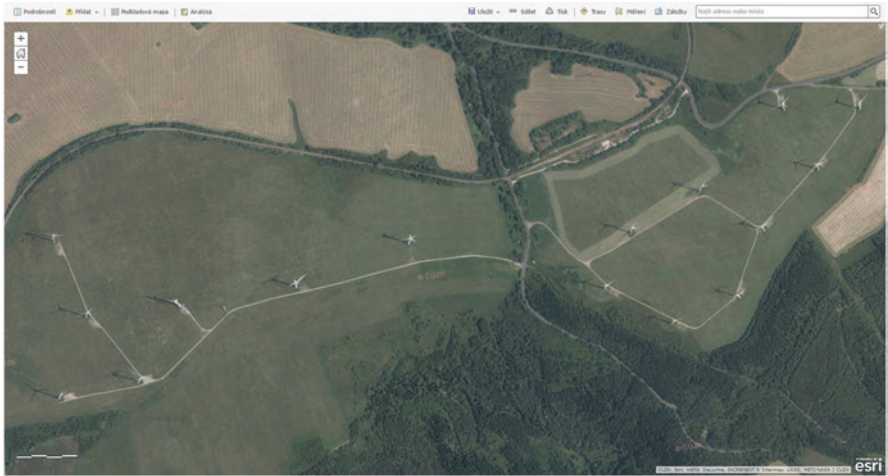

Fig. 6.23 An aerial photograph of the regional wind farm in ArcGIS Online. Source: CUZK, 2016

Fig. 6.23, a digital surface model (DSM) in Fig. 6.24, and a digital elevation model (DEM) in Fig. 6.25. The elevation difference between the DSM grid and the DEM grid can be used for estimation of surface local barriers, such as vegetation, building, and other features. The linked map datasets in ArcGIS Online can be complemented by other data and analyzed, in order to assist in research studies, and to help a local public community, investors, and developers.
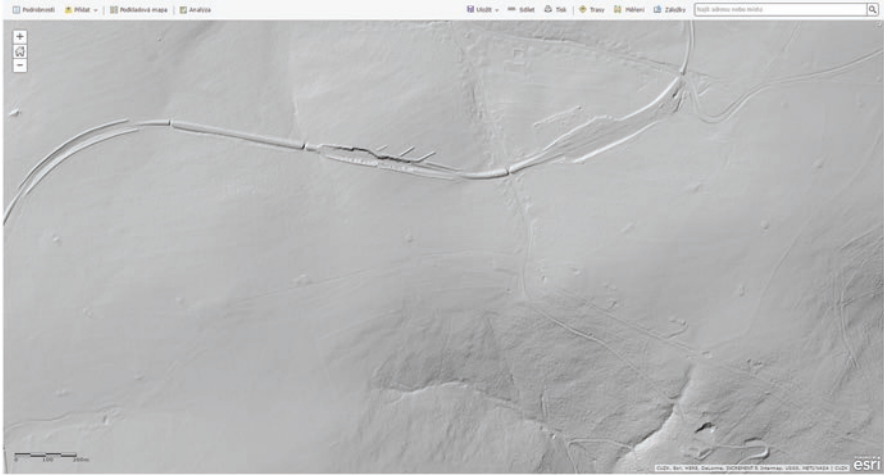
Fig. 6.24 A digital surface model (DSM) of the area of interest in ArcGIS Online. Source: CUZK DMR5G, 2016
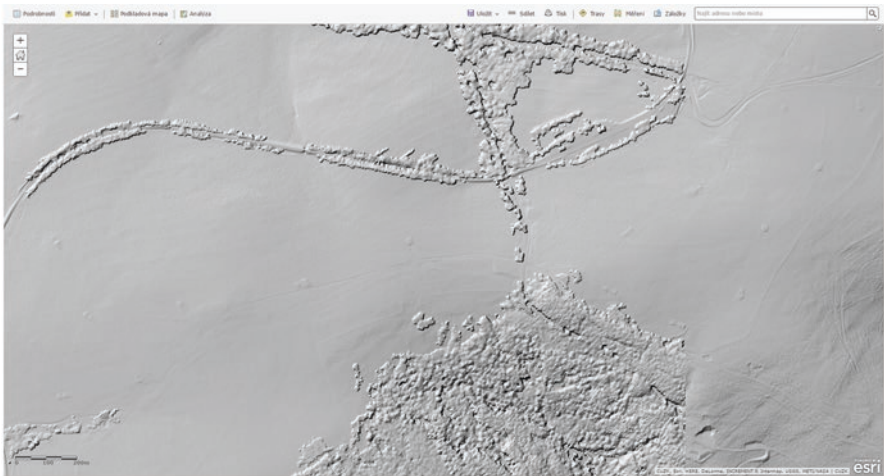
Fig. 6.25 A digital elevation model (DEM) of the area of interest in ArcGIS Online. Source: CUZK DMR1G, 2016

Bibliography

EIA. (2015). *International energy outlook 2015*. Retrieved from http://www.eia.gov/forecasts/ieo/pdf/0484(2016).pdf

GWEC. (2014). *Global wind outlook 2014*. Retrieved from http://www.gwec.net/wp-content/uploads/2014/10/GWEO2014_WEB.pdf

GWEC. (2016). *Global wind report: Annual market update 2015*. Retrieved from http://www.gwec.net/wp-content/uploads/vip/GWEC-Global-Wind-2015-Report_April-2016_19_04.pdf

IEA. (2015). *World energy outlook 2014*. Retrieved from https://www.iea.org/bookshop/477-World_Energy_Outlook_2014

IEA. (2016a). *World energy statistics 2016*. Retrieved from http://www.iea.org/bookshop/723-World_Energy_Statistics_2016

IEA. (2016b). *World energy outlook 2015*. Retrieved from https://www.iea.org/bookshop/700-World_Energy_Outlook_2015

IPCC. (2012). *Special report on renewable energy sources and climate change mitigation*. Retrieved from https://www.ipcc.ch/pdf/special-reports/srren/SRREN_FD_SPM_final.pdf

Dictionaries and Encyclopedia

EIA. (2016). *Energy explained: Your guide to understanding energy*. Retrieved from http://www.eia.gov/energyexplained/index.cfm

Data Sources (Revised in August 2016)

AWS Truepower. Retrieved from http://www.awstruepower.com/

EIA. *International energy statistics*. Retrieved from http://www.eia.gov/cfapps/ipdbproject/IEDIndex3.cfm

EIA. *U.S. energy mapping system—Wind*. Retrieved from http://www.eia.gov/state/maps.cfm?v=Wind

Renewable Energy World. Retrieved from http://www.renewableenergyworld.com/wind-power.html

Chapter 7
Solar Energy: Estimates of Energy Potential and Environmental Issues

The Sun energy falling on the Earth at the rate of about 100 PW/year is enough to support our energy needs about a few thousand times. If new technology could find a practical way of transformation and accumulation, we would have supply by energy our industry and personal consumption without any energy crisis. Although the heat of the Sun stirs up the atmosphere and causes wind and water circulations on the surface of the Earth, a considerable part can be used to generate electricity or used directly. The currently used photovoltaic cells are inefficient and expensive to substitute traditional fossil energy sources. Also the territorial claims are high and output power variable due to meteorological conditions. Despite the Sun giving approximately 1.4 kW per square meter to the Earth, we can use a small part such as about 100–200 W per square meter at the Earth's surface, with higher values at the equator. Although current technology for electricity generation is still too costly for general use, there are many applications for relatively small amounts of electricity needed in remote sites such as navigation lights, road signs, computer networks, power supply, or recharging of consumer electronics. Another way is to use solar energy for domestic water heating. Many houses are equipped with solar panels that can substitute a part of heating energy produced by traditional heating systems on sunny days.

7.1   Description of Solar Energy Sources

The Sun, a source of radiant energy, emits electromagnetic radiation whose irradiance decreases as the square of the distance from the Sun center. At the mean distance of the Earth from the Sun, the solar irradiance is about 1.37 kW m^{-2}. This solar irradiance varies; because the Earth is sphere, the Sun heats equatorial regions more than polar regions. The Earth system including land surfaces, oceans, and atmosphere works to even out solar heating imbalances through evaporation of surface water, convection, rainfalls, winds, and ocean circulation. This circulation is

known as Earth's heat engine. Over the course of a year, the Earth system absorbs an average of approximately 240 W, which drives the biosphere. In addition to redistribution of solar heat from the equator toward the poles, the heated surface and lower atmosphere simultaneously radiate heat back to space, because, otherwise, the Earth would endlessly heat up. This energy net flow represents the basic Earth's energy budget. When the flow of incoming solar energy is balanced by an equal flow of heat to space, Earth is in radiative equilibrium, and global temperature is relatively stable. Anything that increases or decreases the amount of incoming or outgoing energy can disturb Earth's radiative equilibrium.

The solar irradiance is the maximum possible power that the Sun can deliver to a planet at Earth's average distance from the Sun, but just a part reaches the Earth's surface. Complex interaction with the Earth's atmosphere, surface, and other objects has to be taken into account by monitoring and modeling. A part of solar radiation that is neither reflected nor scattered, and which directly reaches the surface, is the direct radiation. A part that is scattered by the atmosphere, and which reaches the ground, is the diffuse radiation. A little radiation reflected by the surface and reaching an inclined plane is the reflected radiation. The described radiations together create global radiation. Solar energy mapping and analysis are mostly dealing with the direct normal irradiation (DNI), the global horizontal irradiation (GHI), and the global tiled irradiation (GTI). The preliminary assessment of solar resources in the world can be provided with the maps for DNI or GHI. As an example, the world irradiation map developed by Solargis for DNI and GHI is illustrated in Figs. 7.1 and 7.2, respectively. The maps present the long-term average of solar energy dealing with an annual sum and a daily sum in kWh m^{-2}.
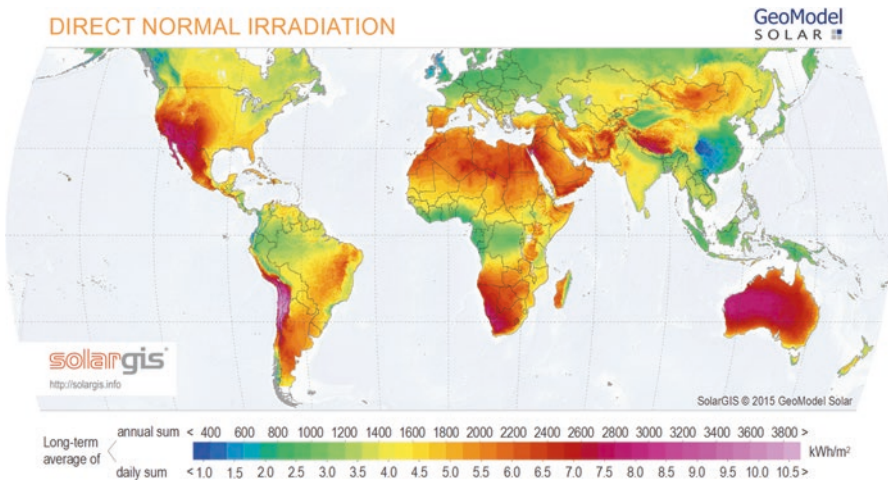

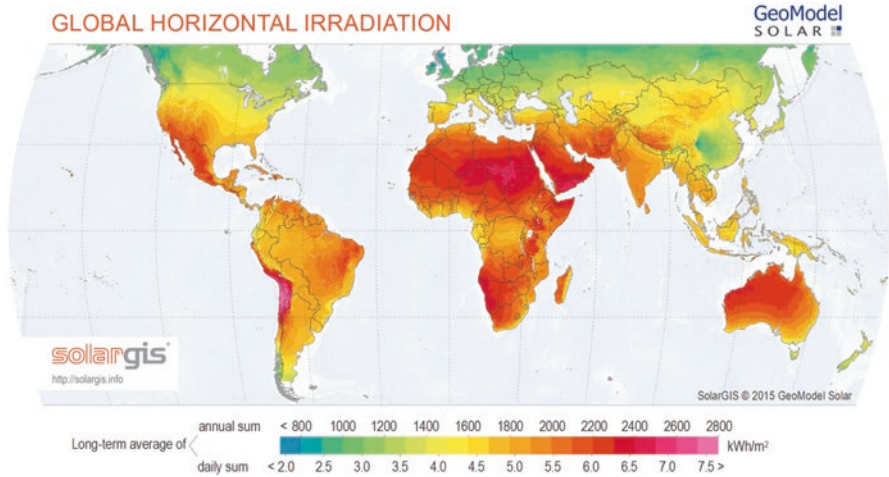**Fig. 7.1** A world solar resource map of DNI (the long-term average of an annual sum and a daily sum in kWh m^{-2}). Source: Solargis, 2016, http://solargis.com/products/maps-and-gis-data/free/download/world

Fig. 7.2 A world solar resource map of GHI (the long-term average of an annual sum and a daily sum in kWh m^{-2}). Source: Solargis, 2016, http://solargis.com/products/maps-and-gis-data/free/download/world

The DNI is involved in thermal and photovoltaic concentration technology. It is an amount of solar radiation received per unit area by a surface that is always held normal to the rays that come in a straight line from the direction of the Sun at its current position in the sky. Typically, solar power systems can maximize the amount of irradiance annually received by a surface with keeping it normal to incoming radiation.

The GHI is the total amount of shortwave radiation received from above by a horizontal surface. This value is of particular interest to photovoltaic installations and includes both DNI and DIF (diffuse horizontal irradiance) that does not arrive on a direct path from the Sun, but has been scattered by molecules and particles in the atmosphere and comes equally from all directions.

The GTI or total radiation received on a surface with defined tilt and azimuth is the sum of the scattered radiation, direct, and reflected. It is used to be a reference for photovoltaic (PV) applications and can be occasionally affected by shadow.

Modeling of irradiation is based on long-term data from ground sensors and satellite systems. Some satellite-based irradiance models are able to estimate the solar radiation without the need of installing ground sensors at all sites of interest. Most of the irradiance models range from physical-based models, which explore observed Earth's radiance by solving radiative-transfer equations, to empirical models, which use statistical approach to provide prediction in accordance with the observed satellite data complemented by data from sensors at the Earth's surface. Data from satellites assist in identification of cloud properties and help to explore the physical processes of atmospheric attenuation of solar radiation. Satellite data can be also used for improvement of the accuracy of the forecast based on numerical weather models in the post-processing phase. An example focused on basic steps in
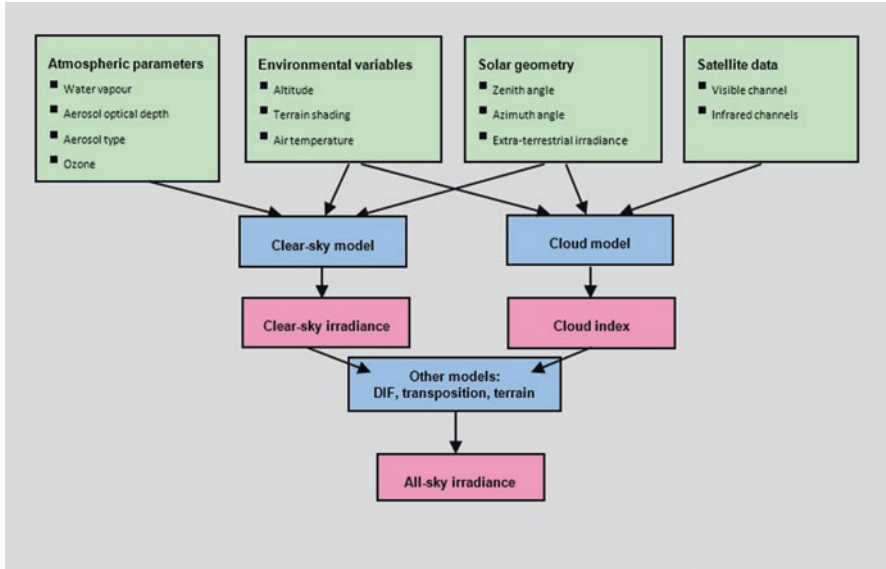
Fig. 7.3 The basic steps in the satellite-based irradiance models dealing with Solargis algorithms. Source: Solargis, 2016, http://solargis.com/support/knowledge-base/methodology/solar-radiation-modeling/

the satellite-based irradiance models dealing with Solargis algorithms is illustrated with a flow diagram in Fig. 7.3.

Modeling of solar irradiance can be split into three steps. After calculation of the clear-sky irradiance, the satellite data including information from several geostationary satellites are used to quantify the attenuation effect of clouds by means of cloud index calculation in order to couple the clear-sky irradiance with cloud index to retrieve all-sky irradiance. The output of this procedure is direct normal and global horizontal irradiance. Finally, direct normal and global horizontal irradiance are used for computing diffuse and global tilted irradiance (irradiance in plane of array, on tilted, or tracking surfaces) and/or irradiance corrected for shading effects from surrounding terrain or objects.

The initial time step of solar resource parameters is 15 min for MSG satellite area, 30-min for MFG and MTSAT satellite area, and up to 3 h for GOES satellite area. The atmospheric parameters such as aerosols and water vapor are represented by daily data. Spatial resolution of Meteosat, GOES, and MTSAT data involved in the calculation scheme is approximately 3 km. Model outputs are resampled to 2 arc minutes regular grid in WGS84 geographical coordinate system (approximately 4 × 4 km). The spatial resolution of outputs is enhanced up to 3 arc seconds (approximately 90 m at the equator, less toward the poles).

The MSG (Meteosat Second Generation) satellites operated by EUMETSAT (European Organization for the Exploitation of Meteorological Satellites) under the Meteosat Transition Programme (MTP) and the Meteosat Second Generation
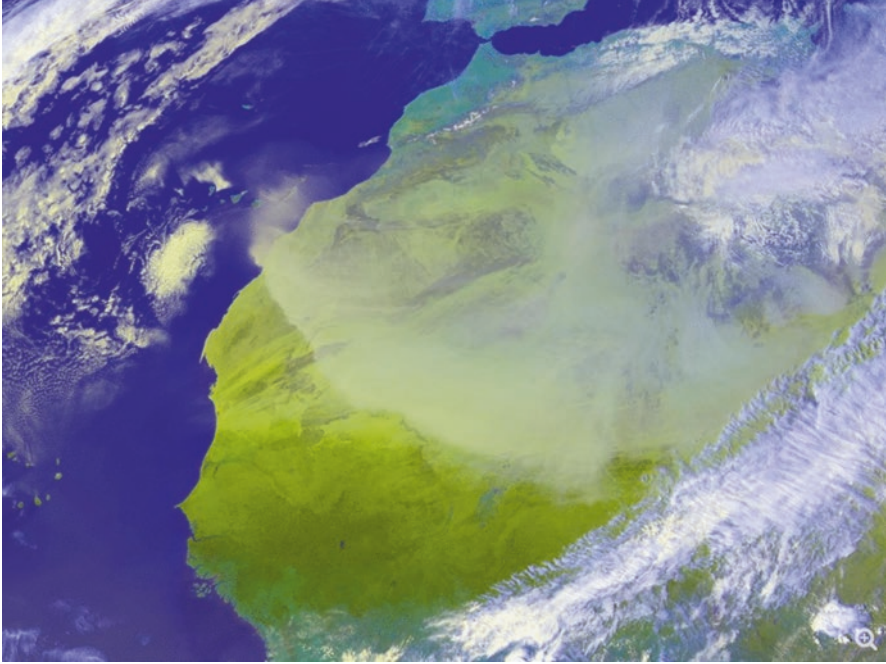
Fig. 7.4 The satellite image of a dust storm and clouds captured by MSG-1. Source: ESA, 2016, http://m. esa.int/Our_Activities/Observing_the_Earth/Meteosat_Second_Generation/MSG_overview2

(MSG) programme are used mainly by meteorologists. The satellites continually return the detailed imagery of Europe, Africa, and parts of the Atlantic and Indian Ocean every 15 min. The first MSG-1 satellite became operational on 29 January 2004, when it was redesignated Meteosat-8. Other satellites were lunched consecutively. Currently the service is provided by Meteosat-10 and the aging Meteosat-9. In addition, Meteosat-8 provides the backup, including taking over rapid-scanning during planned outages of Meteosat-9. The satellite image of a dust storm and clouds captured by MSG-1 is illustrated in Fig. 7.4.

The MTSAT (Multifunctional Transport Satellites) are a series of weather and aviation control satellites, which are geostationary and operated by the Japanese Ministry of Land, Infrastructure, Transport and Tourism and the Japan Meteorological Agency (JMA). The satellites provide coverages that include Japan and Australia.

The GOES (Geostationary Operational Environmental Satellite system), operated by the US NESDIS (National Environmental Satellite, Data, and Information Service), supports weather forecasting and meteorology research. Spacecraft and ground-based elements of the system work together to provide a continuous stream of environmental data. Many images are available through the NOAA geostationary satellite server web page: http://www.goes.noaa.gov/index.html.

The total solar irradiance is the maximum possible solar energy that the Sun can deliver to a planet at Earth's average distance from the Sun, but basic geometry
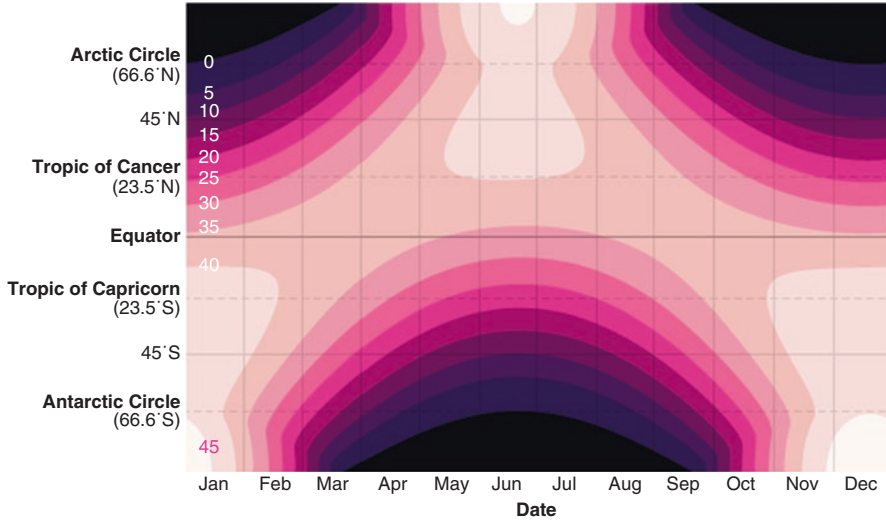
Fig. 7.5 Variations of the solar radiation received at Earth's surface by time and latitude. Source: NASA, 2016, http://earthobservatory.nasa.gov/Features/EnergyBalance/page3.php

limits the actual solar energy intercepted by the Earth, because only half the Earth is ever lit by the Sun at one time, which halves the total solar irradiance. Only the point directly under the Sun receives full-intensity solar radiation. From the equator to the poles, the irradiance meets the Earth at smaller angles, and the light gets spread over larger surface areas. Thus, the solar radiation received at Earth's surface varies by time and latitude (Fig. 7.5). Higher daily amounts of incoming solar energy are at high latitudes in summer, rather than at the equator. In winter, some polar latitudes receive no light at all. The southern hemisphere receives more energy during December than the northern hemisphere does in June because the Earth is slightly closer to the Sun during that part of its orbit.

A seasonal variability in solar radiation can be illustrated with image maps that provide a monthly average of solar resource information on grid cells. As an example, the image mapping national solar photovoltaics (PV) resource potential for the United States is in Fig. 7.6. The map images providing monthly average and annual average daily total solar resource, averaged over surface cells of 0.1° in both latitude and longitude (approximately 10 km in size), are illustrated in Figs. 7.7 and 7.8 for June and December, respectively. The map images are based on the satellite radiation model, which was developed for the US Department of Energy by the National Renewable Energy Laboratory of the State University of New York/Albany in cooperation with other universities. The model uses hourly radiance images from geostationary weather satellites, daily snow cover data, and monthly averages of atmospheric water vapor, trace gases, and the amount of aerosols in the atmosphere to calculate the hourly total Sun and sky insolation falling on a horizontal surface. Information about atmospheric water vapor, trace gases, and aerosols is derived
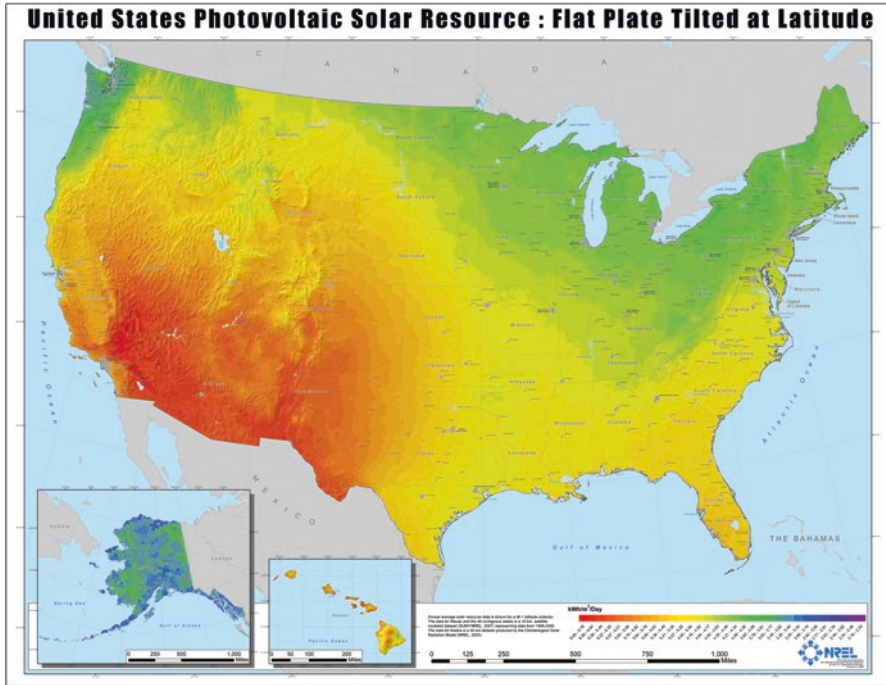
Fig. 7.6 The map illustrating annual mapping of national solar photovoltaics (PV) resource potential for the United States, averaged over surface cells of 0.1° in both latitude and longitude (approximately 10 km in size) from 1998 to 2005 data. The daily values are in kWh m^{-2}. Source: NREL, 2016, http://www.nrel.gov/gis/solar.html

from other sources. Existing ground measurement stations are used for validation of the model. As a result, the model predictions are estimated to be accurate to approximately 10% of a true measured value within the grid cell. But the local cloud cover can vary significantly even within a single grid cell due to terrain effects and other microclimate influences. The model results assist in estimates of the insolation values, which represent the resource available to a flat plate collector, such as a photovoltaic panel, oriented due south at an angle from horizontal to equal to the latitude of the collector location. The typical applications are solar photovoltaics (PV) system installations. Information about projects dealing with mapping and GIS for solar applications are available through the web page: http://www.nrel.gov. Solar datasets focused on an area of the United States are also available through the online map-search GIS application. Other GIS tools can directly estimate the energy production and cost of energy of grid-connected photovoltaic (PV) energy systems. These tools allow users such as homeowners, installers, and manufacturers to easily develop estimates of the performance of their potential PV installations.

More detailed information about solar radiation and photovoltaic electricity potential for Europe and Africa is provided by PVGIS (Photovoltaic Geographical
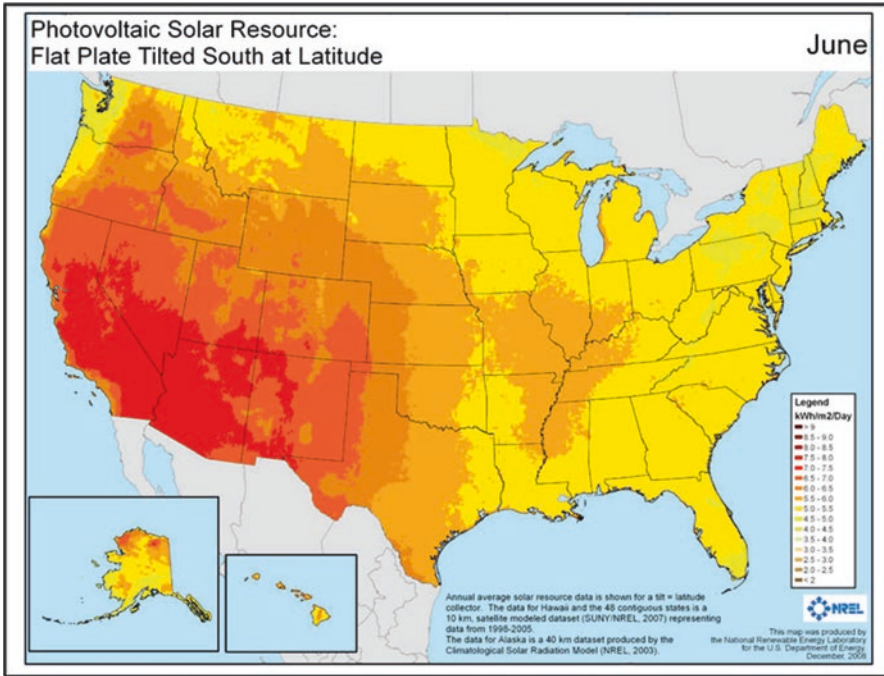
Fig. 7.7 The map illustrating average and annual average daily total solar resource in June, averaged over surface cells of 0.1° in both latitude and longitude (approximately 10 km in size) from 1998 to 2005 data. The daily values are in kWh m⁻². Source: NREL, 2016, http://www.nrel.gov/gis/solar.html

Information System), which provides a map-based inventory of solar energy resource. The regional and country maps can be used for assessment of the electricity generation from photovoltaic systems in Europe, Africa, and Southwest Asia. Datasets, interactive map application, and animations are available through the web page http://re.jrc.ec.europa.eu/pvgis/about_pvgis/about_pvgis.htm. The offered maps represent yearly sum of global irradiation on horizontal and optimally inclined surface and many other options. The datasets represent the average of the period 1998–2011 (north of 58° N, the data represent the 10-year average of the period 1981–1990).

7.2   Potential Sources of Solar Energy

Solar energy can be utilized by a wide range of solar technologies dealing directly with water and space heating and other processes of heat generation in industry, commerce, and transport. Separated technology represents electricity production, which provides conversion of sunlight into electricity, either directly using photovoltaics or indirectly using concentrated solar power.
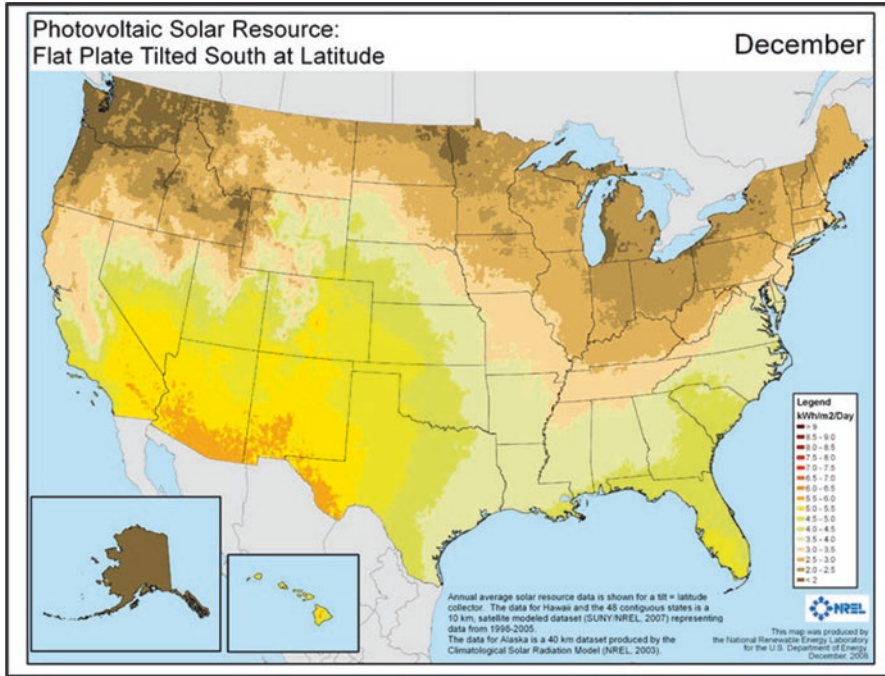
Fig. 7.8 The map illustrating average and annual average daily total solar resource in December, averaged over surface cells of 0.1° in both latitude and longitude (approximately 10 km in size) from 1998 to 2005 data. The daily values are in kWh m^{-2}. Source: NREL, 2016, http://www.nrel.gov/gis/solar.html

The incident power P (W) of the direct sunlight with an average intensity I (W m^{-2}), which incidents normally on an area A (m^2), is

$$P = I \cdot A, \tag{7.1}$$

and the incident energy E (J) is the power multiplied by time t (s):

$$E = P \cdot t. \tag{7.2}$$

For example, the incident power of the direct sunlight of the average intensity 300 W m^{-2}, which incidents on a solar thermal collector or photovoltaic cell of the area 0.1 m^2, is

$$P = I \cdot A = 300 \cdot 0.1 = 30\,\text{W} = 0.03\,kW,$$

and the incident energy in 1 day (24 h or 24 × 60 × 60 s) is

$$E = \text{P} \cdot t = 30 \cdot 24 = 30\,\text{W} = 720\,Wh = 0.72\,kWh$$
$$\text{or } E = P \cdot t = 30 \cdot 24 \cdot 60 \cdot 60 = 2,592,000\,Ws = 2.592\,MJ.$$

The next part is dedicated to production of electricity by photovoltaics in the framework of the electricity mix. Besides aerospace research, the utilization of solar

energy by photovoltaics in remote areas represents an irreplaceable source of electrical energy for the local energy consumption such as electronic devices, smaller industrial installations, and residential consumption. Due to variability in production of electricity, these energy systems are used to be complemented by energy storage tools mostly based on accumulators and batteries. Generally, solar energy sources based on photovoltaics technology can also complement main electricity sources in the local and global scale, but other equipment is needed to transfer the direct current to the alternating current and voltage demand.

The energy of a photon is:

$$E_\gamma = h \cdot \upsilon = h \frac{c}{\lambda}, \tag{7.3}$$

where h is the Planck constant, c speed of light, and λ wavelength ($h \cong 4.136 \cdot 10^{-15}$ eV s; $c \cong 2.998 \cdot 10^8$ m s^{-1}; $h \cdot c \cong 1240$ eV nm). The photon flux F is the number of photons per square meter per second, which can be expressed as:

$$F = \frac{I}{E_\gamma} \tag{7.4}$$

where I is the light intensity.

For example, the energy of a photon of the green light ($\lambda = 510$ nm) is:

$$E_\gamma = h \cdot \upsilon = h \frac{c}{\lambda} = \frac{hc}{\lambda} = \frac{1240}{510} = 2.43\,eV = 2.43 \cdot 1.6 \cdot 10^{-19} = 3.89 \cdot 10^{-19}\,\text{J},$$

and the flux F for a source of the green light of intensity 300 W m^{-2} is:

$$F = \frac{I}{E_\gamma} = \frac{300}{3.89 \cdot 10^{-19}} = 7.74 \cdot 10^{20} \text{ photons m}^{-2}\,\text{s}^{-1}.$$

Solar energy passing through the atmosphere to the Earth's surface is reduced by absorption. The effect of absorption by water vapor, carbon dioxide, and methane is high in the infrared region, corresponding to photon energies below 1.7 eV (wavelengths up 0.7 μm). The energy of the photons in a visible part of the solar spectrum ranges from 1.7 eV (0.7 μm) to 3 eV (0.4 μm). In case of photovoltaics, the cells are made from semiconductor materials. When light falls on a silicon p-n junction, some of the photons can create the electron-hole pairs through the photoelectric effect, in which a photon is absorbed by an electron, promoting it from the valence to the conduction band. The minimum energy that the photon must have equals the band gap, which is 1.1 eV for silicon-based semiconductor materials, and corresponds to a wavelength of approximately 1100 nm ($E\gamma = hc/\lambda = 1240/1100$ eV). It determines an efficiency of the electricity production, which is afterward decreased by other losses. An actual overview of the best research-cell efficiencies is in Fig. 7.9.

An installation of photovoltaics for an energy supply of the electrical system of the International Space Station (ISS) is illustrated in Fig. 7.10. It allows to safely
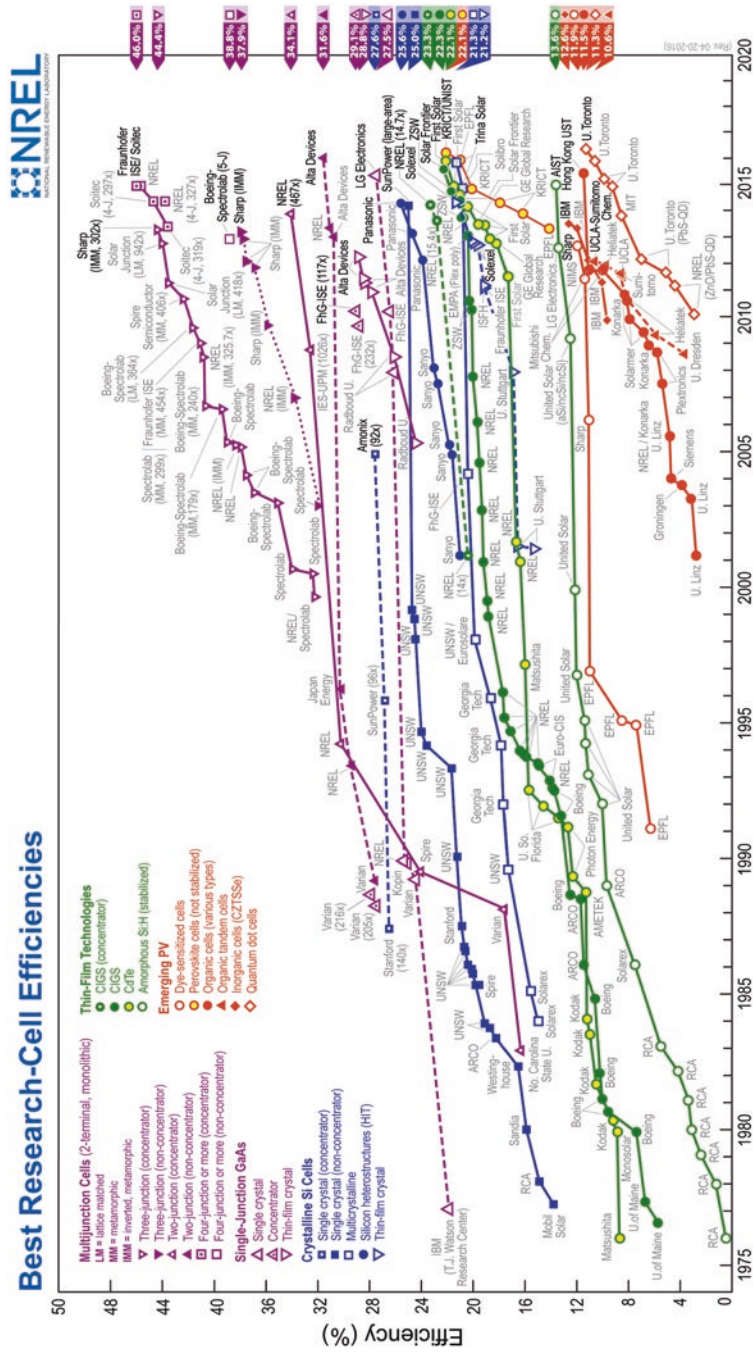
Fig. 7.9 The actual chart of the best research-cell efficiencies. Source: NREL, 2016, regularly updated on the web page http://www.nrel.gov/ncpv/images/efficiency_chart.jpg
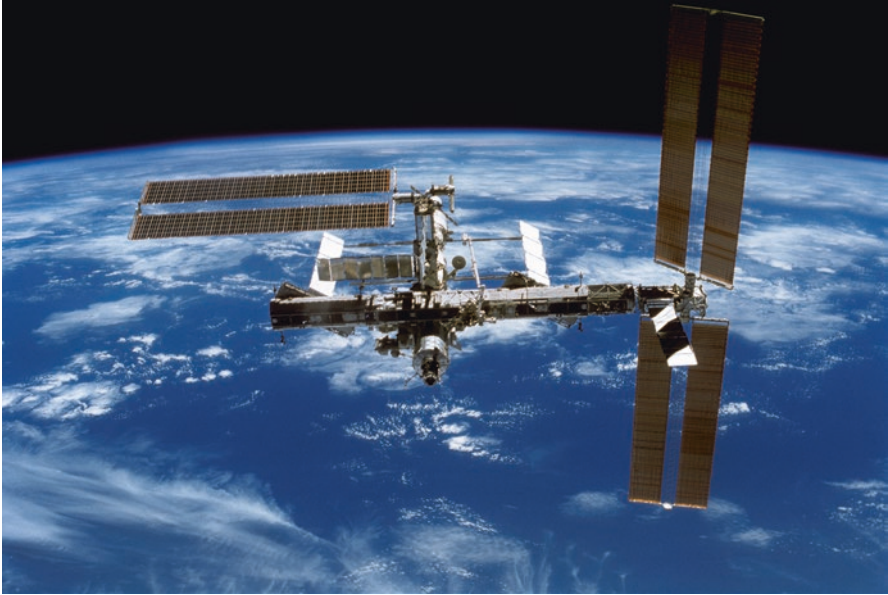
Fig. 7.10 Photovoltaics for energy supply of the International Space Station (ISS). Source: www.pixabay.com, 2016
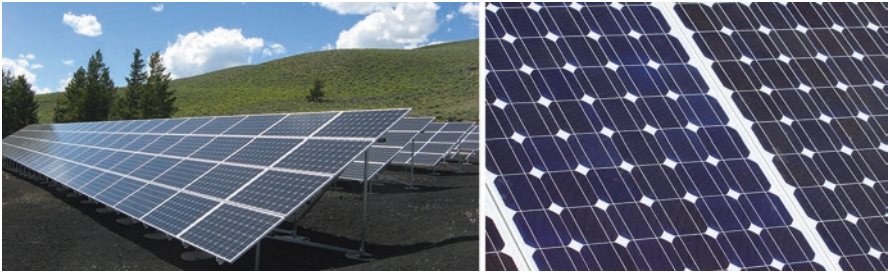

Fig. 7.11 A solar photovoltaic arrays and panels (on the *right side*). Source: www.pixabay.com, 2016

operate the station and to perform scientific experiments. The cells are assembled in large arrays to produce high power levels. An installation of photovoltaics on the Earth's surface, which represents quite often configuration of the solar power plants, is illustrated in Fig. 7.11. Samples focused on conversion of solar energy to thermal energy to generate high temperatures for industry or power generation and to heat water for use in buildings or swimming pools are in Fig. 7.12.

The installed capacity in terms of photovoltaics is the maximum output of the solar panels in the direct current, which can vary substantially from the maximum output from the inverter in alternating current that is available for final consumption in the energy mix. Despite this fact, photovoltaics increased from less than 1 GW of installed capacity in 2000 to 39 GW in 2010 and 176 GW in 2014. The EU accounted more than three quarters of the photovoltaic capacity in 2010. A further 57 GW has

Fig. 7.12 A solar tower for high temperatures and heating of water (on the *right side*). Source: www.pixabay.com, 2016
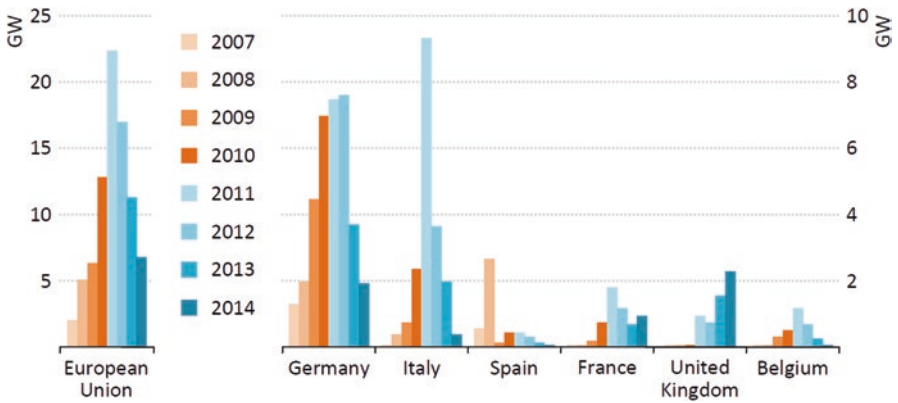

Fig. 7.13 Photovoltaics capacity additions in the EU and selected countries in 2007–2014. Source: IEA World Energy Outlook 2015

been added for the next period mostly by strong deployment in Germany. The EU also established a market for solar PV, which helped to drive down capital costs over the past decade and prompted many claims that solar PV is now nearly competitive with other forms of electricity generation. In Asia, China and Japan have made a strong entrance in the global solar market for the last decade. Particularly, Japan has scaled-up its deployment of photovoltaics since the accident at Fukushima I, adding 7 GW in 2013, which doubled the installed photovoltaic capacity, and afterward other 9.7 GW in 2014. Deployment of solar devices in the United States has been concentrated in California, which has more than nine times the installed photovoltaic capacity in any other state. It is expected that the EU and the United States have already reached a peak in annual capacity additions (Fig. 7.13). Japan will set to peak in the near future. Demand for photovoltaics is also expected to grow rapidly in India and in Southeast Asian countries. The New Policies Scenario estimates that Solar Systems based mainly on photovoltaics establish themselves as a key low-carbon technology in many regions, exceeding 1000 GW of installed capacity globally by 2040 (Fig. 7.14). Photovoltaics in buildings have been dominated to
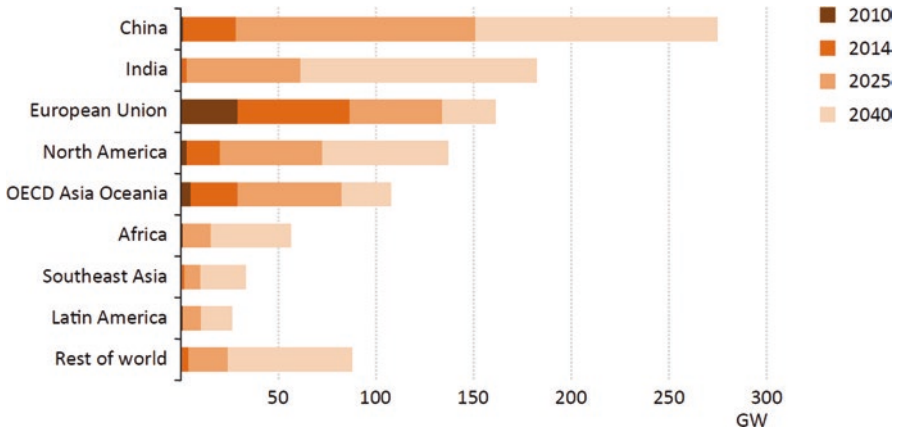
Fig. 7.14 Photovoltaics installed capacity by region and forecasts by the New Policies Scenario. Source: IEA World Energy Outlook 2015

Table 7.1 Top 15 selected largest operational photovoltaic power stations (>200 MW)

Name	Country	Capacity MW$_p$	Generation GWh	Year
Longyangxia Dam Solar Park	China	850	824	2013, 2015
Solar Star (I and II)	United States	579		2015
Topaz Solar Farm	United States	550	1301	2014
Desert Sunlight Solar Farm	United States	550	1287	2015
Huanghe Hydropower Golmud Solar Park	China	500		2014
Copper Mountain Solar Facility	United States	458	1087	2015
Kamuthi Solar Power Project	India	360		2016
Charanka Solar Park	India	345		2012
Cestas Solar Farm	France	300	380	2015
Agua Caliente Solar Project	United States	290	626	2014
Antelope Valley Solar Ranch	United States	266	525	2015
Mount Signal Solar	United States	265.7		2014
California Valley Solar Ranch	United States	250	399	2013
Mesquite Solar project	United States	207	413	2013
Gonghe Industrial Park Phase I	China	200		2013

Source: Wikipedia, 2016

date, accounting for over 60% of the global capacity. This trend looks to continue through to 2040.

Once the cost of solar electricity has fallen, the number of grid-connected solar installations has grown and larger solar power stations with hundreds of megawatts are being built. A number of solar thermal power stations were first developed in the 1980s. A list of selected largest operational photovoltaic and thermal power stations with installed capacity of more than 200 MW is in Tables 7.1 and 7.2, respectively. An example of a large operational photovoltaic power station is Topaz Solar Farm in San Luis Obispo County in California. The power station became operational in

Table 7.2 Top six selected largest operational solar thermal power stations (>200 MW)

| Name	Country	Location	Capacity	Type	Year
Ivanpah Solar Power Facility	United Sates	San Bernardino County, California	392	Power tower	2014
Solar Energy Generating Systems	United Sates	Mojave Desert, California	359	Parabolic trough	
Mojave Solar Project	United Sates	Barstow, California	280	Parabolic trough	2014
Solana Generating Station	United Sates	Gila Bend, Arizona	280	Parabolic trough	2013
Genesis Solar Energy Project	United Sates	Blythe, California	250	Parabolic trough	2014
Solaben Solar Power Station	Spain	Logrosán	200	Parabolic trough	2012

Source: Wikipedia, 2016
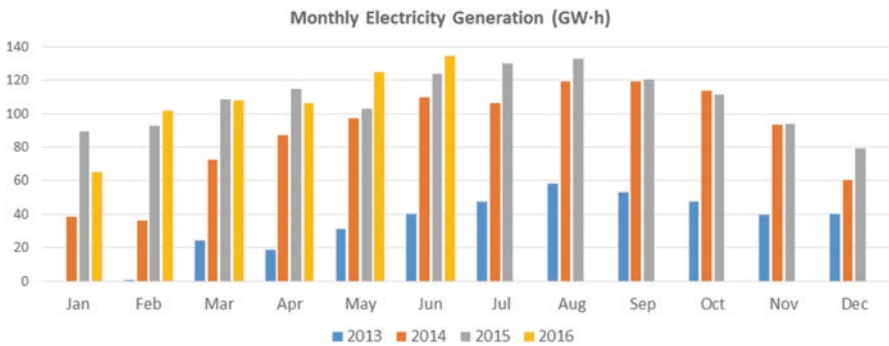
Fig. 7.15 Topaz Solar Farm in San Luis Obispo County in California: monthly electricity generation in GWh. Source: EIA Electricity Data Browser, 2016, http://www.eia.gov/electricity/data/browser/#/plant/57695

November 2014. The installation includes nine million CdTe photovoltaic modules based on thin-film technology. An annual generation is expected to be 1100 GWh, and the capacity factor (the ratio of its actual output over a period of time, to its potential output if it were possible for it to operate at full nameplate capacity continuously over the same period of time) is 23%. Its monthly electricity generation in GWh is in Fig. 7.15. The site of the power station illustrates Fig. 7.16. Examples of solar thermal power stations are in Figs. 7.17 and 7.18.

7.3 Environmental Effects of Photovoltaic Power Plants

Solar installations have a number of attributes that allow their advantageous integration into an energy mix. For applications with low power consumption, such as lighting or solar-derived hot water, solar technologies have a comparative advantage in comparison

Fig. 7.16 Topaz Solar Photovoltaic Farm in San Luis Obispo County in California. Source: Google Earth, 2016

Fig. 7.17 Ivanpah Solar Electric Generating System in the California Mojave Desert. Source: Google Earth, 2016

to nonrenewable fuel technologies. They also allow small decentralized applications as well as larger centralized ones. By combining with other renewables such as biomass or wind power, the system capacity factor and emissions profiles can be improved.

Photovoltaic power generation varies systematically during a day and a year and randomly according to weather conditions at a specific location. These variations have
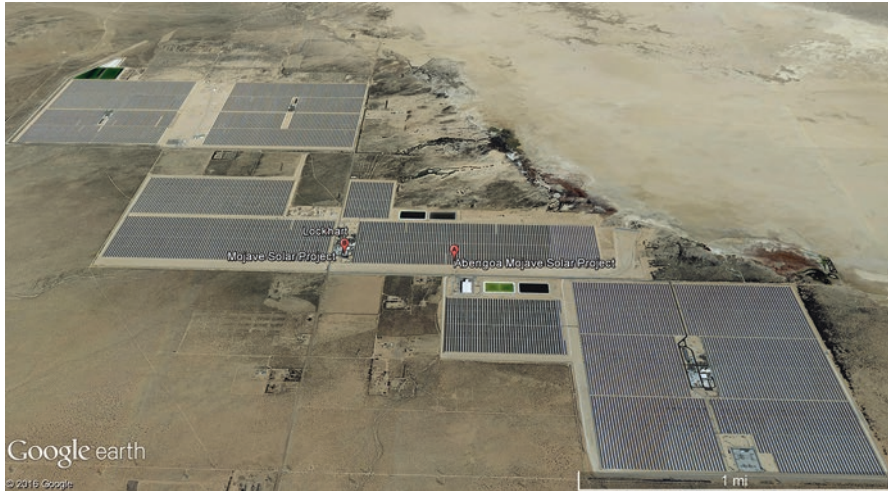
Fig. 7.18   Mojave Solar Project in the California Mojave Desert. Source: Google Earth, 2016

long-term and short-term impacts on voltage and power flow in the local transmission and distribution system, which can potentially constrain integration of photovoltaics into electrical grid. The solar thermal power station, even without storage, the inherent thermal mass in the collector system, and spinning mass in the turbine tend to significantly reduce the impact of rapid solar transients on electrical output, which leads to a reduction of short-term impacts on the electrical grid. Thus, integration of photovoltaics with solar thermal-based systems can reduce the impact of rapid solar transients on the electrical output, as well as improve the capacity factor. Long-term variability can be reduced by integrating Solar Systems with fossil fuel generators, especially with gas-fired integrated solar combined-cycle systems, which offer better fuel efficiency and extended operating hours.

Environmental impacts of Solar Systems are often viewed as greenhouse gas reduction when producing electricity. The use of solar energy systems also reduces the release of pollutants, such as particulates, sulfur dioxide, and noxious gases from the older fossil fuel plants that it replaces. But solar energy installations may create other types of air, water, land, and ecosystem impacts, depending on how they are managed. Some amounts of toxic, explosive gases as well as corrosive liquids are used by industry especially in production of photovoltaic panels in dependence on the cell type and the level of advancement of used technology. Furthermore, some solar technologies in certain regions may require water usage for cleaning to maintain performance and overall management of occupied sites. Estimates of greenhouse gas emissions related to various types of photovoltaic modules is in Fig. 7.19.

The majority of greenhouse gas emissions are between 30 and 80 gCO_2eq/kWh. The estimated emission levels are about an order of magnitude lower than those of natural gas-fired power plants.
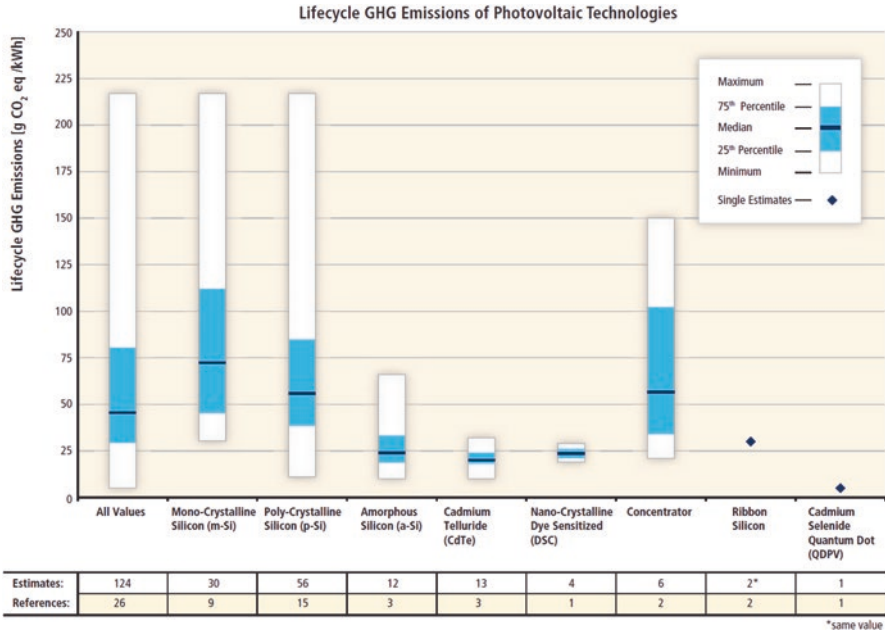
Fig. 7.19 Estimates of greenhouse gas emissions related to various types of photovoltaic modules with a number of references. Source: IPCC (2012) Special Report on Renewable Energy Sources and Climate Change Mitigation

Land use is another form of environmental impact in case of large Solar Systems. Protected areas and environmentally sensitive lands may represent significant barriers for solar installations development. For roof-mounted solar photovoltaic or thermal systems, this is not an issue.

Social impacts and benefits of utilization of solar energy are significant in the developing world, where about 1.4 billion people do not have access to electricity. The local Solar System base and grids can provide electricity to many areas for which connection to a main grid is cost prohibitive. Besides the replacement of indoor-polluting kerosene lamps and inefficient cook stoves, it can provide street lighting for security, improved health by providing refrigeration for food products, and support communications devices. Also, new job creations are not a negligible factor for the local communities, as well as for the large industrial complexes.

7.4   Risk Assessment of Photovoltaic Power Plants with GIS

Like in the assessment of other renewables, GISs can also assist in many steps, which are involved in the decision-making procedures for assessment of solar energy sources. Solar radiation tools implemented in GIS extensions can calculate

the solar energy potential in sites such as building rooftops, as well as in the areas of planned large solar installations. Besides estimating the solar potential, multi-criteria spatial analysis is able to determine the most favorable locations for photo-voltaics power plants or solar thermal power plants based on the cost of transmission, locations of load centers in the electrical grid, and other environmental, economic, and social criteria. Spatial methods also support risk assessment analysis in order to exclude sites such as national parks and wilderness areas. The results include thematic map layers with classes of solar potential, voltage of transmission lines, and, option-ally, forecasts dealing with the expansion of solar devices and their impacts on the environment. These model predictions can be used by government decision-makers or by local authorities to provide optimal installations of Solar Systems. In the United States, NREL (National Renewable Energy Laboratory) provides calculation of solar potential such as solar maps for photovoltaics and concentrating solar power. Many other institutions such as Solargis (http://solargis.com/), PVGIS (http://re.jrc. ec.europa.eu/pvgis/), and GeoSUN Africa (http://geosun.co.za/) are involved in services relating to the assessment of solar energy sources.

ArcGIS Solar Radiation tools support mapping the effects of the Sun over a geo-graphic area for specific time periods. Mapping and analysis for a landscape and specific location are provided by the Area Solar Radiation tool and the Points Solar Radiation tool. These methods are complemented by a number of GIS case-oriented tools that support raster data management, multi-criteria analysis, and display. The general description of methods implemented in Solar Radiation tools is in Table 7.3.

Other GIS advanced methods and functions, which can assist in spatial analysis, can be found in 3D analysis tools, spatial analysis tools, and optionally in network analysis tools. Analysis and spatial modeling for assessment of solar energy sources can benefit from their implementation in the decision-making procedures. The described tools dealing with solar radiation estimates are mostly optional extensions of the existing GIS software packages.

Table 7.3 Methods included in Solar Radiation tools for assessment of solar energy sources in the ArcGIS environment

Solar Radiation tools	Support mapping the effects of the Sun over a geographic area for specific time periods
Area Solar Radiation	– Derives incoming solar radiation from a raster surface
	– The output radiation raster has units of watt hours per square meter (Wh m^{-2}) and the direct duration raster output has units of hours
Points Solar Radiation	– Derives incoming solar radiation for specific locations in a point feature class or location table
	– The output feature class representing the global radiation or amount of incoming solar insolation (direct + diffuse) calculated for each location has units of watt hours per square meter (Wh m^{-2})
Solar Radiation Graphics	– Derives raster representations of a hemispherical viewshed, Sun map, and sky map, which are used in the calculation of direct, diffuse, and global solar radiation

Source: ESRI ArcGIS Resource Center, 2016

7.5   Case-Oriented Studies

Estimation of solar energy potential is based on the GIS methods. Both case studies are focused on the same area of interest, an urban site in Prague (the Czech Republic) situated in a middle part of Europe. Using GIS can give developers information about the solar energy potential in sites such as building rooftops, as well as in smaller unused areas in the urban environment.

7.5.1   Processing of Data About Solar Energy in GIS

A case study is focused on data management of digital surface model (DSM) in Fig. 7.20 and deriving incoming solar radiation in 2014 with the GIS method Area Solar Radiation in Fig. 7.21. The attached point layer shows a location of the reference sensor and of a site for estimates of incoming solar radiation with the GIS method Point Solar Radiation. The seasonal variability of solar radiation is evident for June (Fig. 7.22) and December (Fig. 7.23).

7.5.2   Mapping Potential Sources of Solar Energy in a Local Scale

This case study provides an extension of the previous study. The incoming solar radiation at a site of a reference sensor is estimated with the GIS method Point Solar Radiation and displayed by the column chart in Fig. 7.24. The series of columns
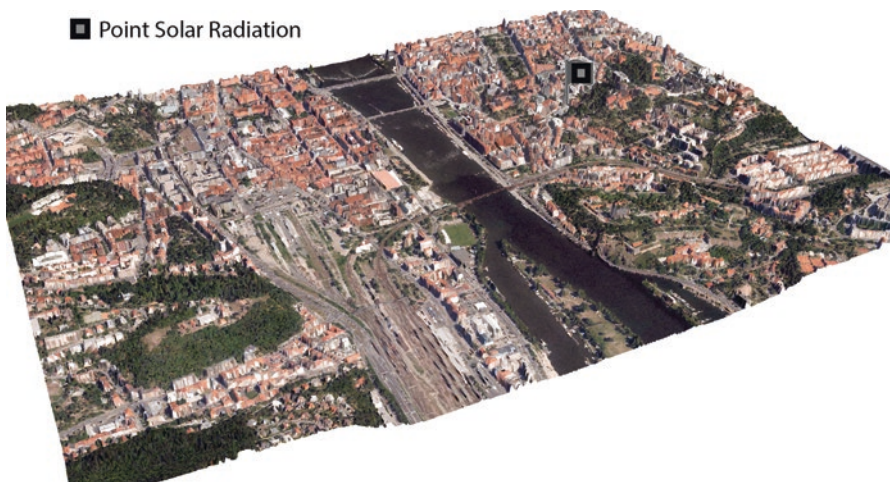

Fig. 7.20 Digital surface model (DSM) complemented by ortofoto and by a reference point (marked by *rectangle*)
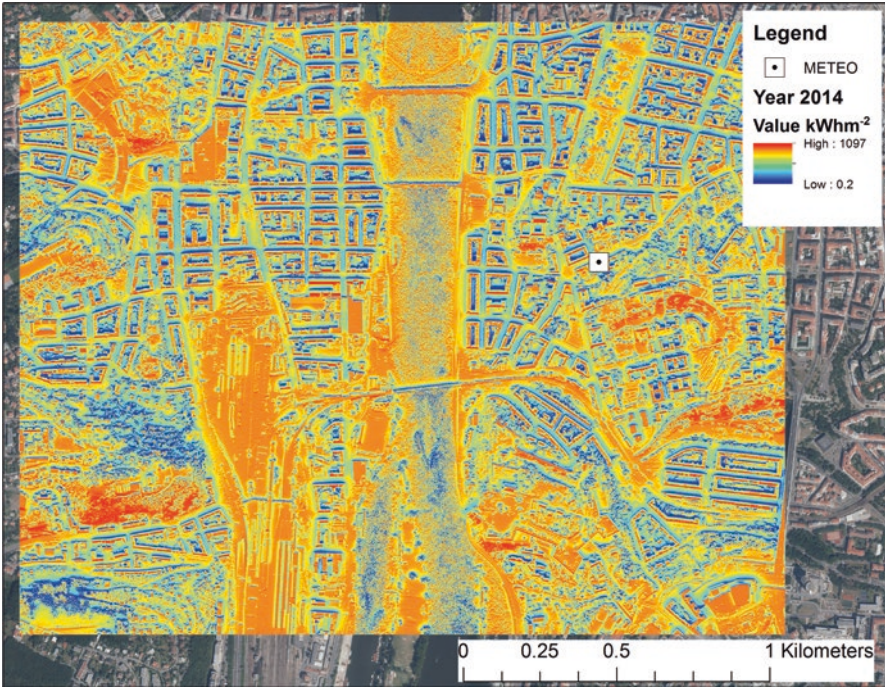
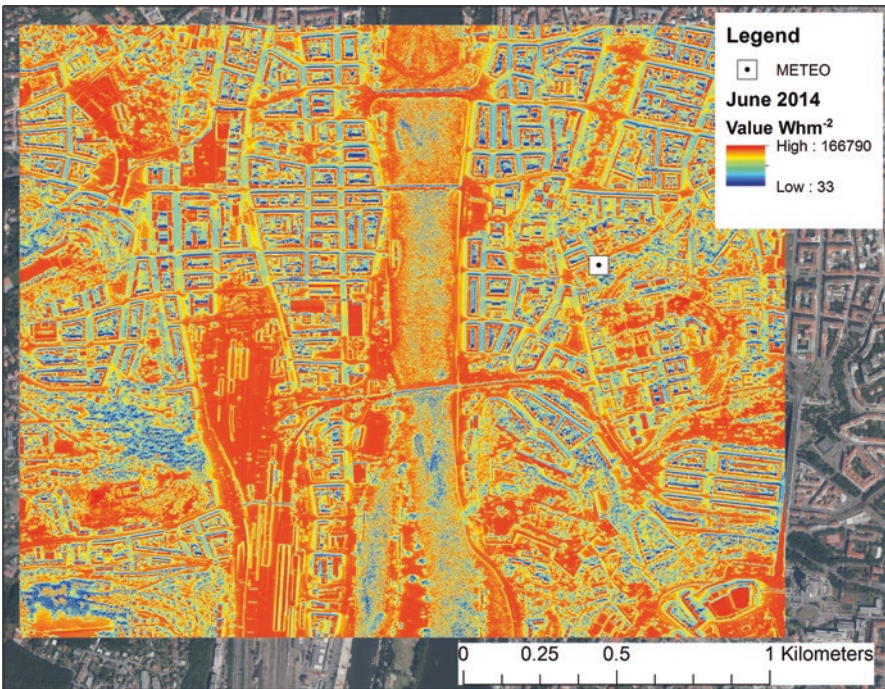**Fig. 7.21** A map illustrating the output radiation raster (Wh m^{-2}) in 2014 (cell size 1 m)

Fig. 7.22 A map illustrating the output radiation raster (Wh m^{-2}) in June, 2014 (cell size 1 m)
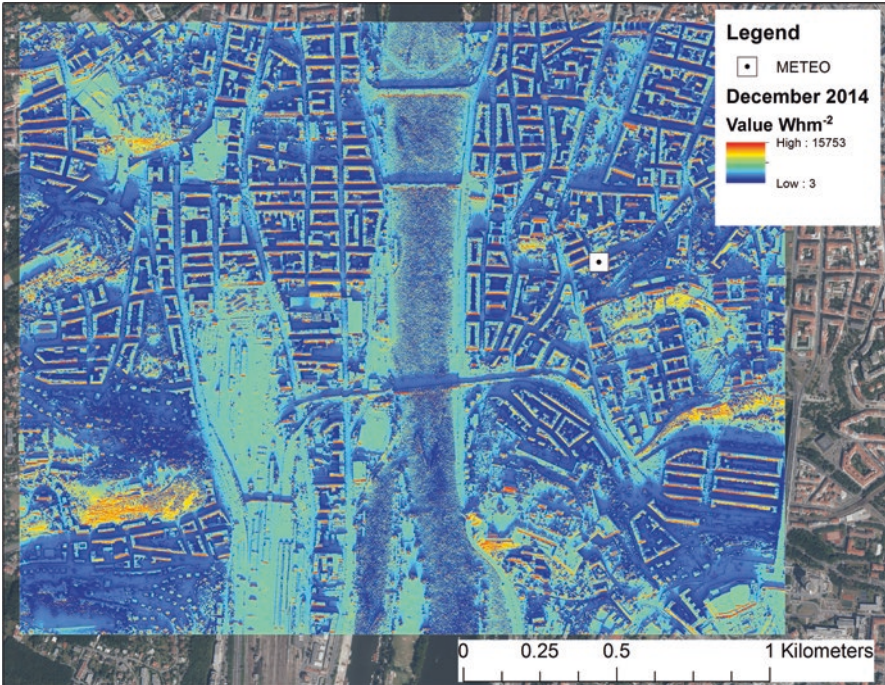
Fig. 7.23 A map illustrating the output radiation raster (Wh m^{-2}) in December, 2014 (cell size 1 m)
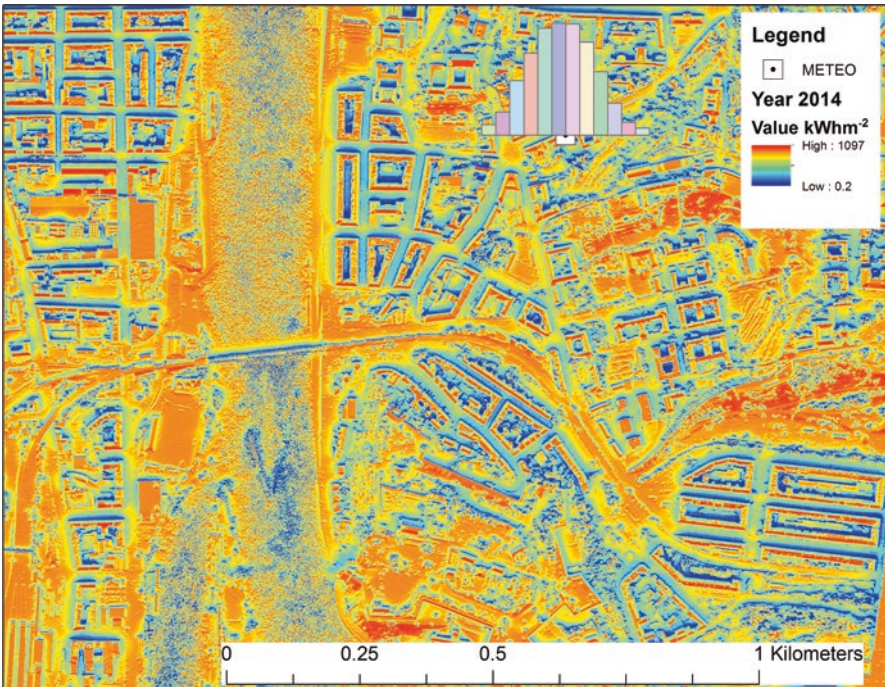

Fig. 7.24 A map illustrating the output radiation raster (Wh m^{-2}) in 2014 (cell size 1 m) and point solar radiation with column diagram at the location marked by a *rectangle*
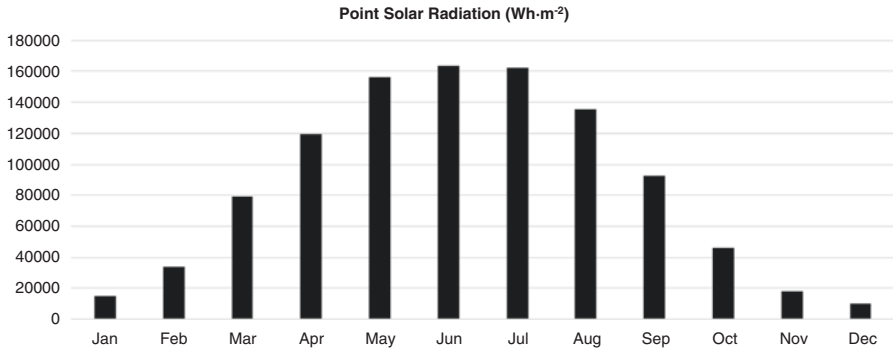
Fig. 7.25 The series of columns indicated incoming solar radiation during individual months (January–December 2014); the values were calculated by the GIS method Point Solar Radiation

represent incoming solar radiation of individual months (January–December, 2014). The mapping is complemented by the raster layer with incoming solar radiation in 2014 from the previous case study in a more detailed scale. The column chart is also presented in Fig. 7.25, in order to provide a more detailed view on the seasonal variability calculated by the GIS method Point Solar Radiation. Finally, the result from spatial modeling compared with regular measurements by solar sensors indicated good coincidence.

Bibliography

EIA. (2015). *International energy outlook 2015*. Retrieved from http://www.eia.gov/forecasts/ieo/pdf/0484(2016).pdf

IEA. (2015). *World energy outlook 2014*. Retrieved from https://www.iea.org/bookshop/477-World_Energy_Outlook_2014

IEA. (2016a). *World energy statistics 2016*. Retrieved from http://www.iea.org/bookshop/723-World_Energy_Statistics_2016

IEA. (2016b). *World energy outlook 2015*. Retrieved from https://www.iea.org/bookshop/700-World_Energy_Outlook_2015

IPCC. (2012). *Special report on renewable energy sources and climate change mitigation*. Retrieved from https://www.ipcc.ch/pdf/special-reports/srren/SRREN_FD_SPM_final.pdf

Perez, R., Ineichen, P., Moore, K., Kmiecikm, M., Chain, C., George, R., et al. (2002). A new operational satellite-to-irradiance model. *Solar Energy, 73*(5), 307–317.

Dictionaries and Encyclopedia

EIA. (2016). *Energy explained: Your guide to understanding energy*. Retrieved from http://www.eia.gov/energyexplained/index.cfm

Data Sources (Revised in August, 2016)

EIA. *Electricity data browser*. Retrieved from http://www.eia.gov/electricity/data/browser/#/plant/57695

EIA. *International energy statistics*. Retrieved from http://www.eia.gov/cfapps/ipdbproject/IEDIndex3.cfm

GeoSUN Africa. Retrieved from http://geosun.co.za/

NREL. *Solar mapping*. Retrieved from http://www.nrel.gov/gis/solar.html

NREL. *The actual chart of the best research-cell efficiencies*. Retrieved from http://www.nrel.gov/ncpv/images/efficiency_chart.jpg

PVGIS. Retrieved from http://re.jrc.ec.europa.eu/pvgis/

Renewable Energy World. Retrieved from http://www.renewableenergyworld.com/solar-energy.html

Solargis. Retrieved from http://solargis.com/

Chapter 8
Biomass: Assessment of Bioenergy Potential Within Existing Energy Systems

Biomass is generally represented by an organic material that can be used to produce heat or allowed to decay and emit natural gas. In the form of wood, this has been done for centuries. It is still widely used as a predominant heating source in poorer countries. The uncontrolled use can lead to desertification. It is an environment-friendly source that does not add to global warming since the carbon dioxide produced when it is burned equals the amount absorbed by the photosynthesis that originally produced it. But carbon savings are decreased by additional services that are necessary for its agricultural production, such as transportation and needed agricultural operations. Unsuitable agricultural practices can rise to erosion. An expansion of biofuel production affects water availability and pesticide use. The growth of industrial crops for biofuels requires large areas of land, which can lead on a large scale of exploitation to disaster. Also the massive switch from food production to growing industrial crops will lead to the growing shortage of food, especially in developing countries.

8.1 Description of Bioenergy Sources

Biomass is used to be described as any organic decomposing matter derived from plants or animals available on a renewable basis. Biomass bioenergy sources include wood and agricultural crops, municipal organic wastes, and animal manure. Recently, these sources are also represented by herbaceous and woody energy crops, which are grown preferentially for this purpose. Biomass-based energy is the oldest source of consumer energy used by mankind. It is still the widely accessible source of renewable energy over the world. It currently accounts about 10% of global primary energy supply, but most of this is traditional use of biomass for heating and cooking, which provides basic energy in many households in developing countries. Probably about 2.6 billion people worldwide rely on the traditional use of biomass as a primary source of energy, but detailed information is not covered by any statistics.
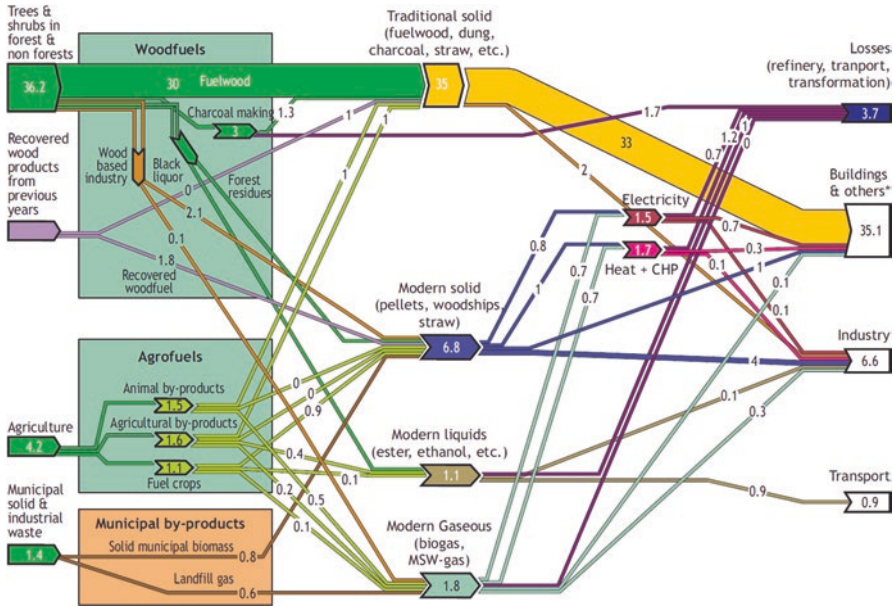
Fig. 8.1 Approximate global bioenergy flows in EJ per year in 2004 and their conversion routes to produce heat, electricity, and biofuels for use by the major sectors. Source: IPCC, 2007

Annual global traditional use of biomass is estimated to be more than 33 EJ per year, which includes both the traditional use and the modern technology. Traditional use of biomass is used to be included in the category: solid biomass. Biomass is an extensively applicable source of energy, because it can be provided as a solid, liquid, or gaseous fuel. It is used for generating electricity and transport fuels, as well as heating in the building sector, in industry, and in transport. Many forms of bioenergy can be stored at times of low demand, which allows to supply variable seasonal demands in generating electricity and transporting services.

Approximate global bioenergy flows and their conversion routes to produce heat, electricity, and biofuels are illustrated in Fig. 8.1. By these estimates, bioenergy sources provide annually about 46 EJ per year of combustible biomass and wastes, liquid biofuels, renewable municipal solid wastes, solid biomass and charcoal, and gaseous fuels. It can be over 10% of global primary energy, but with over two-thirds consumed in developing countries as traditional biomass for household use. Approximately about 8.6 EJ per year of modern biomass is used for heat and power generation. Traditional bioenergy conversions are often based on inefficient combustion combined with higher levels of air pollution and unsustainable use of biomass resources such as native vegetation. Modern technologies include more efficient conversions and effective ways of air pollution control. A number of conversion technologies are under continuous development to produce bioenergy carriers for small utilizations, as well as for large-scale applications. The utilization of many technologies is also dependent on regional climatic conditions and local tradition. Biomass heating is mainly used in countries with a good resource availability and
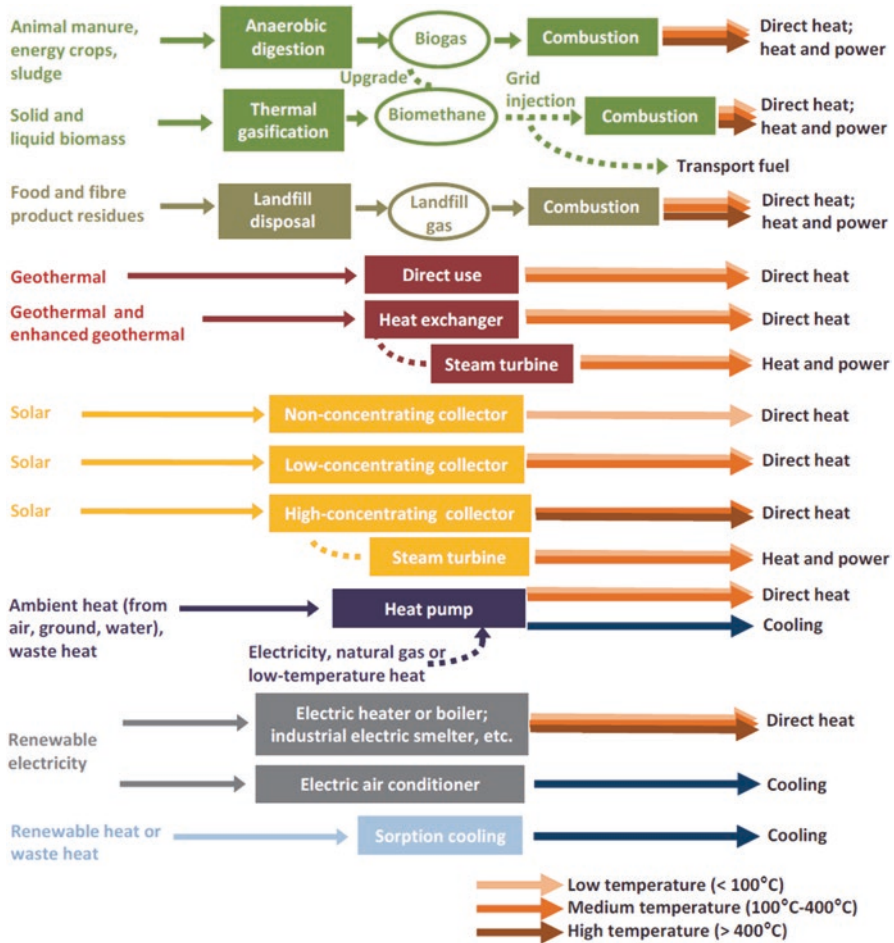
Fig. 8.2 An overview of different renewable energy sources and main technologies to convert them into direct heat, or heat and power. Source: IEA Heating without global warming, 2014

particularly where district heating systems are already in use, mainly in Scandinavian countries, or central European countries, in some regions of the United States and Canada. An overview of the different renewable energy sources and main technologies to convert them into direct heat, or heat, and power is shown in Fig. 8.2.

Biomass utilization for cooking: It has been represented by the use of solid biomass in open fires or simple stoves at very low combustion efficiencies (10–20%) for centuries. In many cases, the combustion of traditional biomass resources causes substantial indoor smoke pollution with severe health impacts. More advanced systems include a chimney for avoiding particle emissions with a higher thermal efficiency (up to 50%). Ethanol or gas cookstoves provide alternatives to traditional biomass stoves with very low emissions and efficiencies up to 70%. However, fuel intake and availability can be an issue, and relatively high fuel costs can occur.

Modern solid biomass heating systems: Solid biomass heating systems range at various scales from small devices, such as boilers (5–100 kW) often running on solid wood logs or wood pellets, to larger-scale applications such as boilers for farms, commercial buildings, or in industry reaching higher capacities (100–500 kW) and running on a variety of feedstocks. They often use grate furnaces for a two-phase combustion consisting of gasification and subsequent burning of the gases with overall thermal efficiencies of up to 90%. Large heating plants for central heating or industrial use have higher capacities (1–50 MW) and are capable of using more diverse biomass types. Larger heating plants are often based on fluidized bed combustion that ensures effective combustion and heat transfer. Despite more expensive technology, the key advantage of fluidized bed boilers is their high feedstock flexibility and high efficiency.

Liquid biofuels: These biofuels are mostly divided into a few generations, but the same fuel might be classified differently depending on applied technology, resources, and greenhouse gas emission balance. Definitions are often based on the maturity of a technology and classification such as conventional and advanced liquid biofuels. Conventional biofuel technologies include proven procedures that are already producing biofuels on a commercial scale. These biofuels, referred to as first-generation biofuels, include sugar- and starch-based ethanol, oil-crop-based biodiesel and straight vegetable oil, as well as biogas derived through anaerobic digestion. Common and typical feedstocks include sugarcane and sugar beet, starch-bearing grains like corn and wheat, oil crops like rape, soybean and oil palm, and, in some cases, animal fats and used cooking oils. Advanced biofuel technologies are conversion technologies, which are still in the research and demonstration phase, commonly referred to as second or third generation. These advanced technologies include hydrotreated vegetable oil based on animal fat and plant oil, as well as biofuels based on lignocellulosic biomass, such as cellulosic ethanol, biomass-to-liquid diesel, and biosynthetic gas. The research of a number of novel technologies, such as algae-based biofuels, and the conversion of sugar into diesel-type biofuels using biological or chemical catalysts have been established in the last years.

Biogas systems: Biogas can be widely used in many applications such as heat and power in buildings and industry, or as fuel in natural gas vehicles. Biogas is produced through anaerobic digestion of feedstocks such as organic waste, animal manure, and sewage sludge, or from dedicated green energy crops such as maize, grass, and crop wheat. Although biogas is used to generate heat and electricity, it can be also upgraded to biomethane and injected into the natural gas grid. Household biogas applications consist of small digester, in which organic household wastes are digested under anaerobic conditions into a biogas that can be temporary stored in rubber balloons and used for household utilizations in cooking and heating. Since the digester in household systems is usually not heated, biogas productivity may decrease with low temperatures in a winter season, because the bacterial activity slows. Larger biogas applications (150 kW–20 MW) are represented by dedicated biogas installations, which derive biogas by digesting sewage sludge, manure, and energy crops. Mixed manure and energy crop systems are often used by farms.

Biogas plants can also convert the biogas on-site into electricity and operate in cogeneration mode with a typical ratio of electricity output to heat of 1:2. In dependence on local costs of natural gas, some applications can upgrade biogas to biomethane by cleaning the gas and increasing the methane content to around 95%. Then the upgraded biomethane can be injected into the natural gas grid and used for power generation, as well as for producing heat in industry and buildings.

The use of biomass in a heating system is illustrated in Fig. 8.3. It uses wood chips and optionally other feedstocks such as agricultural, forest, urban, and industrial residues and wastes, to produce heat in the local scale for the attached residential buildings. The use of biomass limits the long-term effect on the environment, because the carbon in biomass is a part of the natural carbon cycle. A buffer tank provides thermal stores, which are crucial for the efficient operation of all biomass boilers where the system loading fluctuates rapidly, or the volume of water in the complete hydraulic system is relatively small.

Biogas power plant based on anaerobic digestion is illustrated in Fig. 8.4. An anaerobic digestion is a collection of processes by which microorganisms

Fig. 8.3 The use of biomass (wood chips) in a heating systems and a buffer tank for thermal stores (on the *right side*)


Fig. 8.4 Devices of a biogas power plant: the anaerobic digesters and the power generator (on the *right side*)

break down biodegradable material in the absence of oxygen. Feedstocks include biodegradable waste materials, such as agricultural wastes, grass clippings in attached residential sites, leftover food, sewage, and animal waste. The produced biogas is used for power generation and electricity supply of the local population.

8.2   Potential Bioenergy Sources

Total production of the biomass of plants and animals on land is estimated to be about $1.2 \cdot 10^{11}$ t each year and approximately contains around $5 \cdot 10^{10}$ t of carbon. It makes the annual amount of bioenergy production around $2 \cdot 10^{21}$ J (2,000,000,000 TJ). It could represent a continuous thermal power output around 65 TW, which is several times the global power consumption. But, a part of approximately 1.5 TW of thermal power is only used from the total biomass production, which is estimated to be about 10%. The similar amount of bioenergy is produced by the oceans, but none of this can be used as a direct bioenergy source due to its inaccessibility. From this part of bioenergy, only a small amount about 12% of bioenergy ends up as a direct food supply of people including farm animals. The main part of bioenergy is currently used for heating and cooking, mostly by an inefficient way.

An approximate annual estimate of the electric power from a biomass-fired power plant that burns biomass grown over an area is based on an annual efficiency of photosynthesis in real conditions of a crop field. During photosynthesis carbon dioxide and water are converted to oxygen and carbohydrate:

$$CO_2 + H_2O + h\upsilon \rightarrow O_2 + [CH_2O] \tag{8.1}$$
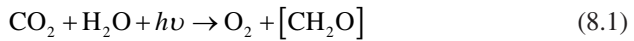
where $h\upsilon$ is light quanta, energy of photons, and $[CH_2O]$ stands for carbohydrate. The obtained energy per kilogram depends on the degree of oxidation of the carbon. The input energy is represented by sunlight, where the photons at the red and blue parts of the visible spectrum are absorbed by the chlorophyll pigments of the plants. It excites electrons to form molecules in a series of complex chemical reactions, the electron transport pathway. The maximum efficiency of this process is around 33%. But it is significantly decreased by the efficiency of the selective absorption of solar photons in the visible spectrum and by reflection and transmission losses of plants. Thus, theoretical efficiency in optimal conditions is estimated about 12%. In real conditions, biomass grown annually in the field can utilize about one-third of the solar radiation during the growing period, but only around one-fifth of the radiation falls on plants in their environment. Some converted energy must be used by respiration, and the remaining around 60% is utilized by biomass growth. The overall annual efficiency of photosynthesis to convert sunlight to biomass is in the field conditions:

$$\begin{aligned}
&(\text{theoretical efficiency}) \times (\text{annual utilization during the growth period}) \\
&\times (\text{real sunlight transition}) \times (\textit{net} \text{ production}) = \text{total efficiency} \\
&= (0.12) \times (0.33) \times (0.2) \times (0.6) \approx 0.5\%
\end{aligned} \tag{8.2}$$

As an example for the average annual amount of solar energy 1000 kWh m^{-2} falling on an area of 1×1 km (1000×1000 m), the average total annual amount of solar energy is

$$E_{km^2 year^{-1}(solar)} = A\, E_{m^2 year^{-1}} = 1000^2\ 1000 = 10^9\, kWh\, km^{-2}$$
$$= 1\, TWh\, km^{-2} = 3600\, TJ\, km^{-2} year^{-1}.$$

and the available average annual biomass production can be estimated according to total photosynthesis efficiency:

$$E_{km^2\ year^{-1}(biomass)} = \left(\text{total efficiency}\right) E_{km^2 year^{-1}(solar)} = 0.005\ 3600 = 18\, TJ\, km^{-2} year^{-1},$$

which is as an average estimate during a year about 0.5–0.6 MW km^{-2}. This energy content is highly dependent on the plants and growing conditions. If it is taken as an approximate estimate for biomass power supply, the biomass utilization could generate about 0.2 MW km^{-2} (2 kW ha^{-1}) of electrical power. The average annual amount of electricity can be about $0.2 \times (24 \times 365)$ MWh km^{-2} = 1752 MW h km$^{-2} \approx 1.75$ GWh km^{-2}.

In comparison with other renewables, bioenergy can be used in all sectors, including transport, where it can directly displace oil-product consumption. Global bioenergy use by sector in 2012 and its comparison to future prediction by the new policy scenarios are illustrated in Fig. 8.5. Traditional use of solid biomass in the building sector, such as using of solid biomass in households, will grow by replacing low-efficiency applications with new installations and extended development of modern bioenergy systems such as wood pellet water heaters or space heaters. The significant increase of bioenergy applications is expected in power generation, because this combustible fuel allows the power output to be controlled more readily in distinction with more variable renewables like wind power and solar power. A continuous growth
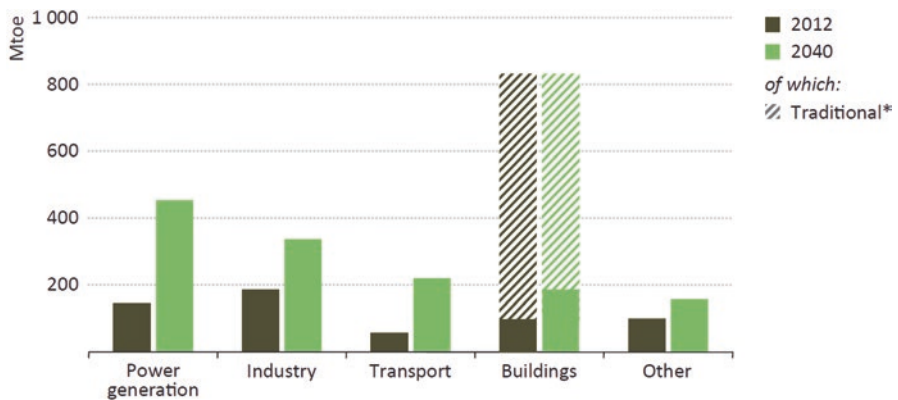
* Refers to traditional use of solid biomass in households.

Fig. 8.5 Global bioenergy use by sector in 2012 and its comparison to future predictions in 2040 based on IEA New Policies Scenario. Sources: IEA Outlook 2014

of bioenergy as a source of process heat and steam is expected in industry. But, a great potential of bioenergy is in a contribution to the energy transformation, including as a source of heat and power in refineries producing liquid biofuels.

Predictions, such as New Policies Scenario by IEA, suppose an increase of global demand for bioenergy to 2000 Mtoe in 2040. The share of modern bioenergy utilizations could rise to over two-thirds, because consumption in power generation and transport more than triple and use in industry increases by 80%. Growth in both OECD and non-OECD countries will also promote improved efficiency of modern bioenergy applications. Thus, the consumption of traditional use of solid biomass by households in non-OECD countries will decline over time due to the entrance of modern bioenergy installations by urbanization and industrialization of underdeveloped areas.

Bioenergy can also gain an advantage over other renewables by utilization of domestic resources that are able to meet the majority of rising demand in many regions and local sites with available biomass resources, which tend to be the least-cost supply option, due to high cost of transporting services. All biomass resources can contribute to the increasing supply, including nonfood crops grown specifically for use in the energy sector, forestry and agricultural residues, forestry products preserving sustainable development, as well as new feedstocks, such as algae. The potential for production of bioenergy is enormous further ahead in comparison with long-term predictions and many new scenarios. Despite relatively high transport cost and the abundance of potential domestic supply, it is expected that net trade in bioenergy in the regional scale will increase by several times for the next decades. Innovative government policies and measures supporting the consumption of biofuels and use of bioenergy to generate power and produce heat will result in better supply of domestic resources. Advanced technologies are going to be utilized in biofuels for transport and in solid biomass for power generation and heat production. For example, biomass feedstocks are processed, dried, and compressed into biomass pellets in order to increase the energy density and uniformity of the product, which can significantly reduce transportation costs and improve the competitiveness in relation to fossil fuels and domestic resources.

In the next decades, the European Union will continue to expand the demand on the international market, as the largest net importer of biofuels, in order to increase the share of renewable energy in its energy mix. Despite strong growth in biofuel production, also the United States will import large amounts of biofuels, especially sugarcane-based ethanol from Brazil, which establishes itself as the main supplier to the world market. Other important players are China, India, and Korea. Bioenergy installed power generation capacity by region and long-term prediction based on IEA New Policies Scenario are displayed in Fig. 8.6.

8.3 Environmental Effects of Using Bioenergy Sources

By the IPCC special report on Renewable Energy Sources and Climate Change Mitigation from 2011, it is estimated that renewables accounted for 12.9% of the 492 EJ of total primary energy supply in 2008, where the largest contributor was
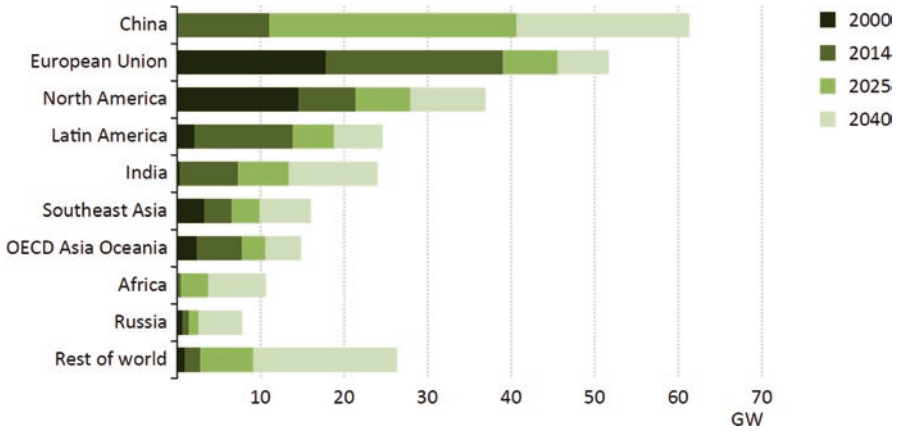
Fig. 8.6 Bioenergy installed power generation capacity by region and long-term prediction based on IEA New Policies Scenario. Sources: IEA Outlook 2015
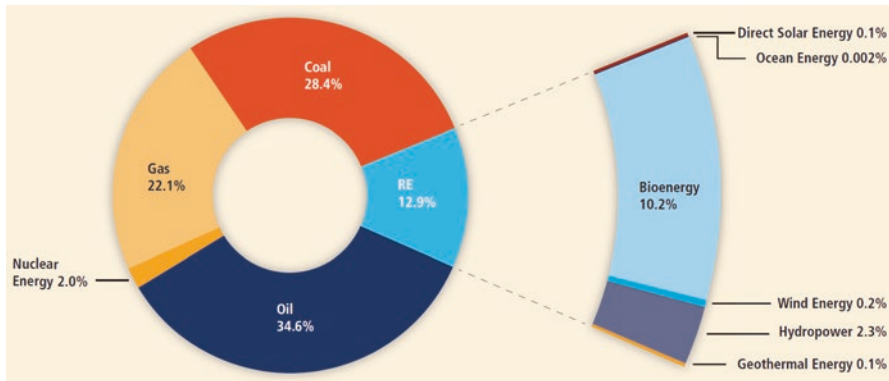

Fig. 8.7 The composition of energy sources in total global primary energy supply in 2008 where systems based on modern biomass contribute about 38% of the total biomass share. Source: IPCC, 2011

bioenergy by its 10.2%, with the majority about 60% used in traditional heating and cooking applications in developing countries and with rapidly increasing use of systems based on modern biomass, as well as other renewables. The composition of energy sources in total global primary energy supply in 2008 is presented in Fig. 8.7.

A model schema dealing with integration of renewables into heating and cooling networks is presented in Fig. 8.8. It enables for multiple energy sources to be connected to various consumers. Centralized heat production can manage the use of thermal energy in the cost-effective way that reduces air pollution in comparison to having many small individual heating and cooling devices. The user can also benefit from a professionally managed central system, which avoids individual operating and maintaining of the separated devices, as well as provides substitution of fossil fuels.
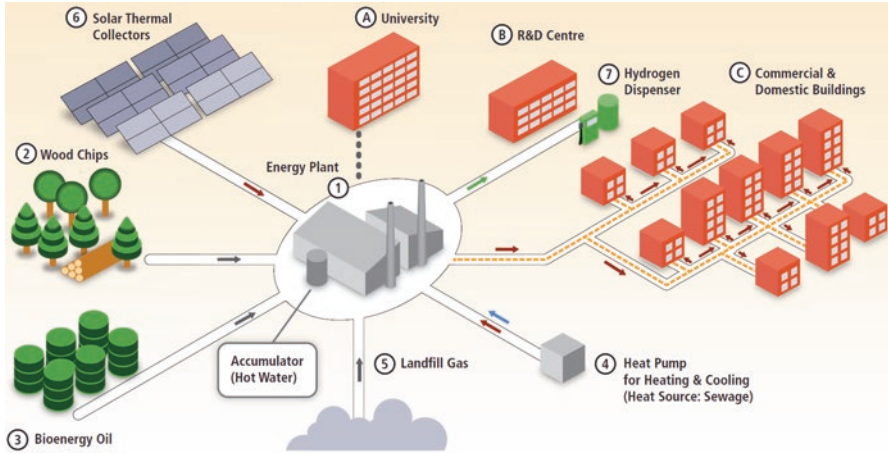
Fig. 8.8 A model schema dealing with the integration of renewables into heating and cooling networks, in order to provide the cost-effective way that reduces air pollution. Source: IPCC, 2011
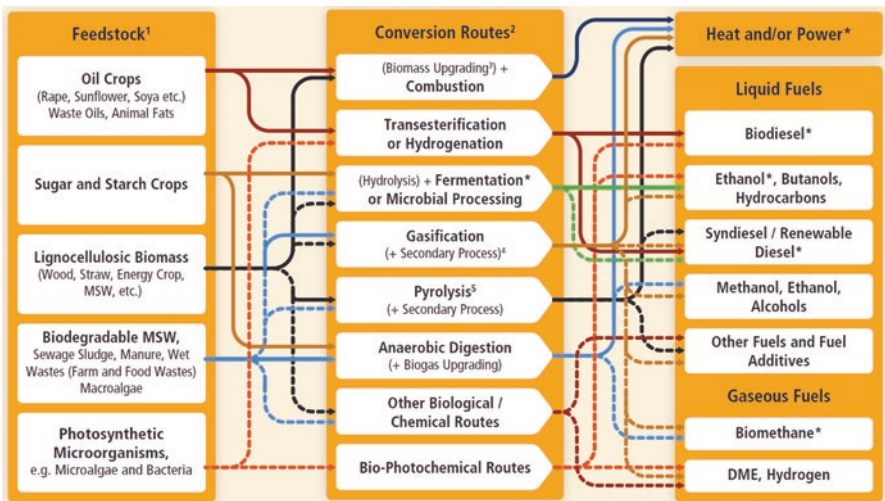

Fig. 8.9 Schematic view of conversion procedures including feedstocks, conversion routes, and products (commercial conversions and products are marked with *solid lines* and *asterisks*, respectively; developing bioenergy routes are indicated with *dotted lines*). Source: IPCC, 2011

Bioenergy technology and applications range from home cooking with stoves to large district combined heat and power systems, from first-generation liquid biofuels to next advanced technologies and from local biogas installations to integration bioenergy applications into heating and cooling networks. The conversion procedures including feedstocks, conversion routes, and products are illustrated in Fig. 8.9.

A number of biomass initiatives have been started worldwide to produce bioenergy for a few last decades. Using dedicated crops, agricultural residues and forestry also

affect discussion on the sustainability of bioenergy, and particularly the indirect impact of biofuels on land-use change. Increasing attention to sustainable use of biomass is reflected in research and policy plans developed in various levels by countries worldwide.

In the United States, the Department of Energy investigated "A Billion-Ton Report" on biomass supply for bioenergy and bioproduct industry. The "2016 Billion-Ton Report: Advancing Domestic Resources for a Thriving Bioeconomy" is the third in a series of national biomass resource assessments, which evaluates the most recent estimates of potential biomass that could be available for new industrial uses in the future. The first volume of this report is focused on resource analysis-projecting biomass potentially available at specified prices. The second volume evaluates changes in environmental sustainability indicators associated with select production scenarios in volume 1. Other key issues based on previous analyses are dealing with (1) updating the farmgate/roadside analysis using the latest available data and specified enhancements; (2) adding more feedstocks, including algae and specified biomass energy crops; and (3) expanding the analysis to include a scenario study to illustrate the cost of transportation to biorefineries under specified logistical assumptions. The "2016 Billion-Ton Report" interactive version offers datasets about potential energy crop production, agricultural residue availability, and forestry production, as well as the potential economic availability of biomass resources delivered to biorefineries. The interactive web-based tools, designed for the Bioenergy Knowledge Discovery Framework (KDF), offer detailed data visualization for potential bioenergy components based on bioenergy resources (agriculture, forest, and wastes), selection of data aggregation (county or state), selection of result type (production, production density, harvested acres, or yield), and other selection criteria such as scenario, feedstock, biomass price (per dry ton), and year. An example of bioenergy exploration over an area of the East Coast of the United States is illustrated in Fig. 8.10. The main benefits of the KDF are a common collaboration toolkit and data resource that offer information about the latest bioenergy research. It includes information about potential energy crop production, agricultural residue availability, forestry production, the potential economic availability of biomass resources delivered to biorefineries, as well as data analyses and model predictions.

In Europe, the European Commission also carry out many activities. The report on the sustainability of solid and gaseous biomass for heat and electricity generation includes information on current and planned EU actions to maximize the benefits of using biomass while avoiding negative impacts on the environment. The full report is downloadable on the web page: https://ec.europa.eu/energy/sites/ener/files/2014_biomass_state_of_play_.pdf. The EU biomass consumption in electricity, heating, and transport is illustrated in Fig. 8.11.

The assessment of greenhouse gas emission savings of biomass can be based broadly on the simplified methodology contained in the Commission report on biomass sustainability published in 2010. The approximate estimate of the total emissions from the use of the fuel before energy conversion used for the fossil fuel comparator is
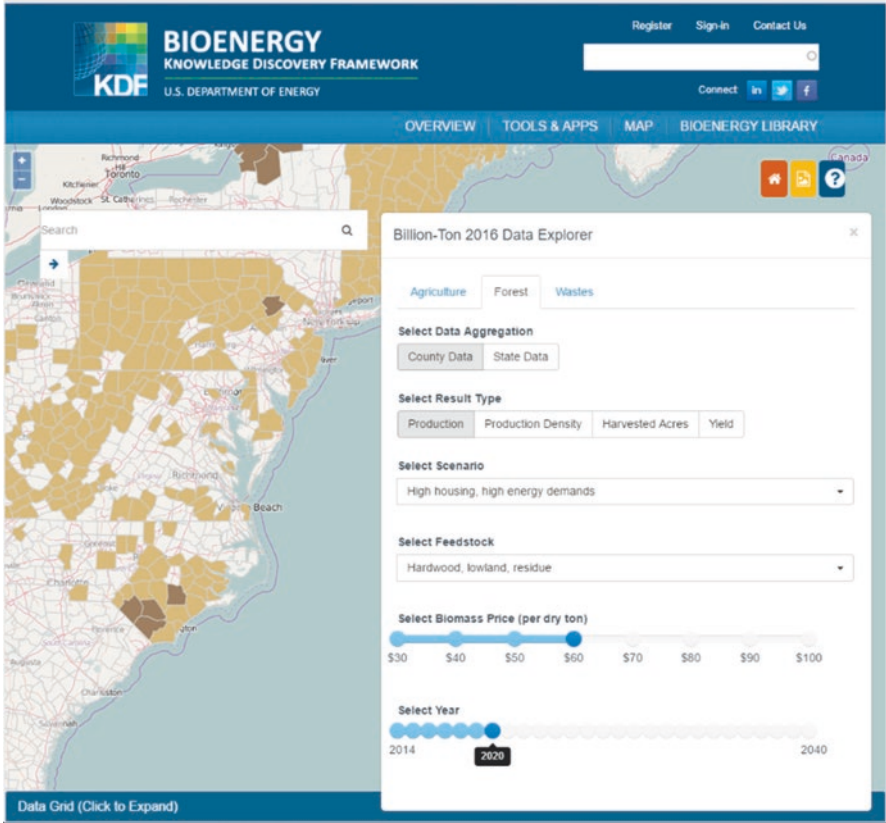
Fig. 8.10 An example of bioenergy exploration over an area of the East Coast of the United States. Source: Bioenergy KDF, 2016, https://bioenergykdf.net/billionton2016/overview
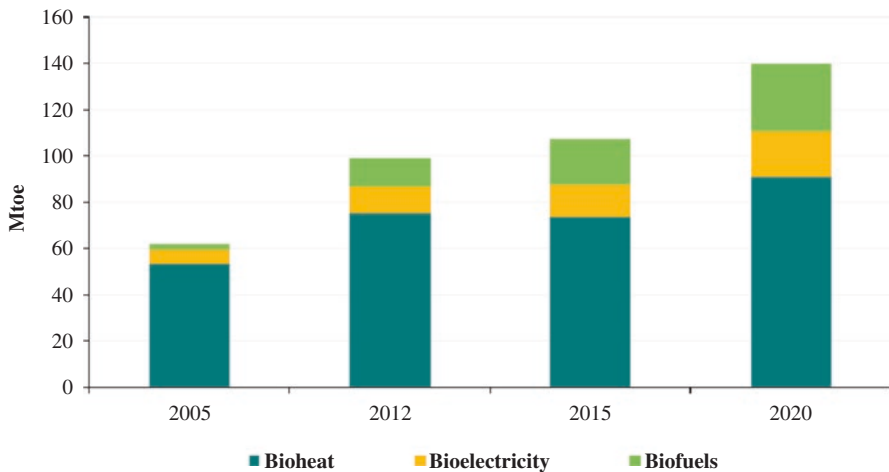

Fig. 8.11 The EU biomass consumption in electricity, heating, and transport. Source: National renewable energy action plans (NREAPs) and 2011 progress reports

$$E = e_{ec} + e_l + e_p + e_{td} + e_u - e_{sca} - e_{ccs} - e_{ccr}, \tag{8.3}$$

where e_{ec} are emissions from the extraction or cultivation of raw materials, e_l annualized emissions from carbon stock changes caused by land-use change, e_p emissions from processing, e_{td} emissions from transport and distribution, e_u emissions from the fuel in use, e_{sca} emission savings from soil carbon accumulation via improved agricultural management, e_{ccs} emission savings from carbon capture and geological storage, and e_{ccr} emission savings from carbon capture and replacement. The resulting savings are presented in Fig. 8.12 for solid biomass. The presented default greenhouse gas values are obtained by applying an electrical efficiency of 25% and a thermal efficiency of 85%. The similar resulting savings for biogas and biomethane are presented in Fig. 8.13. The resulting savings are calculated for selected biomass pathways, on the basis of default values compared against a fossil fuel comparator (the Staff Working Document accompanying the Renewable Energy Directive 2009/28/EC). As a reference distance for solid woody biomass, the long transport shipping distance was calculated with reference to distances to Rotterdam harbor. In real conditions, greenhouse gas savings can be improved in a number of ways, such as by transporting the biomass feedstock for shorter distances. Also, a
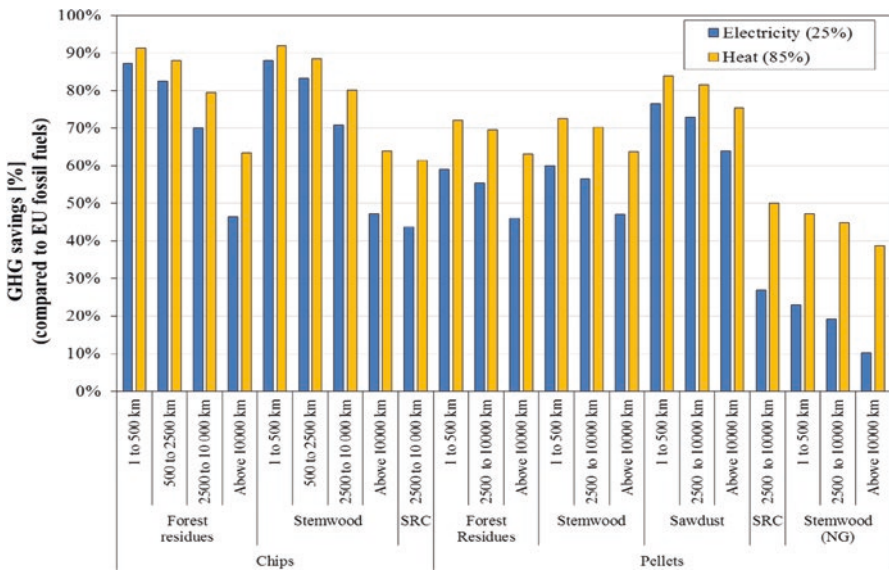

Fig. 8.12 The default greenhouse gas saving performance of solid biomass (default greenhouse values are obtained by applying a standard electrical efficiency of 25% and a standard thermal efficiency of 85%; SRC is short rotation coppice; the calculations are based on greenhouse gas data from eucalyptus cultivation in tropical areas; stem wood (NG) is pellets produced using natural gas as process fuel; all the other pathways are based on wood as process fuel; distances refer to the following regions: 1–500 km is intra-EU trade, 500–2500 km are imports from Russia and Baltic countries, 2500–10,000 km are imports from South East USA and South America, more than 10,000 km are imports from Western Canada). Source: Joint Research Centre 2014
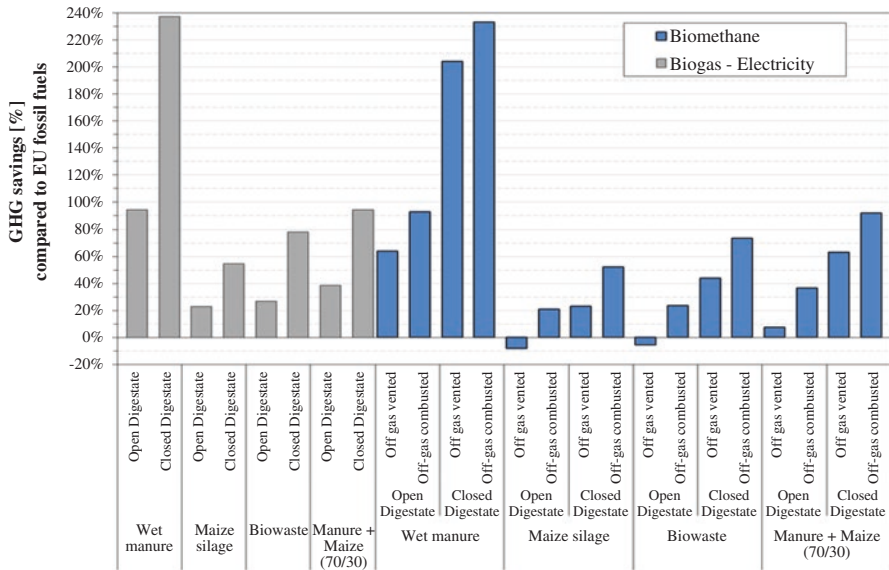
Fig. 8.13 Default greenhouse gas saving performance of biogas and biomethane (manure/maize ≈ 70/30 is an illustrative example of co-digestion of a mixture composed of 70% manure and 30% maize silage on a wet mass basis; results obtained for different mixture compositions are in JRC 2014). Source: Joint Research Centre 2014

conservative electrical efficiency of 25% can be increased to the average efficiency of modern bioelectricity plants, which is around 30–35% and up to 40% with co-firing. For saving performance of solid biomass, the greenhouse emissions can change significantly depending on the used amount of fertilizer, the amount of energy used in processing, as well as the transport mode and distance. In case of forest and agriculture residues, the savings are generally above 70% compared to fossil fuel alternatives. However, lower savings can occur for short rotation coppices such as eucalyptus in tropical countries, in cases of high fertilizer use in agriculture and when natural gas is used for drying pellets.

The default greenhouse emission performance of biogas and biomethane can vary significantly in dependence on the feedstock and the conversion technology used at the plant level. In particular, the greenhouse gas performance is sensitive to the amount of energy crops used and to the leakage of methane emissions during biogas processing, biogas combustion, and storage of digestate. Thus, the greenhouse gas performance of biogas and biomethane plants is used to be improved by using higher shares of waste, animal manure, and slurry as feedstock while improving as much as possible the operational performance and efficiency of the installation itself. Limiting the use of dedicated annual energy crops in the production of bioenergy can contribute to avoid direct and indirect negative impacts resulting from high monoculture production in some areas. Thus, EU Member States are progressively limiting support for the use of annual energy crops for biogas production by setting maximum thresholds for the use of cereals and other starch-rich crops, sugars, and

Table 8.1 Estimated energy content and relative proportion of agriculture production

Energy content biomass crops and residues	Commodity (EJ)	Share	Residues (EJ)	Share
Cereals	41.2	34%	50.8	65%
Oil crops	11.8	10%	11.9	15%
Sugar (cane)	19.8	16%	7.5	10%
Fruits and vegetables	26.2	21%	1.3	2%
Roots and tubers	12.2	10%	1.2	2%
Sugar beets	3.8	3%	0.4	0%
Less important crops	6.9	6%	4.4	6%
Subtotal (inclusive crops less in quantity)	**121.8**	**100%**	**77.6**	**100%**
		Share		
Crops and residues	**199.4**	**63%**		
Grassland	**114.6**	**37%**		
Total	**314.0**			

Source: PBL Netherlands Environmental Assessment Agency report, 2014, http://www.pbl.nl/en/

oil crops by financial support from the Rural Development programs. The existing bioenergy installations can achieve greenhouse gas savings of at least 70% compared to the fossil fuel comparators.

The total energy content of all crops is estimated to be around 200 EJ per year, of which 60% (122 EJ) is from the main crops and 40% (78 EJ) from residues (Table 8.1. The energy content of grasslands is estimated to be around 115 EJ per year, and the total energy content of primary agricultural biomass is estimated around 315 EJ per year. The livestock-related energy content is estimated at about 20 EJ per year. As secondary production, it is not included in the total primary production. But only a small proportion about 5% (420 Mt. ≈ 11 EJ) of the energy content of crops and residues is used for energy and material production. It mostly comes from crops, such as sugarcane and corn. As examples, global biomass flows based on estimates in 2010 resulting from agriculture and from forestry are illustrated by the Sankey diagram in Figs. 8.14 and 8.15, respectively. Using energy density data for all common commodities, the mass datasets have been converted to energy datasets in exajoules (EJ). A distinction is made between biomass from agriculture and forestry. Agricultural biomass is divided into crops and residues (food, feed, fodder, energy, and materials) and livestock (meat, dairy products, fat, energy, and materials, excluding fisheries). Forestry biomass is divided into industrial roundwood (for construction, furniture, and paper) and fuelwood (PBL Netherlands Environmental Assessment Agency report, 2014).

8.4 Risk Assessment of Bioenergy Sources with GIS

While utilization of bioenergy can reduce greenhouse gas emissions, and production of feedstocks creates additional employment and income with positive socioeconomic benefits for farmers and rural communities, there are also potential negative aspects.
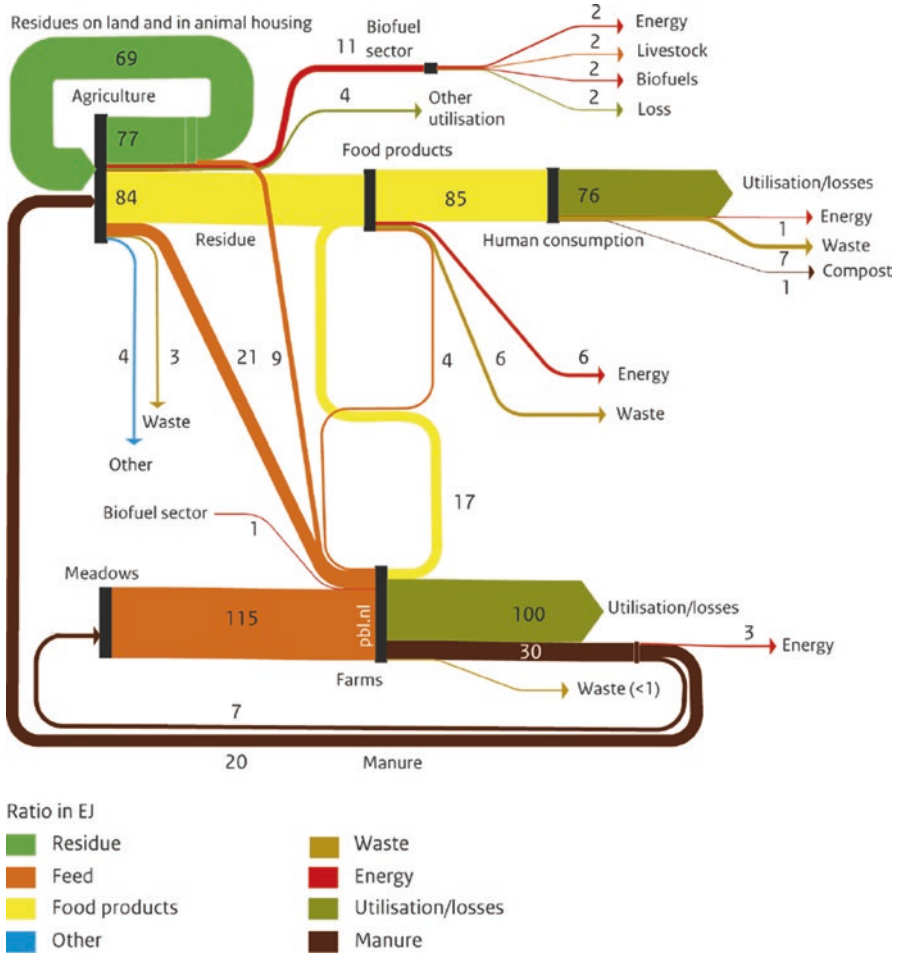
Fig. 8.14 Global biomass flows based on estimates in 2010 resulting from agriculture in exajoules (EJ). Source: PBL Netherlands Environmental Assessment Agency report, 2014, http://www.pbl.nl/en/

The large-scale deployment of bioenergy can create competition with existing uses of biomass, such as for food and feed or forest products, or can compete for land used for their production. Finally, this competition can create upward pressure on agricultural and forestry commodity prices and thus affect food security. The extensive use of bioenergy leads to direct and indirect land-use changes, such as erosion and surface water pollution. In more intensive land use with pressure on water resources, anthropogenic disruption of ecosystems and loss of biodiversity result in increased greenhouse gas emissions. Thus, powerful instruments and procedures are needed in order to minimize the potential negative aspects and maximize the social, environmental, and economic benefits of bioenergy production and use.
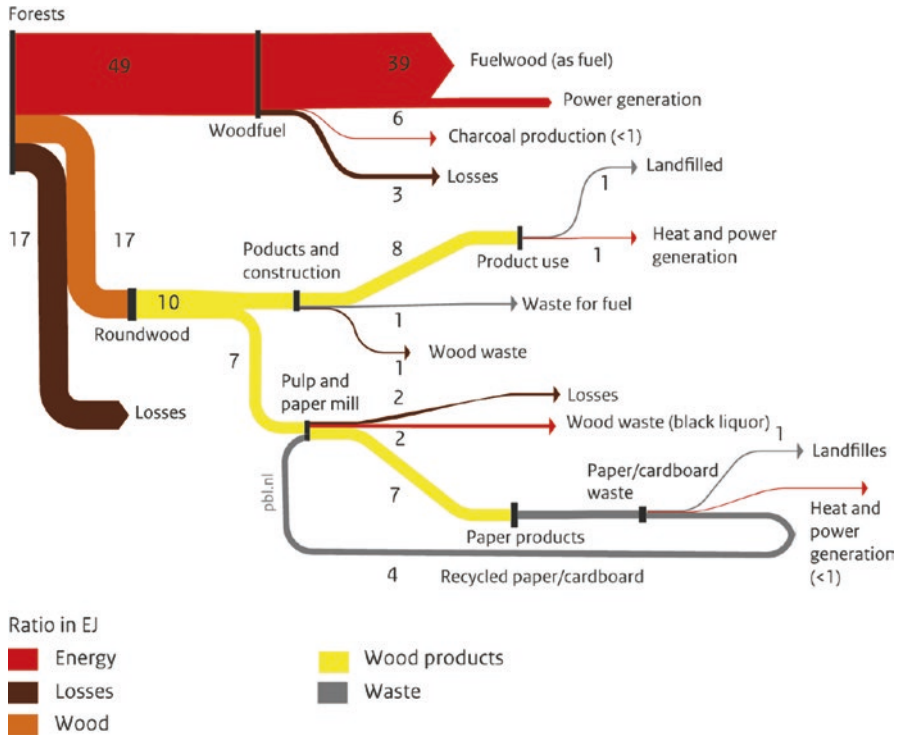
Fig. 8.15 Global biomass flows based on estimates in 2010 resulting from forestry in exajoules (EJ). Source: PBL Netherlands Environmental Assessment Agency report, 2014, http://www.pbl.nl/en/

Only then can bioenergy contribute to meeting energy demand and reducing greenhouse gas emissions in a sustainable way.

Using GIS for assessment of bioenergy sources can help to determine the most favorable locations for feedstock production and its transportation lines. Spatial modeling tools in GIS enable analysis of land-use management and network analysis for transportation with a number of optional extensions. The results can be used to provide optimal integration of renewables into heating and cooling networks, in order to provide the cost-effective way that reduces air pollution. Multi-criteria analysis can examine economic development and social potential based on local a wide range of data such as land use, transportation facilities, urban cartography, regional territorial planning, digital elevation model, lithology, climatic types, civil and industrial users, manufacturing centers, national parks, and protected areas. The results of GIS analysis can include mapping areas of feedstock potential, optimal location of bioenergy installations, as well as optimization of transport networks and electrical grids. This assessment can also show the strong competitiveness of bioenergy sources in comparison with traditional fossil fuels.

8.5   Case-Oriented Studies

Assessment of bioenergy sources and installations of biomass plants are based on the GIS tools. Both case studies present the GIS abilities to solve a wide range of tasks dealing with estimation of potential biomass sources and optimization of transportation in order to provide the cost-effective way. It can give developers information about the bioenergy potential, as well as data sources for risk assessment procedures.

8.5.1   Processing of Data About Bioenergy in GIS

A case study is focused on the assessment of the suitability of land for production of bioenergy crops in Ireland. A map layer opened in ArcGIS Online shows mapping of suitability of land for the production of *Miscanthus* (Fig. 8.16).

Miscanthus (known as elephant grass) is a high-yielding energy crop that grows over 3 m tall and produces a crop every year without the need for replanting. The rapid growth, low mineral content, and high biomass yield favorite this plant as a suitable biofuel source. The suitability of land for production is classified as high, medium, low, unsuitable, or unavailable (protection areas or urban and industrial sites). Besides mapping for the production of bioenergy crops, the additional map layers show the location of wastewater treatment plants and the distance from every location to the main road network, which is classified in a stepped approach (50–100 m, 100–500 m, 500–1000 m, 1000–2000 m, and more than 2000 m) (Fig. 8.17). The described map layers together with other criteria such as energy demand, local employment, and environmental protection can be used for multi-criteria analysis in order to optimize regional and local heating and electrical systems.

8.5.2   Mapping Potential Sources of Bioenergy in a Local Scale

This case study is focused on the assessment of bioenergy sources in a local urban environment. The area of interest is complemented by map layers dealing with proposed locations of bioplants, street network, and ortofoto (Fig. 8.18. The results of network analysis for waste collection based on the method "Service Area Analysis" is presented in Fig. 8.19.

An urban environment produces a high amount of biowastes, which can be partially utilized for bioenergy production. The described case study provides a more detailed analysis of waste collection in order to optimize transport management, which can minimize costs and reduce air pollution. ArcGIS Network Analysis tools are used to maintain network datasets and provide Service Area Analysis. The results determine the area of accessibility within a given cutoff cost from bioplant locations.
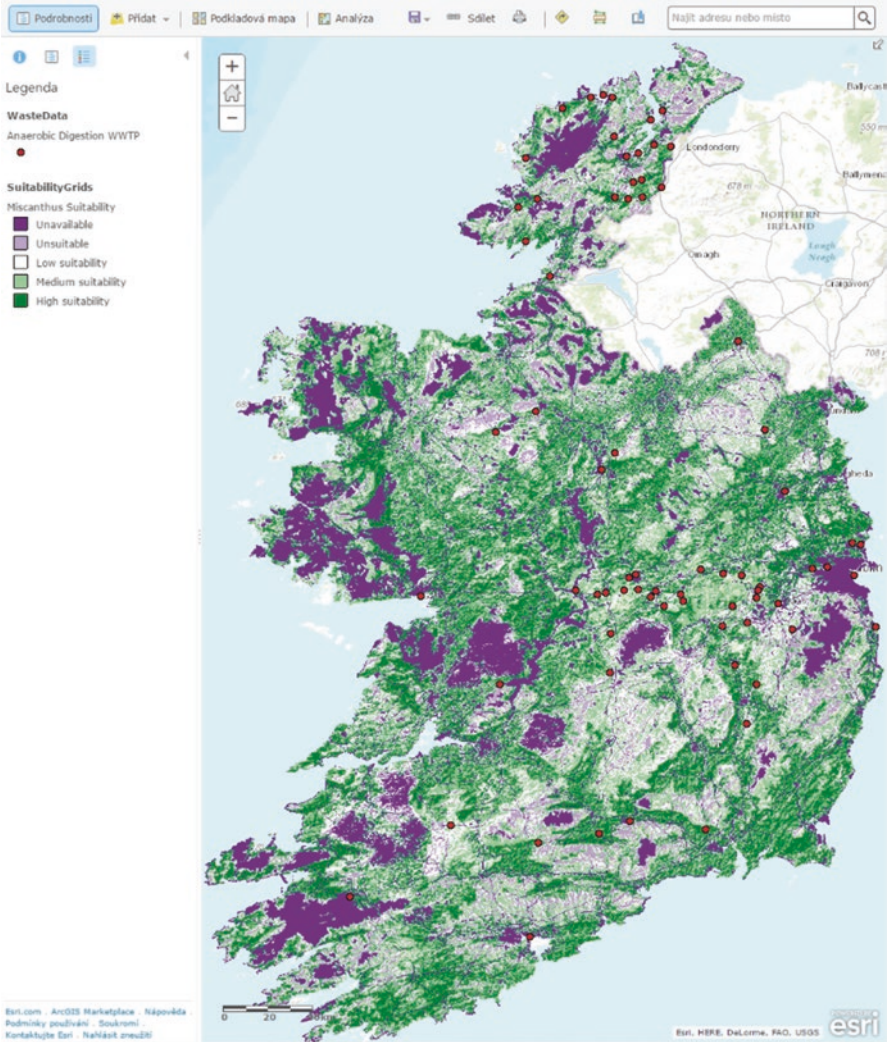
Fig. 8.16 A map layer opened in ArcGIS Online for mapping of suitability of land for the production of *Miscanthus*. The suitability is classified as high, medium, low, unsuitable, or unavailable (protection areas or urban and industrial sites). Source: an ArcGIS Online dataset, which is a subset of a dataset used by the Department of Agriculture, Fisheries and Food (DAFF), the dataset is maintained as the "Land Parcel Information System (LPIS)"

The created polygons represent the distance that can be reached from a bioplant within a specified distance. These polygons are called as service area polygons and are calculated as 3 km, 6 km, and 9 km service areas for nine proposed locations of bioplants. The results of this study can be included into a wider range of datasets to assist in research studies and to help a local public community, investors, and developers.
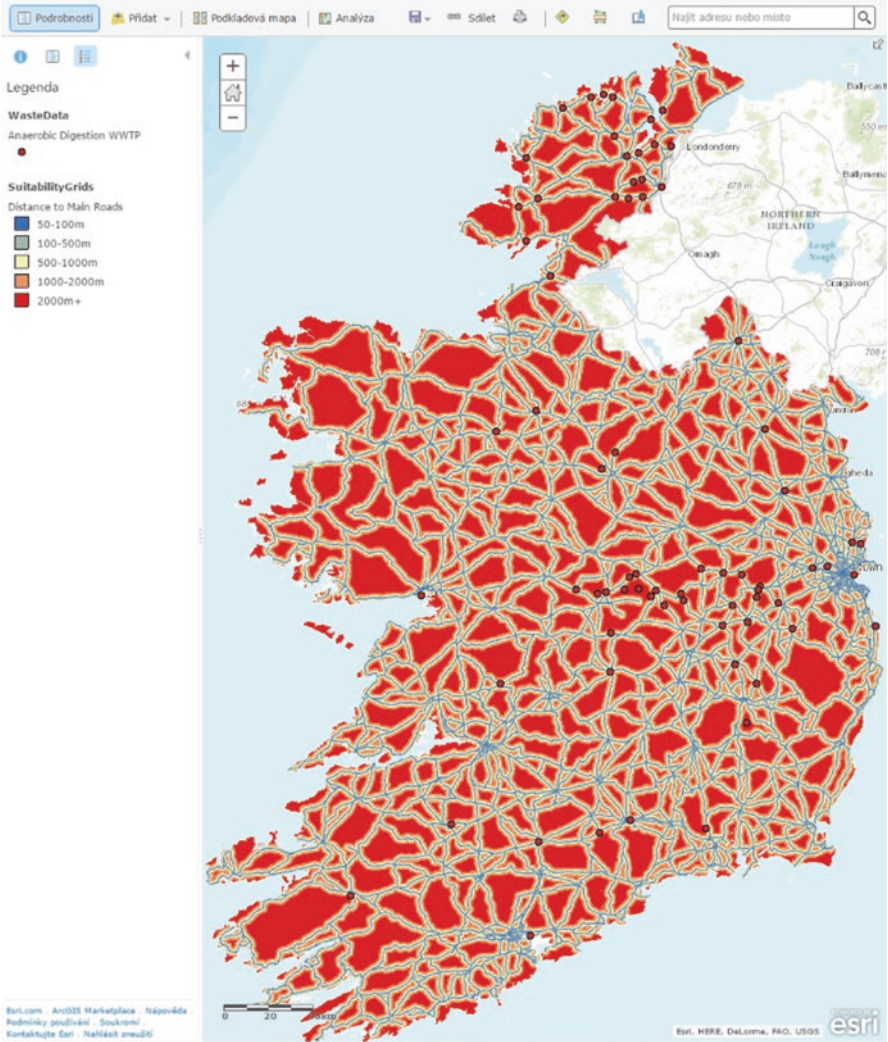
Fig. 8.17 A map layer for assessment of the suitability of land for production of bioenergy crops such as *Miscanthus* in Ireland. The suitability is classified as high, medium, low, unsuitable, or unavailable in case of protection areas or urban and industrial sites. Source: the ArcGIS Online dataset, which is a subset of a dataset used by the Department of Agriculture, Fisheries and Food (DAFF), the dataset is maintained as the "Land Parcel Information System (LPIS)"

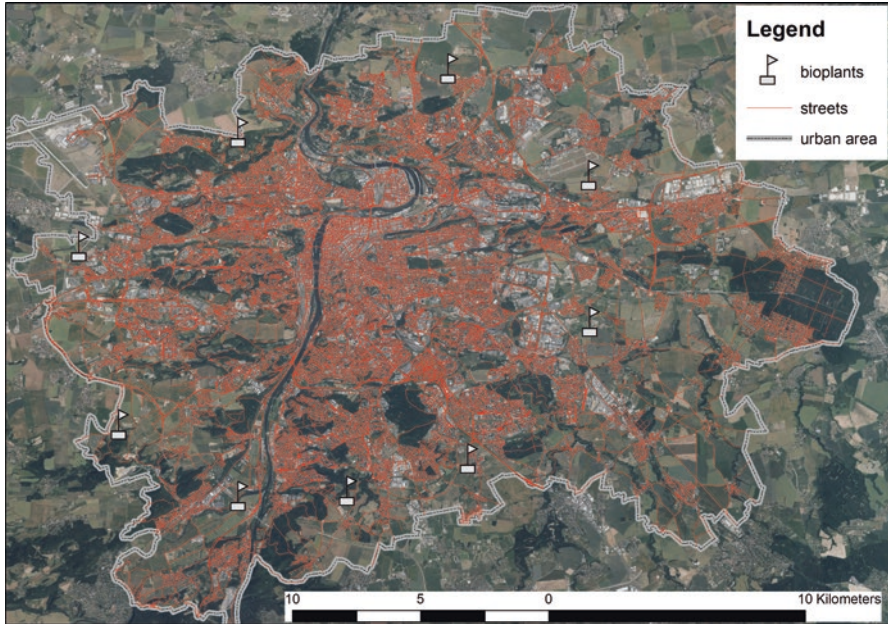**Fig. 8.18** The area of interest complemented by proposed locations of bioplants, street network, and ortofoto
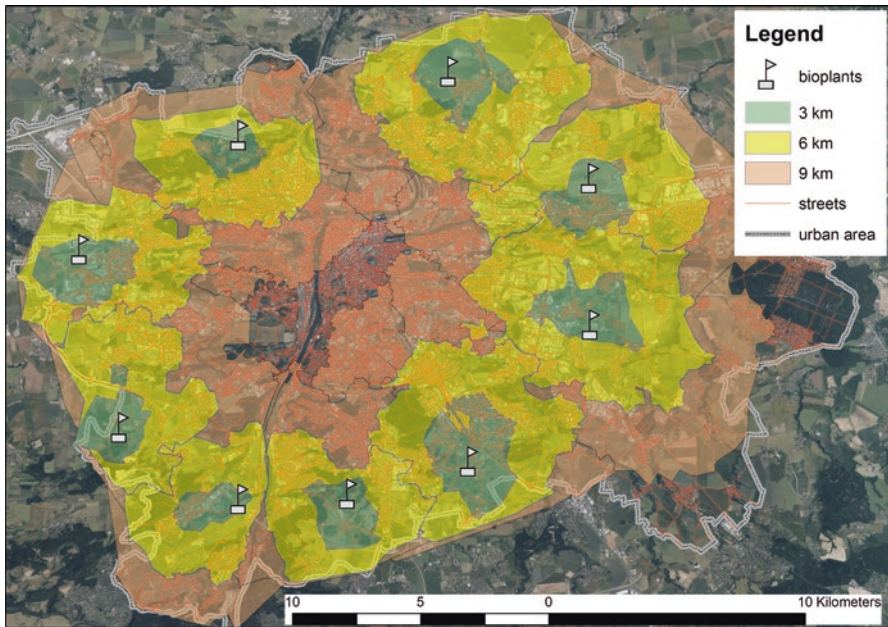

Fig. 8.19 The results of network analysis based on the Service Area Analysis in the Network Analyst

Bibliography

EEA (2016). *Renewable energy in Europe 2016. Recent growth and knock-on effects*. Retrieved from http://www.eea.europa.eu/publications/renewable-energy-in-europe-approximated

EIA (2015). *International energy outlook 2015*. Retrieved from http://www.eia.gov/forecasts/ieo/pdf/0484(2016).pdf

EIA (2016). *2016 Billion-Ton Report—Advancing domestic resources for a thriving bioeconomy*. Retrieved from https://bioenergykdf.net/billionton2016/overview

European Commission (2013). *EU energy, transport and GHG emissions trends to 2050—Reference scenario, 2013*. Retrieved from http://ec.europa.eu/transport/media/publications/doc/trends-to-2050-update-2013.pdf

European Commission (2014). *State of play on the sustainability of solid and gaseous biomass used for electricity, heating and cooling in the EU*. Retrieved from http://ec.europa.eu/energy/sites/ener/files/2014_biomass_state_of_play_.pdf

European Commission (2015). *EU energy in figures: Statistical pocketbook, 2015*. Retrieved from http://ec.europa.eu/energy/sites/ener/files/documents/PocketBook_ENERGY_2015%20PDF%20final.pdf

European Commission (2016). *EU reference scenario 2016—Energy, transport and GHG emissions—Trends to 2050*. Retrieved from https://ec.europa.eu/energy/sites/ener/files/documents/20160713%20draft_publication_REF2016_v13.pdf

IEA (2007a). *Good practice guidelines—Bioenergy project development biomass supply*. Retrieved from https://www.iea.org/publications/freepublications/publication/biomass.pdf

IEA (2007b). *Renewables for heating and cooling—Untapped potential*. Retrieved from http://www.iea.org/publications/freepublications/publication/renewable_heating_cooling_final_web.pdf

IEA (2012a). *World energy outlook 2012*. Retrieved from http://www.iea.org/publications/freepublications/publication/world-energy-outlook-2012.html

IEA (2012b). *Technology roadmap bioenergy for heat and power*. Retrieved from http://www.iea.org/publications/freepublications/publication/technology-roadmap-bioenergy-for-heat-and-power-.html

IEA (2012c). *Technology roadmap biofuels for transport*. Retrieved from http://www.iea.org/publications/freepublications/publication/biofuels_roadmap_web.pdf

IEA (2013a). *Production costs of alternative transport fuels—Influence of crude oil price and technology maturity*. Retrieved from https://www.iea.org/publications/freepublications/publication/FeaturedInsights_AlternativeFuel_FINAL.pdf

IEA (2013b). *Technology roadmap energy and GHG reductions in the chemical industry via catalytic processes*. Retrieved from https://www.iea.org/publications/freepublications/publication/Chemical_Roadmap_2013_Final_WEB.pdf

IEA (2015a). *World energy outlook 2014*. Retrieved from https://www.iea.org/bookshop/477-World_Energy_Outlook_2014

IEA (2015b). *Heating without global warming—Market developments and policy considerations for renewable heat*. Retrieved from https://www.iea.org/publications/freepublications/publication/FeaturedInsight_HeatingWithoutGlobalWarming_FINAL.pdf

IEA (2016a). *World energy statistics 2016*. Retrieved from http://www.iea.org/bookshop/723-World_Energy_Statistics_2016

IEA (2016b). *World energy outlook 2015*. Retrieved from https://www.iea.org/bookshop/700-World_Energy_Outlook_2015

IPCC (2014). *Climate change 2014 mitigation of climate change*. Retrieved from https://www.ipcc.ch/pdf/assessment-report/ar5/wg3/ipcc_wg3_ar5_full.pdf

PBL Netherlands Environmental Assessment Agency (2014). *Integrated analysis of global biomass flows in search of the sustainable potential for bioenergy production 2014*. Retrieved from http://www.pbl.nl/en/

Dictionaries and Encyclopedia

EIA (2016). *Energy explained: Your guide to understanding energy*. Retrieved from http://www.eia.gov/energyexplained/index.cfm

Data Sources (Revised in August, 2016)

Bioenergy Knowledge Discovery Framework (KDF). (2016). Retrieved from https://bioenergykdf.net/billionton2016/overview

EIA. *International energy statistics*. Retrieved from http://www.eia.gov/cfapps/ipdbproject/IEDIndex3.cfm

Renewable Energy World. Retrieved from http://www.renewableenergyworld.com/solar-energy.html

Chapter 9
Nuclear Power: Historical Overview, Bright Side, and Environmental Issues

Heat generated by the fission represents higher order amounts of energy in comparison with other energy sources such as fossil or renewable. Nuclear reactors can transform 60TJ of energy from 1 kg of uranium 235, which can give, assuming 30% efficiency of conversion, 3 GWh of electricity. For example, a small 1 cm reactor fuel pellet produces the same amount of energy as 1.5 tonnes of coal. Actually, energy from nuclear reactors ranks among major sources of energy such as coal, oil, and gas. For example, France producing 80% of its electricity by nuclear power and exports this energy to surrounding countries. Due to the limited resources of fossil fuels, hundreds of fossil-fuel power stations must be replaced. It cannot be mainly done by renewable sources of energy, but the renewable source can complement these high-performance sources of energy. Up-to-date nuclear reactors are reliable and operate over 90% of the time, and the remainder of the time is mostly covered by essential maintenance that is scheduled in advance. The number of unplanned shutdowns has fallen to about one in 7000 per day. The main disadvantage of nuclear reactors during their operation is the long period to come up to full power than other power stations. But temporary electricity failures by nuclear reactors can be quickly replaced by alternative sources such as gas power stations that can be rapidly activated in case of a sudden need. The concern about nuclear radiation has diverted attention from other hazardous to our health, but the nuclear industry is responsible for less than 0.01%.

9.1 Description of Nuclear Power and Historical Overview

Nuclear power is an abundant source of low-carbon energy that can help in reduction of greenhouse gas emissions in comparison with fossil fuels. There are two forms of nuclear energy that are used for energy supply. The controlling fission, the reaction used in current reactors, and the controlling fusion, the energy source in stars, which actually represent a great challenge in research and development.

Energy can be released in the fission of heavy nuclei or in the fusion of light nuclei. The released energy is dependent on binding energy, which is required to disassemble the nucleus (neutrons and protons) of an atom into its component parts. A nucleus is bounded together by a short-range attractive force. Its mass is less than the sum of the masses of its constituent nucleons and the difference gives the total binding energy through Einstein's relation:

$$\Delta EB = \Delta MB \cdot c2 \tag{9.1}$$

where ΔE_B is the total binding energy, ΔM_B the mass difference, and c the speed of light (approximately $3 \cdot 10^8$ ms^{-1}). Binding energy per nucleon of the isotopes is shown in Fig. 9.1, which shows that binding energy are maximum in the middle of the period table and less for the lighter and heavier isotopes. It is the energy that would be required to pull apart the nucleus into its constituent nucleons and determines whether a nucleus is stable or unstable.

For example, the energy release due to the fission of ^{235}U (mass numbers $A_1 = 235$, $E_{B1} \approx 7.6$ MeV), which results in two lighter stable nuclei (mass numbers $A_2 \approx 140$, $A_3 \approx 93$, and $E_{B2} \approx 8.35$ MeV, $E_{B3} \approx 8.7$ MeV, respectively) is:

$E_R = [A_1 \cdot (E_{B2} - E_{B1}) + (A_3 \cdot (E_{B3} - E_{B1}))] = [140 \cdot (8.35–7.6) + (93 \cdot (8.7–7.6))] \approx$ 210 MeV $\approx 3.2 \cdot 10^{-11}$ J.
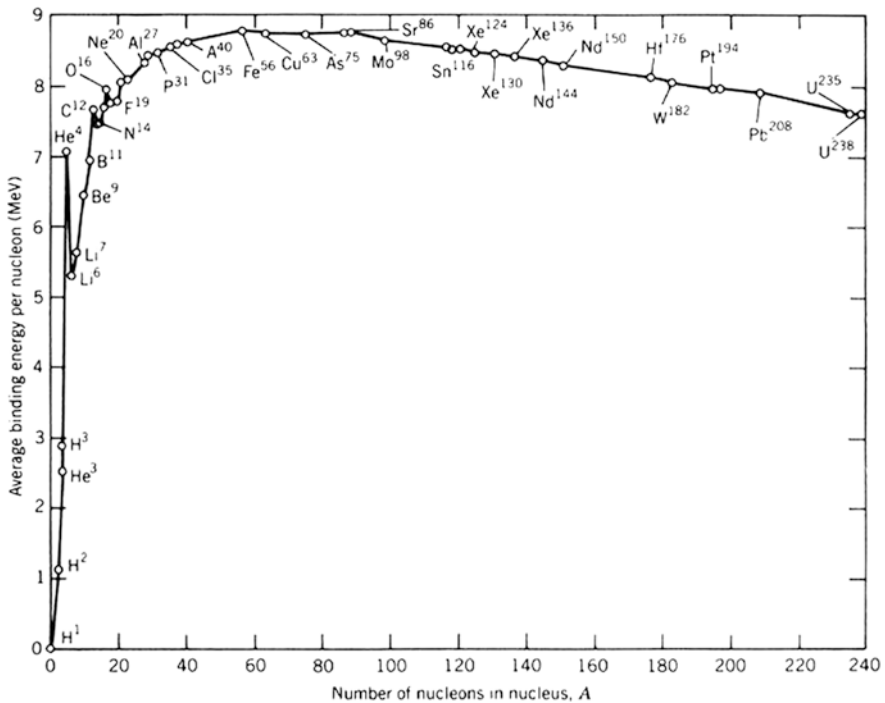

Fig. 9.1 Binding energy per nucleon of the isotopes with maximum binding energy in the middle of the period table and less for the lighter and heavier isotopes

Table 9.1 The comparison of the nuclear fission and the nuclear fusion

	Nuclear fission	Nuclear fusion
Definition	Fission is the splitting of a large atom into two or more smaller ones	Fusion is the fusing of two or more lighter atoms into a larger one
Natural occurrence of the process	Fission reactions occur in lower levels in uranium deposits	Fusion occurs in stars, such as the sun
By-products of the reaction	Fission produces many highly radioactive particles	Only few radioactive particles are produced by fusion reaction
Conditions	Critical mass of the substance and high-speed neutrons are required	High density and high temperature environment is required
Energy requirement	Takes little energy to split two atoms in a fission reaction	Extremely high energy is required to bring two or more protons close enough
Energy released	The energy released by fission is much higher than that released in chemical reactions, but lower than the energy released by nuclear fusion	The energy released by fusion can be several times higher than the energy released by fission
Energy production	Fission is used in nuclear power plants	Fusion is an experimental technology for producing power
Fuel	The primary fuel used in power plants is uranium	The primary fuel used in experimental fusion power plants hydrogen isotopes (deuterium and tritium)

The final released energy deposited in surrounding materials is about 200 MeV due to radiation and other interactions. It is much more energy in comparison with chemical combustion reaction ($C + O_2 \rightarrow CO_2 + 4$ eV, ~10^{-19} J). But in dependence on mass of atoms and used resources, the released energy of 1 tonne of uranium can be compared to about 20,000 tonnes of coal in real conditions (Andrews & Jelley, 2013).

As an example of the fusion, the energy release, when deuterium ^2H ($A_1 = 2$, $E_{B1} = 1.1$) and tritium ^3H ($A_2 = 3$, $E_{B2} = 2.6$) nuclei fuse to helium ^4He ($A_3 = 4$, $E_{B3} = 7.1$) with the release of a neutron, is:

$$E_R = A_3 \cdot E_{B3} - (A_1 \cdot E_{B1} + A_2 \cdot E_{B2}) = 4 \cdot 7.1 - (2 \cdot 1.1 + 3 \cdot 2.6) \approx 18 \text{ MeV}.$$

In dependence on mass of atoms and technology, the energy released by fusion can be several times higher than the energy released by fission. A comparison of the both principles of energy supply by the nuclear fission and the nuclear fusion is shown in Table 9.1.

Nuclear fission: The world's first nuclear reactor to achieve criticality was Chicago Pile-1 (CP-1), which represented a part of the military Manhattan Project. The first man-made self-sustaining nuclear chain reaction was initiated in CP-1 on 2 December 1942, under the supervision of Enrico Fermi. The first commercial facility for energy production using nuclear reactors was the Calder Hall Plant, in Windscale (Sellafield), Great Britain. The first large-scale US nuclear plant was opened in Shippingport, Pennsylvania, in 1957. During two decades, nearly 40 power production nuclear reactors were launched in the United States, the largest being Unit One of the Zion Nuclear Power Station in Illinois, with a capacity of 1155 MW.

Fig. 9.2 Kashiwazaki-Kariwa Nuclear Power Plant in Japan with the nameplate capacity 7965 MW (7 operational reactors: 5 × BWR 1067 MW; 2 × ABWR 1315 MW). Source: Google Earth, 2016

During the 1990s, Germany and especially France expanded their nuclear plants, focusing on smaller and thus more controllable reactors. China launched its first two nuclear facilities in 2007, producing a total of 1866 MW. Fission installations represent powerful forms of energy production, but have a number of built-in inefficiencies. The nuclear fuel, usually uranium 235, is expensive to mine and purify. The fission reaction creates heat that is used to boil water for steam to turn a turbine that generates electricity, which represents cumbersome and expensive transformation. Other significant source of inefficiency is that clean-up and storage of nuclear waste is very expensive and requires security to ensure public safety. The largest nuclear-generating station in the world by net electrical power rating (nameplate capacity 7965 MW; capacity factor 48%; average generation 33,317 TWh) is Kashiwazaki-Kariwa Nuclear Power Plant in Japan on the coast of the Sea of Japan, from where it gets cooling water, Fig. 9.2.

Nuclear fusion: The devices for nuclear fusion are in a stage of research and experimental development. For fusion to occur, the atoms must be confined in the magnetic field and raised to a temperature of 100 million Kelvin or more, which takes an enormous amount of energy to initiate fusion. Other challenge is the need to properly contain the plasma field for long-term energy production. Researchers are still trying to overcome these challenges because fusion devices are safer and more powerful energy production systems than fission reactors. ITER (International Thermonuclear Experimental Reactor) is being built in collaboration of 35 nations next to the Cadarache facility in southern France, Fig. 9.3. The world's largest fusion tokamak, a magnetic fusion device has been designed to prove the feasibility of fusion as a large-scale and carbon-free source of energy (https://www.iter.org/).

Fig. 9.3 The construction of the world's largest fusion tokamak in southern France. Source: https://www.iter.org/

World uranium mining production is shown in Table 9.2. In 2015, the leading countries in production with over two-thirds of the world's production of uranium from mines were Kazakhstan (39%), Canada (22%), and Australia (9%). An increasing amount of uranium, about 48%, was produced by in situ leaching. Over half of uranium mine production is from state-owned mining companies. In 2015, 11 companies marketed 89% of the world's uranium mine production. Known recoverable resources of uranium in 2013 are given in Table 9.3 and attached map layer in Fig. 9.4. The long-term world uranium production and demand are illustrated in Fig. 9.5.

As an example, fuel consumption of the nuclear reactor having total power $P_T = 500$ MW and a number of fissions $C = 3 \cdot 10^{10}$ $W^{-1} \cdot s^{-1}$ (fissions per Watt-second) is determined. The reactor fission rate is:

$$F_r = P_T \cdot C = 500 \cdot 10^6 \cdot 3 \cdot 10^{10} = 1.5 \cdot 10^{19} \text{ s}^{-1} \text{ (fissions per second).}$$

If the fuel occupies 6% of the reactor volume 38.5 m^3, the fuel volume is:

$$V_f = 0.06 \cdot 38.5 = 2.31 \text{ m}^3 = 2.31 \cdot 10^6 \text{ cm}^3.$$

The ^{235}U nuclei per cm^3 is (uranium density: $\rho_U = 18.68$ g·cm^3; uranium relative atomic mass: $A_r = 238.07$; Avogadro's constant $N_A = 6.023 \cdot 10^{23}$ mol^{-1}):

$$N_U = (\rho_U/A_r) \cdot N_A = (18.68/238.07) \cdot 6.023 \cdot 10^{23} = 0.472 \cdot 10^{23} \text{ cm}^{-3}.$$

Table 9.2 World uranium mining production from mines in tonnes

Country	2007	2008	2009	2010	2011	2012	2013	2014	2015
Kazakhstan	6637	8521	14,020	17,803	19,451	21,317	22,451	23,127	23,800
Canada	9476	9000	10,173	9783	9145	8999	9331	9134	13,325
Australia	8611	8430	7982	5900	5983	6991	6350	5001	5654
Niger	3153	3032	3243	4198	4351	4667	4518	4057	4116
Russia	3413	3521	3564	3562	2993	2872	3135	2990	3055
Namibia	2879	4366	4626	4496	3258	4495	4323	3255	2993
Uzbekistan (estimate)	2320	2338	2429	2400	2500	2400	2400	2400	2385
China (estimate)	712	769	750	827	885	1500	1500	1500	1616
United States	1654	1430	1453	1660	1537	1596	1792	1919	1256
Ukraine (estimate)	846	800	840	850	890	960	922	926	1200
South Africa	539	655	563	583	582	465	531	573	393
India (estimate)	270	271	290	400	400	385	385	385	385
Czech Republic	306	263	258	254	229	228	215	193	155
Romania (estimate)	77	77	75	77	77	90	77	77	77
Pakistan (estimate)	45	45	50	45	45	45	45	45	45
Brazil (estimate)	299	330	345	148	265	326	192	55	40
France	4	5	8	7	6	3	5	3	2
Germany	41	0	0	8	51	50	27	33	0
Malawi			104	670	846	1101	1132	369	0
Total world	41,282	43,764	50,772	53,671	53,493	58,489	59,331	56,041	60,496
Tonnes U$_3$O$_8$	48,683	51,611	59,875	63,295	63,084	68,976	69,969	66,089	71,343
% of world demand	64%	68%	78%	78%	85%	86%	92%	85%	90%

Source: World Nuclear Association, 2016

Table 9.3 Estimated recoverable resources of uranium in 2013 in tonnes

Country	U (tonnes)	%
Australia	1,706,100	29%
Kazakhstan	679,300	12%
Russia	505,900	9%
Canada	493,900	8%
Niger	404,900	7%
Namibia	382,800	6%
South Africa	338,100	6%
Brazil	276,100	5%
United States	207,400	4%
China	199,100	4%
Mongolia	141,500	2%
Ukraine	117,700	2%
Uzbekistan	91,300	2%
Botswana	68,800	1%
Tanzania	58,500	1%
Jordan	40,000	1%
Other	191,500	3%
World total	5,902,900	

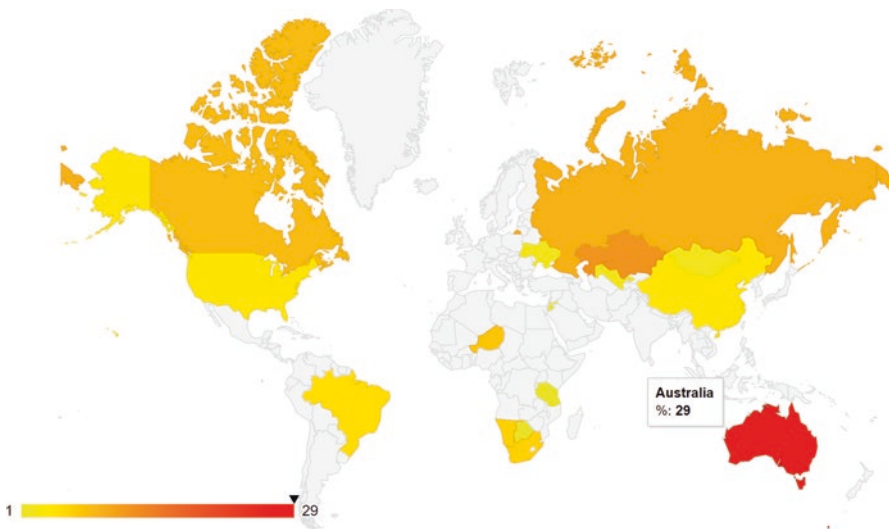Source: World Nuclear Association, 2016

Fig. 9.4 Mapping of estimated recoverable resources of uranium in 2013 in tonnes. Source: World Nuclear Association, 2016
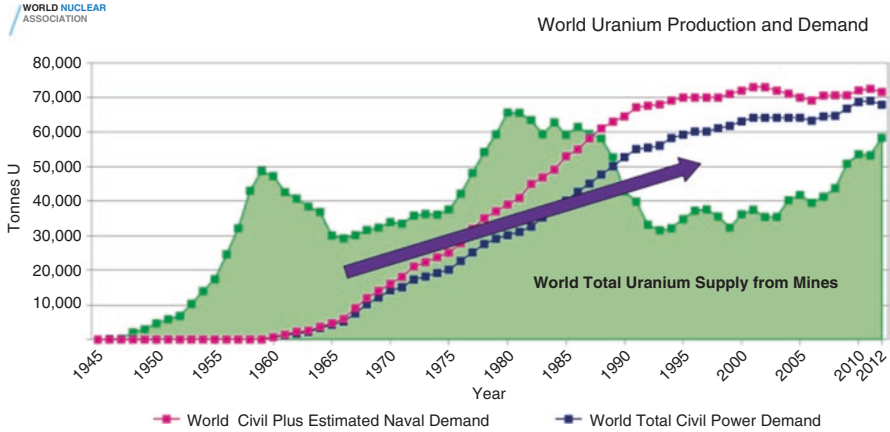
Fig. 9.5 The long-term world uranium production and demand. Source: World Nuclear Association, 2016

If the fuel is 99.3% of ^{238}U and 0.7% ^{235}U, the ^{235}U nuclei in the reactor is:

$$N_{235U} = 0.007 \cdot N_U \cdot V_f = 0.007 \cdot 0.472 \cdot 10^{23} \cdot 2.31 \cdot 10^6 = 7.64 \cdot 10^{26}.$$

The consumed ^{235}U fissionable material is:

$$F_{235U} = F_r \cdot G_m/N_A = 1.5 \cdot 10^{19} \cdot 235/6.023 \cdot 10^{23} = 0.00585 \text{ g} \cdot \text{s}^{-1}.$$

If the plant operates 8760 h/year (8760·3600 s) at an 80% load factor, the annual consumption of fissionable material is:

$$A_c = F_{235U} \cdot (8760 \cdot 3600) \cdot 0.8 = 0.00585 \cdot (8760 \cdot 3600) \cdot 0.8 = 147{,}588 \text{ g year}^{-1}$$
$$\approx 148 \text{ kg} \cdot \text{year}^{-1}.$$

The ^{235}U consuming by fission is higher due to the loses by absorption, which is expressed as ratio $\alpha = (^{235}$U total capture cross section$)/(^{235}$U fission cross section$)$. The annual consumption for a typical reactor with $\alpha = 1.2$ is:

$$A_{ct} = \alpha \cdot A_c = 1.2 \cdot 148 = 178 \text{ kg} \cdot \text{year}^{-1}.$$

The allowable percentage of burnup (^{235}U and ^{238}U) depends on a number of parameters such as the total integrated radiation dosage, radiation energy level, the effect on fuel material dimensional stability, thermal conductivity, and reduction in effective multiplication factor. Assuming a maximum allowable burnup of 20%, which is a typical value, the maximum allowable atom burnup:

$$B_{ma} = (\text{percentage of burnup}) \cdot N_U \cdot V_f = 0.002 \cdot 0.472 \cdot 10^{23} \cdot 2.31 \cdot 10^6 = 2.18 \cdot 10^{26}$$
atoms.

The average fuel-cycle time can be estimated as:

$$A_f = B_{ma}/F_r = 2.18 \cdot 10^{26}/1.5 \cdot 10^{19} = 1.45 \cdot 10^7 \text{ s} \approx 168 \text{ days}$$

The procedure can be used generally for any reactor designed to generate power. The methods are based on the work reported in Power magazine by Henry C. Schwenk and Robert H. Shannon. A number of calculations were published in the Hicks G. and Tyler P.E. in the Handbook of Energy Engineering Calculations.

9.2   Mapping of Existing Power Plant Installations

During the past half century, the nuclear power has become a significant source of the global energy supply for growing electricity demand in some regions, as well as a solution how to avoid emissions of greenhouse gases and other air pollutants. Yet some countries have rejected the use of nuclear power due to the risk of accidents and dangerous nuclear wastes. In 2013, the total installed nuclear capacity accounted for 11% (392 GW) of electricity generation. Nuclear plant construction accelerated during the 1960s and 1970 after the oil price shock (1973–1974). While OECD countries, such as European countries and the United States, accounted for the majority of new nuclear builds during that time, there was a resurgence in new nuclear builds in the late 2000s, driven by non-OECD countries, mainly China, seeking to meet fast-growing electricity demand and to reduce air pollution, Fig. 9.6. The accident at Three Mile Island in the United States in 1979 with no external radiological health effects heightened public opposition to nuclear power and slowed license approvals around the world, mainly in the United States. The accident at Chernobyl in Ukraine in 1986 further depressed activity, especially in Europe. The accident at Fukushima Daiichi in Japan in 2011 strengthens public opposition to nuclear power around the world again. From economic point of view, in the 1990s, gas and electricity markets in many OECD countries were deregulated and gas prices were low, which caused that investment in new nuclear plants became less attractive than investment in alternatives, particularly combined-cycle gas turbines.
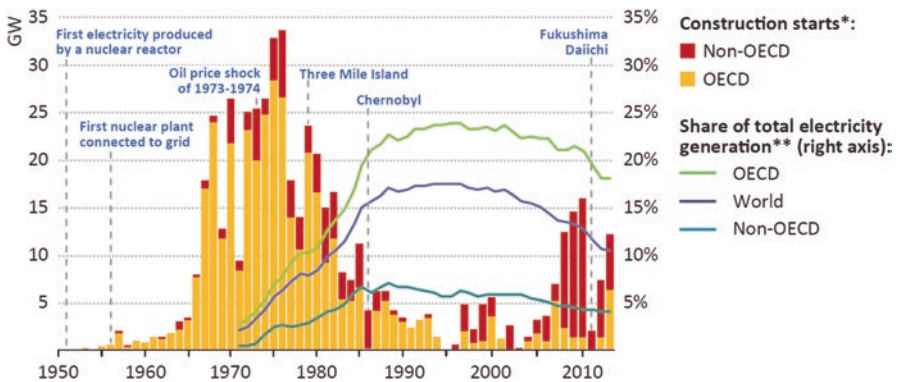

Fig. 9.6   Reactor construction starts and timeline of events. Source: IEA Outlook, 2014
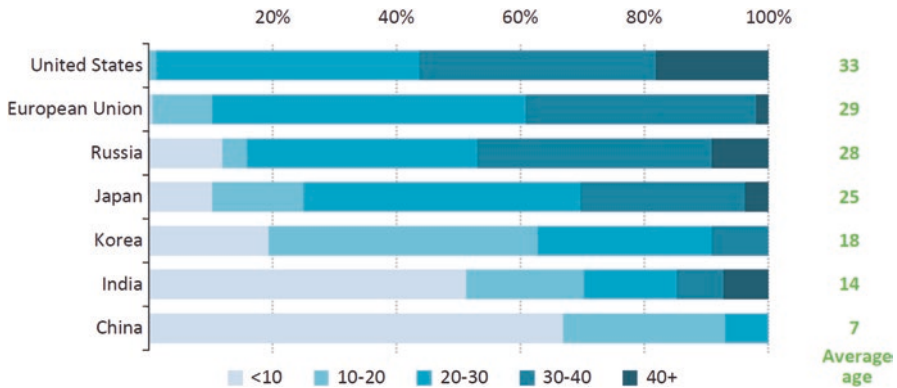
Fig. 9.7 The age profile of nuclear capacity by selected region and operational period. Source: IEA Outlook, 2014

There is still about 80% of nuclear capacity in OECD countries, but more than three-quarters is over 25 years old, raising important questions in the medium-term about lifetime periods. But, around half of the capacity in non-OECD countries (excluding Russia) is less than 15 years old, and about the 76 GW of nuclear capacity is under construction with three-quarters in non-OECD countries (40% in China). The average age of nuclear capacity worldwide is 27 years. The expected technical lifetimes for reactors are 30–60 years, depending on the reactor type and location. The age profile of nuclear capacity by selected region is illustrated in Fig. 9.7.

In many OECD countries, activities have been focused on improving capacity factors, achieving power uprates, and extending the lifetime of existing reactors. Depending on the reactor type, the uprate potential for nuclear reactors can be between 2 and 30% of the original licensed capacity. The most common reactor type, the pressurized-water reactor has its uprate potential around 20%. Extensive uprates involve complex plant modifications that may take several years to complete and higher costs. Between 1977 and 2013, the US Nuclear Regulatory Commission approved 149 uprates in the United States, which represented total power around 7 GW corresponding to building 5–7 new large-scale reactors. Most of new builds in recent years have taken place in markets in which electricity prices are regulated or in markets where government-owned entities build, own, and operate plants. In competitive markets, the risks in constructing and operating new plants have been too high to attract investment though some governments have offered subsidies to mitigate these risks. Nuclear power statistics by region based on estimates for 2013 is given in Table 9.4, where the start of construction is the date of the first major placing of concrete. Japan's nuclear reactors are operable, but they have largely been idled since the accident at Fukushima Daiichi in 2011.

The nuclear capacity in operation is mostly constituted by light-water reactors. They are represented by two main types: pressurized-water reactors (PRs), which

Table 9.4 Nuclear power by region based on estimates for 2013

	Operational reactors	Installed capacity (GW)	Electricity generation (TWh)	Share of electricity generation	Under construction (GW)
OECD	324	315	1	961	18%
United States	100	105	822	19%	6.2
France	58	66	424	74%	1.7
Japan*	48	44	9	1%	2.8
Korea	23	22	139	26%	6.6
Canada	19	14	103	16%	0
Germany	9	13	97	15%	0
United Kingdom	16	11	71	20%	0
Other	51	41	297	11%	2.7
Non-OECD	110	78	517	4%	56
Russia	33	25	171	16%	9.1
China	20	17	117	2%	32
Ukraine	15	14	83	44%	2
India	21	5.8	32	3%	4.3
Other	21	16	113	2%	9.5
World	434	392	2478	11%	76

Source: IEA Outlook, 2014
* Although Japan's nuclear reactors are operable, they have largely been idled since the accident at Fukushima Daiichi in March 2011

make up around two-thirds of installed nuclear capacity, and boiling-water reactors (BWRs), which account for about one-fifth. The main difference of mentioned types of reactors is in steam production. BWRs make steam within the reactor core by contact of water with the nuclear fuel assembly. PWRs prevent boiling in the reactor core by keeping the cooling water under high pressure but require an intermediate component called a steam generator to transfer the heat from the core and convert it into steam. Reactor technologies have continued to evolve based on operational experience since the 1950s. The accident forced developers to improve monitoring and safety systems. The stage of development is in broad terms called generations of reactors. The first-generation reactors were built in the 1950s and 1960s followed by the second-generation reactors, which comprise the majority of the reactors in operation today. They were mostly built after 1970. A new series of reactors is represented by the third generation, which first became commercially available in the 1990s and aims to enhance safety in comparison to the preceding systems. The third-generation reactors make up more than half of the capacity under construction globally. Future reactor technologies and associated fuel cycles will seek continued improvements such as aim to optimize the nuclear fuel cycle, which means using fuel resources more efficiently and minimizing the environmental impacts of waste. Other research seeks to increase the temperature at which the reactor operates from about 300 °C to more than 500 °C or even 1000 °C. The fourth-generation
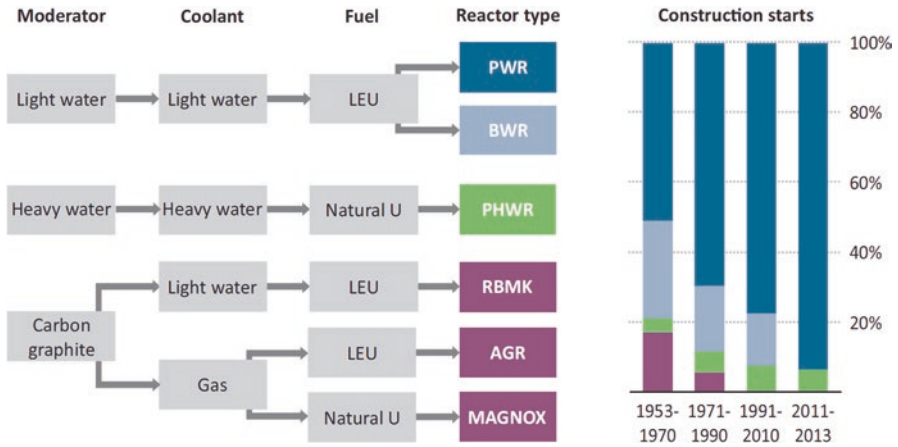
Fig. 9.8 Overview of basic nuclear reactor technologies and their share of construction starts (*LEU*—low-enriched uranium, *Natural U*—natural or slightly enriched uranium, *PWR*—pressurized-water reactor, *BWR*—boiling-water reactor, *PHWR*—pressurized heavy-water reactor, *RBMK*—high power channel-type reactor, *AGR*—advanced gas-cooled reactor, *MAGNOX* magnesium nonoxidizing). Source: IEA Outlook, 2014

reactor concepts seek to make changes to fuel use and spent fuel management. The proposed fast reactors do not use moderators to slow neutrons to encourage a chain reaction, but they require fuel that is enriched to higher levels than in today's reactors. They are also designed to achieve high safety levels by using passive systems and to reduce the lifetime of the produced radioactive wastes. Overview of basic nuclear reactor technologies and their share of construction starts are illustrated in Fig. 9.8.

Government policy is the most crucial for the prospects for nuclear power. Each country has its priorities, which influence energy security, economic and environmental conditions. If there is an opportunity for public involvement in decision-making, government policy can be strongly influenced by public views toward nuclear power development. Finally, economic considerations are a major determinant for construction of a nuclear power plant. It also includes assessment of the lifetime costs of generating electricity by nuclear power in comparison to other power generation technologies, Table 9.5.

Operating costs for nuclear plants consist of the cost of fuel and non-fuel operation and maintenance. The costs for middle-term and long-term radioactive waste disposal and plant decommissioning should also be considered to be operating costs. Some countries have designated funds to cover these expenses, which are set aside during plant operation. Costs in the life cycle of a typical nuclear power plant are illustrated in Fig. 9.9. The timeframe corresponds to the typical period over which a plant is decommissioned and high-level wastes are removed from the plant site to permanent disposal facilities. After operational start, nuclear plants are relatively cheaper to run than coal- and gas-fired plants with higher fuel costs. Due to the high

Table 9.5 Comparison of nuclear power and other power generation technologies

|	Nuclear	Coal steam	Gas CCGT	Wind onshore and solar PV
Investment cost	Very high	Moderate	Low	Moderate-high
Construction time	4–10 years	4–5 years	2–3 years	0.5–2 years
Operational cost	Low	Low-moderate	Low-high	Very low
Operational characteristics	Baseload, limited flexibility	Baseload, moderate flexibility	Mid-load, high flexibility	Variable output, low-load factor
CO_2 emissions	Negligible	High-very high	Moderate	Negligible
Key risks	Regulatory (policy changes), public acceptance, market	Regulatory (CO_2 and pollution), public acceptance, market	Regulatory (CO_2), market	Regulatory (policy changes)

Source: IEA Outlook, 2014
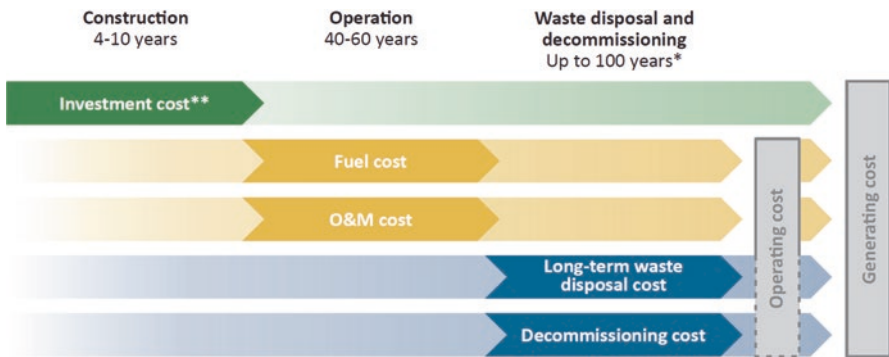
Fig. 9.9 Costs in the life cycle of a nuclear power plant (* timeframe corresponds to the typical period over which a plant is decommissioned and high-level waste is removed from the plant site to a permanent disposal facility; ** the total investment costs including plant construction financing cost). Source: IEA Outlook, 2014

investments costs and the fuel-cycle management, nuclear plants usually generate electricity continuously, in order to recover their large upfront expenditure. The time-frames and subtotal costs for different stages in the life cycle of a nuclear power plant may vary by project and by region. A plant can also incur investment costs during its operation such as refurbishment of technology and monitoring systems, as well as extra costs for higher safety of spent nuclear fuel for long-term disposal after a plant is closed. Nuclear fuel costs include uranium mining (40–50% of the total), conversion (5%), enrichment (25–35%), and fuel fabrication (15–25%). These costs are still lower and less volatile than the cost of fossil-fuel inputs to power generation.

A number of countries, such as the United States, the United Kingdom, Japan, France, Germany, Russia, China, and India, have plans to support investment in new nuclear plants, to grant operational licenses, to provide retirements for old generations

Table 9.6 Related policies and targets in selected countries with operable nuclear reactors

Country	Key policies and targets
Argentina	15–18% share of nuclear in the electricity mix
Belgium	Phase out nuclear by 2025
China	Increase nuclear capacity to 58 GW by 2020 (with further 30 GW under construction); preferential tariffs for electricity generation from new nuclear
France	A new energy law is anticipated in early 2015; it may cap nuclear capacity at the present level, with a view to reducing its share in the electricity mix
Germany	Phase-out nuclear by the end of 2022
India	Increase share of nuclear in electricity mix to 5% by 2020, 12% by 2030, and 25% by 2050
Japan	Reduce reliance on nuclear power, but recognize it as an important source of baseload electricity; potential for operating lifetimes to be extended from 40 to 60 years
Korea	Increase nuclear capacity to 29% of installed capacity by 2035
Russia	Increase nuclear capacity to 50 GW by 2035 (22.5% of electricity mix)
Sweden	Construction of new reactors permitted at existing sites, but only to replace current units
Switzerland	Reactors will not be replaced when they reach the end of their design life, implying a phaseout by 2034
Ukraine	Maintain the current share of nuclear in electricity mix.
United Kingdom	Agreed to a "contract-for-difference" with the EDF that reduces the investment risk for Hinkley Point C (which would be the first new unit built since 1995)
United States	Loan guarantees and production tax credits to support investment in new nuclear; operating license extensions granted to 60 years for most plants

Source: IEA Outlook, 2014

of reactors, as well as to manage fuel waste. The United States provides a number of incentives to support investment in new nuclear plants, which include a loan guarantee fund that is available for up to 80% of the cost of building a new plant and transfers the risk of default to the government. The US government is also planning to provide operating license extensions granted to 60 years for most plants. France is preparing a new energy law that may cap nuclear capacity at the present level with a view to reducing its share in the electricity mix. Some European countries closed older reactors and stopped new projects of nuclear power plants after the accidents in Chernobyl and Fukushima. Some countries (China, Korea, Russia, and India) increase nuclear capacity in order to supply growing energy demands, Table 9.6.

Nuclear power can help to decline the share of fossil fuels in total generation of electricity. The regional trends for electricity produced from coal, however, are quite different from a view of the IEA New Policies Scenario. While OECD countries expect a 44% decline in coal-fired generation from 2013 to 2040, non-OECD countries assume an increase of more than 60%. The reduction of coal use in the both OECD and non-OECD countries reflects action to reduce greenhouse gas emissions and local air pollution, but some non-OECD countries still use coal as a secure, affordable, and reliable way to meet booming electricity demand, Figs. 9.10, 9.11, 9.12, and 9.13.
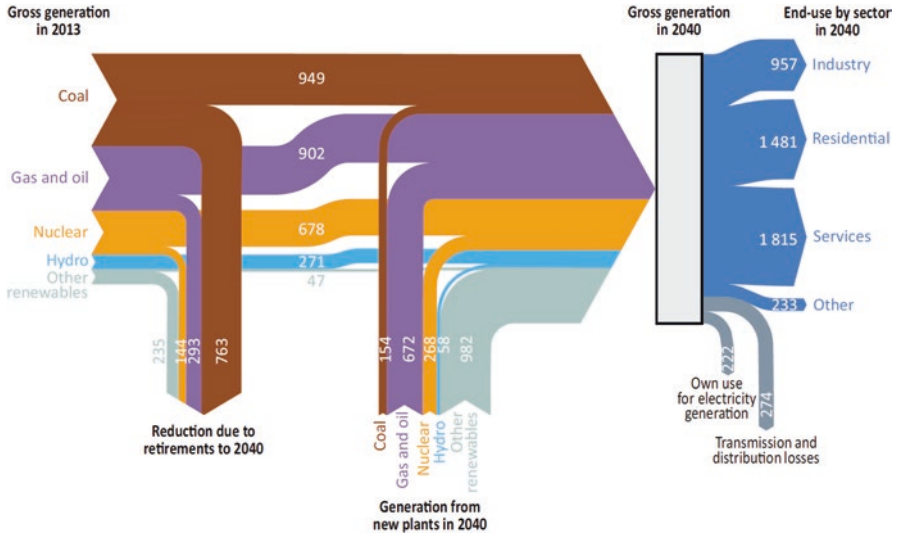
Fig. 9.10 The United States: power generation by fuel and demand by sector (TWh). Source: IEA Outlook, 2015
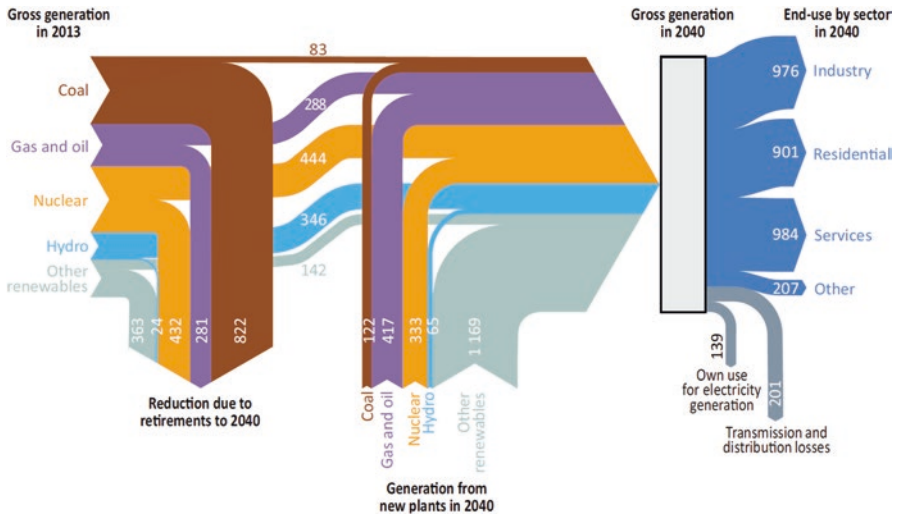

Fig. 9.11 The European Union: power generation by fuel and demand by sector (TWh). Source: IEA Outlook, 2015
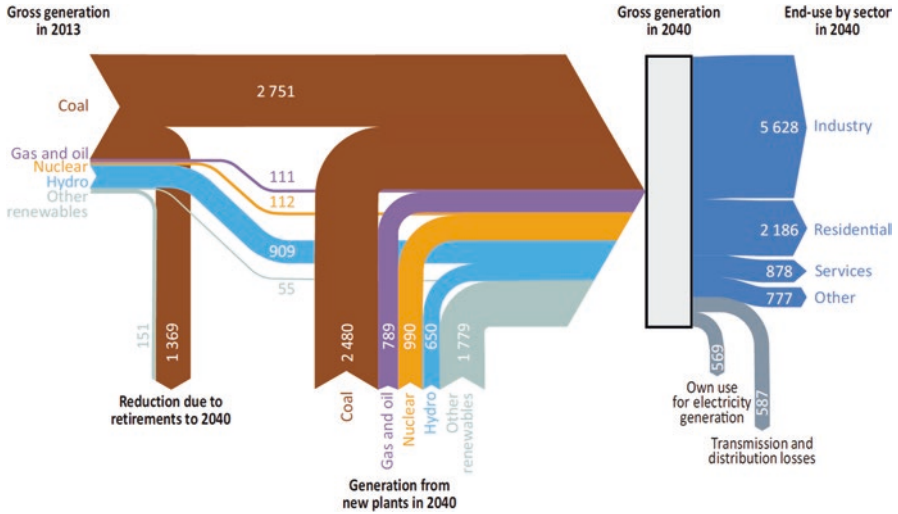
Fig. 9.12 China: power generation by fuel and demand by sector (TWh). Source: IEA Outlook, 2015
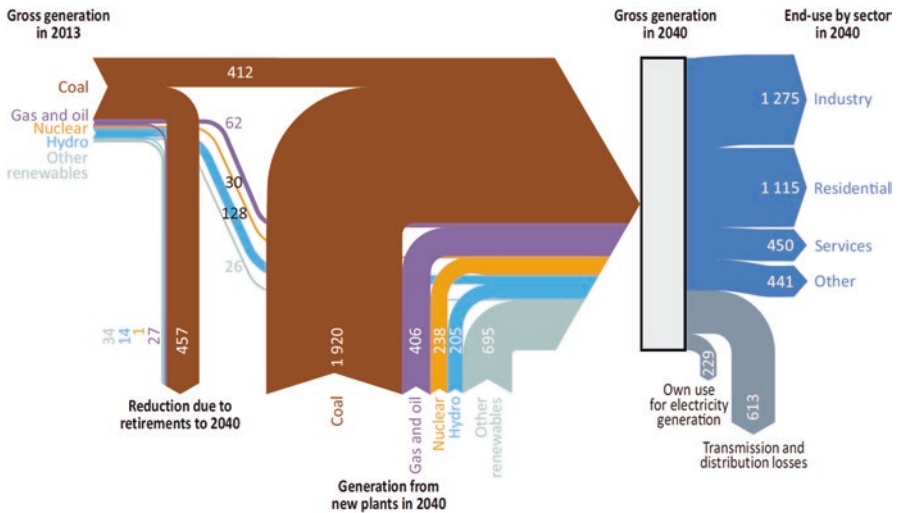

Fig. 9.13 India: power generation by fuel and demand by sector (TWh). Source: IEA Outlook, 2015

9.3   Environmental Effects of Using Nuclear Energy

Nuclear power offers a low-carbon source of electricity generation, and therefore an important option for mitigation of climate change. At the same time, the nuclear fuel-cycle produces radioactive waste that must be safely isolated for centuries to
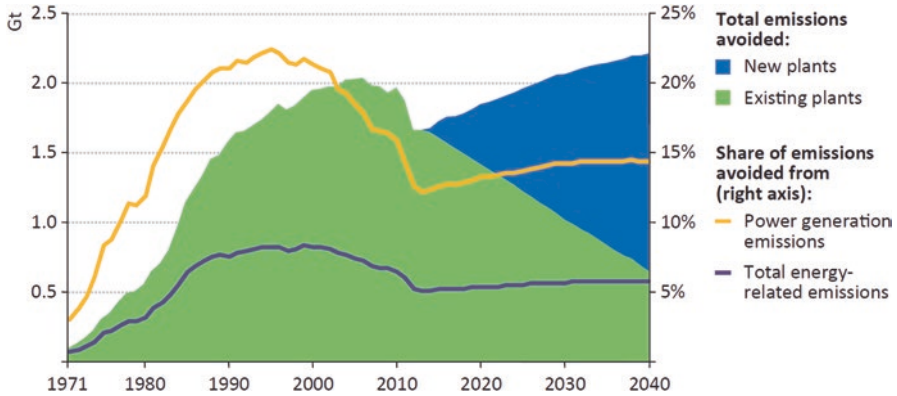
Fig. 9.14 The trends in global energy-related carbon dioxide emissions and carbon dioxide emissions avoided by nuclear in the IEA New Policies Scenario. Source: IEA Outlook, 2014

protect human health and the environment. Nuclear power plants also use large amounts of water for cooling like other thermal power plants, which can be risks to nuclear facilities and stress to local water resources. It produces low greenhouse gas emissions in the period of electricity generation. Some emissions result from the use of fossil fuels at different stages of the nuclear fuel cycle and in plant construction. The gradual de-carbonization of power supply is assumed due to the introduction of more efficient plants and a shift in the power mix toward renewable sources and toward natural gas rather than coal. Nuclear power as a means of limiting carbon dioxide emissions is useful in regions that rely heavily on larger energy sources and plan the substitution for fossil fuels. The trends in global energy-related carbon dioxide emissions and carbon dioxide emissions avoided by nuclear in the IEA New Policies Scenario are shown in Fig. 9.14. It is estimated that nuclear power can avoid the release of over 56 Gt of carbon dioxide globally between 1971 and 2012.

The nuclear fuel cycle generates radioactive waste, which consists of spent nuclear fuel and waste streams from reprocessing. The highly radioactive waste makes its management and disposal the principal challenge at the back-end of the nuclear fuel cycle. Because nuclear wastes remain more radioactive than its natural surroundings for thousands of years, it must be safely isolated to protect human health and the environment. It is estimated that reactors worldwide have generated over 349,000 tonnes of spent nuclear fuel since 1971 and that this is currently increasing by around 9000 tonnes per year (IEA Outlook, 2014). Some of the spent nuclear fuel has been reprocessed in France, Japan, Russia, and the United Kingdom, the rest is in temporary storage at reactor sites or more centralized facilities. The world cumulative spent nuclear fuel discharged since 1971 based on the IEA New Policies Scenario is illustrated in Fig. 9.15.
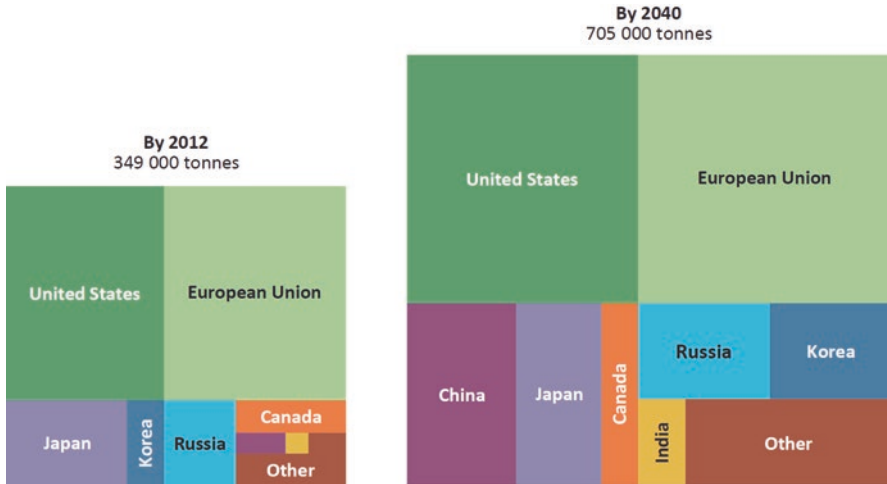
Fig. 9.15 The world cumulative spent nuclear fuel discharged since 1971 based on the IEA New Policies Scenario. Source: IEA Outlook, 2014

9.4   Risk Assessment of Nuclear Power Plants with GIS

The decision-makers in countries with growing economy often turn to nuclear power as the feasible alternative for energy. The site selection is a key phase, which may significantly affect the safety and cost of the facility during its entire life cycle. The siting of nuclear power plants represents one of multi-criteria problems, which makes it complex. GIS can support spatial analysis in order to provide risk assessment of many interrelated factors.

9.5   Case-Oriented Studies

The attached case studies are focused on mapping of existing operational installations of nuclear reactors and main accidents (1957–2011), in order to analyze their potential influence on population in the global and regional scale.

9.5.1   Risk Assessment of Operational Nuclear Installations and Their Global Environmental Impacts

Assessment of nuclear energy sources in the global scale is illustrated in Figs. 9.16 and 9.17 with ArcGIS Online tools. Risk assessment is based on existing nuclear installations over the world and global population density.
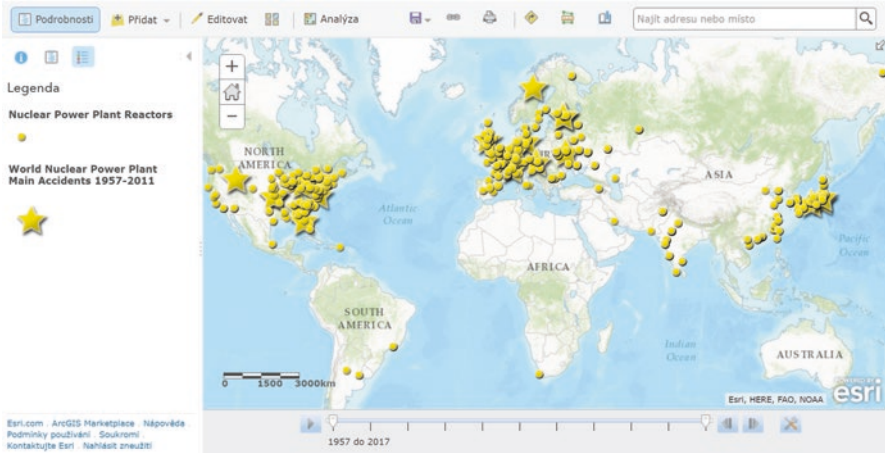
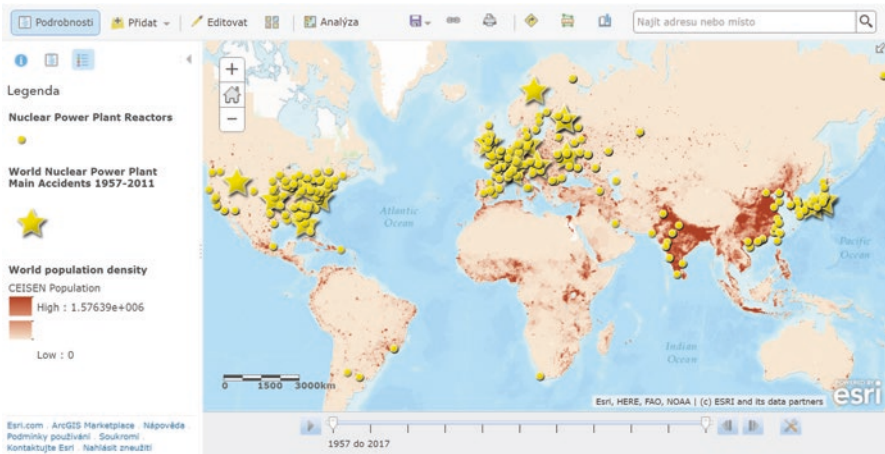**Fig. 9.16** Mapping of installations of nuclear reactors and main accidents (1957–2011) in the global scale

Fig. 9.17 Risk assessment based on world population density, nuclear installations, and main accidents (1957–2011)

9.5.2 Risk Assessment of Operational Nuclear Installations and Their Regional Environmental Impacts

Like in the previous case study, risk assessment is based on existing nuclear installations and population density, but the exploration is provided in the regional scale of a part of Asia. There are a number of new nuclear installations in China and Korea. The spatial distribution of main nuclear accidents is related with

Fukushima I in 2011 and other minor accidents in Japan. The world population density is represented by map layer which is color coded based on the number of persons per square mile (per every 1.609 km^2). Population datasets originate from national population censuses, the UN demographic yearbooks. The nuclear installations in densely populated areas place higher demands on their security (Figs. 9.18 and 9.19).
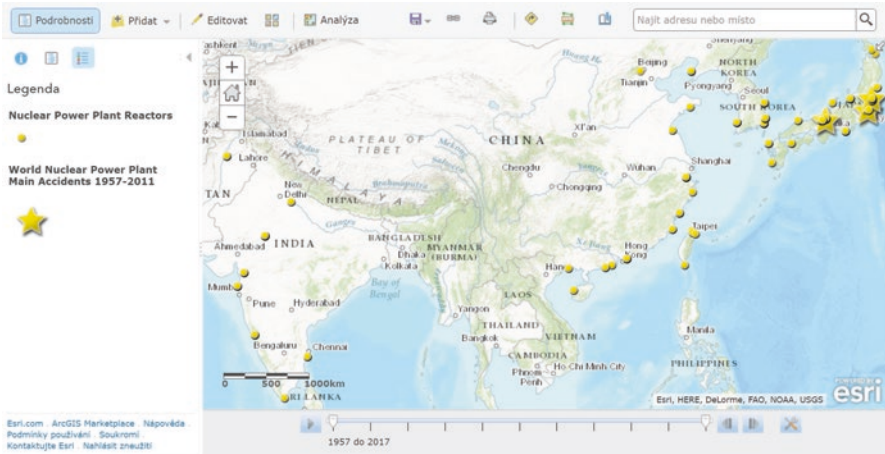

Fig. 9.18 Mapping of installations of nuclear reactors and main accidents (1957–2011) in the regional scale
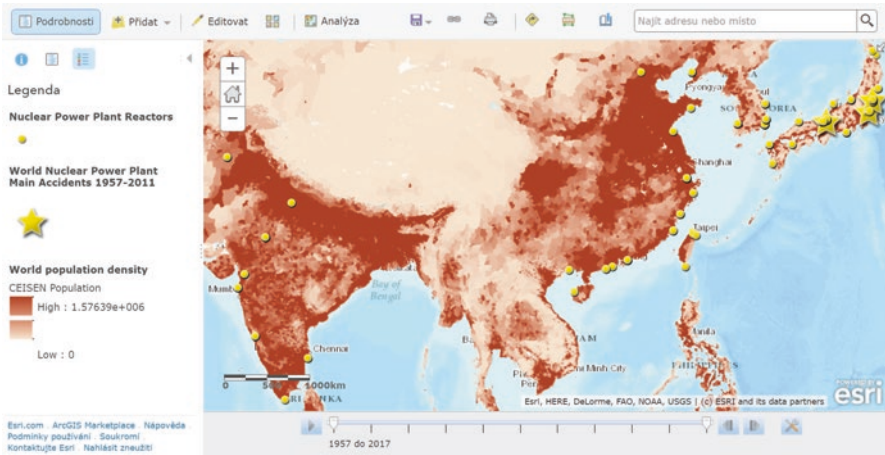

Fig. 9.19 Risk assessment based on world population density, nuclear installations, and main accidents (1957–2011) in the regional scale

Bibliography

Andrews, J., & Jelley, N. (2013). *Energy science: Principles, technologies, and impacts* (2nd ed.). Kindle Edition. Oxford: Oxford University Press.

EIA. (2015). *International energy outlook 2015*. Retrieved from http://www.eia.gov/forecasts/ieo/pdf/0484(2016).pdf

European Commission. (2015). *EU energy in figures: Statistical pocketbook, 2015*. Retrieved from http://ec.europa.eu/energy/sites/ener/files/documents/PocketBook_ENERGY_2015%20PDF%20final.pdf

Fay, J. A., & Golomb, D. S. (2012). *Energy and the environment: Scientific and technological principles* (1st ed.). New York: Oxford University Press.

IAEA. (2015). *Climate change: Making a difference through nuclear technologies*. Retrieved from https://www.iaea.org/sites/default/files/climatechangebulletin-june2015_0.pdf

IAEA. (2016). *Decommissioning and environmental remediation*. Retrieved from https://www.iaea.org/sites/default/files/bull571_april2016_1.pdf

IEA. (2015). *World energy outlook 2014*. Retrieved from https://www.iea.org/bookshop/477-World_Energy_Outlook_2014

IEA. (2016a). *World energy statistics 2016*. Retrieved from http://www.iea.org/bookshop/723-World_Energy_Statistics_2016

IEA. (2016b). *World energy outlook 2015*. Retrieved from https://www.iea.org/bookshop/700-World_Energy_Outlook_2015

IPCC. (2014). *Climate change 2014 mitigation of climate change*. Retrieved from https://www.ipcc.ch/pdf/assessment-report/ar5/wg3/ipcc_wg3_ar5_full.pdf

NEA. (2015). *Nuclear energy: Combating climate change*. Retrieved from https://www.oecd-nea.org/ndd/pubs/2015/7208-climate-change-2015.pdf

NEA. (2016). *Five years after the Fukushima Daiichi accident: Nuclear safety improvements and lessons learnt*. Retrieved from https://www.oecd-nea.org/nsd/pubs/2016/7284-five-years-fukushima.pdf

Tyler, G., & Hicks, P. E. (2012). *Handbook of energy engineering calculations* (1st ed.). Kindle Edition. New York: McGraw-Hill Education.

World Nuclear Association. (2016). *World nuclear performance report 2016*. Retrieved from http://www.world-nuclear.org/our-association/publications/online-reports/world-nuclear-performance-report-2016.aspx

Dictionaries and Encyclopedia

EIA. (2016). *Energy explained: Your guide to understanding energy*. Retrieved from http://www.eia.gov/energyexplained/index.cfm

Data Sources (Revised in September, 2016)

EIA: International Energy Statistics. Retrieved from http://www.eia.gov/cfapps/ipdbproject/IEDIndex3.cfm

International Atomic Energy Agency. (2016). Retrieved from https://www.iaea.org/resources/databases

JAEA Library. (2016). Retrieved from http://tenkai.jaea.go.jp/english/

U.S. NRC Library. (2016). Retrieved from http://www.nrc.gov/reading-rm.html

World Nuclear Association. (2016a). *Reactor database*. Retrieved from http://www.world-nuclear.org/information-library/facts-and-figures/reactor-database.aspx

World Nuclear Association. (2016b). *Information library*. Retrieved from http://www.world-nuclear.org/information-library.aspx

Chapter 10
Energy Storage: Assessment of Selected Tools in Local and Global Scales

Over short periods of time, the amount of generated electricity is relatively fixed, but demand for electricity fluctuates throughout the day. Thus, technology for storing electrical energy is needed to manage the amount of power required to supply customers at times when need is greatest, during peak load. Also it can help to make renewable energy, whose power output cannot be controlled by grid operators, without interruptions of power supply and smooth. Suitable local energy storage can balance microgrids to achieve a good match between generation and load. Storage devices can achieve a more reliable power supply for industrial facilities, and hold considerable promise for transforming the electric power industry. Energy storage technology is applied to a wide range of areas that differ in power and energy requirements. It includes batteries, electrochemical capacitors, superconducting magnetic storage, pumped-storage hydroelectricity, and flywheels. Also new technology seeks to improve energy storage density in electrolytes and nano-structured electrodes.

10.1 Electricity Transmission, Distribution, and Storage Systems

Energy storage technologies can support energy security, as well as climate change goals by providing valuable services in energy systems. Their approach will lead to more integrated and optimized energy systems by improving energy resource use efficiency, helping to integrate higher levels of variable renewable resources, supporting higher production of energy where it is consumed, increasing energy access, and improving electricity grid stability and flexibility. While some energy storage technologies, such as pumped hydroelectric reservoirs, are well tried, most are still in the early stages of development and currently struggle to compete with other non-storage technologies due to high costs. But, governments can help accelerate the research and deployment of energy storage technologies by supporting targeted promising projects. The actual status of energy storage technologies
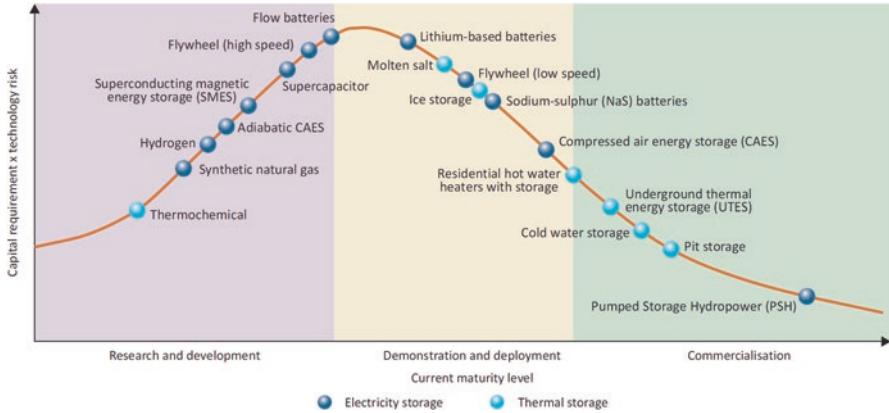
Fig. 10.1 The actual status of energy storage technologies. Source: IEA Technology Roadmap: Energy Storage, 2014

divided into research and development phase, demonstration and deployment level, and commercial utilization is illustrated in Fig. 10.1.

Generally, energy storage systems can absorb energy and store it for a period of time before releasing it to supply power devices. Through this process, storage systems can bridge temporal gaps between energy supply and demand. Energy storage devices can be utilized on large and small scales in distributed and centralized manners throughout the energy grid. Energy storage technologies are used to be categorized by output, which can be electricity or thermal. Energy storage deployment can be developed across the supply, transmission and distribution, and demand parts of the energy system. The best location for individual storage device depends on the services these technologies will supply to specific locations in the energy grid. The smart grid and other new energy infrastructure technologies may impact the structure for storage systems in the future. The basic schema for storage deployment is illustrated in Fig. 10.2, which contains utilization of storage systems across the supply, transmission and distribution, and demand parts of the grid.

10.2   Energy Storage Principles

The current global installed capacity for energy storage struggle from a lack of accessible datasets as well as conflicting definitions of various technologies. Some datasets exist in the United States, Japan, and some regions in Europe for a specific subset of energy storage technologies such as large-scale, grid-connected electricity storage systems. These datasets indicate that at least 140 GW of large-scale energy storage is currently installed in electricity grids over the world. The majority about 99% of this capacity comprises pumped-storage hydropower. The rest about 1% covers a mix of other storage systems, such as battery, compressed air energy
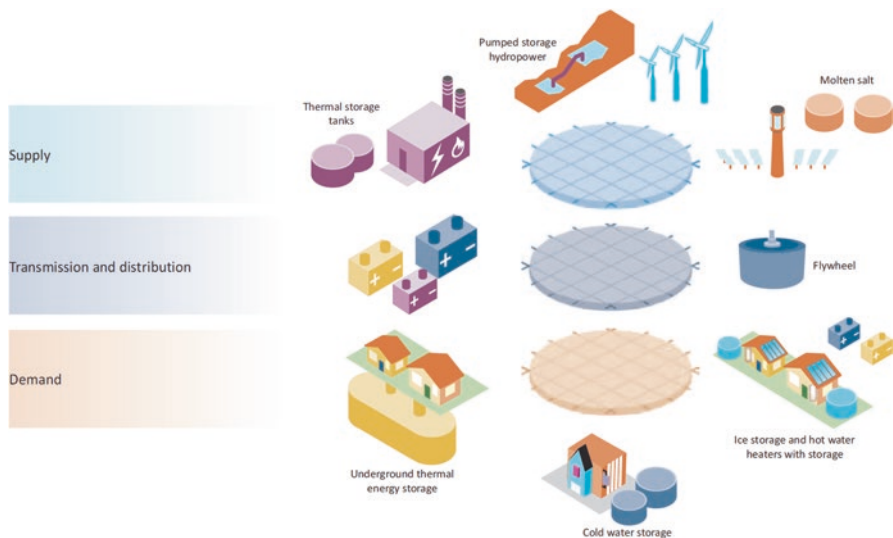
Fig. 10.2 The basic schema for storage deployment with utilization of storage systems across the supply, transmission and distribution, and demand parts of the grid. Source: IEA Technology Roadmap: Energy Storage, 2014
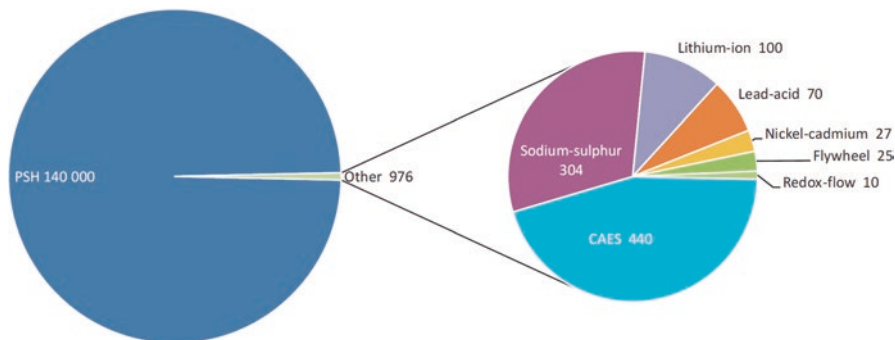

Fig. 10.3 Global installed grid-connected electricity storage capacity in MW (*PSH* pumped-storage hydropower, *CAES* compressed air energy storage). Source: IEA Technology Roadmap: Energy Storage, 2014

storage, and a wide range of various minor systems, Fig. 10.3. Energy storage systems are also utilized for thermal energy storage applications such as domestic hot water tanks, or ice and chilled water storage. Underground thermal energy storage systems are frequently used in Canada, Germany, and other European countries.

Electricity storage systems are used to be grouped into three main time categories: short-term, long-term, and distributed battery storage. The short-term storage systems have high cycle lives and power densities, but lower energy densities. Thus, they are best suited for supplying of short bursts of electricity in the energy grids.

These storage systems (supercapacitors and superconducting magnetic energy storage) are still great challenge for research and development. The long-term storage systems have been the most widespread method for long-term electricity storage for several decades. These technologies often require high upfront investment costs due to typically large project sizes and geographic requirements (pumped-storage hydropower or compressed air energy storage). There are a number of systems in commercial operation. The distributed battery storage can be used for both short- and long-term applications and benefits from being highly scalable and efficient. It has already achieved limited deployment in both distributed and centralized systems for mobile and stationary applications at varying scales. Widespread deployment is hampered by challenges in energy density, power performance, lifetime, charging capabilities, and costs. A specific technology is represented by hydrogen storage that can be used for long-term energy applications, where electricity is converted into hydrogen, stored, and then reconverted into the desired end-use form. These storage systems have significant potential due to their high energy density, quick response times, and potential for use in large-scale energy storage applications, but a lack of existing infrastructure for large-scale applications such as hydrogen storage for fuel-cell vehicles is available in the local and regional scales. A list of selected energy storage systems for electricity and thermal storage is presented in Table 10.1.

Thermal storage systems can store thermal energy for later use as heating or cooling capacity in applications such as seasonal storage. Some thermal energy storage technologies have already realized significant levels of utilization in electricity and heat networks. In dependence on an operational temperature, the thermal storage devices are utilized as low-temperature (<10 °C) applications, medium temperature (10–250 °C), and high-temperature (>250 °C) applications. Low-temperature applications represent cold-water storage tanks in commercial and industrial facilities that are already installed around the world to supply cooling capacity. Underground thermal energy storage systems have been successfully developed in order to provide both heating and cooling capacity in countries such as Canada, Germany, the Netherlands, and Sweden. Low-temperature applications also provide thermochemical storage based on reversible chemical reactions, where the cooling capacity is stored in the form of chemical compounds. It can achieve higher energy storage densities and is used for the transportation of temperature-sensitive products. The medium temperature applications have been utilized, for example, in New Zealand, Australia, and France that use storage capabilities in electric hot water storage heaters. The underground thermal energy storage systems have been successfully deployed on a commercial scale to provide heating capacity in the Netherlands, Norway, and Canada. Also thermochemical storage systems can discharge thermal energy at different temperatures, which make them an appealing option for medium temperature applications. The high-temperature applications are based on molten salts, which can be used, for example, to dispatch power from concentrating solar power facilities by storing several hours of thermal energy for use in electricity generation. But the high-temperature thermochemical energy storage and waste heat utilization systems offer many potential opportunities.

Table 10.1 Description of selected energy storage systems

Pumped-storage hydropower (PSH)	– Utilizes elevation changes to store energy for later use. Water is pumped from a reservoir at a lower elevation to a reservoir at a higher elevation during off-peak periods. Subsequently, water can flow back down to the lower reservoir, generating electricity like in a conventional hydropower plant
Compressed air energy storage (CAES)	– Utilizes pressure changes to store energy for later use. Systems use off-peak electricity to compress air, storing it in underground caverns or storage tanks. This air is later released to a combustor in a gas turbine to generate electricity during peak periods
Batteries	– Use chemical reactions with two or more electrochemical cells to enable the flow of electrons. Many types of batteries have been developed during a few decades. The current technologies are dealing often with lithium-based batteries
Chemical-hydrogen storage	– Uses hydrogen as an energy carrier to store electricity, for example, through electrolysis. Electricity is converted, stored, and then reconverted into the desired end-use form, which can be electricity, heat, or liquid fuel
Flywheels	– Store electricity as rotational energy. Flywheels are mechanical devices that spin at high speeds. This energy is later released by slowing down the flywheel's rotor, releasing quick bursts of energy
Supercapacitors	– Store energy in large electrostatic fields between two conductive plates separated by a small distance. Electricity can be quickly stored and released using this technology in order to produce short bursts of power
Superconducting magnetic energy storage (SMES)	– Stores energy in a magnetic field. This field is created by the flow of direct current (DC) electricity into a super-cooled coil. In low-temperature superconducting materials, electric currents encounter almost no resistance, so they can cycle through the coil of superconducting wire for a long time without losing energy
Hot/cold-water storage in tanks	– Meet heating or cooling demand. The devices are highly used in domestic hot water heaters, which frequently include storage in the form of insulated water tanks
Thermochemical storage	– Uses reversible chemical reactions to store thermal energy in the form of chemical compounds. Energy can be discharged at different temperatures, dependent on the properties of the thermochemical reaction
Ice storage	– Is a form of the latent heat storage based on a material phase change as it stores and releases energy. It refers to transition of a medium between solid, liquid, and gas states
Solid media storage	– Store energy in a solid material for later use in heating or cooling such as bricks or concrete. Some electric heaters also include solid media storage to assist in regulating heat demand
Underground thermal energy storage (UTES)	– Pump heated or cooled water underground for later use as a heating or cooling resource. Water is pumped into (and out of) either an existing aquifers or man-made boreholes

Source: IEA Technology Roadmap: Energy Storage, 2014.

Fig. 10.4 The Seneca pumped-storage generating station in northwest Pennsylvania takes advantage of the local topographical conditions by filling a reservoir at a higher elevation than the dam below. Source: Google Earth, 2016

The future utilizations of storage systems will depend on improving the technologies and costs drop, the implementation of new pricing and valuation schemes for the services storage, and the cost and efficiency of alternatives. The next description contains a few examples of pumped-storage hydropower (PSH) that represents a long-proven storage technology, but the facilities are very expensive to build, may cause environmental impacts, and extensive permitting procedures. Furthermore, it requires the site with specific topologic and geologic conditions. An example of operational pumped hydroelectric reservoirs in Pennsylvania is illustrated in Fig. 10.4. It takes advantage of the local topographical conditions. The device can be operated as a 435 MW hydroelectric power plant, generating power to supply demand for electricity during the daytime peak hours. Overnight, a reversible hydroelectric turbine is powered by low-cost electricity and provides pumping water from the lower reservoir up to the upper reservoir.

Another relatively proven storage technology is represented by compressed air energy storage (CAES), which provides an efficient solution to meeting peak requirements by taking advantage of lower cost, off-peak energy to generate energy during peak demand periods. An example of an operational device is shown in Fig. 10.5. A 110 MW plant with a capacity of 26 h was built in McIntosh, Alabama in 1991. The storage capacity is about a 19 million cubic foot solution mined salt cavern. The expansion phase requires combustion of natural gas at one-third the rate of a gas turbine producing the same amount of electricity.

A high-temperature application based on thermal energy storage to continue generating electricity is illustrated in Fig 10.6. The solar power station (150 MW) uses a thermal storage system, which absorbs a part of the heat produced in the solar field

Fig. 10.5 Compressed air energy storage at McIntosh power plant in Alabama. Source: PowerSouth Energy Cooperative, A Touchstone Energy Cooperative, 2016, http://wwwpowersouth.com

Fig. 10.6 The Andasol solar power station (150 MW), Europe's first commercial plant to use parabolic troughs, located near Guadix in Andalusia, Spain. Source: Google Earth, 2016

during the day. This heat is then stored in a molten salt mixture (60% sodium nitrate and 40% potassium nitrate) in order to produce electricity by a turbine when the sky is overcast. It almost doubles the number of operational hours at the solar thermal

Fig. 10.7 Tesla Gigafactory (planned annual battery production capacity of 35 GWh). Source: https://www.tesla.com/, 2016

power plant per year. A fully loaded storage system can hold around 1 GWh of heat, enough to run the turbine for about 7.5 h at full-load, in case it rains or after sunset.

Battery, which uses chemical reactions to enable electrical energy, is widely used in many mobile electronic applications. Rechargeable batteries can be charged, discharged into a load, and recharged many times, while a non-rechargeable batteries are supplied fully charged, and discarded once discharged. Batteries are produced in many shapes and sizes, ranging from button cells to megawatt systems that are used to stabilize an electrical distribution networks. A number of different combinations of electrode materials and electrolytes are used, such as lead–acid, nickel cadmium (NiCd), nickel metal hydride (NiMH), lithium ion (Li-ion), and lithium ion polymer (Li-ion polymer). An example focused on automobile industry, Tesla Gigafactory, is illustrated in Fig. 10.7. The name Gigafactory comes from the factory's planned annual battery production capacity of 35 GWh. This mission is to accelerate the world's transition to sustainable energy in order to produce power for electric vehicles in sufficient volume to force change in the automobile industry. There is planned production rate of 500,000 cars per year.

Flywheels store electricity as rotational energy. They can be utilized in a continuously variable transmission. For example, trains can use energy, which is recovered from the drive train during braking and stored in a flywheel. This stored energy is then used during acceleration. In motor sports, this energy can be used to improve acceleration, but the same technology can be applied to road cars to improve fuel efficiency and reduce emissions, Fig. 10.8.

Advanced energy storage technologies are currently limited in use by higher production costs and represent great challenge to practical utilization. Besides pumped hydroelectric storage, majority of the storage technologies are in the early stages of development for widespread utilization. They can serve an array of functions around

Fig. 10.8 A flybrid
systems kinetic energy
recovery system built for
use in formula one. Source:
Wikimedia, 2016
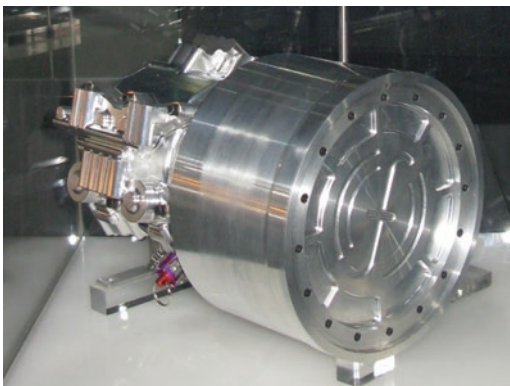
the electric power system, from assuring power quality to deferring electric power
system infrastructure upgrades to integrating variable generation from wind and
solar generators. Without stored electricity or heat, power system operators must
increase or decrease generation to meet the changing demand in order to maintain
acceptable levels of power quality and reliability. Currently, generating capacity is
set aside as reserve capacity to provide a buffer against fluctuations in demand. In
that way, if the reserve capacity is needed, it can be dispatched or sent to the grid
without delay. There are extra costs, at times significant, to requiring the availability
of generating capacity to provide reserves and regulation of power quality. But, the
efficient way of utilization of energy storage systems could eliminate the need for
extra generating capacity to fill that role.

Existing or potential storage technologies are adapted for different uses. Electricity
storage technologies are designed to respond to changes in the demand for electric-
ity, which can be provided on different timescales. Approximate comparison of
described power energy storage principles to capacity and discharge time is shown
in Fig. 10.9. The pumped hydroelectric storage or compressed air energy storage
represent higher capacity technologies capable of outputting electricity for extended
periods of time in order to moderate the extremes of demand over longer timescales.
Demand fluctuations on shorter timescales of a few minutes down to fractions of a
second can be supplied by rapidly responding technologies, such as flywheels,
supercapacitors, or a variety of batteries, which are often of smaller capacity.

10.3   Environmental Effects of Using Selected Storage Systems

Utilization of storage systems brings indirect environmental benefits. The electri-
city storage systems can help to integrate more renewable energy into the electricity
grid and to reduce use of less efficient generating units that would otherwise only
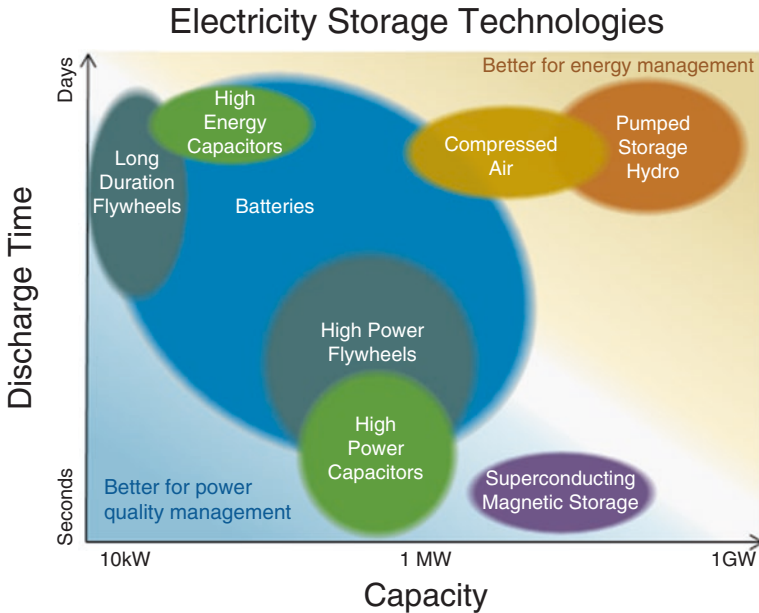
Electricity Storage Technologies

Fig. 10.9 Approximate comparison of described power energy storage principles to capacity and discharge time. Source: EIA, Today in Energy, December 2011, http://www.eia.gov/todayinenergy/detail.cfm?id=4310

run at peak times. Furthermore, the added capacity by electricity storage can decrease the need to build additional power plants or transmission lines. The negative impacts of storage systems depend on the type and efficiency of storage technology. For example, large pumped hydroelectric storages can influence local ecosystems like hydropower plants. In case of batteries, the use of raw materials, such as lithium and lead, can cause potential environmental hazards if they are not disposed of or recycled properly. In addition, some electricity is wasted during the storage process. An approximate comparison of environmental effects of using selected storage systems with conventional energy technologies is illustrated in Fig. 10.10. It aggregates values from individual projects and the final impacts in particular cases can be slightly different in dependence on local conditions. These issues are also discussed in the framework of the Energy Technology Perspectives (ETP) 2DS, which describes transformation of technologies across all energy sectors by 2050 to give an 80% chance of limiting average global temperature increase to 2 °C. The scenario sets the target of cutting energy-related carbon dioxide emissions by more than half by 2050 (compared with 2009). Energy storage will compete with other options in the energy grids to provide the flexibility needed to accommodate the energy resources, which sets the context for the vision for future storage technologies.
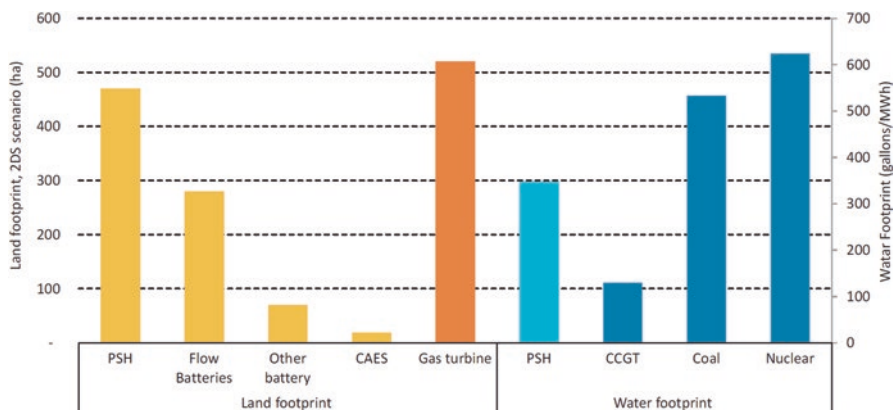
Fig. 10.10 An approximate comparison of environmental effects of using selected storage systems with conventional energy technologies (*PSH* pumped-storage hydropower, *CAES* compressed air energy storage, *CCGT* combined cycle gas turbine). Source: IEA Technology Roadmap: Energy storage, 2014

10.4   Case-Oriented Studies

Increased electricity generation from renewables, such as wind power and photovoltaic, requires development of energy storage systems, in order to integrate highly variable renewable energy into the grid. Only large-scale energy storage systems, such as pumped-storage hydropower and compressed air energy storage, can help to increase the penetration of renewables. Besides increased energy storage capacity, a number of other benefits include black start capabilities, grid stability, spinning and auxiliary reserve, peak shaving, and regulation control.

GIS can help to explore possibilities of using energy storage systems, such as pumped-storage hydropower or compressed air energy storage, which are geographically related to suitable places. The significant role of GIS is also in the risk assessment stages of project development. The resulting analysis can provide information about environmental perspective of storing electricity from renewables and consequent reduction in carbon dioxide production.

10.4.1   Environmental Evaluation of Selected Energy Storage Installations for Electricity Grids

The attached case study is focused on utilization of pumped-storage hydropower (PSH) and compressed air energy storage (CAES). Information about environmental impacts is derived from the report "Environmental performance of existing energy storage installations,", which has been produced in the framework of a

project "Facilitating energy storage to allow high penetration of intermittent renewable energy" (www.store-project.eu). The magnitude of the environmental impacts for selected categories was classified to three levels such as high, medium, and low. The high level represents a significant impact by its character, magnitude, and duration or intensity, which alters a sensitive aspect of the environment. The medium level is related to a moderate impact, which alters the character of the environment in a manner that is consistent with existing and emerging trends. The low level is without noticeable consequences or represents a slight impact, which causes noticeable changes without affecting its sensitivity. The evaluation is presented for six selected installations of energy storage systems located in Europe: five different PHS in terms of age, technology, and environmental conditions, and only one CAES, Table 10.2.

The identified direct and indirect environmental impacts during operation are summarized in Fig. 10.11. The presented negative environmental impacts are dealing with human impacts, effects on ecology and natural systems, and links to physical environment. The list of selected environmental impacts can be complemented by other phenomena in dependence on a particular installation. Due to the life span of the presented energy storage systems, most impacts associated with their operation are proposed to be long term.

The benefits of described storage systems based on PSH and CAES from an environmental perspective are a partial elimination of the variability of electricity production (mainly from renewable sources), and an overall consequent reduction in carbon dioxide production. The Huntorf CAES facility indicates very few environmental impacts during operation, but it is a hybrid system, which is dependent on an external heat source (natural gas) to replace the heat lost during the compression stage. The remaining PSH systems can have high negative impacts on ecology and natural systems, as well as on physical environment related to the construction of a dam for hydro generation results in alteration of the natural flow regime of the river. The heavily modified environment by previously constructed dams results in a significantly lower environmental impact of the PSH.

10.4.2   Mapping of Environmental Impacts with GIS for the Energy Storage Installation Kopswerk II

The topography of the Alps is well suited for hydropower and pumped-storage hydropower (PSH). The PSH Kopswerk II can be integrated into the electricity grid with renewables not only in Austria but also in its neighboring regions in Germany. Kopswerk II is an open PSH with its upper reservoir, the Kops, at a height of 1800 m, which boasts a storage capacity of 127 GWh. The lower reservoir, the Rifa, is located approximately 800 m below, Fig. 10.12. Assessment of environmental impacts in ArcGIS Online is based on CORINE Land Cover shown in Fig. 10.13, the satellite image in Fig. 10.14, and changes of Normalized Difference Vegetation Index (NDVI) shown in Fig. 10.15.

Table 10.2 Selected installations of energy storage systems for environmental evaluation located in Europe

Type, location, and commissioning	Description of energy a storage system, installed capacity, and its potential environmental impacts
CAES, Huntorf (Northwest of Germany in Niedersachsen), commissioned in 1978	It is the first CAES facility installed worldwide. The installed capacity of 290 MW was upgraded to 321 MW in 2007. It has a storage capacity of 0.64 GWh and has the ability to operate at peak load for about 2 h per day. It uses two large underground salt caverns to store the compressed air. Each of the caverns is located at a depth between 650–800 m and is approximately 40 m in diameter. During decompression, the system requires natural gas, as its external heat source, to recover the stored compressed air. Due to extra energy for compression and heating during decompression, this type of CAES is therefore not considered to be a pure electricity storage technology, but rather a hybrid system
PSH, Thissavros (Greece, Nestos River Basin), basin is already regulated with dams in Bulgaria, commissioned in 1997	It has an installed capacity of 381 MW and provides electricity generation, peak power, and water for irrigation together with a further dam downstream of Thissavros called Platanovrisi (commissioned in 1999). Although habitat loss due to land inundation to create Thissavros reservoir is an impact of construction, the long-term effects on flora and fauna are attributed to the operational phase. Since Thissavros does not have a fish pass to facilitate fish migration, it causes ecosystem isolation in Platanovrisi and Thissavros reservoirs. The dam has also inhibited the river role in sediment transport. Thus, the beaches in the delta region have been found to have much higher erosion rates
PSH, Kopswerk II (Austria in the region of Vorarlberg), commissioned in 2008	An installed capacity is 450 MW. The facility utilizes the already-existing upper reservoir, Kops and the lower reservoir, Rifa. Thus, no extra impoundment was needed to operate Kopswerk II. The pre-developed environment was already changed to such a degree that the addition of Kopswerk II has brought very little environmental impact during operation. But the water level in the Kops has fluctuated more frequently since the addition of Kopswerk II as the storage system operates on a daily basis
PSH, Goldisthal (Germany, River Schwarza), commissioned in 2003	The facility has an installed capacity of 1060 MW. The lower dam also boasts a small hydropower facility that produces an additional 1.6 GWh annually from the water discharged to the downstream environment. The upper reservoir is situated approximately 300 m above the lower reservoir. Now, the system is deconstructed to allow for free fish passage along the river Schwarza and Saale
PSH, Bolarque II (Spain, Tagus River), commissioned in 1975	It utilizes the already existing Bolarque reservoir as the lower reservoir (commissioned in 1910). Upstream are two further dams Entrepenas and Buendia, and downstream of Bolarque dam is another dam Zorita. Bujeda reservoir was created as the upper reservoir almost 300 m above. Thus, the storage system was constructed into an already highly stressed and regulated environment. From this point of view, Bolarque II has almost no environmental impacts during operation
PSH, Turlough Hill (Ireland), commissioned in 1974	It utilizes the existing lake, Lough Nahanagan as the lower reservoir, and the man-made upper reservoir is located 300 m above. The installed capacity is 292 MW. The main environmental impact is daily lowering of the lower lake during pumping mode, which affects the shore line vegetation in terms of species cover

Source: "Facilitating energy storage to allow high penetration of intermittent renewable energy" (www.store-project.eu)

		CAES	Pump-back PHES	Semi-open PHES			Closed-loop PHES
Potential Issues/EIA terms of reference		Huntorf	Thissavros	Kopswerk2	Goldisthal	Bolarque2	Turlough Hill
Human Impact	Population	L	L	L	L	L	L
	Traffic	L	L	L	L	L	L
	Cultural Heritage	L	L	L	L	L	L
	Material Assets	L	L	L	L	L	L
Ecology and Natural Systems	Biodiversity	L	H	L	H	L	H
	Fisheries	L	H	L	M	L	M
	Air and Climate	L-H*	L-H*	L-H*	L-H*	L-H*	L-H*
	Landscape and Visuals	L	M	L	M	M	M
	Water Resources & Quality	L	H	L	M	L	M
Physical Environment	Noise & Vibration	L	L	L	L	L	L
	Soils, Geology & Sediment Transport	L	H	L	M	L	L
	Hydrology & Hydrogeology	L	H	M	H	L	H

- Recommended to review each individual case study
- Inclusion of combined impacts with existing land uses and pressures
- Limited raw data

Fig. 10.11 Summary of negative environmental impacts during operation highlighted by case studies (PHES—pumped hydro energy storage source marked in text as PSH—pumped-storage hydropower). Source: www.store-project.eu

Land use mapping is based on CORINE Land Cover (CLC), which is a geographic land cover/land use database encompassing most of the countries of Europe. An inventory of land cover in 44 classes is organized hierarchically in three levels at a scale of 1:100,000. The first level (five classes) corresponds to the main categories of the land cover/land use, such as artificial areas, agricultural land, forests and semi-natural areas, wetlands, and water surfaces. The second level (15 classes) covers physical and physiognomic entities at a higher level of detail. The third level composed of 44 classes, which are presented in this study for classes of the forest semi-natural areas, is shown in Fig. 10.13. Data layers on land cover are useful for the environment policy, regional development, and agriculture, as well as for impact assessment of the described pumped-storage hydropower. It can also provide information on other themes, such as soil erosion, and vegetation disturbance.

Vegetation analysis is provided by satellite image's band combination (5 4 3), which is helpful for vegetation studies. It complements CORINE Land Cover data and gives a view on living condition of vegetation. In Fig. 10.14, healthy vegetation is symbolized by bright green and soils are mauve. The used image was compiled from Global Land Survey (GLS) datasets, which were created by
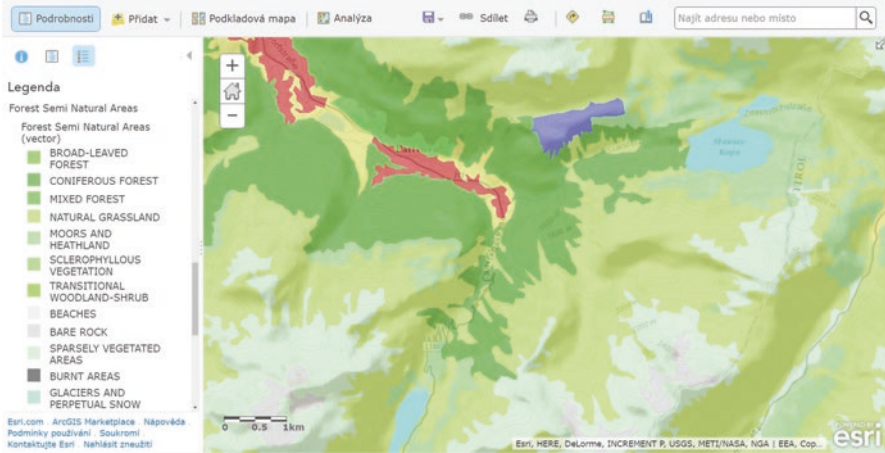
Fig. 10.12 Kopswerk II with its upper reservoir, the Kops (*right side* of an image), and its lower reservoir, the Rifa (*left side* of an image); complex run-off system Vorarlberg. Source: Google Earth, 2016; Illwerke vkw, 2008

the U.S. Geological Survey (USGS) and the National Aeronautics and Space Administration (NASA) using Landsat images. The data layers can support global assessments of land cover, land cover-change, and ecosystem dynamics such as disturbance and vegetation health.

The vegetation changes in period 1990–2005 are highlighted by using the NDVI as shown in Fig. 10.15. In spite of that the described pumped-storage hydropower

Fig. 10.13 Assessment of environmental impacts based on CORINE Land Cover in ArcGIS Online
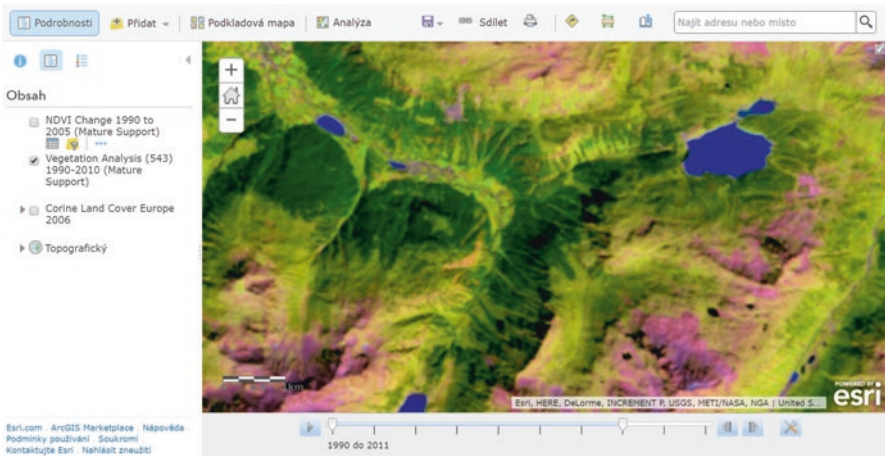
Fig. 10.14 Assessment of environmental impacts based on Landsat image bands (5 4 3) in ArcGIS Online

was commissioned in 2008, it can provide impact assessment of the hydropower systems operating before or in those years. The changes are generated by combining multi-temporal imagery of Global Land Survey (GLS) Landsat NDVI, where red, green, and blue color in the color composition is linked to NDVI in 2005, NDVI in 1990, and NDVI in 2005, respectively. Most areas in the image will be grey, indicating no change because each pixel has relatively the same value in each band. Areas that show up green were brighter in 2005, while areas that show up in magenta were brighter in 1990 than 2005.
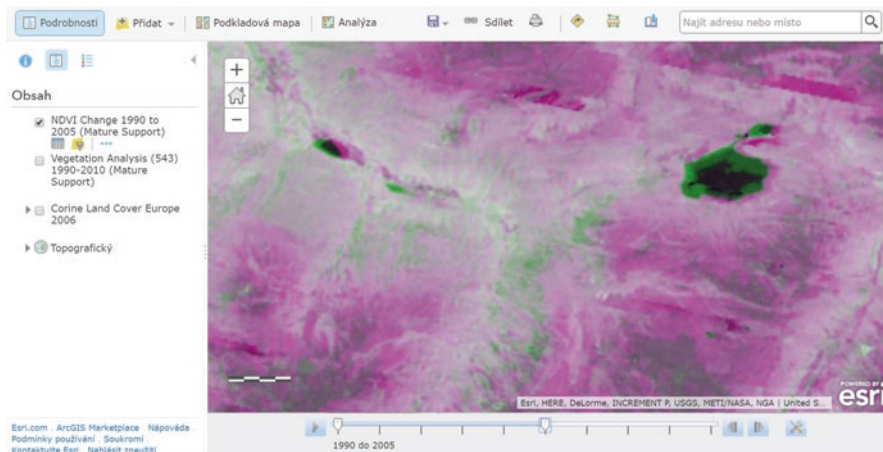
Fig. 10.15 Assessment of environmental impacts based on NDVI changes in the period 1990–2010 in ArcGIS Online

Kopswerk II is part of a more complex system of hydropower plants and reservoirs common in the alpine region. The Kops reservoir functions as an annual storage for the hydropower systems connected to it and as daily peaking storage for Kopswerk II. Kopswerk II consists of three sets of Pelton turbines, pumps, and generators with the installed capacity of 450 MW, but at Kopswerk II the turbines and pumps are separate in comparison to the most pumped-storage hydropower systems that have the turbine and pump integrated into one machine. This set up allows Kopswerk II to utilize the principle of hydraulic short circuit during pumping mode (Illwerke vkw, 2010).

The surrounding area of the reservoir Kops is sparsely populated by smaller towns. The most dominant features are hills, forests, and rivers. Thus, the human impacts are negligible.

The area around the Kops is designated as Natura 2000 site with a number of protected birds. The water has low levels of organic or inorganic nutrients with no significant oxygen deficit. Fish do not naturally occur, and do not reproduce as water temperature in the Kops reservoir is too low. Thus, rainbow trout is introduced into the reservoir for recreational fishing. Fish deaths have been observed in the upper reservoir due to high fluctuations in water levels where isolated areas can become dried out. Also, the impacts on ecology and natural systems are minimal.

Sediment transport has been an issue in the Kops reservoir about 10 years ago, due to weathering sediments flowing into the Kops during major and minor rainfall events, avalanches, and snowmelts. But sediment management has helped to prevent serious consequences of sediment accumulating in front of spillways.

Kopswerk II utilizes an already-existing upper and lower reservoir and its own operating environmental impacts of pumped-storage hydropower are low. It also confirms impact assessment based on remote sensing data, which is introduced in this case study.

Bibliography

Andrews, J., & Jelley, N. (2013). *Energy science: Principles, technologies, and impacts* (2nd ed.). Kindle Edition. Oxford: Oxford University Press.

EIA. (2015). *International energy outlook* 2015. Retrieved from http://www.eia.gov/forecasts/ieo/pdf/0484(2016).pdf

European Commission. (2015). *EU energy in figures: Statistical pocketbook*, 2015. Retrieved from http://ec.europa.eu/energy/sites/ener/files/documents/PocketBook_ENERGY_2015%20PDF%20final.pdf

European Commission. (2016). *DG ener working paper: The future role and challenges of energy storage*. Retrieved from https://ec.europa.eu/energy/sites/ener/files/energy_storage.pdf

HSBC. (2014). *Energy storage: Power to the people*. Retrieved from http://www.qualenergia.it/sites/default/files/articolo-doc/Energy%20Storage.pdf

IEA. (2014a). *Technology roadmap energy storage*. Retrieved from https://www.iea.org/publications/freepublications/publication/TechnologyRoadmapEnergystorage.pdf

IEA. (2014b). *Energy storage technology roadmap technology annex*. Retrieved from https://www.iea.org/media/freepublications/technologyroadmaps/AnnexA_TechnologyAnnexforweb.pdf

IEA. (2014c). *Energy technology perspectives 2014 harnessing electricity's potential*. Retrieved from http://www.iea.org/publications/freepublications/publication/EnergyTechnologyPerspectives2014.pdf

IEA. (2015). *World energy outlook* 2014. Retrieved from https://www.iea.org/bookshop/477-World_Energy_Outlook_2014

IEA. (2016a). *Energy technology perspectives 2016—Towards sustainable urban energy systems*. Retrieved from http://www.iea.org/bookshop/719-Energy_Technology_Perspectives_2016

IEA. (2016b). *World energy statistics* 2016. Retrieved from http://www.iea.org/bookshop/723-World_Energy_Statistics_2016

IEA. (2016c). *World energy outlook* 2015. Retrieved from https://www.iea.org/bookshop/700-World_Energy_Outlook_2015

IEC. (2011a). *Electrical energy storage*. Retrieved from http://www.iec.ch/whitepaper/pdf/iecWP-energystorage-LR-en.pdf

IEC. (2011b). *Smart grid standardization roadmap*. Retrieved from http://www.iec.ch/smartgrid/downloads/sg3_roadmap.pdf

Illwerke VKW. (2010). *Kopswerk II Das Grösste Pumpspeicherkraftwerk der Vorarlberger Illwerke AG*.

IRENA. (2015). *Renewables and electricity storage: A technology roadmap for REmap 2030*. Retrieved from https://www.irena.org/DocumentDownloads/Publications/IRENA_REmap_Electricity_Storage_2015.pdf

IVA. (2016). *Energy storage: Electricity storage technologies, IVA's electricity crossroads project*. Retrieved from http://www.iva.se/globalassets/rapporter/vagval-el/201604-iva-vagvalel-ellagring-rapport-english-e-ny.pdf

Landry, M., & Gagnona, Y. (2015). Energy storage: Technology applications and policy options. *Energy Procedia, 79*, 315–320.

Pacific Northwest Nationa Laboratory. (2013). *Compressed air energy storage: Grid-scale technology for renewables integration in the Pacific Northwest*. Retrieved from http://caes.pnnl.gov/pdf/PNNL-22235-FL.pdf

Store. (2012). *Facilitating energy storage to allow high penetration of intermittent renewable energy*. Retrieved from www.store-project.eu

Dictionaries and Encyclopedia

EIA. (2016). *Energy explained: Your guide to understanding energy*. Retrieved from http://www.eia.gov/energyexplained/index.cfm

Data Sources (Revised in September, 2016)

ECES. Retrieved from http://www.iea-eces.org/homepage.html

EIA. *International energy statistics*. Retrieved from http://www.eia.gov/cfapps/ipdbproject/IEDIndex3.cfm

PowerSouth Energy Cooperative. (2016). *Compressed air energy storage*. McIntosh Power Plant, Alabama. Retrieved from http://www.powersouth.com/files/CAES%20Brochure%20[FINAL].pdf

Chapter 11
Advanced Assessment Tools for Spatial and Temporal Analysis of Energy Systems

Spatial and temporal modeling can be extended by other computer tools focused on optimization of fuel and power supply. Multi-criteria analysis is used for regional energy planning and development because the optimization of energy systems requires physical, economic, environmental, and social considerations. The more complex energy supply models can be used for predicting the feature. They deal with technological innovations and efficiency improvements, which can provide better optimization on the local and global scale. Many of the assessment tools are used to support decision-making. Renewable energy sources can be included in the models as a component that helps to reduce the environmental impacts of energy consumption. In order to develop an efficient power grid, it is important to know the exact capacity of various renewable energy sources because each renewable energy source has a different energy generation capacity. Optimized deployment of innovated existing power sources and renewable energy sources will reduce the operational and maintenance costs of the energy generated units. In general, cost minimization and power maximization under defined environmental restrictions are the two main objectives in the described assessment tools.

11.1 Integration of Spatial and Temporal Data in a Geodatabase

Research in this area combines expertise in GIS, economics, and engineering to provide analysis and model prediction. The way energy is converted, provided, and consumed has an enduring impact on the environment and economy. It requires the development of clean and cost-effective energy sources that continue to support economic growth while attaining climate policy objectives. In order to provide effective development and management of such energy supplies, multi-criteria analysis including spatial and time interaction is needed to generate new knowledge on the interdependencies and interactions between policymakers, energy suppliers, and consumers.
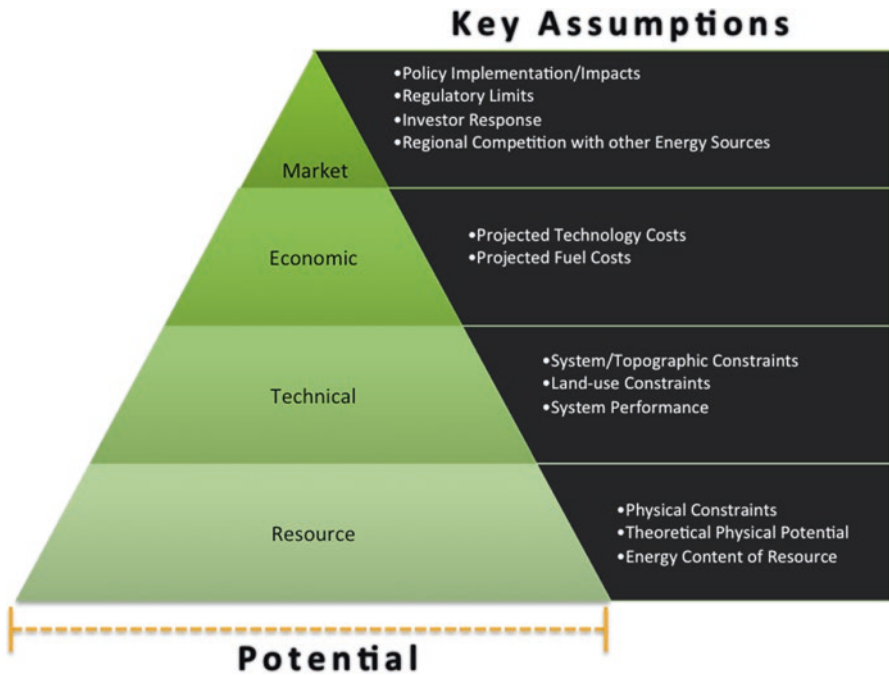
Fig. 11.1 The relations of key assumptions illustrated by the pyramid multilevel structure, which includes key assumptions on the level of resource, technical, economic, and market conditions. Source: Technical Report NREL/TP-6A20-51946, July 2012, http://www.nrel.gov/docs/fy12osti/51946.pdf

It includes multiple aspects of energy policy containing market regulation, infrastructure, and factors influencing consumer adoption of new technologies. The relations of key assumptions are illustrated by the pyramid structure in Fig. 11.1.

The GIS results provided by thematic maps can better visually inform developers, environmentalists, and public, in order to support a healthier and safer environment. There are many prepared model templates on the ArcGIS platform, such as energy utilities, environmental regulated facilities, petroleum, pipeline, and transportation (http://support.esri.com/technical-article/000011644). For example, ArcGIS Electric Distribution contains ready-to-use data models that can be configured and customized for use at electric utilities. A keystone of this new data model is superior modeling of electric devices and circuits that capture the behavior of real-world objects such as transformers and feeders.

11.2   Assessment of Renewables by Multi-Criteria Analysis in the GIS Environment

Sustainable concept in energy systems requires balanced conditions between energy, the economy, and environmental and social aspects. Future energy systems require an optimized solution among emissions, supply security, and the market economy.

Recent attention focused on global warming and fluctuations in energy prices caused by the great concentration of fossil resources in politically unstable regions have increased the interest in renewables and clean combustion technology. In order to achieve sustainability without compromising the potential for future generations, new analyses based on energy-economic models are needed on the scale of regional energy policies, renewable energy systems, and the regional environment.

11.2.1   Spatial Analysis and Modeling

Multi-criteria analysis for regional energy planning and development has been used for a number of decades. Formerly, a number of modeling tools were developed in response to the first oil embargo. Recently, global warming has become one of the most significant topics for decision-makers. These models have been developed to predict the impact of increased carbon dioxide concentrations on the climate and to present alternative economic strategies for minimizing emissions. The optimization of energy systems requires both economic and environmental considerations. The more complex energy-economic models are not only numerical tools for predicting the future, but also management tools for decision-making that include information about environmentally sound technologies. They deal with multidisciplinary fields that encompass the economy and the environment (Nakata, 2004). Technological innovations and efficiency improvements implemented in these models can provide better optimizations on the local and global scale.

Renewables are well recognized in models as a component, which can reduce the environmental impacts of energy consumption, as well as improves the local economy and increases public participation in local environmental management. Many countries are significantly focused on this research because of the need to comply with regulations requiring increases in renewable energy sources as a percentage of the overall power supply. In this case, renewables can be used for many applications, such as heating and generation of electricity with minimum greenhouse gas emissions. In comparison with conventional fossil fuel-based power-generating systems, the energy-generating units associated with renewables are less reliable because of their variable supply. But integration of renewables coupled with conventional fossil fuel-based sources can improve reliability in regular energy supply on a regional scale. Thus, renewables by themselves are often extended to include an energy storage system that encompasses hybrid renewable energy sources, as their electricity generation capacity depends on location and time. In order to develop an efficient power grid, it is important for the regional authority to know the exact capacity of various renewable energy sources because each renewable energy source has a different electricity generation capacity. Optimized deployment of renewables can reduce the operational and maintenance costs of the energy-generating units. In general, cost minimization and power maximization under defined environmental and social restrictions are the two main objectives for development power supply grids. Many analyses and optimization techniques have been proposed for balancing these two objectives and a number of studies have been published about the methods and tools used to evaluate the availability of renewable energy.

The increasing attention paid to the role of small decentralized renewable energy developments can play an important role in the expansion of renewable energy sources and alter energy-consumption behavior through active community engagement. Remote sensing and GIS-based techniques are often used to develop a methodology for evaluation of the regional-scale potential for community-based renewable energy sources. This approach combines a range of technologies including hydropower, wind power, solar photovoltaic and bioenergy. Spatial analysis of satellite and aerial images together with existing map layers encompass a mix of localized renewable energy developments. GIS can support spatial multi-criteria analysis and assessment for siting wind and solar farms and biomass plants. It can also support the evaluation of potential renewable energy from installed developments in relation to solar and wind potential and biomass potential from energy crops on a regional scale.

11.2.2   Input Datasets for Assessment of Potential Energy Sources Using GIS

The assessment of potential energy sources using GIS can determine which land cover classes are affiliated with high solar, wind, hydro, and biomass potential over a period of several decades. The remote sensing data and multi-criteria GIS modeling techniques are used to identify sites, which are suitable for solar farms, wind and biofuel production, and small hydro energy plants. The input data layers are complemented by multispectral images captured by Landsat satellites in the 1985–2016 period.

The area of interest for the presented case study encompasses surface coal mines in the northwestern region of the Czech Republic in Europe, where the impacts of surface mining and reclamation constitute a dominant force in land cover changes. The area covers approximately 1875 km^2, Fig. 11.2. Massive surface mining has been carried out regularly since the early 1970s. Environmental remediation has been performed at selected sites since the 1990s.

The satellite images are used to evaluate the biomass potential using the Normalized Difference Vegetation Index (NDVI). The images captured by Landsat satellites in 1990 (Landsat 5 TM), 2000 (Landsat 7 ETM+), 2006 (Landsat 5 TM), and 2011 (Landsat 5 TM) and corresponding NDVI layers are illustrated in Fig. 11.3. The satellite images are complemented by data layers from the CORINE (Coordination of information on the environment) land cover project for land cover mapping in 1990 and 2000 in Fig. 11.4, and 2006 and 2012 in Fig. 11.5. The CORINE land cover nomenclature is used for selection of mineral extraction sites (1.3.1.), dump sites (1.3.2.), and all the agricultural classes (2.x.x.) that take priority over other land cover classes for utilization of renewable energy sources.

The principal input spatial datasets for wind power, and solar energy represents estimation of the average wind speed 100 m above the surface, and average solar energy per year, respectively, which is illustrated by data layers in Fig. 11.6. It complements mapping of weirs, which can be used for utilization of small hydro energy plants, together with the population density and transport, in order to optimize energy supply in the local scale, Fig. 11.7.
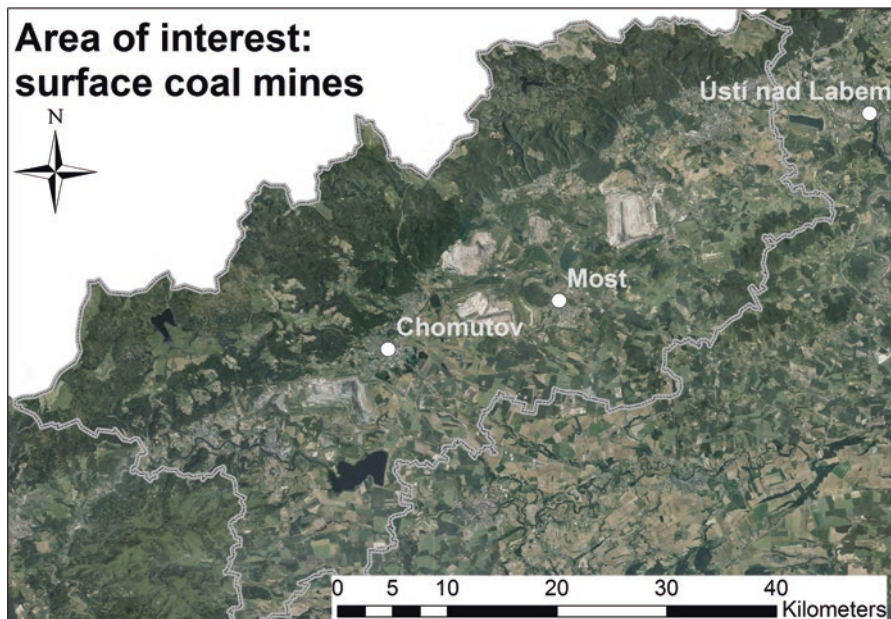
Fig. 11.2 The area of interest for the presented case study encompasses surface coal mines in the northwestern region of the Czech Republic in Europe, the impacts of surface mining and reclamation constitute a dominant force in land cover changes

11.2.3   Spatial Data Processing and Multi-Criteria Analysis in the GIS Environment

The described multi-criteria analysis is based on GIS spatial methods and functions. It contains a few steps that include creation of the GIS project with the input datasets and the appropriate output data layers, transforming input datasets into the required data formats, and reclassification of the potential energy supply from renewables, weighting the spatial datasets according to a percentage influence, and combining weighted spatial datasets to produce a map displaying suitable locations of renewables. While a map layer for each source of renewable energy shows the relative energy contribution, the application of multi-criteria analysis can indicate the overall accessibility of renewable energy and suitability of using renewables at each site. The input spatial datasets for multi-criteria analysis must be reclassified to a common scale and processed with raster algebra tools to identify suitable sites.

Reclassification of solar energy within a range of 1–10 is based on the yearly sum of global irradiation on horizontal inclined surface. It represents the 10-year average for the 1981–1990 period, and all the data values are given as kWh m^{-2}. The original data within the range 970–1010 kWh m^{-2} are divided into ten equal intervals, which are linked to the values (1–10) for subsequent processing with multi-criteria analysis.
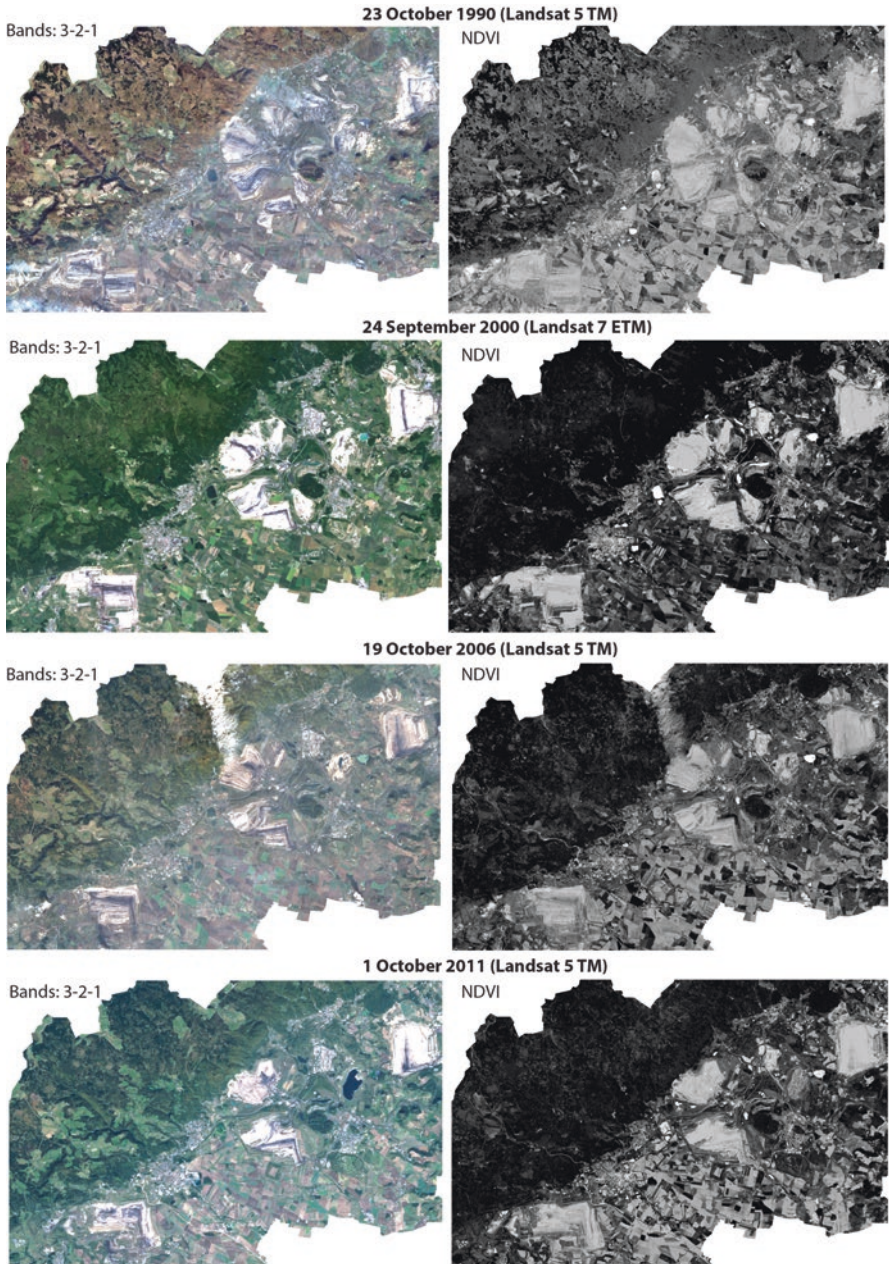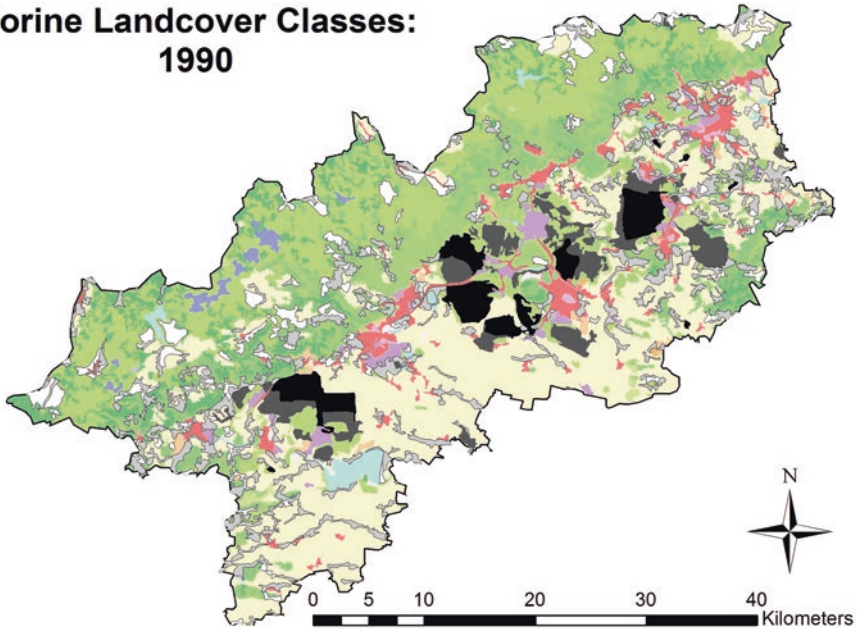
Fig. 11.3 Multispectral images: 1990 Landsat 5 TM, 2000 Landsat 7 ETM+, 2006 Landsat 5 TM, 2011 Landsat 5 TM (on the *left side*) complemented by corresponding NDVI images (on the *right side*)
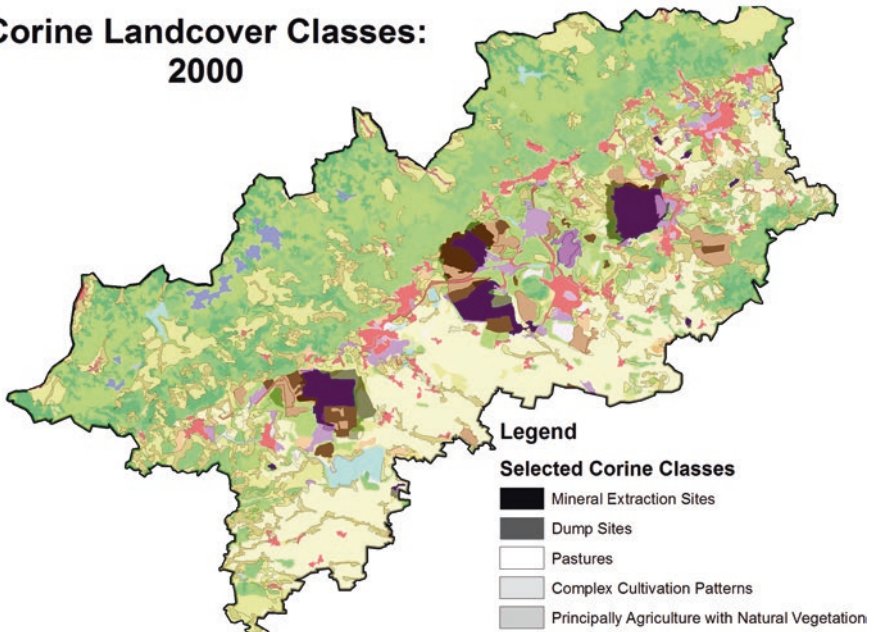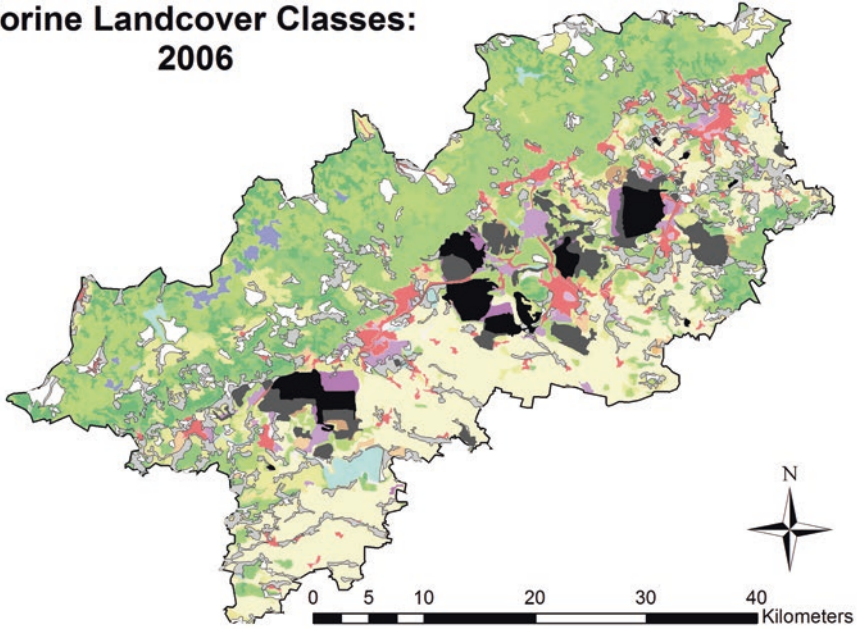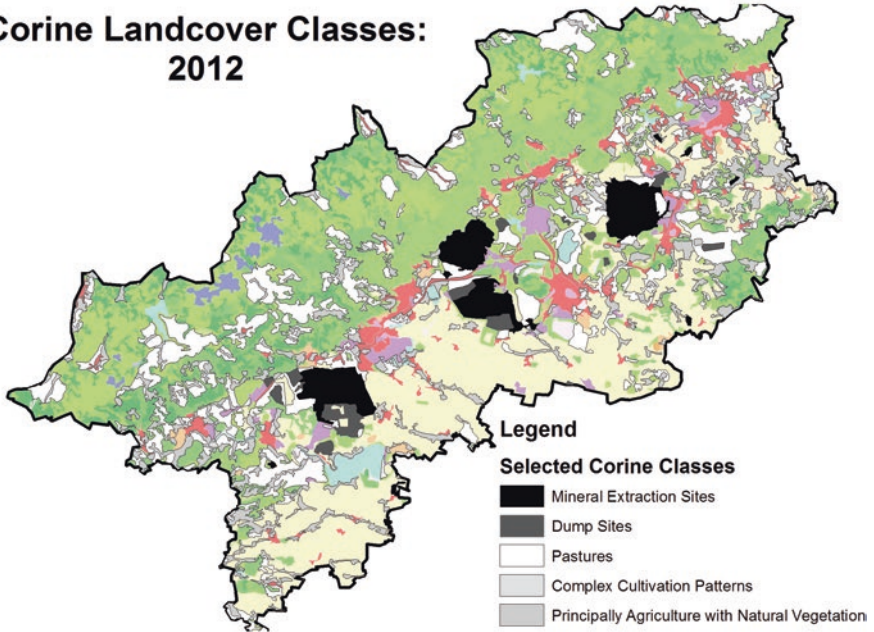
Fig. 11.4 Land cover mapping in 1990 and 2000 (CORINE), where the mineral extraction sites, dump sites, and all the agricultural classes that take priority over other land cover classes for utilization of renewables

Fig. 11.5 Land cover mapping in 2006 and 2012 (CORINE), where the mineral extraction sites, dump sites, and all the agricultural classes that take priority over other land cover classes for utilization of renewables
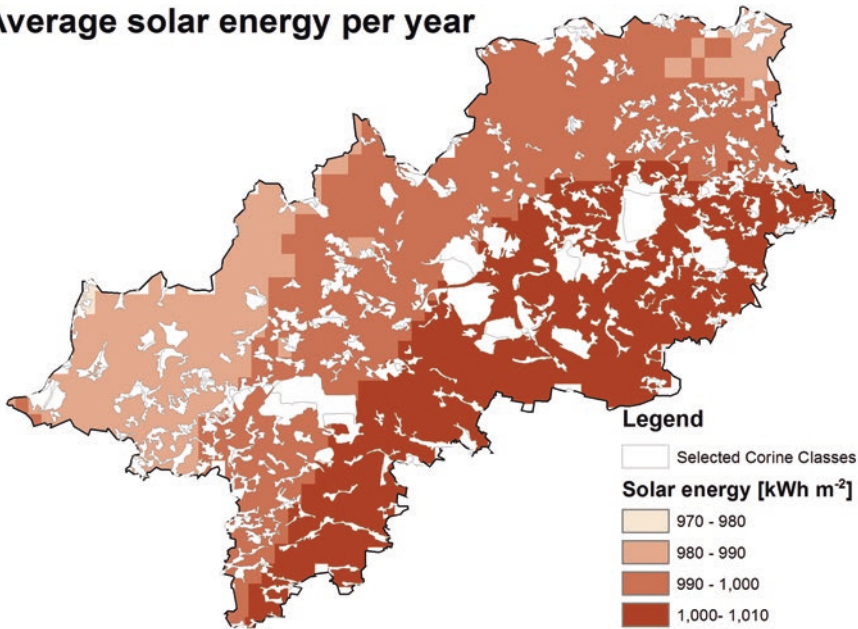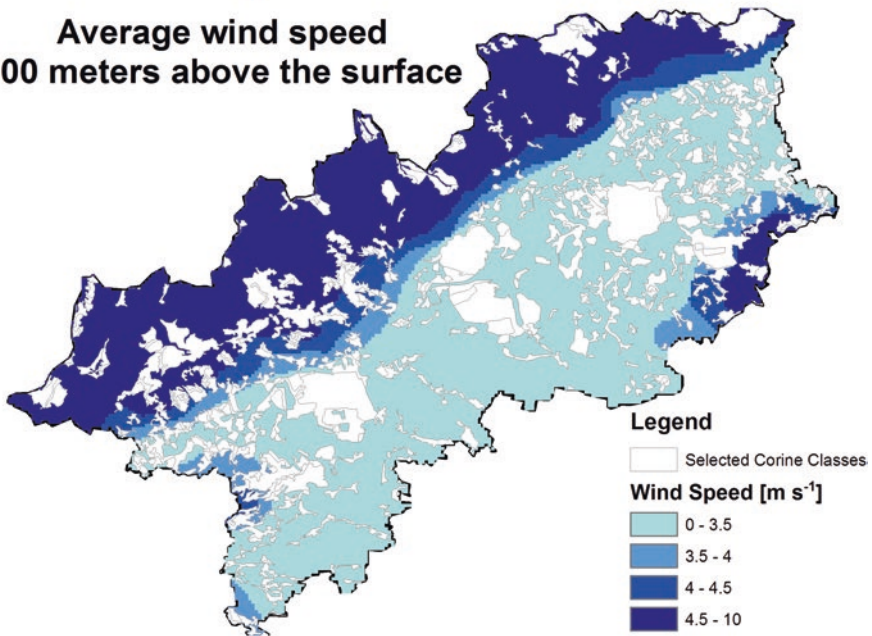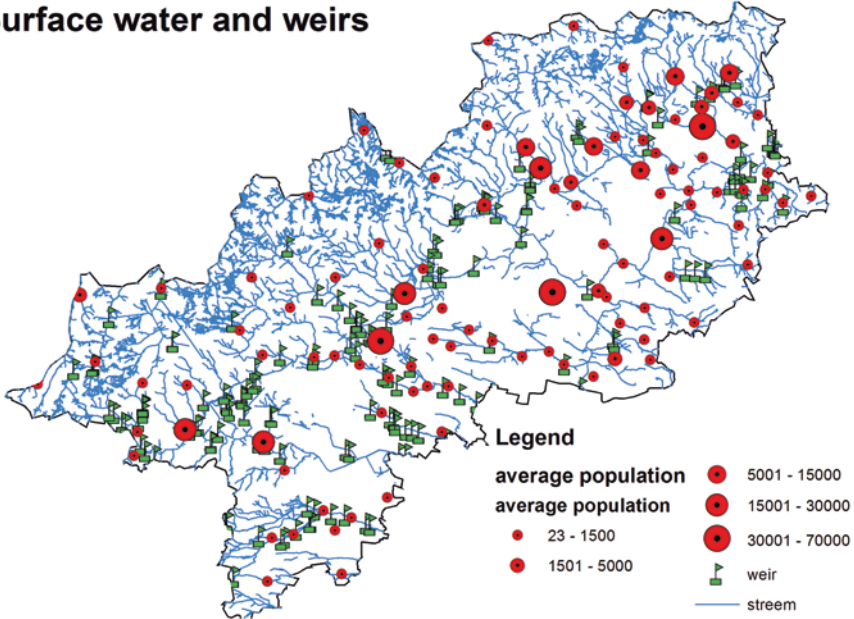
Fig. 11.6 Estimation of the average wind speed 100 m above the surface and the average solar energy per year

Surface water and weirs
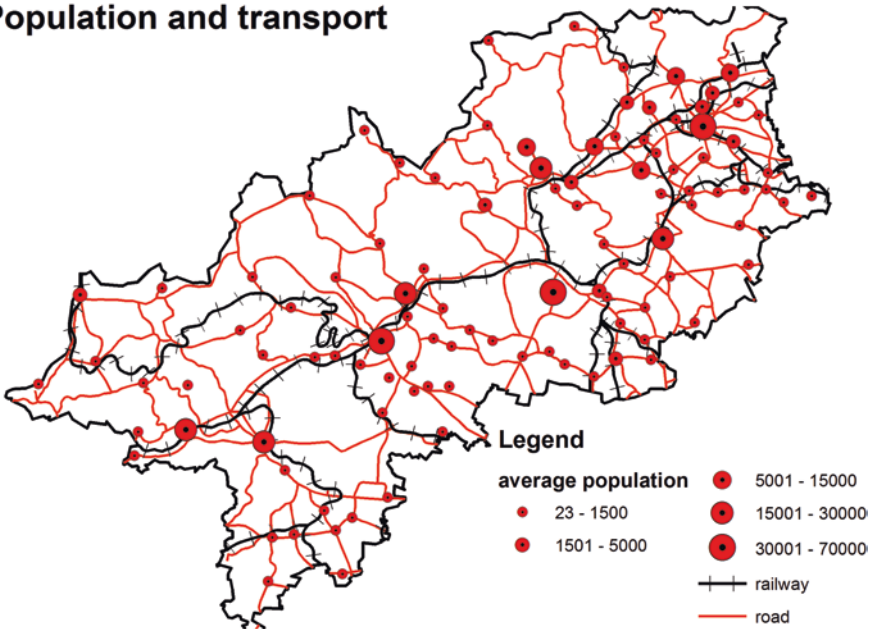

Population and transport

Fig. 11.7 Mapping of weirs, which can be used for utilization of small hydro energy plants, together with the population density and transport, in order to optimize energy supply in the local scale

Reclassification of wind potential in the same range of the values (1–10) is derived from the wind speed 100 m above the surface. The original data are based on mathematical models and presented through the Web Map Service (WMS) on the Internet.

The hydropower is based on the location of weirs as potential sites for utilization of small hydro energy plants. Because of the high variability of surface water flows during the analyzed period of 1985–2015, the reclassification of available hydro energy is based on a distance from the nearest small hydro energy plant, which can dominate in economic and market calculations. Thus, the grid of distances created for the whole region is reclassified within the same range of the values (1–10).

Reclassification of the biomass potential within the range of the values (1–10) employs NDVI, which is used for a simplified estimate of the live green vegetation. A dense vegetation canopy tends to positive values. Reclassification of the biomass potential within the range of the values (1–10) is used experimentally for a positive value of NDVI (0–1). The negative values are appended to class 1 in the range of the values (1–10).

After establishing a common scale for reclassified datasets, the map algebra is used to combine them to rate each subarea in the grid of the region. The average values of four input classified datasets represent the rates for cells in the grid. In this step, the values of the input grids can be weighted in order to change the equal percentage influence. In the next step, the number of suitable sites is reduced by land cover classes from CORINE to mining sites and agricultural areas. The output grid indicates suitable locations for utilization of renewables on a scale of preferences.

Due to the massive mining activities in the last decades, the presented case study is also focused on long-term land cover changes in 1985–2015. But the multi-criteria analysis for land cover classes in 1990, 2000, 2006, and 2012 shows only moderate changes in the mapping of suitable sites for utilization of selected renewables. Finally, the results represent map layers showing the energy availability on the scale of a number of preference classes (1–7), where the first class is linked to a minimum and the last class to a maximum for 1990, 2000, 2006, and 2012, Fig. 11.8. These classes are linked to output classes (3–10) of the multi-criteria analysis (classes 1–2 are excluded due to the low availability of renewable energy). The attached histograms show moderate variability of preference classes due to the land cover changes caused by mining activities and mapping of the biomass potential by NDVI. The results in the histograms also indicate a slight increase in more preferable classes for utilization of renewable energy.

11.2.4   Final Comments and Recommendations

The southern part of the region has greater potential for solar development. This part also contains the majority of agricultural flatland, which can be used for larger solar development. The density of settlements becomes applicable for this source of renewable energy. The middle part also contains a large area of surface mines with mine disposal and remediation sites.
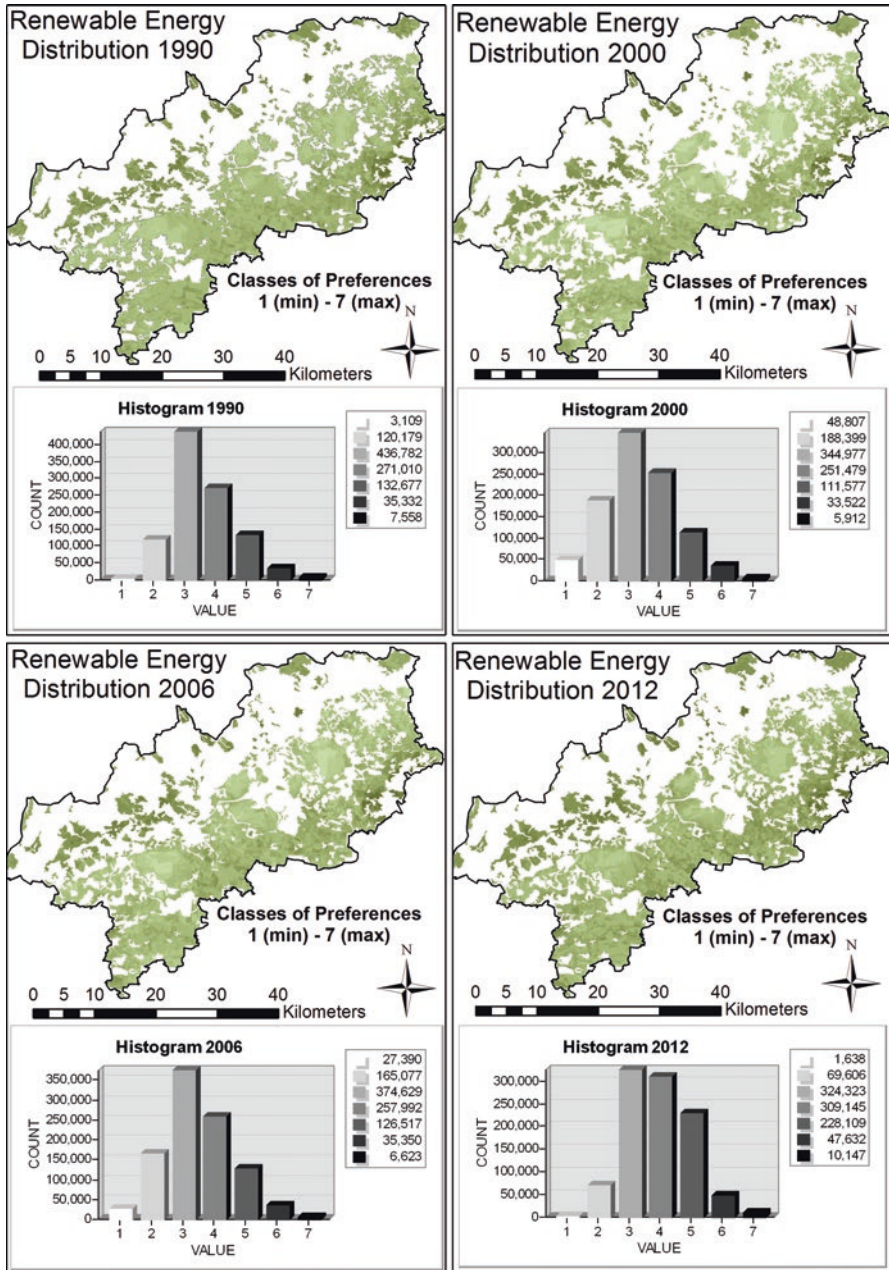
Fig. 11.8 Resulting map layers showing the renewable energy availability on the scale of the preference classes (1–7), where the first class is linked to a minimum and the last class to a maximum in 1990, 2000, 2006, and 2012

Highly preferable sites for small wind farms are located in the northwestern part of the region on the slopes of the Ore Mountains. The western part of the Ore Mountains includes the highest peak, Klinovec, with an altitude of 1244 m. While the mountains slope gently away in the northern part close to the German border, the southern slopes are steeper. The northern parts of the mountains with higher altitude are preferable for utilization of standalone wind turbines and small wind farms, but this area contains a minority of agricultural land cover classes and is sparsely populated.

The southern part of the Ore Mountains contains rather steep slopes with many small streams that form brooks and rivers in the valleys in the middle part of the region. Many weirs in this part can be utilized for small hydro energy plants. In addition, the density of settlements creates a demand for electricity consumption and road networks to manage the hydropower systems. The accessibility of these sources of renewable energy is finally selected as a main factor for multi-criteria analysis, due to the high seasonal variability of surface water flows on the southern part of the Ore Mountains.

Approximate estimates of biomass resources and their bioenergy potential can be approximated by the NDVI using data from remote sensing. In spite of a weak link between NDVI and the biomass potential, long-term monitoring by satellite images yields a wide range of information about landscape development and progress for utilization of renewable energy. It is less useful for highly variable biomass in agricultural sites, but can indicate the biomass potential of spontaneous vegetation in many areas following massive surface coal mining in the period of land remediation. Evaluation of biomass resources in the long-term period by satellite images shows moderate variability.

The delineation of mineral extraction/dump sites and all agricultural classes (in 1990, 2000, 2006, and 2012), which are accounted as potential sites for renewables, can be based on CORINE land cover datasets. Other land cover classes, including forests with many small protected areas (nature reserves and natural monuments), are excluded from the multi-criteria analysis.

The results of multi-criteria analysis yield mapping of the energy potential on a scale of a few preference classes (1–7). Multi-criteria analysis requires well-defined input variables and weights that logically influence the results. Thus, many improvements will be needed to adapt selected methods in the future. In the presented case study, the same weights have been used for multi-criteria analysis for a basic insight.

At the present time, the most important source of energy is represented by fossil fuels, which are also distributed outside the region. In the future, the utilization of sources of renewable energy will be increasingly necessary. In addition, more complex multi-criteria analysis will be required to meet the demands of investors, governmental agencies, and environmentalist. Classification derived from a minimum and maximum of the energy potential will have to be replaced by the real energy output for all the sources of renewable energy in order to estimate the total energy potential from these sources. The weights in the multi-criteria analysis will also have to be accommodated to local social and economic needs. This approach must be based on local projects that can evaluate the financial input and profit together with environmental insight and other criteria.

None of the selected sources of renewable energy (solar photovoltaic, wind power, hydropower, and bioenergy) can fully meet the energy requirements of the local population in this region. The combination of several sources of renewable energy based on local efficiency will be able to replace only part of the energy sources based on fossil fuels. However, after the coal reserves have been exhausted, economic, social and environmental factors will have to be reevaluated in order to stabilize the economy of the region.

The way in which energy is used will change in response to a number of fundamental challenges, such as access to efficient commercial energy sources, meeting the expanding and shifting energy market in an urbanized world, preventing pollution and minimizing avoidable risk by utilizing suitable technological solutions and reducing energy imports from politically unstable regions. In developing suitable energy-economic models for specific renewable energy purposes, it is important to employ a suitable tool to consider geographical regions, energy classification, and economic parameters. In relation to the environment, environmentally friendly technologies can be more expensive than low-cost technology based on coal- or gas-fired plants. They are also dependent on liberalization of the energy markets and reconciliation of environmental goals. Using data from remote sensing, such as multispectral images complemented by NDVI and the CORINE database, in the multi-criteria analysis for long-term periods can reduce financial resources currently allocated toward finding and assessing suitable areas.

Bibliography

Ahamed, T., Tian, L., Zhang, Y., & Ting, K. C. (2011). A review of remote sensing methods for biomass feedstock production. *Biomass and Bioenergy, 35*(7), 2455–2469.

Angelis-Dimakis, A., Biberacher, M., Dominguez, J., Fiorese, G., Gadocha, S., Gnansounou, E., et al. (2011). Methods and tools to evaluate the availability of renewable energy sources. *Renewable and Sustainable Energy Reviews, 15*(2), 1182–1200.

Arnette, A., & Zobel, C. W. (2012). An optimization model for regional renewable energy development. *Renewable and Sustainable Energy Reviews, 16*(7), 4606–4615.

Arnold, U. (2015). Economic risk analysis of decentralized renewable energy infrastructures— A Monte Carlo Simulation approach. *Renewable Energy, 77*, 227–239.

Aslani, A., & Wong, K.-F. V. (2014). Analysis of renewable energy development to power generation in the United States. *Renewable Energy, 63*, 153–161.

Blaschke, T., Biberacher, M., Gadocha, S., & Schardinger, I. (2013). "Energy landscapes": Meeting energy demands and human aspirations. *Biomass and Bioenergy, 55*, 3–16.

Calvert, K., Pearce, J. M., & Mabee, W. E. (2013). Toward renewable energy geo-information infrastructures: Applications of GIScience and remote sensing that build institutional capacity. *Renewable and Sustainable Energy Reviews, 18*, 416–429.

Celik, A. N., Muneer, T., & Clarke, P. (2009). A review of installed solar photovoltaic and thermal collector capacities in relation to solar potential for the EU-15. *Renewable Energy, 34*(3), 849–856.

Cristeaa, C., & Jocea, A. F. (2019). GIS application for wind energy. *Energy Procedia, 85*, 132–140.

Dagdougui, H., Ouammi, A., & Sacile, R. (2011). A regional decision support system for onsite renewable hydrogen production from solar and wind energy sources. *International Journal of Hydrogen Energy, 36*(22), 14324–14334.

El Baroudy, A. A. (2016). Mapping and evaluating land suitability using a GIS-based model. *Catena, 140*, 96–104.

Erdinc, O., & Uzunoglu, M. (2012). Optimum design of hybrid renewable energy systems: Overview of different approaches. *Renewable and Sustainable Energy Reviews, 16*(3), 1412–1425.

Fais, B., Blesl, M., Fahl, U., & Voß, A. (2014). Comparing different support schemes for renewable electricity in the scope of an energy systems analysis. *Applied Energy, 131*, 479–489.

Fiorese, G., & Guariso, G. (2010). A GIS-based approach to evaluate biomass potential from energy crops at regional scale. *Environmental Modelling and Software, 25*(6), 702–711.

Gormally, M., Whyatt, J. D., Timmis, R. J., & Pooley, C. G. (2012). A regional-scale assessment of local renewable energy resources in Cumbria, UK. *Energy Policy, 50*, 283–293.

Grassi, S., Chokani, N., & Abhari, R. S. (2012). Large scale technical and economical assessment of wind energy potential with a GIS tool: Case study Iowa. *Energy Policy, 45*, 73–85.

Grassi, S., Junghans, S., & Raubal, M. (2014). Assessment of the wake effect on the energy production of onshore wind farms using GIS. *Applied Energy, 136*, 827–837.

Hammer, A., Heinemann, D., Hoyer, C., Kuhlemann, R., Lorenz, E., Müller, R., et al. (2003). Solar energy assessment using remote sensing technologies. *Remote Sensing of Environment, 86*(3), 423–432.

Höhn, J., Lehtonen, E., Rasi, S., & Rintala, J. (2014). A Geographical Information System (GIS) based methodology for determination of potential biomasses and sites for biogas plants in southern Finland. *Applied Energy, 113*, 1–10.

Hwang, T., Song, C., Bolstad, P. V., & Band, L. E. (2011). Downscaling real-time vegetation dynamics by fusing multi-temporal MODIS and Landsat NDVI in topographically complex terrain. *Remote Sensing of Environment, 115*(10), 2499–2512.

Inman, R. H., Pedro, H. T. C., & Coimbra, C. F. M. (2013). Solar forecasting methods for renewable energy integration. *Progress in Energy and Combustion Science, 39*(6), 535–576.

Iqbal, M., Azam, M., Naeem, M., & Khwaja, S. (2014). Optimization classification, algorithms and tools for renewable energy: A review. *Renewable and Sustainable Energy Reviews, 39*, 640–654.

Jahangiri, M., Ghaderi, R., Haghani, A., & Nematollahi, O. (2016). Finding the best locations for establishment of solar-wind power stations in Middle-East using GIS: A review. *Renewable and Sustainable Energy Reviews, 66*, 38–52.

Jangid, J., Bera, A. B., Joseph, M., Singh, V., Singh, T. P., Pradhan, B. K., et al. (2016). Potential zones identification for harvesting wind energy resources in desert region of India—A multi criteria evaluation approach using remote sensing and GIS. *Renewable and Sustainable Energy Reviews, 65*, 1–10.

Janke, J. R. (2010). Multicriteria GIS modeling of wind and solar farms in Colorado. *Renewable Energy, 35*(10), 2228–2234.

Kumar, S., & Bansal, V. K. (2016). A GIS-based methodology for safe site selection of a building in a hilly region. *Frontiers of Architectural Research, 5*, 39–51.

Larsson, S., & Nilsson, C. (2005). A remote sensing methodology to assess the costs of preparing abandoned farmland for energy crop cultivation in northern Sweden. *Biomass and Bioenergy, 28*(1), 1–6.

Lasanta, T., & Vicente-Serrano, S. M. (2012). Complex land cover change processes in semiarid Mediterranean regions: An approach using Landsat images in northeast Spain. *Remote Sensing of Environment, 124*, 1–14.

Liu, J., Pattey, E., & Jégo, G. (2012). Assessment of vegetation indices for regional crop green LAI estimation from Landsat images over multiple growing seasons. *Remote Sensing of Environment, 123*, 347–358.

Long, H., Li, X., Wang, H., & Jia, J. (2013). Biomass resources and their bioenergy potential estimation: A review. *Renewable and Sustainable Energy Reviews, 26*, 344–352.

Matejicek, L. (2014). Integration of simulation models for watershed management and data from remote sensing in geographic information systems. In *Proceedings of the 7th International Congress on Environmental Modelling and Software, June 15–19, San Diego, California, USA*.

Matejicek, L. (2015). Multicriteria analysis for sources of renewable energy using data from remote sensing. In *The International Archives of the Photogrammetry, Remote Sensing and Spatial Information Sciences*, XL-7/W3.

Matejicek, L., & Kopackova, V. (2010). Changes in croplands as a result of large scale mining and the associated impact on food security studied using time-series Landsat images. *Remote Sensing, 2*(6), 1463–1480.

Menegaki, A. N. (2013). Growth and renewable energy in Europe: Benchmarking with data envelopment analysis. *Renewable Energy, 60*, 363–369.

Miura, T., Huete, A., & Yoshioka, H. (2006). An empirical investigation of cross-sensor relationships of NDVI and red/near-infrared reflectance using EO-1 Hyperion data. *Remote Sensing of Environment, 100*(2), 223–236.

Muselli, M., Notton, G., Poggi, P., & Louche, A. (1999). Computer-aided analysis of the integration of renewable-energy systems in remote areas using a geographical-information system. *Applied Energy, 63*, 141–160.

Nakata, T. (2004). Energy-economic models and the environment. *Progress in Energy and Combustion Science, 30*(4), 417–475.

Natarajan, K., Latva-Käyrä, P., Zyadin, A., & Pelkonen, P. (2016). New methodological approach for biomass resource assessment in India using GIS application and land use/land cover (LULC) maps. *Renewable and Sustainable Energy Reviews, 63*, 256–268.

Noorollahi, Y., Yousefi, H., & Mohammadi, M. (2016). Multi-criteria decision support system for wind farm site selection using GIS. *Sustainable Energy Technologies and Assessments, 13*, 38–50.

Nygaard, I., Rasmussen, K., Badger, J., Nielsen, T. T., Hansen, L. B., Stisen, S., et al. (2010). Using modeling, satellite images and existing global datasets for rapid preliminary assessments of renewable energy resources: The case of Mali. *Renewable and Sustainable Energy Reviews, 14*(8), 2359–2371.

Pereira, E. J. D. S., Pinho, J. T., Galhardo, M. A. B., & Macêdo, W. N. (2014). Methodology of risk analysis by Monte Carlo method applied to power generation with renewable energy. *Renewable Energy, 69*, 347–355.

Perpiña, C., Martínez-Llario, J. C., & Pérez-Navarro, Á. (2013). Multicriteria assessment in GIS environments for siting biomass plants. *Land Use Policy, 31*, 326–335.

Sarralde, J. J., Quinn, D. J., Wiesmann, D., & Steemers, K. (2014). Solar energy and urban morphology: Scenarios for increasing the renewable energy potential of neighbourhoods in London. *Renewable Energy, 73*, 1–8.

Siyal, S. H., Mörtberg, U., Mentis, D., Welsch, M., Babelon, I., & Howells, M. (2015). Wind energy assessment considering geographic and environmental restrictions in Sweden: A GIS-based approach. *Energy, 83*, 447–461.

Šúri, M., Huld, T., Dunlop, E. D., & Ossenbrink, H. (2007). Potential of solar electricity generation in the European Union member states and candidate countries. *Solar Energy, 81*(10), 1295–1305.

Tafarte, P., Das, S., Eichhorn, M., & Thrän, D. (2014). Small adaptations, big impacts: Options for an optimized mix of variable renewable energy sources. *Energy, 72*, 80–92.

Thomas, A., Bond, A., & Hiscock, K. (2013). A GIS based assessment of bioenergy potential in England within existing energy systems. *Biomass and Bioenergy, 55*, 107–121.

Troldborg, M., Heslop, S., & Hough, R. L. (2014). Assessing the sustainability of renewable energy technologies using multi-criteria analysis: Suitability of approach for national-scale assessments and associated uncertainties. *Renewable and Sustainable Energy Reviews, 39*, 1173–1184.

Wang, S., & Koch, B. (2010). Determining profits for solar energy with remote sensing data. *Energy, 35*(7), 2934–2938.

Yue, C. D., & Wang, S. S. (2006). GIS-based evaluation of multifarious local renewable energy sources: A case study of the Chigu area of southwestern Taiwan. *Energy Policy, 34*(6), 730–742.

Zhang, F., Johnson, D. M., & Sutherland, J. W. (2011). A GIS-based method for identifying the optimal location for a facility to convert forest biomass to biofuel. *Biomass and Bioenergy, 35*(9), 3951–3961.

Data Sources (Revised in September, 2016)

CORINE Land Cover. Retrieved from http://www.eea.europa.eu/publications/COR0-landcover

Institute for Energy and Transport (IET). Retrieved from http://re.jrc.ec.europa.eu/pvgis/

USGS Global Visualization Viewer. Retrieved from http://glovis.usgs.gov/

GIS Data Sources (Revised in September, 2016)

CENIA. *ArcGIS server*. Retrieved from https://geoportal.gov.cz/web/guest/wms. *Wind potential and topographic layers (Czech Republic)*. Retrieved from http://geoportal.gov.cz/arcgis/services

CENIA DMR 5G Hill Shaded Terrain Model (WMS). *Digital model of a relief (Czech Republic)*. Retrieved from http://ags.cuzk.cz/arcgis/services/dmr5g/ImageServer/WMSServer?request=GetCapabilities&service=WMS

CUZK ortofoto (WMS). *Aerial photographs (Czech Republic)*. Retrieved from http://geoportal.cuzk.cz/WMS_SM5V_PUB/WMService.aspx